Energy-efficient Train Timetabling

Scheepmaker, G.M.

DOI
10.4233/uuid:9e59cd4f-06da-4adf-b3a1-0067bda2d34d

Publication date
2022

Document Version
Final published version

Citation (APA)
Scheepmaker, G. M. (2022). *Energy-efficient Train Timetabling*. [Dissertation (TU Delft), Delft University of Technology]. Trail / TU Delft. https://doi.org/10.4233/uuid:9e59cd4f-06da-4adf-b3a1-0067bda2d34d

Energy-efficient Train Timetabling

Gerben Misha SCHEEPMAKER

The research leading to this dissertation was funded by the Netherlands Railways (NS). The Netherlands Research School for Transport, Infrastructure and Logistics TRAIL is greatly acknowledged.

Cover image: Gerben Scheepmaker

Energy-efficient Train Timetabling

Dissertation

for the purpose of obtaining the degree of doctor
at Delft University of Technology
by the authority of the Rector Magnificus, Prof.dr.ir. T.H.J.J. van der Hagen
chair of the Board for Doctorates
to be defended publicly on
Monday 17th, January 2022 at 10:00 o'clock

by

Gerben Misha SCHEEPMAKER
Master of Science in Civil Engineering
Delft University of Technology, the Netherlands
born in Alkmaar, the Netherlands

This dissertation has been approved by the promotor:
Prof.dr. R.M.P. Goverde

Composition of the doctoral committee:

Rector Magnificus	Chairperson
Prof.dr. R.M.P. Goverde	Delft University of Technology, promotor

Independent members:

Prof.dr.ir. S.P. Hoogendoorn	Delft University of Technology
Prof.dr.ir. B.H.K. de Schutter	Delft University of Technology
Prof.dr. F. Corman	ETH Zürich, Switzerland
Dr. A.R. Albrecht	University of South Australia, Australia
Dr.ir. M.M. de Weerdt	Delft University of Technology
Dr. R.M. Lentink	Netherlands Railways

TRAIL Thesis Series no. T2022/1, the Netherlands Research School TRAIL

TRAIL
P.O. BOX 5017
2600 GA Delft
The Netherlands
E-mail: info@rsTRAIL.nl

ISBN: 978-90-5584-305-3

Printed in the Netherlands

Do or do not, there is no try.

Jedi Master Yoda (Star Wars)

Preface

If someone asked me during my childhood what I wanted to be when I grew up, my answer was that I wanted to be a train driver at the Netherlands Railways (NS). And today part of my childhood dream has come true. First, during my MSc thesis at NS (and during my PhD research) I had numerous occasions with a train driver in the cab to experience energy-efficient train driving in real-time. Second, I work at NS since 2013. During my MSc study at Delft University of Technology (TU Delft) I also became interested in doing a PhD research on the topic of railway timetabling and operations, and I discussed this with Rob Goverde. During my MSc thesis he offered me a position for PhD research at his research group. However, I preferred to work at NS after my MSc, because I already found a job there at the Department of Logistics. During my first year at NS, Rob convinced the head of the Department of Logistics to propose a part-time (two days per week in a period of four years) PhD research at TU Delft, in which I would remain in service for NS and my research was completely funded by NS. The only constraint was that the research topic should be related to the work done at the Department of Logistics. This basically means that I was able to choose my own PhD research topic, which is quite unique. I preferred to continue the topic of my MSc thesis on energy-efficient train driving and incorporating energy-efficient train driving into timetable design. I did my PhD research in the period 2014-2022 and I would like to thank all people involved in my research.

First, I would like to thank Rob Goverde for supporting me with my PhD research as both my daily supervisor and promoter. You always made time for me when I had some questions and your critical review improved the quality of my work significantly. You helped me to see the broader picture, when I sometimes got stuck into the details of my research. In addition, you helped me to develop my knowledge in mathematics and operations research. Thank you for your patient, critical thinking and guidance during my PhD research.

Second, I would like to thank the committee members of my PhD defense: Serge Hoogendoorn, Bart de Schutter, Francesco Corman, Amie Albrecht, Mathijs de Weerdt and Ramon Lentink. Thank you for reviewing my PhD thesis and propositions that helps me to improve the quality. In addition, special thanks to Amie for hosting me at the University of South Australia as a visitor researcher and

to exchange knowledge on the field of energy-efficient train control and timetabling. Also special thanks to Ramon Lentink for being my supervisor during my PhD research at NS since 2016. You really helped me to consider the practical implementation of the scientific research and enabled me to form a bridge (as Civil Engineer) between scientific research and practice (at NS).

Third, special thanks to Ralph Luijt and Vincent Verbeet who enabled me to do a part-time PhD research funded and commissioned by NS. Ralph, also thank you for your support in finding a position at NS.

Fourth, I would like to thank the other authors for collaborating in different papers. Thanks to Leo Kroon for his input in timetable optimization in our literature review paper regarding energy-efficient train control and timetabling, and for being my supervisor at NS in the period 2014 to 2016. I would like to thank Hellen Willeboordse, Jan Hoogenraad, and Ralph Luijt for cooperating on a paper where we analyze the effects of different driving strategies on different key performance indicators for railway undertakings. It is great to see that our research results are currently used by NS to determine the preferred driving strategy. I would like to thank Peter Pudney, Amie Albrecht, and Phill Howlett for co-writing a paper about the distribution of the running time supplements and comparing different methods to solve the optimal control problem. It was an honor to work together with your research group that has more than 30 years of experience with energy-efficient train control. It was great to have a better understanding of the working of the driver advisory system Energymiser and to compare the system with my direct solution method. Thanks to Pengling Wang for your cooperation in our paper on pseudospectral optimal train control and helping me to further exploit the knowledge of the MATLAB toolbox GPOPS.

Fifth, I would like to thank NS, TU Delft, and TRAIL Research School for their support in my research. Thanks to NS for supporting and funding my PhD research. Special thanks to Wilmet van Dijk, Ramon Lentink, Dennis Huisman, Erwin Abbink and Erik Sigger for the possibility to extend my part-time PhD research contract of NS from 4 to 6 years. I would like to thank the secretaries of the following (former) departments for their practical support during my PhD research: Logistics, Timetable Development and Design, and Performance Management and Innovation. I would also like to thank all my (former) NS colleagues for their support during my research and their help in applying my knowledge from my PhD in practical advice for NS regarding energy-efficient train driving and timetable design. Thanks to the secretary of the department of Transport and Planning for the practical support in my scientific research. I would also like to thank my (former) colleagues from the Digital Rail Traffic Lab for exchanging knowledge and ideas during our PhD research. Also thanks to the Graduate School of TU Delft that enabled me to develop different skills related to conducting research,

improving knowledge in my research area, and personal development. I would like to thank TRAIL Research School for their support in education and their practical support during my research.

Finally, I would like to thank my family and friends for supporting me in my research. Special thanks to my friends Simon den Hengst and Henno Smaling for being my paranymphs during my PhD defense. My special thanks also goes to my wife Kim. Thank you for giving me the opportunity to do this research (even during the evenings and the weekends) and supporting me in writing. You always surprised me with your very useful ideas and feedback during programming in MATLAB. And Noa, my daughter, you are a great help in keeping daddy happy and smiling, especially when you take over my work behind my desktop computer while saying "Noa op de pjuter, papa". Finally, most of all I would like to thank God and bring Him my praise, because without Him nothing was possible (John 15:5).

Veenendaal, the Netherlands, December 2021

Gerben Scheepmaker

Contents

Chapter 1

Introduction

1.1 Context and background

Global warming is a worldwide problem and its effects are increasingly visible nowadays. For instance: rising sea level, more extreme weather conditions, and melting ice on earth's polar region. The main cause of the global warming are the greenhouse gasses, because they radiate the energy back to the earth causing increasing temperatures on the earth. One of the main greenhouse gasses is carbon dioxide (CO_2) of which pollution has increased drastically since the Industrial Revolution (National Geographic, 2017).

In Europe 20% of the total emissions is caused by the transport sector. Although the main part is caused by road transport, the railways consider about 3.3% of the total CO_2 emissions in Europe (IAE & UIC, 2014). As a consequence, for railways in Europe the UIC (International Union of Railways) and CER (Community of European Railway and Infrastructure Companies) have set targets to decrease the amount of CO_2 emissions by 30% in 2020 and 50% in 2030 compared to 1990 (UIC, 2012). Therefore, railway companies in Europe have taken measures to decrease the amount of CO_2 emissions (sustainability). The reduction of CO_2 emissions for railways is directly related to energy. In addition to sustainability, there is the environmental requirement to reduce the energy usage. Railways are already more energy friendly than other modes, but it can still be improved. Reducing the energy cost is another intrinsic incentive for railway companies to reduce the energy consumption.

Railways in general can contribute to the total reduction of the CO_2 emissions by the modal shift from road to rail. Although this means that more energy is needed to transfer people and freight for the railways, the total amount of energy consumption (and thus the CO_2 emissions) for the complete transport sector will reduce. Railways are in general more efficient compared to road transport with

less pollution of greenhouse gasses per passenger kilometer (EEA, 2021), because most railway lines in Europe are electrified. In addition, renewable energy sources are (partially) used to generate the electricity like solar, wind and hydro power. However, the focus of this thesis is not on the modal shift.

Railway undertakings (RUs) can save energy in various ways, such as the improvement of the streamlining of rolling stock (aerodynamics), efficient use of the heating, cooling and lighting of trains during parking, or storage of regenerated energy during braking. González-Gil et al. (2014) compared different measures for energy saving by looking at the total investment cost and the return in energy savings. The highest energy savings can be gained by wayside energy storage systems, but the investment costs are very high.

One of the measures that leads to relatively high energy savings with low investment costs is energy-efficient train driving or eco-driving and optimized timetables for energy-efficient train driving (González-Gil et al., 2014). The aim of energy-efficient train driving is to minimize total traction energy consumption of the train given the scheduled running time in the timetable. The total available time includes *running time supplements*. These supplements are the extra time above the technical minimum running time in the timetable in order to cope with running time variations and to recover from small delays (Scheepmaker & Goverde, 2015). The train driver can apply energy-efficient train driving, and arrive exactly on-time (i.e., not too early and not too late) at the next stop during undisturbed situations.

The energy savings during energy-efficient train driving are quite substantial, because the rolling resistance of a train is very low. This is mainly due to the low friction between steel wheels and steel tracks. Furthermore, trains are quite heavy. This provides a high potential for coasting, where the train driver pulls off the traction of the train and the train remains rolling. For instance, the Netherlands Railways (NS) yearly saves about 5% of energy by using the energy-efficient train driving approach of *Energie Zuinig Rijden* (Luijt et al., 2017). Energy-efficient train driving can be applied in different ways. For instance, NS focuses on coasting (see Figure 1.1), while the Swiss Federal Railways (SBB) focuses on cruising (maintain a constant maximum speed) (see Figure 1.2). The difference in the applied driving strategy by each RU is caused by multiple factors, such as the catenary system (i.e., voltage and current), the topography (i.e., gradient), the timetable (i.e., amount and distribution of the running time supplements), the rolling stock type (i.e., regenerative braking), the importance of each key performance indicator that influences the driving strategy (i.e., punctuality or the workload for the train driver), and the culture (i.e., the acceptance rate of influencing the driving strategy of a train driver). For instance, at NS the energy-efficient train driving strategy started with a simple (manual) method developed by

a train driver (called the UZI method) based on coasting that can easily be applied by all train drivers. The advantages of this approach were the low investment cost, the relatively high energy savings, the low workload for the train driver, and the high acceptance rate by the train drivers (Luijt et al., 2017). In addition, a bottom-up approach was used at NS (first introduce energy-efficient train driving at the train drivers and later involve the management) to bring a change in driving behavior within the organization. Based on the success of this coasting driving strategy the train drivers themselves asked for further digital assistance to improve their energy-efficient driving strategy and to decrease their workload. Train drivers can be assisted in applying energy-efficient train driving by using *driver advisory systems* (*DASs*), that give the train driver speed advice in order to minimize energy consumption (Panou et al., 2013). In addition, *automatic train operation* (*ATO*) enables even more energy savings compared to a DAS, because an algorithm is in potential better (i.e., more accurate and with less fluctuation) able to follow the optimal driving strategy with real-time information compared to a train driver (i.e., absence of human behavior).

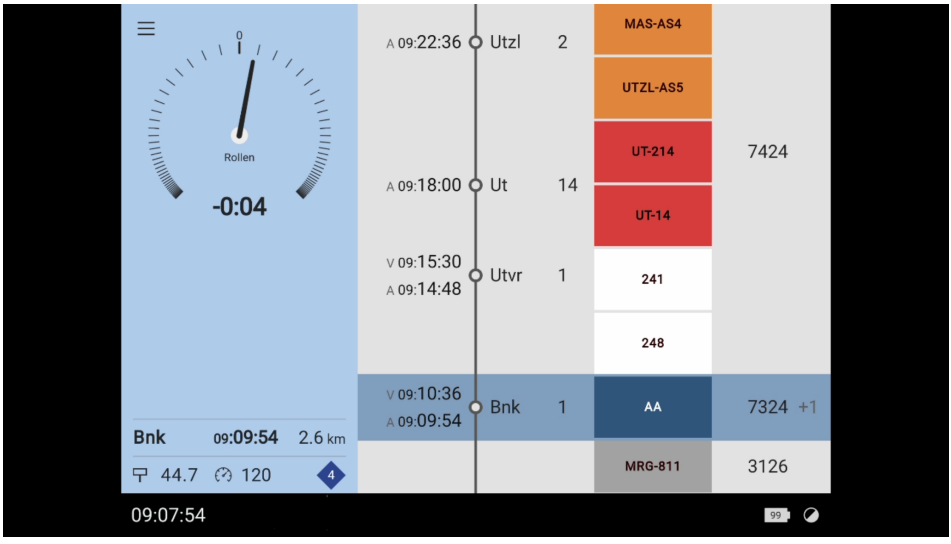

Figure 1.1: Coasting advice (left blue part that indicates in Dutch "Rollen") from the RTA App on the TimTim for train drivers at NS (De Jong, 2019).

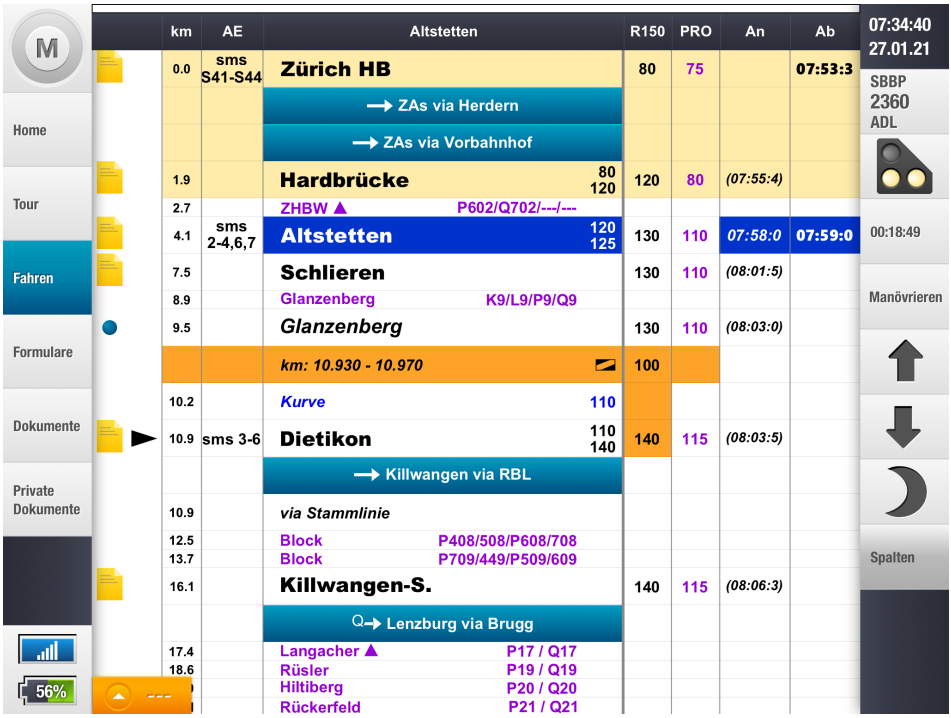

Figure 1.2: Cruising speed advice (column "PRO") from RSC-ADL on the LEA App for train drivers at SBB (Graffagnino et al., 2019; Graffagnino & Tuchschmid, 2019).

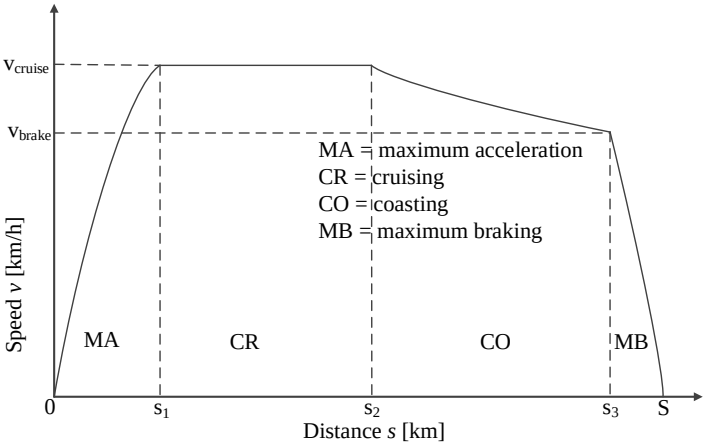

Figure 1.3: Speed profile of a basic energy-efficient driving strategy with switching points between driving regimes at s_1, s_2 and s_3 for a flat track with sufficient running time supplements.

The challenge in practice for a DAS or ATO is to compute in real-time the optimal train trajectory over the available running time that minimizes the total energy consumption, especially when considering realistic conditions such as varying gradients and varying speed limits. The train trajectory consists of the speed profile for a train including the switching points between different *driving regimes* (i.e., acceleration, cruising, coasting, and braking). Therefore, train trajectory optimization regarding energy minimization or *energy-efficient train control* (*EETC*) is extensively studied in literature during the last thirty years (Scheepmaker et al., 2017). The aim of the EETC problem is to find the energy-optimal driving strategy that uses the least amount of traction energy. *Pontryagin's Maximum Principle* (*PMP*) is used in order to derive the necessary optimality conditions (Pontryagin et al., 1962). PMP tries to find the control settings for optimal switching between different driving regimes by maximizing the Hamiltonian function. The necessary conditions characterize the optimal driving regimes, consisting of: maximum acceleration (MA), cruising (CR), coasting (CO) and maximum braking (MB). Algorithms are used to compute the optimal order and sequence of the driving regimes in order to derive the energy-optimal driving strategy. A simple example of the optimal driving strategy on a flat track with sufficient running time supplements is shown in Figure 1.3. This figure clearly illustrates the sequence of the driving regimes (MA-CR-CO-MB) as well as the switching points s_1, s_2 and s_3 between these regimes. Note that the optimal cruising speed can be lower than the speed limit. The optimal cruising speed can also be higher than the speed limit, in which case the train will follow the speed limit. The optimal control strategy will typically then compensate with less coasting (Albrecht et al., 2016a). The EETC problem becomes more complex when considering realistic conditions, such as varying gradients, varying speed limits, regenerative braking, multiple stops and multiple trains on a corridor or network. During regenerative braking the train uses the engine as a generator in order to gain energy. This energy can be used by the train itself for lighting or heating, or it can be fed back to the catenary system to supply surrounding trains with energy. It is also possible to store the regenerated energy within the train or around the track (González-Gil et al., 2013).

The EETC problem can be solved using different methods that can be classified into indirect and direct solution methods (Betts, 2010; Rao, 2014). These methods differ in the way they translate the optimal control problem into a numerical problem. The indirect methods use a boundary value problem (BVP) and direct solution methods use a nonlinear programming problem. Also heuristic methods are used to solve the EETC problem.

For indirect solution methods the necessary optimality conditions are derived using PMP, which leads to a two-point boundary value problem (Ross, 2005). The optimal control problem is thus translated into a BVP, which makes it an indirect solution method to solve the original optimal control problem. The BVP also depends on the optimal control structure that again depends on the solution of the BVP. Therefore, usually constructive methods are used that use knowledge about the optimal control structure. Most research on EETC is focused on indirect solution methods. The optimal train control problem in literature started simple (flat tracks) and gradually increased in complexity to become more realistic (i.e., including varying gradients, speed limits, and regenerative braking), as discussed in the papers of for instance Howlett & Pudney (1995), Khmelnitsky (2000), Liu & Golovitcher (2003), and A. Albrecht et al. (2016b,a).

For direct solution methods collocation is used to discretize the state and control variables and translate the problem into a nonlinear programming problem (Betts, 2010). Algorithms are available to solve the nonlinear programming problem. Direct solution methods are efficient for complex optimal control problems, because they do not need information about the optimal control structure as input to solve the problem (Rao, 2014). Pseudospectral methods are direct solution methods that have been intensively applied for optimal control problems in aerospace engineering (Ross & Karpenko, 2012). A limited number of papers on optimal train control use direct solution methods, for instance, Y. Wang et al. (2013), P. Wang & Goverde (2016a), and Ye & Liu (2016). All these papers apply the pseudospectral method where the state and control are approximated by global polynomials and orthogonal collocation is used for the differential equations (Ross & Karpenko, 2012). In this thesis the pseudospectral method is used to compute the optimal train trajectory while the optimal control structure is checked using PMP.

Even more energy can be saved (with low investment costs) when considering the timetable design phase (*energy-efficient train timetabling* or *EETT*) (González-Gil et al., 2014), since the amount and distribution of the running time supplements determine the impact of energy-efficient train trajectories. Research on timetable design is mainly focused on the robustness of the timetable, see the surveys of Caprara et al. (2007), Lusby et al. (2011), and Cacchiani & Toth (2012). Timetable *robustness* means that the timetable can cope with design errors, variations of parameters and changing operational conditions (Goverde et al., 2016). A limited number of papers considers the topic of energy-efficient train timetabling (Scheepmaker et al., 2017). Most research in this area is focused on synchronization of accelerating and regenerative braking trains, where the regenerated energy of the braking train can be used for the accelerating train. Examples can be found in the papers of T. Albrecht (2004), Peña-Alcaraz et al. (2012), Li & Lo (2014b),

and X. Yang et al. (2015). However, another possibility for EETT is the amount and/or distribution of the running time supplements for optimizing energy-efficient train trajectories. Examples of papers considering the optimal amount and/or distribution of the running time supplements for energy-efficient train driving can be found in Pudney et al. (2009), Sicre et al. (2010), and Su et al. (2013, 2014).

However, from a practical point of view, minimizing the total energy consumption is not the only objective for a railway undertaking. Timetables in practice are manually developed in timetable design tools. The primary aim is to find a feasible timetable with a balance between travel times and capacity consumption. The timetable is not necessary conflict-free and, therefore, timetable feasibility and robustness is checked using simulation. Other objectives are minimizing total travel time for the passenger, minimizing the infrastructure occupation and maximizing the robustness of the timetable. The *infrastructure occupation* is defined as the amount of time that the infrastructure is blocked by train paths from a given timetable structure in a given time window (UIC, 2013).

Scientific research on the topic of multiple-objective optimization for timetabling without energy-efficient train driving can be found in the surveys of Caprara et al. (2007), Lusby et al. (2011), and Cacchiani & Toth (2012). Most research is focused on a macroscopic (aggregate) level of the infrastructure data with conflict detection based on headway norms. However, research considering a *microscopic level* of the infrastructure and conflict detection based on the blocking times of trains is limited (Cacchiani et al., 2014, 2015), because more details are needed for modelling which results in an increased size of the model for the decision variables and constraints (Zhang et al., 2019). Scientific research on the topic of multiple-objectives on a microscopic level considering energy-efficient train trajectories is even more limited. In the European rail project ON-TIME energy-efficient train trajectory optimization was considered to fine-tune the timetable on a corridor level, after the feasibility (realistic running times and conflict-free timetable based on blocking time theory (Pachl, 2009, 2014)), stability (absorb delays without rescheduling) and robustness of the timetable were determined (Goverde et al., 2016). The fine-tuning model considers robust energy-optimal speed profiles by including stochastic dwell time distributions at intermediate stops. The combination of energy-efficient train trajectories and minimizing delays for multiple-trains on single-track lines using headway norms is considered by P. Wang & Goverde (2017). The approach is extended by P. Wang & Goverde (2019) to optimize the energy-efficient train trajectories for trains on a general railway network by re-allocating the running time supplements in the timetable, while conflicts are detected using headway norms during the optimization. The feasibility of the optimal timetable is afterwards checked using blocking times. Furthermore, there are currently no RUs in practice that have applied energy-

efficient train trajectory optimization into their timetable design. NS would like to investigate the possibilities to incorporate energy-efficient train trajectory optimization into the timetable design process, since energy-efficient train trajectories helps the train driver to reduce the fluctuation of the running times in practice.

1.2 Research objective and research questions

Both scientific research and railway practice show the need to incorporate energy-efficient train driving in the timetable design process and to balance energy-efficient train trajectory optimization with other objectives during the design phase, such as the total running time, the infrastructure occupation and robustness of the timetable. Therefore, the aim of this thesis is to incorporate energy-efficient train driving into the timetable design. In order to structure this thesis, the following key research questions are considered:

1. How can the optimal driving strategy be determined that minimizes total traction energy consumption? (Chapter 2)
2. How can nonlinear regenerative braking be included in the energy-optimal driving strategy? (Chapter 3)
3. How can existing train driving strategies be improved to minimize energy consumption? (Chapter 4)
4. How can the optimal distribution of running time supplements be determined to optimize energy-efficient driving of a train over multiple stops along the line? (Chapter 5)
5. How can energy-efficient train driving be included in timetable optimization considering multiple objectives? (Chapter 6)

1.3 Thesis contributions

In this section the main contributions of the thesis are summarized. The contributions are separated into scientific contributions (Section 1.3.1) related to theory and methodology, and societal relevance (Section 1.3.2).

1.3.1 Scientific contributions

The scientific contributions of this thesis can be grouped into the following six topics:

1. *Review of energy-efficient train control and energy-efficient train timetabling.*
   A thorough literature review is provided on the topics of EETC and EETT with the focus on the difference in the mathematical models and algorithms (Chapter 2). For EETC a distinction is made between the traction control (discrete or continuous), the braking behavior (with or without regenerative braking) and the solution method (indirect solution method, direct solution method or heuristics). For EETT a distinction is made between the braking behavior (with or without regenerative braking) and the algorithm (genetic algorithm, simulation, dynamic programming or gradient search) to solve the problem.

2. *Analyzing the difference in the EETC for mechanical and/or (nonlinear) regenerative braking.*
   The EETC problem including realistic braking behavior considering mechanical and (nonlinear) regenerative braking is formulated, and the optimal control structure and the necessary optimally conditions are derived. The differences between mechanical and/or (nonlinear) regenerative braking on the energy-efficient train control are analyzed on different scenarios by using algorithms based on the Radau pseudospectral method (Chapter 3).

3. *Comparing different train driving strategies.*
   Current driving strategies in practice are mainly focused on cruising or coasting. A comparison is made between a cruising (*reduced maximum speed*, *RMS*), coasting (*maximal coasting*, *MC*) and the EETC driving strategy on different scenarios using different evaluation criteria. The criterion of energy consumption indicates where existing driving strategies can be improved to minimize the total energy consumption (Chapter 4). The optimal control problems for the EETC, MC and RMS driving strategy are formulated and solved using algorithms based on the Radau pseudospectral method.

4. *Insight in the optimal distribution of the running time supplements in the timetable for a single train over multiple stops.*
   A problem formulation and application of the EETC problem for a single train over multiple stops regarding the distribution of the running time supplements is presented (Chapter 5). This also leads to general timetable design principles for incorporating energy-efficient train driving into timetabling.

5. *Balance between energy-efficient train trajectories, total running time, infrastructure occupation, and robustness.*

A multiple-objective optimization problem is formulated and solved that considers the trade-off between running time, infrastructure occupation, timetable robustness and energy-efficient train driving for multiple interacting following trains on a corridor (Chapter 6). A brute force algorithm is used to tackle the multiple-objective optimization by computing the optimal solutions using the weighted sum and the standard Euclidean distance method. The result leads to a balanced conflict-free timetable by considering the blocking times.

6. *Developing and implementing a prototype to solve the optimal train trajectory and the multi-objective timetable optimization problem.*
   The developed models and implemented algorithms in this thesis have led to the MATLAB prototype tool called PROMO (PseudospectRal Optimal train control MOdel). Four different driving strategies with different braking behavior (i.e., mechanical and/or regenerative braking) have been incorporated in PROMO based on the Radau pseudospectral method with the optimal control structure using PMP: the minimum running time, a coasting and a cruising strategy, and the EETC driving strategy (Chapters 3–4). Furthermore, PROMO has also been applied to compute the optimal amount and distribution of the running time supplements in the timetable and provides the blocking times, according to the blocking time theory (Chapters 5–6). A brute force search algorithm has been used in a multi-objective optimization problem to minimize the total running time, infrastructure occupation, energy consumption and to maximize the robustness of the timetable (Chapter 6). The robustness of the timetable has been considered by evaluating the buffer times between two consecutive trains.

1.3.2 Societal relevance

The thesis has the following contributions to society:

1. *Energy-efficient train driving contributes to sustainability.*
   Reducing the energy consumption of trains by energy-efficient train driving reduces the amount of fuel or electricity, the energy costs and in the end the amount of CO_2 emissions which contributes to sustainability (global warming) (Chapter 2). Direct reduction of CO_2 emission is achieved for fuel engine trains. However, most trains are electrified and even use green energy from sources such as wind, solar or hydropower. Indirect reduction of CO_2 emission for these trains is achieved, because they need less electricity that can be used for other sectors.

2. *Comparison between different practical driving* strategies on multiple key performance indicators.
   In practice railway undertakings apply different driving strategies in order to save energy. However, there are more key performance indicators (KPIs) that affect the operational performance of RUs. The KPIs considered in this research are safety, timeliness, energy consumption, workload for the driver, the environment, cost of maintenance and brand image. For instance, energy-efficient driving strategies reduce the environmental pollution by the average amount of pass-by-noise (noise hindrance), reduce the cost of maintenance needed for rolling stock and infrastructure, and increase the brand image from passenger perspective by reduction of unplanned stops. A KPI toolbox has been developed that enables for instance infrastructure managers (IMs), railway undertakings and policy makers to evaluate the most appropriate driving strategy (Chapter 4).

3. *Balanced timetable design by considering multiple objectives.*
   A balanced multiple-objective timetable is determined by minimizing the total travel time, infrastructure occupation, energy consumption and maximizing the robustness of the timetable. Incorporating energy-efficient train driving in timetable design leads to realistic speed profiles for the train driver that enables on time running and reduces the fluctuations in operational performance. A balanced timetable is able to withstand disturbances and small delays, reduces the total travel times, infrastructure occupation (efficient use of the infrastructure assets), and energy consumption, which is beneficial for the IMs, the RUs and the passengers (Chapter 6).

1.4 Collaborations in the thesis

Five scientific papers form the core of this thesis. Three papers have been written with multiple co-authors in addition to the supervisor. Their contributions to the papers are listed below:

- **Chapter 2**: Gerben M. Scheepmaker, Rob M. P. Goverde, Leo G. Kroon (2017) Review of energy-efficient train control and timetabling, *European Journal of Operational Research*, 257(2), 355–376. The co-authors were responsible for the basic model description for EETC and EETT.

- **Chapter 4**: Gerben M. Scheepmaker, Helen Y. Willeboordse, Jan H. Hoogenraad, Ralph S. Luijt, R. M. P. Goverde (2020) Comparing train driving strategies on multiple key performance indicators, *Journal of Rail Transport Planning & Management*, 13, 100163. The second and third co-authors were responsible for the methodology section for the KPIs safety,

workload, cost of maintenance, environment and brand image, as well as the results of the platform clearing scenarios. The fourth author peer reviewed the paper and provided input from practice (operation) into the paper.

- **Chapter 5**: Gerben, M. Scheepmaker, Peter J. Pudney, Amie R. Albrecht, Rob M. P. Goverde, Phil G. Howlett (2020) Optimal running time supplement distribution in train schedules for energy-efficient train control, *Journal of Rail Transport Planning & Management*, 14, 100180. The second, third and last co-authors were responsible for the description and results of the indirect solution method of Energymiser.

1.5 Outline of the thesis

In this section the outline of this thesis is described. A visual representation of the outline can be found in Figure 1.4. Basically the chapters of the thesis are structured on the topics of EETC and EETT. Chapter 2 considers the literature review on the topic of EETC and EETT which gives the background information and the knowledge gap in this research area.

The focus of Chapter 3 is on the EETC problem, in which the theoretical basis for the EETC problem is formulated, as well as the connection with the Radau pseudospectral method, which is the method used to solve the optimal control problem in this thesis. Chapter 3 also compares the difference in driving strategy between EETC with mechanical and/or constant/nonlinear regenerative braking. Different driving strategies in practice are compared with the theoretical optimal EETC and evaluated for different KPIs in Chapter 4.

Chapter 5 and Chapter 6 continue with the EETT problem. Chapter 5 focuses on a single train in order to determine the optimal distribution of the running time supplements over multiple stops. The aim is to minimize the total traction energy consumption given a total running time for the complete trajectory. Chapter 6 considers the interaction with other surrounding trains and, therefore, incorporates the effect of the infrastructure occupation and robustness of the timetable. The aim is to determine the relationship between the objectives of minimizing total traction energy consumption and the total running time, infrastructure occupation and robustness of the timetable. Finally, the conclusions and recommendations for future research are provided in Chapter 7.

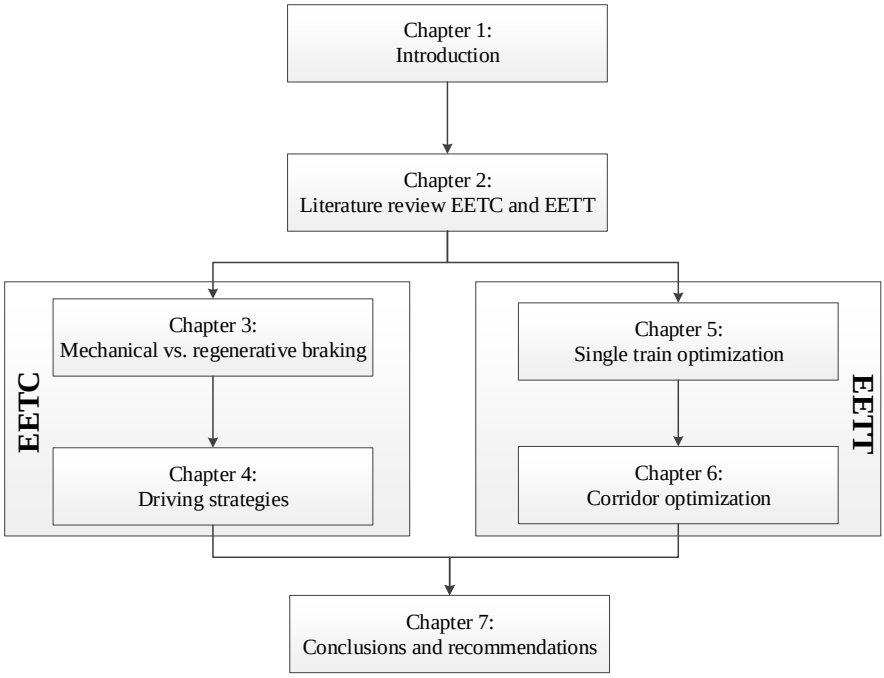

Figure 1.4: Visualization of the outline of the thesis.

Chapter 2

Review of energy-efficient train control and timetabling

Apart from minor updates, this chapter has been published as:
Scheepmaker, G. M., Goverde, R. M. P., Kroon, L. G. (2017) Review of energy-efficient train control and timetabling, *European Journal of Operational Research*, 257(2), pp. 355–376.

2.1 Introduction

Global warming is an increasingly important topic these days. One of the causes of global warming is the increasing amount of carbon dioxide (CO_2) emissions which comes for a large part from transport. Therefore, the European Union (EU) set targets to decrease these CO_2 emissions. One of the sectors affected by these measures is the railway sector. For the railway sector targets are set by the UIC (International Union of Railways) and CER (Community of European Railway and Infrastructure Companies). The short term target is to decrease CO_2 emissions by 30% over the period 1990 to 2020, with a further decrease by 50% in 2030 (UIC, 2012). Furthermore, energy consumption of railway companies should be decreased in 2030 by 30% compared to 1990. A further incentive for railway undertakings to reduce energy consumption is the reduced operating costs and enlarged competitive advantages involved.

As a consequence, railway companies in Europe have started research on opportunities to decrease energy consumption in order to be sustainable and more profitable in the future. Several ways to achieve this goal are as follows:

- An operator can deploy rolling stock that is more energy-efficient (due to

more efficient engines or streamlining).

- An operator may better match the capacities of the trains with the demand, so that fewer empty seats are moved around.
- An operator can deploy measures concerning heating, cooling, lighting, etc. of parked trains during nights in order to save energy.
- *Energy-efficient train control* (*EETC*) or *eco-driving* may be applied, in which a train is driven with the least amount of traction energy, given the timetable.
- The timetable may be constructed in such a way that it allows EETC most effectively, resulting in *energy-efficient train timetabling* (*EETT*).

This chapter focuses on the last two options: energy-efficient train control (EETC) and energy-efficient train timetabling (EETT). A good overview of different measures in order to decrease energy consumption for urban rail transport can be found in González-Gil et al. (2014).

EETC has been and is a hot topic in the literature. Much research effort aims at finding the optimal driving strategies of a train that minimize energy consumption (Khmelnitsky (2000); Liu & Golovitcher (2003); A. Albrecht et al. (2016a,b)). Most of this research is based on optimal control theory, and in particular on *Pontryagin's Maximum Principle* (*PMP*) (Pontryagin et al., 1962), to derive the optimal control. This leads to optimal *driving regimes* such as maximum acceleration, cruising, coasting and maximum braking, see Figure 2.1. The problem is then to find the optimal sequence of these driving regimes and the switching points between the regimes for a range of different circumstances and train types. The optimal driving strategy must then be translated into feasible and understandable advice to train drivers in real-time. This generated considerable research in developing *Driver Advisory Systems* (*DAS*) that provide specific speed advice to the train drivers with the main challenge to incorporate the current delays into the advice (Kent, 2009; ON-TIME, 2013; Panou et al., 2013). Energy savings between 20% to 30% have been reported when applying EETC in a DAS compared to normal train operation, for example see Franke et al. (2000) and ON-TIME (2014a).

The impact of train operation on energy savings depends on the timetable. More recently this led to research on the topic of optimal running time supplements (Scheepmaker & Goverde, 2015). A *running time supplement* is the extra running time on top of the technically minimum running time between two stations which is included in the timetable primarily to manage disturbances in operations and to recover from small delays. However, if a train is punctual then these supplements can be used for energy-efficient driving. Nevertheless, in practice

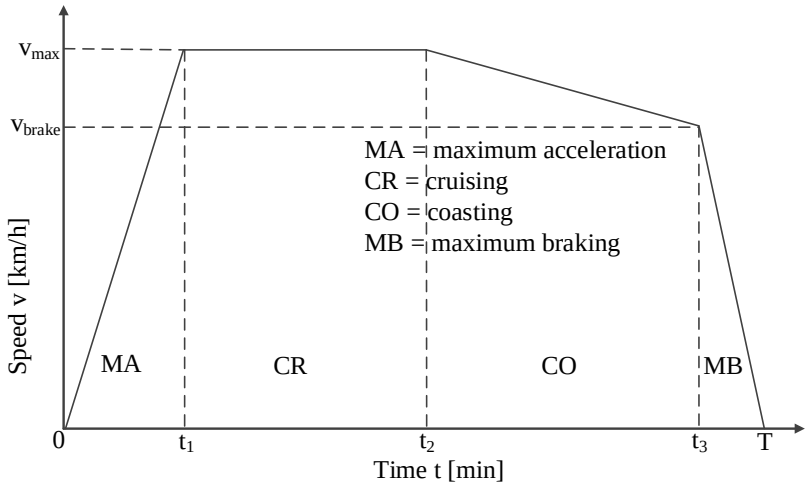

Figure 2.1: Optimal driving regimes for energy-efficient driving on flat track as function of time with switching points at t_1, t_2 and t_3.

energy efficiency is not yet considered in the construction of timetables which sometimes leads to allocating most running time supplements before main stations where punctuality is measured at the cost of insufficient supplements or even unrealizable running times earlier on the route. Another recent stream of research considers the synchronization of accelerating and braking trains to support *regenerative braking*, like T. Albrecht (2004). With regenerative braking, kinetic energy is converted into electricity that is fed back to the power supply system to be used by other (nearby) trains. A more detailed description about the working of regenerative braking and different regenerative braking technologies for urban transport can be found in the review paper of González-Gil et al. (2013). Energy savings up to 35% have been reported after timetable optimization compared to using the normal timetable, for example see T. Albrecht & Oettich (2002) and Sicre et al. (2010).

This chapter provides a thorough review of the literature on energy-efficient train control and timetabling, starting with the first simple models from the 1960s of a train running on a level track to the advanced models and algorithms of the last decade dealing with varying gradients and speed limits, and including regenerative braking. The focus is on the differences between the mathematical models and algorithms in terms of applicability, accuracy and computation time, and their main conclusions on the structure of the optimal driving strategy.

Our method is based on a literature study focused on EETC and EETT. We structured the publications based on the frameworks shown in Figure 2.2 and Figure

2.9. This review chapter includes publications up to January 2016. The recent literature is given in the literature review sections of Chapters 3, 5, and 6. The recent paper by X. Yang et al. (2016) also provides a review of EETC and EETT with a focus on urban rail. In contrast to that paper, we consider general railway systems and focus on the differences in the mathematical problem formulations and solution approaches.

Section 2.2 introduces a basic EETC problem and outlines the mathematics involved. Section 2.3 reviews the EETC literature building on the concepts and terminology of the basic model. The application of EETC in EETT is the topic of Section 2.4, which reviews the related literature on the optimization of running time supplements and the synchronization of accelerating and braking trains. Finally, Section 2.5 ends this literature review with the main conclusions and an outlook to future research directions of EETC and EETT.

2.2 A basic model and solution approaches

This section considers a basic optimal train control problem to define the basic notation and illustrate the main modelling concepts which will be extended later in this chapter. This problem was analysed by Milroy (1980) in the late 1970s as one of the first optimal train control problems. Here, we give a modern analysis. A rigorous mathematical treatment and further extensions are given in Howlett & Pudney (1995) and A. Albrecht et al. (2016a,b).

2.2.1 A basic energy-efficient train control model

Consider the problem of driving a train from one station to the next along a flat track within a given allowable time T in such a way that energy consumption is minimized. The train speed $v(t)$ at time t is governed by a tractive or braking effort $F(t)$ and a resistance force $R(v)$ according to the Newton force equilibrium

$$\rho m \dot{v}(t) = F(t) - R(v(t)), \tag{2.1}$$

where $\dot{v} = dv/dt$ is the derivative of speed to time, m is the train mass and ρ the dimensionless rotating mass factor (Brünger & Dahlhaus, 2014). The force F is the tractive effort of the engine for $F \geq 0$ and the braking effort due to the brakes for $F < 0$. The maximum tractive effort $F_{\max}$ is a non-increasing function of speed, which is approximated by a piecewise linear, quadratic and/or hyperbolic function of speed depending on the engine (Brünger & Dahlhaus, 2014). The maximum braking force $F_{\min}$ is usually approximated based on a constant braking rate (independent of speed). The resistance force is given by the Davis equation $R(v) = R_0 + R_1 v + R_2 v^2$ with non-negative coefficients $R_i \geq 0, i \in \{0, 1, 2\}$, which

is a strictly increasing quadratic function in speed (Davis, 1926). The constant and linear coefficients are rolling resistances and depend on mass, while the quadratic term is the air resistance which is mass independent.

It is convenient to normalize the equations as mass-specific by the specific resistance $r(v) = R(v)/\rho m = r_0 + r_1 v + r_2 v^2$ and the specific tractive effort $u(t) = F(t)/\rho m$ with $u(t) \in U = [-u_{\min}, u_{\max}(v(t))]$ for $t \in [0,T]$, where

$$u_{\max}(v) = \frac{F_{\max}(v)}{\rho m} > 0 \text{ and } u_{\min} = \frac{F_{\min}}{\rho m} > 0.$$

Recall that $r(v)$ is strictly increasing and $r_i \geq 0$, $i \in \{0,1,2\}$.

The energy consumption to be minimized is the work done by the traction power $P(t) = F(t)v(t)$ over time, i.e., $\int u^+(t)v(t)dt$, where the integral is only over the (positive) specific tractive effort denoted as

$$u^+(t) = \max(u(t), 0). \tag{2.2}$$

Note that in this example we assume that braking does not cost nor generate energy. We finally get the basic optimal train control problem

$$J = \min_u \int_0^T u^+(t)v(t)dt \tag{2.3}$$

subject to

$$\dot{x}(t) = v(t) \tag{2.4}$$
$$\dot{v}(t) = u(t) - r(v(t)) \tag{2.5}$$
$$x(0) = 0, x(T) = X, v(0) = 0, v(T) = 0 \tag{2.6}$$
$$v(t) \geq 0, u(t) \in [-u_{\min}, u_{\max}(v(t))], \tag{2.7}$$

where $x(t)$ is the distance travelled over time, and X is the total distance travelled. The variables (x, v) are the state variables and u is the control variable.

2.2.2 Pontryagin's Maximum Principle (PMP)

This optimal control problem has the standard form $\min_u \int_0^T f_0(x,v,u)dt$, subject to the ordinary differential equations $\dot{x}(t) = f_1(x,v,u)$ and $\dot{v}(t) = f_2(x,v,u)$ with boundary conditions for x and v and (algebraic) path constraints $g_i(x,v,u) \geq 0$, $i = 1,\ldots,n$, as given in (2.7). Note that the control is bounded from above by a mixed constraint that depends on the state v. Necessary conditions for these optimal control problems are given by Pontryagin's Maximum Principle (Pontryagin et al., 1962). According to the PMP the optimal control variable $\hat{u}$ should be selected

from the admissible control variables that maximize the Hamiltonian

$$H(x,v,\varphi,\lambda,u) = -f_0(x,v,u) + \varphi f_1(x,v,u) + \lambda f_2(x,v,u), \tag{2.8}$$

where (φ,λ) are the co-state (or adjoint) variables which satisfy the differential equations

$$\dot{\varphi}(t) = -\frac{\partial \tilde{H}}{\partial x}(x,v,\varphi,\lambda,\mu,u) \quad \text{and} \quad \dot{\lambda}(t) = -\frac{\partial \tilde{H}}{\partial v}(x,v,\varphi,\lambda,\mu,u) \tag{2.9}$$

without boundary conditions. Here, $\tilde{H}$ is the augmented Hamiltonian (or Lagrangian)

$$\tilde{H}(x,v,\varphi,\lambda,\mu,u) = H(x,v,u,\varphi,\lambda,u) + \sum_{i=1}^{n} \mu_i g_i(x,v,u), \tag{2.10}$$

with respect to the additional path constraints $g_i(x,v,u) \geq 0$, where μ_i are Lagrange multipliers satisfying the complementary slackness conditions $\mu_i \geq 0$ and $\mu_i g_i(x,v,u) = 0$. Moreover, the Karush-Kuhn-Tucker (KKT) necessary condition $\partial \tilde{H}/\partial u = 0$ must be satisfied by the optimal solution.

Note that the differential equations (2.4) and (2.5) of the state variables satisfy $\dot{x}(t) = \partial \tilde{H}/\partial \varphi = v$ and $\dot{v}(t) = \partial \tilde{H}/\partial \lambda = u - r(v)$, so that we end up with a special boundary value problem of four differential equations in four variables with four boundary conditions. Unfortunately, the boundary conditions are both the initial and final conditions for the state equation, and none for the co-state equation. (If the final state is free, then the final co-states must be zero, $\varphi(T) = \lambda(T) = 0$, which is easier to solve.)

For the example problem we get the following Hamiltonian:

$$H(x,v,\varphi,\lambda,u) = -vu^+ + \varphi v + \lambda(u - r(v)), \tag{2.11}$$

and augmented Hamiltonian

$$\tilde{H}(x,v,\varphi,\lambda,\mu,u) = H(\cdot) + \mu_1(u_{\max}(v) - u) + \mu_2(u + u_{\min}), \tag{2.12}$$

with the additional differential equations for the co-state (φ,λ)

$$\dot{\varphi}(t) = 0 \quad \text{and} \quad \dot{\lambda}(t) = \lambda r'(v) - \varphi + u^+ - \mu_1 u'_{\max}(v). \tag{2.13}$$

From the first equation of (2.13) it follows that $\varphi = \varphi_0$ is a constant. Moreover, from the complementary slackness conditions follows that $\mu_1 = 0$ if $u < u_{\max}(v)$, and $\mu_1 \geq 0$ if $u = u_{\max}(v)$ (maximum acceleration).

According to the PMP the optimal control is

$$\hat{u}(t) = \arg\max_{u \in U} H(\hat{x}(t), \hat{v}(t), \hat{\varphi}(t), \hat{\lambda}(t), u), \tag{2.14}$$

where $(\hat{x}, \hat{v})$ and $(\hat{\varphi}, \hat{\lambda})$ are the state and co-state trajectories associated to the control trajectory $\hat{u}$. Typical for an optimal train control problem is that the Hamiltonian is (piecewise) linear in the control variable u, by which the optimal control may not be uniquely defined from the necessary conditions on some non-trivial interval. For the example problem, the Hamiltonian (2.11) can be split around $u = 0$, yielding

$$H(x, v, \varphi, \lambda, u) = \begin{cases} (\lambda - v)u + \varphi v - \lambda r(v) & \text{if } u \geq 0 \\ \lambda u + \varphi v - \lambda r(v) & \text{if } u < 0, \end{cases} \tag{2.15}$$

which is linear both for non-negative and negative values of u. Discarding for the moment the control constraints $u \in U$, the optimal control must satisfy the necessary optimality condition $\partial H / \partial u(x, v, \varphi, \lambda, u) = 0$, giving $\lambda - v = 0$ for $u \geq 0$ and $\lambda = 0$ for $u < 0$, which are independent of the value of the control variable u (besides its sign). Taking also the control constraints (2.7) into account, the optimal control is characterized as

$$\hat{u}(t) = \begin{cases} u_{\max}(v(t)) & \text{if } \lambda(t) > v(t) & \text{(MA)} \\ u \in [0, u_{\max}] & \text{if } \lambda(t) = v(t) & \text{(CR)} \\ 0 & \text{if } 0 < \lambda(t) < v(t) & \text{(CO)} \\ -u_{\min} & \text{if } \lambda(t) \leq 0 & \text{(MB).} \end{cases} \tag{2.16}$$

The optimal control is illustrated in Figure 2.1. Clearly, the maximum control $\hat{u} = u_{\max}$ implies maximum acceleration (MA), zero control $\hat{u} = 0$ implies coasting (CO), i.e., rolling with the engine turned off, and the minimum control $\hat{u} = -u_{\min}$ implies maximum braking (MB). The singular solution defined by $\lambda(t) = v(t)$ corresponds to speed-holding or cruising (CR), i.e., driving at a constant optimal cruising speed using partial tractive effort $\hat{u} \in [0, u_{\max}]$. To see this, note that the singular solution only holds over some nontrivial interval if also the derivatives are the same, $\dot{\lambda}(t) = \dot{v}(t)$. Moreover, $\mu_1 = 0$ since $u < u_{\max}(v)$ except maybe at some isolated points as otherwise we are back in regime (MA). Then from (2.5), (2.13), $\lambda(t) = v(t)$ and $u > 0$, it follows that the optimal cruising speed must satisfy

$$\varphi_0 = vr'(v) + r(v). \tag{2.17}$$

This equation has a unique solution v_c which gives the optimal cruising speed over some interval. Recall that $r(v)$ is a non-negative strictly-increasing quadratic function and thus convex in v. Then also $\psi(v) = vr(v)$ is a non-negative strictly-

increasing convex function for $v \geq 0$ with $\psi'(v) = vr'(v) + r(v)$, and in particular $\psi'(v) \geq \psi'(0) = r(0) = r_0$. Hence, by (2.17) a unique optimal cruising speed exists if $\varphi_0 > r_0$. Also note that this implies $\varphi_0 > 0$ and thus the solution $\lambda = 0$ with $u < 0$ cannot hold except at a single time point, since in this case we get $\dot{\lambda}(t) = -\varphi_0 < 0$ and therefore λ is not constant over a nontrivial interval. So without loss of generality, we added the singular point $\lambda = 0$ in (2.16) to the (MB) regime. Later, we will see that the singular solution $\lambda = 0$ may occur when considering gradients.

However, finding the optimal cruising speed usually takes some creativity since (2.17) has two unknowns v and φ_0. An additional equation can be obtained from the PMP which also states that the Hamiltonian is constant along the optimal control and state trajectories (if the cost and dynamic equations are independent of time), i.e.,

$$H(\hat{x}(t), \hat{v}(t), \hat{\lambda}(t), \hat{\varphi}(t), \hat{u}(t)) = C \quad \text{for all} \quad t \in [0, T]. \tag{2.18}$$

So the Hamiltonian is kept at its maximum value along the optimal control and state trajectories. In the example problem for the singular solution under $v = \lambda$, (2.18) gives $\varphi_0 v - vr(v) = C$. After substituting (2.17) this gives the additional equation

$$v^2 r'(v) = C \tag{2.19}$$

with the additional unknown C. Note that from (2.19) follows $C \geq 0$. Still we end up with two equations in three unknowns. In general, the cruising speed v_c can be parameterized in either φ_0 or C and then solved for the optimal parameter using a numerical procedure. Nevertheless, v_c can also be considered as a parameter itself.

2.2.3 Solution approaches

The optimal control problem can be reformulated as a boundary value problem in (x, v, φ, λ) connected by the optimal control structure (2.16). Starting with estimates for the initial values $\varphi(0) = \varphi_0$ and $\lambda(0)$, first the optimal cruising speed v_c is computed from (2.17) which is then used for the cruising regime in (2.16). Then the trajectories for (x, v, λ) could in principle be computed as an initial value problem forward in time t using a shooting method (Stoer & Bulirsch, 2002), with $u(t)$ specified by (2.16) depending on the computations of $v(t)$ and $\lambda(t)$. If the computed final values $x(T)$ and $v(T)$ are equal to the boundary conditions (2.6) then we have found the optimal trajectories. Otherwise, the initial values are adjusted and the procedure starts again. However, shooting methods are really sensitive to the initial values and this procedure does not work well in practice.

A different approach to solve the optimal train control problem is by constructive methods. These methods are based on the observation that an optimal driving

trajectory must be a concatenation of the four optimal driving regimes given by (2.16), in the case of flat track. Then the problem is replaced by finding the optimal order of driving regimes and the switching times between regimes, along with a possible optimal cruising speed. For the example problem, the optimal order of the driving regimes is maximum acceleration, cruising, coasting and maximum braking, while the cruising regime may also be absent. The basic decision variables then become the switching time from acceleration to cruising (and thus the cruising speed v_c) and the switching time from cruising to coasting, if both these regimes are optimal, or a direct switching from acceleration to coasting. Note that the switching time to the final braking regime is implicitly determined when the speed trajectory reaches the braking curve in time to reach the destination X at time T. This braking curve can be computed by solving $\dot{v}(t) = -u_{\min} - r(v(t))$ backwards from $v(T) = 0$.

The switching times and the number of driving regimes depend on the terminal time T. For the example problem, the optimal driving trajectory may consist of maximum acceleration to some switching speed, coasting and maximum braking (the case of short distance with sufficient time) or maximum acceleration to the cruising speed, cruising, coasting and maximum braking (long distance with sufficient time). Note that coasting is always present due to the continuity of the co-state variable (in this case that the dynamic equations do not depend explicitly on time), although the coasting regime can be very short depending on the terminal time. The minimal feasible terminal time corresponds to maximum acceleration to the maximum speed, cruising at maximum speed, and maximum braking, i.e., time-optimal driving for the minimal running time $T_{\min}$. Note that the minimal-time train control problem is a slightly different optimal control problem with a variable terminal time that needs to be minimized. Hence, the time-optimal solution is not energy-efficient. In the energy-efficient train control problem the lengths of the coasting and cruising regimes depend on the available running time supplement $T - T_{\min}$. An energy-efficient solution exists only if the scheduled running time exceeds the minimal running time.

2.3 Energy-efficient train control (EETC)

This section gives a literature review of EETC models and solution methods. The review is mainly chronological where the first simple models are extended and adapted to derive more complex models. We will use the concepts and terminology introduced in the description of the basic model in Section 2.2 to provide a consistent terminology throughout the review.

A distinction can be made between models with continuous traction control (such as in Section 2.2) and models with discrete traction throttle settings. More-

over, regenerative braking may be used or not. The review is clustered in these distinct classes.

Another clustering can be obtained through the solution method applied. Two main solution approaches can be distinguished which are both explicitly or implicitly based on the optimal control structure derived from the optimality conditions of Pontryagin's Maximum Principle (PMP) such as discussed in Section 2.2. These are exact solutions by numerical algorithms that solve the differential equations indirectly using the derived optimal control structure, and heuristics that find suboptimal solutions to the dynamic equations by artificial intelligence or search algorithms using knowledge of the optimal control structure. A third solution approach is to solve the optimal control problem by transcribing the problem into a nonlinear optimization problem and solving this problem directly, as opposed to indirectly solving the necessary optimality conditions.

The remainder of this section considers subsequently indirect exact methods without and with regenerative braking, indirect exact methods with discrete control, direct methods, and heuristic methods. An overview of the framework that we used for the classification of EETC can be found in Figure 2.2.

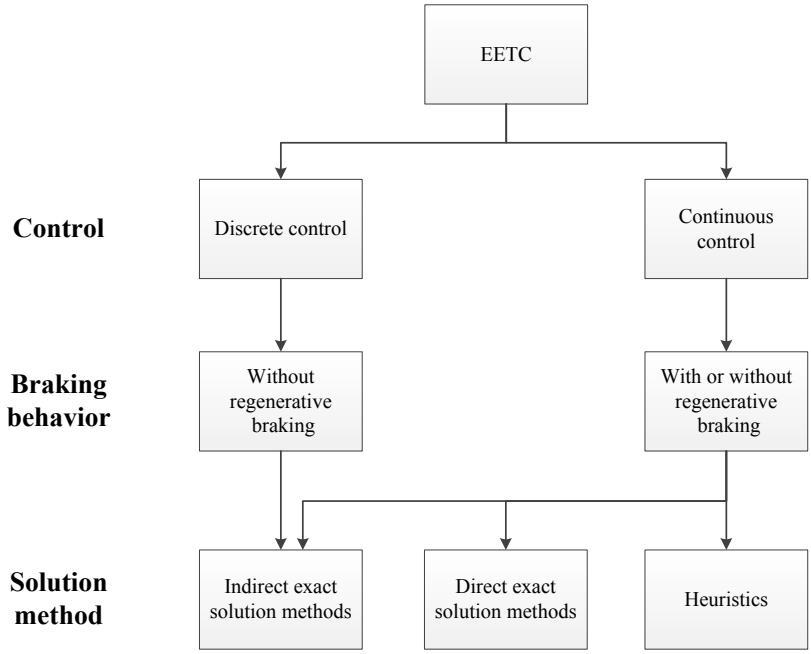

Figure 2.2: Framework of EETC.

2.3.1 Exact methods without regenerative braking

The first study on energy-efficient train control was carried out by Ichikawa (1968) in Japan. His model is similar to the basic model discussed in Section 2.2, but the resistance force was simplified as $r(v) = v$ by which (2.5) reduces to the linear differential equation $\dot{v}(t) = u(t) - v(t)$. Since now both differential equations are linear, Ichikawa could derive analytical expressions for the various regimes by applying the PMP. He gave a complete analysis of all four driving regimes on level tracks:

1. Maximum acceleration (MA),
2. Cruising by partial traction force (CR),
3. Coasting (CO), and
4. Maximum braking (MB),

as well as the resulting optimal control rules. In the conclusions he mentioned that "Considerable idealization has been made on the equations of motion for the train in this report, but the basic point seems to have been revealed about the optimal operation of a train. The author believes that the report will serve to make the beginning of scientific and reliable research on the economization of train operation for which huge amount of energy is consumed everyday." (Ichikawa, 1968, p. 865).

Strobel et al. (1974) continued the research for the optimal control strategy of a train with a model similar to that of Ichikawa (1968), but they modelled the resistance force as a quadratic function of speed with an additional term for gradient resistance. Nevertheless, they then linearized the resistance function and thus could derive analytical expressions for all driving regimes using the PMP as well. As a result of the possible negative slopes they found a second singular solution consisting of partial braking to maintain cruising, although they stated that this solution was "practically without significance" (Strobel et al., 1974, p. 379). Strobel et al. (1974) thus found five driving regimes for varying gradients:

1. Maximum acceleration (MA),
2. Cruising by partial traction force (CR1),
3. Coasting (CO),
4. Cruising by partial braking (CR2), and
5. Maximum braking (MB).

They mentioned that for suburban train traffic the cruising regimes could be neglected. This further simplification allowed them to derive a suboptimal algorithm for real-time computation. They implemented their algorithm and compared the resulting computer-aided train operation with manually controlled train movements in a train simulator, which revealed a substantially improved adherence to timetables and driving energy savings of approximately 15%. Note that the energy savings compared to using technical minimum running times will be higher than the energy savings that are achieved in practice, since not all drivers without DAS drive as fast as possible. The approach was translated into a driver advice about the optimal driving regime. The algorithm of Strobel et al. (1974) formed the basis for the first DAS implemented in board computers of the Berlin S-Bahn (suburban trains) in Germany at the beginning of the 1980s. However, the computations to determine the switching points were made offline, due to the limited computational power of the computers in those days (Oettich & Albrecht, 2001).

T. Albrecht & Oettich (2002) revisited the research of Strobel et al. (1974) to determine the optimal driving strategy for a single train using the linearized resistance equations. They used Simulink to numerically calculate switching curves that could be used to calculate the switching points in the optimal trajectory backwards from the target station. The control algorithm was applied in a DAS on the train driving simulator at Dresden University of Technology (TU Dresden), and in real-time passenger operation at the suburban railway line S1 in Dresden, see T. Albrecht (2005a). The successful real-time test showed energy savings of 15% to 20% compared with manual driving.

Since 1982 a lot of research about optimal train control has been carried out by the University of South Australia (UniSA). The research started with the PhD research of Milroy on continuous train control similar to the basic model of Section 2.2 (Milroy, 1980; Howlett & Pudney, 1995). Milroy (1980) applied the PMP and concluded based on his research on urban railway transport that there are three driving regimes in the optimal driving strategy for urban railways on level track and with a fixed speed limit (see Figure 2.3):

1. Maximum acceleration (MA),
2. Coasting (CO), and
3. Maximum braking (MB).

Later, Howlett proved mathematically based on the PMP that the general optimal driving strategy for level track and a fixed speed limit consists of four driving regimes including cruising (Howlett, 1990), which had already been found by Strobel et al. (1974).

The theoretical ideas of continuous energy-efficient train control were implemented by UniSA in a commercial system named Metromiser. The system

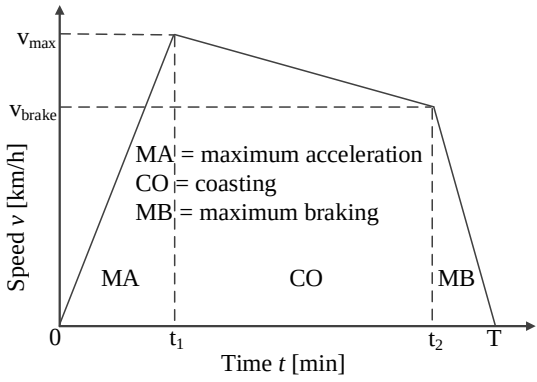

Figure 2.3: Optimal driving regimes without cruising (for metro and suburban railway systems) over time with switching points between driving regimes at t_1 and t_2.

consisted of two parts: a software package for timetable planners to generate energy-efficient timetables, and a DAS for energy-efficient train operation (Howlett & Pudney, 1995). The DAS part of Metromiser advised the train driver when to coast and when to brake in order to minimize energy consumption using light and sound indications (Benjamin et al., 1987; Howlett et al., 1994; Howlett & Pudney, 1995; Howlett, 1996; Cheng, 1997). However, Metromiser assumed a constant effective gradient during coasting and braking phases (Pudney & Howlett, 1994). The first successful runs with the system were done on the (sub)urban trains in Adelaide (Australia) in 1984, and later in Toronto (Canada), Melbourne (Australia) and Brisbane (Australia). The achieved energy savings were more than 15% compared to the trains running without Metromiser, and also punctuality increased. Benjamin et al. (1987) and Howlett et al. (1994) showed that for suburban trains to which Metromiser was applied the coasting phase is the most important driving regime due to the short stop distances.

Around 1990, Netherlands Railways (NS, *Nederlandse Spoorwegen*) also investigated the EETC problem. Van Dongen & Schuit (1989a,b, 1991) investigated the optimal driving strategy and found the four optimal driving regimes by measurements and experience. Static advice about cruising and coasting was included in the timetable for the train drivers on the intercity line between Zandvoort and Maastricht/Heerlen in the Netherlands. Results with the optimal driving strategy indicated energy savings of 10% compared to the normal practice of train operation with reduced constant timetable speeds. Moreover, they found that both optimizing the cruising speed (by applying constant power) and the coasting distance led to the most energy savings. In addition, Van Dongen & Schuit (1989a,b,

1991) found that it is even better not to apply maximum acceleration for the Dutch power supply system with its low voltage, since this led to a high drop in voltage and energy losses. They therefore recommended to apply a low and constant line current in consideration of the low catenary voltage.

Liu & Golovitcher (2003) considered the EETC problem with varying gradients and speed limits. Since both gradients and speed limits are functions of distance, they reformulated the optimal control problem with distance as the independent variable instead of time. This change of independent variable had been proposed before by Howlett et al. (1994) and Pudney & Howlett (1994) to deal with varying speed limits, and by Howlett & Pudney (1995) for both varying speed limits and gradients. With distance x as independent variable, the state variables now become time $t(x)$ and speed $v(x)$, and the energy consumption equals $\int u^+(x)dx$, where now $u(x) = F(x)/\rho m$ with $u(x) \in U = [-u_{\min}, u_{\max}(v(x))]$ for $x \in [0, X]$. Note that

$$\int_0^T u^+(t)v(t)dt = \int_0^T u^+(t)\frac{dx}{dt}dt = \int_0^X u^+(x)dx.$$

The equivalent EETC problem in terms of distance with the additional speed limit upper bounds is then:

$$J = \min_u \int_0^X u^+(x)dx \tag{2.20}$$

subject to the constraints

$$\dot{t}(x) = 1/v(x) \tag{2.21}$$

$$\dot{v}(x) = (u(x) - r(v(x)) - g(x))/v(x) \tag{2.22}$$

$$t(0) = 0, t(X) = T, v(0) = 0, v(X) = 0 \tag{2.23}$$

$$v(x) \in [0, v_{\max}(x)], u(x) \in [-u_{\min}, u_{\max}(v(x))], \tag{2.24}$$

where X is the total distance travelled, $t(x)$ is the time over the distance travelled, and T is the total available running time. The variables (t, v) are the state variables and u is the control variable. Note that now $\dot{v}(x)$ and $\dot{t}(x)$ denote the derivatives of v and t with respect to the independent variable x. The resistance force now consists of a train resistance $r(v)$ and a line resistance $g(x)$, where line resistance $g(x)$ is defined as the specific external force due to track gradient or curvature. It is assumed that tracks have piecewise constant gradients. Note that on uphill slopes $g(x) > 0$ and on downhill slopes $g(x) < 0$. Total resistance may be defined now also as $r(v,x) = r(v) + g(x) = r_2v^2 + r_1v + r_0 + g(x)$, which is thus explicitly a function of both speed and distance.

The optimal control $\hat{u}(x)$ can be derived similar to Section 2.2 by applying

Pontryagin's Maximum Principle as follows. The Hamiltonian is

$$\begin{aligned} H(t,v,\varphi,\lambda,u,x) &= -u^{+} + \frac{\phi}{v} + \frac{\lambda(u - r(v) - g(x))}{v} \\ &= \begin{cases} (\frac{\lambda}{v} - 1)u + \frac{\varphi}{v} - \frac{\lambda}{v}(r(v) + g(x)) & \text{if } u \geq 0 \\ \frac{\lambda}{v}u + \frac{\varphi}{v} - \frac{\lambda}{v}(r(v) + g(x)) & \text{if } u < 0, \end{cases} \end{aligned} \tag{2.25}$$

and the associated augmented Hamiltonian

$$\tilde{H}(x,v,\varphi,\lambda,\mu,u) = H + \mu_1(u_{\max}(v) - u) + \mu_2(u + u_{\min}) + \mu_3(v_{\max} - v),$$

where $\varphi(x)$ and $\lambda(x)$ are the co-state variables satisfying the differential equations

$$\dot{\varphi}(x) = -\frac{\partial \tilde{H}}{\partial t} = 0 \tag{2.26}$$

$$\begin{aligned} \dot{\lambda}(x) &= -\frac{\partial \tilde{H}}{\partial v} \\ &= \frac{\lambda u + \lambda v r'(v) - \lambda r(v) + \varphi}{v^2} - \mu_1 u'_{\max}(v) + \mu_3. \end{aligned} \tag{2.27}$$

Note that the Hamiltonian is now also a function of the independent variable x due to the line resistance $g(x)$. Similar to Section 2.2, the optimal control $\hat{u}(x)$ that maximizes the Hamiltonian for varying gradients is

$$\hat{u}(x) = \begin{cases} u_{\max}((v(x)) & \text{if } \lambda(x) > v(x) & \text{(MA)} \\ u \in [0, u_{\max}] & \text{if } \lambda(x) = v(x) & \text{(CR1)} \\ 0 & \text{if } 0 < \lambda(x) < v(x) & \text{(CO)} \\ u \in [-u_{\min}, 0] & \text{if } \lambda(x) = 0 & \text{(CR2)} \\ -u_{\min} & \text{if } \lambda(x) < 0 & \text{(MB).} \end{cases} \tag{2.28}$$

The optimal speed-distance profile for a level track is illustrated in Figure 2.4.

Liu & Golovitcher (2003) derived the above five driving regimes from the PMP where the cruising regime is split into partial power and partial braking. The latter may occur on negative gradients. They also showed that the optimal cruising speed v_c is the root of (2.19) or the maximum speed, whichever is lower. To determine the sequence of optimal controls they derived four control switching graphs describing the possible switchings between the five driving regimes depending on speed $v(x)$ and speed limit $v_{\max}(x)$ at the switching moment, which could either be $v(x) < v_{\max}(x)$, or $v(x) = v_{\max}(x)$ with $v_{\max}(x)$ remaining constant at x, dropping down or jumping up. In each of these switching graphs, conditions were derived for switching to another regime depending on the value of speed, optimal cruising speed, (changed) speed limit, and the beginning of a steep climb or end of a steep

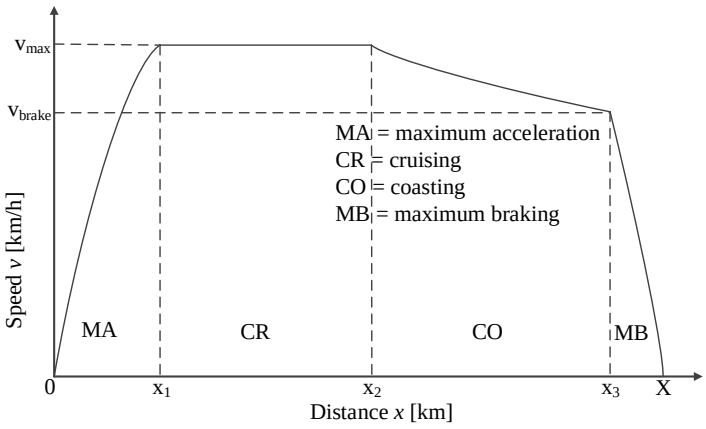

Figure 2.4: Speed profile of a basic energy-efficient driving strategy with switching points between driving regimes at x_1, x_2 and x_3.

descent, see also Golovitcher (2001) for more details. For the final determination of the optimal control, Liu & Golovitcher (2003) divided the distance in intervals with constant line resistance $g(x) = g_n$ on (x_{n-1}, x_n). On each of these intervals the dynamic equation (2.22) is again independent of distance. Thus the Hamiltonian (2.25) is constant there, providing a complementary optimality condition on each interval, cf. (2.18). Based on the optimal driving regimes, the control switching graphs and the complementary optimality conditions, Liu & Golovitcher (2003) finally derived a numerical algorithm consisting of an outer loop that finds the cruising speed v_c on each interval of constant line resistance and an inner loop that builds the optimal trajectory for the given values of v_c. They implemented the algorithm in a simulation and optimization package, which has been applied for crew training and timetable optimization. Several case studies were reported. A simulation of a metro system with *automatic train operation* (*ATO*) showed energy savings of 3% compared to using technical minimum running times. Here a simple control algorithm, which computes the required speed based on the remaining time and distance only, was compared with the energy-efficient algorithm that constantly re-calculates the optimal trajectory to the next station using the track gradient profile to find the optimal speed and locations for switching the control.

Vu (2006) also considered the optimal train control problem in speed and time as function of distance and showed that the optimal control for a specific journey on a non-steep track is unique. Based on this research, Howlett et al. (2009) developed a new local energy minimization principle to calculate the critical switching points on tracks with steep gradients. A steep uphill section is a section in which the

train has insufficient power to maintain a cruising speed when climbing, while a steep downhill section is a section in which the train is increasing speed when applying coasting (Vu, 2006). They showed that a maximum acceleration regime is necessary for a steep uphill section and a coasting regime for a steep downhill section. Furthermore, they showed that the necessary conditions defining the optimal switching points near steep gradients are also necessary conditions for minimization of local energy usage subject to a weighted time penalty. This minimization was adopted as a more efficient means to compute the optimal switching points in the DAS Freightmiser for freight trains, the follow-up of Cruisemiser described in Section 2.3.3. During trial tests in Australia and India in the period between 2002 and 2007, energy savings of about 15% were achieved for freight trains with Freightmiser compared to freight trains without this DAS (Howlett et al., 2008). Freightmiser was also tested on a passenger high speed line in the UK with energy savings of 22% compared to normal operation (Coleman et al., 2010).

A. Albrecht et al. (2013a) proved that the switching points obtained from the local energy minimization principle are uniquely defined for each steep section of track and therefore also deduced that the global optimal strategy is unique. They now reported an implementation of the algorithm in a DAS called Energymiser, the follow up of Freightmiser. Energymiser has been used with energy savings between 7% and 20% compared to normal driving without Energymiser, see A. Albrecht et al. (2015). In addition, A. Albrecht et al. (2014) showed by means of numerical examples using Energymiser that the optimal train control strategy indeed consists of maximum power instead of partial power for acceleration. The power is then applied for a smaller time resulting in a lower total energy consumption. Recently, the French railway undertaking SNCF (*Société Nationale des Chemins de fer Français*) applied Energymiser on their TGV high speed trains using tablets to display driving advice to the train drivers (Albrecht et al. (2016b)).

Aradi et al. (2013) used a predictive optimization model to calculate the energy-efficient speed profile taking into account varying gradients and speed limits. Their algorithm considers both the current location of the train and some distance further ahead to make a prediction about the speed profile. The multi-objective function of the algorithm aims at minimizing the total energy consumption and at maximizing punctuality. Sequential quadratic programming (SQP) was used to solve the model. The model was applied in a case study of a locomotive-hauled train on a 15 km track on the Swiss line between Fribourg and Bern, showing energy savings of 15.3% compared to normal operation.

Scheepmaker & Goverde (2015) also considered the EETC model (2.20)–(2.24) with varying gradients and speed limits and derived the PMP optimality conditions, see also Scheepmaker (2013). To find the switching points, they

developed a two-stage iterative algorithm that calculates the optimal cruising speed using Fibonacci search and the optimal coasting point for the given cruising speed using the bisection method. The algorithm was implemented in MATLAB and applied in a case study on the regional train line between Utrecht Central and Rhenen in the Netherlands. The results from the EETC model were compared with the UZI method applied by train drivers at NS. The UZI method (*Universeel Zuinigrijden Idee*, Dutch for universal energy-efficient driving idea) is a simple coasting strategy for short and long distances derived empirically by an enthusiastic train driver. In the UZI method, for short distances with scheduled running time $t \in \{2, \ldots, 8\}$ minutes, the driver accelerates with maximum power to the coasting speed $v_{\text{coast}}(t) = 60 + 10 \cdot t$ km/h and then starts coasting. For longer distances, the time to start coasting t_{coast} before the arrival time at the next station is defined as a function of the track speed limit as $t_{\text{coast}}(v_{\max}) = 4 + (v_{\max} - 100)/10$ minutes for $v_{\max} \in \{100, \ldots, 140\}$ km/h (Scheepmaker, 2013; Velthuizen & Ruijsendaal, 2011). The results of Scheepmaker & Goverde (2015) showed that extra energy savings compared to the UZI method of at least 5% were possible by using the EETC model which considers both cruising and coasting, as well as the exact running time supplement and the track and train characteristics. Compared to time-optimal running times the energy savings were 15.7%. With respect to an improved timetable with uniform running time supplements the energy savings increased to 15.9% for UZI and 21.8% for the EETC model compared to time-optimal running. An example of an energy-efficient speed profile including varying gradients and speed limits can be found in Figure 2.5. The reported computation time of the EETC algorithm was on average 190 seconds (laptop with 2.1 GHz processor speed and 8 GB RAM) for a train run between two stops (including varying gradients). The method could be used for static energy-efficient speed advice with optimal cruising speed and coasting point information for punctual trains.

Su et al. (2013) considered the EETC problem in time (2.3)–(2.7) on level track with the simplifying assumptions that the maximum traction, maximum braking and resistance forces are all constants. As a result they could derive analytical expressions for all regimes based on the PMP. Su et al. (2014) extended the previous model with maximum traction, maximum braking and resistance forces as functions of speed although the exact functions are not given. Since their focus is on subway systems, they assumed that the maximum speed is the optimal cruising speed. The computation of the energy-efficient speed profile is based on a given amount of energy available for each section between two stops. The algorithm first discretizes the section into parts of equal distances and then starts with maximum acceleration on the first part. Then as long as energy is left the train either accelerates with maximum power if the speed is below the maximum speed

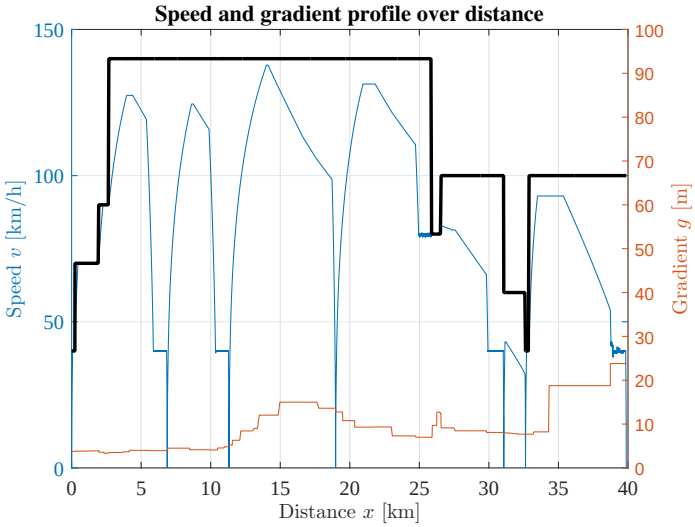

Figure 2.5: Example of an energy-efficient speed profile with varying gradients and speed limits for the line Utrecht Central-Rhenen (adapted from Scheepmaker & Goverde (2015)).

or cruises with an energy consumption that counters the train and line resistances. When all available energy has been used, both speed profiles for coasting until the end of the section and for maximum braking from the end of the section are computed, with the minimum speed of these profiles giving the final coasting and braking regimes (and their intersection). They applied their algorithms on the Beijing Yizhuang metro line in China in a timetabling algorithm, see Section 2.4.

A. Albrecht et al. (2013b) observed that timetabled arrival times are not always efficient when meeting the specified times requires the train to vary its pace throughout the journey and thus to waste energy. Therefore, they proposed to use time windows which define the earliest and latest arrival time at a specific location to improve the energy-efficient driving strategies. In a case study from the UK they showed that 13% extra energy could be saved with a 1-minute time window, and 18% with a 3-minute time window both compared to no time window. T. Albrecht et al. (2013c) also described the use of time windows instead of target times at minor stops and junctions to decrease energy consumption. They mentioned that target windows should only be applied if slight delays of a train do not have immediate consequences to surrounding trains. They extended the algorithm described in T. Albrecht & Oettich (2002) to include time intervals without giving the details. Jaekel & Albrecht (2013) further developed the concept of time windows to so-called Train Path Envelopes (sequences of time windows) to limit the time-distance search space for energy-efficient train control with respect to adjacent trains.

2.3.2 Exact methods with regenerative braking

A different option for energy saving is to incorporate regenerative braking where the kinetic energy of the running train is fed back to the catenary system when the train brakes using the regenerative braking. This energy can then be used by other trains so that the overall energy consumption of the train decreases.

Asnis et al. (1985) studied the energy-efficient train control problem including regenerative braking for level track. They considered the basic problem (2.3)–(2.7) but with the adjusted objective function

$$J = \min_{u} \int_0^T (u^+(t) - \eta u^-(t)) v(t) dt, \tag{2.29}$$

where the second term $\eta u^- v$ gives the energy regenerated by the braking of the train. Here, $u^-(t) = -\min(u(t), 0)$ denotes the specific braking force (the negative part of the control) similar to (2.2), and $\eta \in [0, 1]$ is the recuperation coefficient which determines the efficiency of the regenerative braking system. Note that the problem reduces to the basic problem if $\eta = 0$ (no regenerative braking). The resistance force $r(v)$ was modelled in an abstract way that included the usual quadratic function in speed but with $r_0 = 0$. Asnis et al. (1985) derived necessary conditions by applying PMP, resulting in the following optimal control strategy

$$\hat{u}(t) = \begin{cases} u_{\max}(v(t)) & \text{if } \lambda(t) > v(t) & \text{(MA)} \\ u \in [0, u_{\max}] & \text{if } \lambda(t) = v(t) & \text{(CR)} \\ 0 & \text{if } \eta v(t) < \lambda(t) < v(t) & \text{(CO)} \\ u \in [-u_{\min}, 0] & \text{if } \lambda(t) = \eta v(t) & \text{(RB)} \\ -u_{\min} & \text{if } \lambda(t) < \eta v(t) & \text{(MB).} \end{cases} \tag{2.30}$$

Here the driving regime RB denotes regenerative braking. Hence, the possibility for regenerative braking generates an additional singular solution corresponding to partial braking. Note that we distinguish between the partial braking regime CR2 from (2.28) and the regenerative braking regime RB, since the latter may also contribute energy to the cost function and may thus lead to potential different strategies. However, for level track, Asnis et al. (1985) showed that this singular solution does not occur over a nontrivial interval. Hence, regenerative braking is only used with maximum braking. However, the optimal driving regime sequence may now also contain maximum braking before a coasting regime. Asnis et al. (1985) also derived analytical expressions in the special case of $r(v) = v$. They did not provide an algorithm to construct an optimal driving regime sequence with the associated switching times.

Khmelnitsky (2000) considered the EETC problem with variable gradient profiles and speed restrictions as well as regenerative braking. He used the same objective function (2.29) as Asnis et al. (1985) but using distance as independent variable, by which it transforms to

$$J = \min_{u} \int_0^X (u^+(x) - \eta u^-(x))dx. \tag{2.31}$$

This is equal to (2.20) with an additional term for the regenerative braking.

However, Khmelnitsky (2000) used time $t(x)$ and total energy $E(x) = K(x) + P(x)$ as state variables. Total energy is the sum of kinetic energy $K(x)$ and potential energy $P(x)$ at position x. Potential energy is the energy due to the track height $P(x) = mgh(x)$ which other authors model using the track gradients, and kinetic energy is the energy due to motion $K(x) = \frac{1}{2}mv^2$. The train resistance force is now a function of kinetic energy $w(K) = w_0 + w_1\sqrt{K} + w_2 K$, which equals the usual Davis equation $r(v)$ using the transformation $v = \sqrt{2K/m}$. We use a different notation $w(x)$ to distinguish it from the squared function $r(v)$. The constraints can now be described as:

$$\dot{t}(x) = 1/\sqrt{2K(x)} \tag{2.32}$$

$$\dot{E}(x) = u(x) - w(K(x)) \tag{2.33}$$

$$t(0) = 0, t(X) = T, E(0) = 0, E(X) = E_X \tag{2.34}$$

$$K(x) \in [0, \bar{K}(x)], u(x) \in [-u_{\min}, u_{\max}(K(x))], \tag{2.35}$$

where $\bar{K}(x)$ is the maximum kinetic energy at position x, which can be derived from the speed profile using the transformation $\bar{K} = \frac{1}{2}mv^2_{\max}$. Khmelnitsky (2000) derived the PMP necessary conditions for problem (2.31)–(2.35) and also found the optimal control structure (2.30) with five regimes, but now in terms of distance:

$$\hat{u}(x) = \begin{cases} u_{\max}(K(x)) & \text{if } \lambda(x) > K(x) & \text{(MA)} \\ u \in [0, u_{\max}] & \text{if } \lambda(x) = K(x) & \text{(CR)} \\ 0 & \text{if } \eta K(x) < \lambda(x) < K(x) & \text{(CO)} \\ u \in [-u_{\min}, 0] & \text{if } \lambda(x) = \eta K(x) & \text{(RB)} \\ -u_{\min} & \text{if } \lambda(x) < \eta K(x) & \text{(MB).} \end{cases} \tag{2.36}$$

In order to keep a constant speed (and kinetic energy) along an interval, the tractive or braking force has to change according to the grade profile

$$u(x) = \dot{P}(x) + w(K(x)). \tag{2.37}$$

Hence for varying gradients, Khmelnitsky (2000) showed that both singular solutions could occur in a cruising regime with partial traction or partial braking equal

to the track and train resistance forces on intervals with minor grades or falls where the right-hand side of (2.37) stays within the bounds of traction and braking forces, respectively. Note that the definition of minor grades and falls depends on both the grade profile and the speed. He also proved that the equations $\lambda(x) = K(x)$ and $\lambda(x) = \eta K(x)$ have no more than one root for each minor grade and each minor fall interval, respectively, so that the cruising speeds are well-defined. Moreover, he proved that the smaller the running time, the higher the optimal cruising speeds. For steep grades where the speed decreases even at full traction or for steep falls where speed increased even at full braking, he showed that the cruising phase should be interrupted in advance by maximum acceleration or maximum braking, respectively. Khmelnitsky (2000) solved the problem with a numerical algorithm that first locates the intervals of singular cruising regimes (CR, RB) and then links them together with a sequence of regular driving regimes (MA, CO, MB). For full recovery of braking energy ($\eta = 1$) he remarked that the cruising and coasting regimes merge constituting a unique stabilization regime on intervals with minor grades and falls. A case study on a 40 km railway line with two hills and three different speed limits showed fast computation times within 10 seconds on an IBM PC-586 computer.

Franke et al. (2000) considered the EETC problem with regenerative braking with mass-specific kinetic energy $E(x) = \frac{1}{2}v^2$ and time t as state variable of distance as independent variable. They simplified the resistance equation into the linear equation $w(E) = w_0 + w_2 E$ and thus neglected the term in $\sqrt{E}$. In terms of the normal Davis resistance this discards the linear speed term but not the quadratic speed. Moreover, they approximated the traction and braking force as piecewise constant. The objective function is the integral of electric power $P = uv$ and an additional nonlinear term $P_{\text{loss}}(u, v)$ for the power losses of the propulsion (traction and regenerative braking) system, formulated in speed. Hence, they considered the following optimal control problem:

$$J = \min_u \int_0^X (u(x)v(x) + P_{\text{loss}}(u(x), v(x)))dx, \tag{2.38}$$

subject to

$$\dot{t}(x) = 1/\sqrt{2E(x)} \tag{2.39}$$

$$\dot{E}(x) = u(x) - w(E(x)) - g(x) \tag{2.40}$$

$$t(0) = 0, t(X) = T, E(0) = 0, E(X) = 0 \tag{2.41}$$

$$E(x) \in [0, \bar{E}(x)], u(x) \in [-u_{\min}, u_{\max}(E(x))]. \tag{2.42}$$

Since the simplified dynamic equation in E is linear, they could derive analytical expressions for the various driving regimes and solve the problem by a Discrete

Dynamic Programming (DDP) algorithm. For this, they reformulated the optimal control problem (2.38)–(2.42) as a multistage optimization problem by discretizing the problem into K stages $k = 0, \dots, K-1$, such that the resistance including the grade profile w^k and the traction/braking force u^k could be considered constant in each stage. Stage k covers the distance interval $[x^k, x^{k+1})$ with length $\Delta x^k = x^{k+1} - x^k$. This then results in the Dynamic Programming problem

$$\min \sum_k f_0(E^k, \Delta x^k, u^k, w^k), \tag{2.43}$$

subject to

$$E^{k+1} = f_1(E^k, \Delta x^k, u^k, w^k) \tag{2.44}$$
$$t^{k+1} = t^k + f_2(E^k, \Delta x^k, u^k, w^k) \tag{2.45}$$
$$E^k_{\min} \le E^k \le E^k_{\max}, t^k_{\min} \le t^k \le t^k_{\max} \tag{2.46}$$
$$-u_{\min}(w^k) \le u^k \le u_{\max}(w^k, E^k, E^{k+1}), \tag{2.47}$$

and the given initial state $(t^0, E^0) = (0, 0)$ and scheduled finite state $(t^K, E^K) = (T, 0)$. Here, the function f_0 is obtained using a numerical approximation of (2.38) over each stage with fixed resistance w^k and control u^k, and f_1 and f_2 are the analytical expressions to (2.39) and (2.40) depending on the values of w^k and u^k. The DPP algorithm was implemented in a Nonlinear Model Predictive Controller (NMPC) to optimize the driving strategy in real-time. The algorithm was applied in a case study on the Swiss line Zürich HB-Luzern where in two controlled runs the driver operated the train exactly according to the pre-calculated optimization results. Results from simulations and the pilot runs showed potential energy savings between 10% and 30% compared to mean manual driving strategies and fastest driving. A remarkable result from their model was that no maximum acceleration or maximum braking is applied at high speeds due to the nonlinear power losses.

Baranov et al. (2011) considered the EETC problem with both mechanical and regenerative braking with distance as independent variable. Denote by u_f, u_b and u_r the mass-specific force due to traction, braking and regenerative braking, respectively. Then the optimal train control problem is formulated as:

$$\min_{u_f, u_r} \int_0^X (u_f(x) - \eta u_r(x)) dx,$$

subject to

$$\dot{v}(x) = \left(u_f(x) - u_b(x) - u_r(x) - r(v(x)) - g(x)\right) / v(x),$$

together with (2.21), (2.23), $v(x) \in [0, v_{\max}(x)]$, and the control limits $u_f(x) \in [0, \bar{u}_f(v(x))], u_b(x) \in [0, \bar{u}_b(v(x))], u_r(x) \in [0, \bar{u}_r(v(x))]$. Here, η is a the efficiency factor of regenerative energy returned to the network. Using the PMP, they found seven driving regimes: the three familiar regimes MA, CO and MB (maximum braking with both mechanical and regenerative braking), three cruising regimes with either partial traction (CR), with partial regenerative braking (RB) or with full regenerative braking and partial mechanical braking, and finally a regime with full regenerative braking. An algorithm to construct the optimal control sequence of these driving regimes is mentioned as an open question.

Rodrigo et al. (2013) discretized distance into $n-1$ intervals and transformed the optimal control problem into an optimization problem with speed v_i at the fixed points $i = 1, \ldots, n$ as n decision variables. They therefore expressed the objective function, dynamic equations and constraints as functions of the n-tuple of speed values and solved the resulting optimization problem by the Lagrange multiplier method using MATLAB. They included the option of regenerative braking with an efficiency coefficient and considered two case studies of Madrid's metro Line 8 in Spain. For regenerative braking they concluded that it is optimal to start with maximum acceleration until some average cruising speed. In the central sections, traction and regenerative braking are alternated with preferably braking on downward slopes to generate energy, and at the destination braking is applied to recover as much energy as possible. The average regenerated energy was approximately 23%. When regenerative braking is not possible, however, they found that it is optimal to start with maximum acceleration until a speed is reached that ensures arrival on time using coasting. In central sections partial traction is used for cruising and in case of speed restrictions coasting is preferred before braking if time allows. The energy consumption of mechanical braking was higher than with regenerative braking. The two case studies showed a big increase in computation time if mechanical braking was applied instead of regenerative braking. The computation time for the first case study between the stations Nuevos Ministerios and Colombia was 34.82 s for regenerative braking and 290 s for mechanical braking. In the second case study between the stations Colombia and Mar de Cristal the computation time increased to 90.22 s for regenerative braking up to 1,977 for mechanical braking.

Regenerative braking in the optimal control for metro trains is considered by Qu et al. (2014). They used the objective function (2.31) but assumed full recovery of regenerative braking energy ($\eta = 1$) and no steep slopes. In this case, coasting is not used and the optimal driving strategy consists of a sequence of the three driving regimes maximum acceleration, cruising and maximum braking, see Figure 2.6. They presented an iterative numerical algorithm to compute the optimal cruising speeds for given speed restrictions and scheduled running time.

The authors applied it to a case study based on the Shenzhen Metro Line 1 in China to show that the presence of a speed restriction changes the cruising speeds.

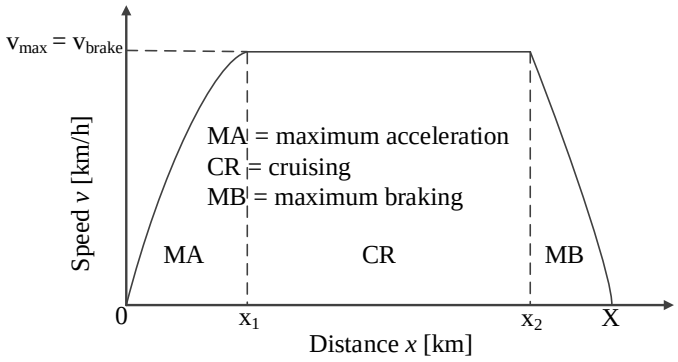

Figure 2.6: Speed profile of an energy-efficient driving strategy without coasting and with switching points between driving regimes at x_1 and x_2.

In the European rail project ON-TIME (Optimal Networks for Train Integration Management across Europe) an iterative algorithm was developed for an on-board DAS to calculate the optimal control of a train (ON-TIME, 2014a). The algorithm is based on PMP and includes regenerative braking as well as traction efficiency with time as independent variable. They thus assumed the five optimal driving regimes as in (2.30), which was used in an iterative gradient-based algorithm that computes the switching times between regimes by iteratively replacing regimes on a subsection as long as the running time can be increased. The regime changes are selected as the ones that provide most energy savings with the smallest change in running times. The three options to increase the running time on a subsection with given start and end speed are (*i*) reducing the duration of maximum acceleration and replacing it with cruising at a lower speed or coasting; (*ii*) reducing the duration of cruising, and (*iii*) replacing part of it by coasting; and reducing the cruising speed. Results on a case study on the Dutch railway network between Utrecht Central and Eindhoven showed energy savings of 20% to 30% by the use of the algorithms compared to non-optimized train driving.

A. Albrecht et al. (2016a,b) discussed the key principles of optimal train control and extended their previous work by including regenerative braking. Their problem statement includes varying (steep) gradients. The problem formulation is the same as the dynamic constraints with respect to distance (2.21)–(2.24) with

the objective equal to (2.31). This leads to the following optimal control strategy:

$$\hat{u}(x) = \begin{cases} u_{\max}(v(x)) & \text{if } \lambda(x) > v(x) & \text{(MA)} \\ u \in [0, u_{\max}] & \text{if } \lambda(x) = v(x) & \text{(CR)} \\ 0 & \text{if } \eta v(x) < \lambda(x) < v(x) & \text{(CO)} \\ u \in [-u_{\min}, 0] & \text{if } \lambda(x) = \eta v(x) & \text{(RB)} \\ -u_{\min} & \text{if } \lambda(x) < \eta v(x) & \text{(MB).} \end{cases} \tag{2.48}$$

The results indicate that regenerative braking should only be included in a cruising phase to maintain a certain cruising speed during a steep downhill section. Moreover, they derived analytical equations for the modified dimensionless co-state variable $\eta = \lambda/v - 1$. Phase plots of the state and modified-co-state variables were drawn for constant gradients to find the optimal switching points between control regimes for different initial conditions. They implemented their model in MATLAB and successfully tested it on two examples with steep uphill and steep downhill sections, and checked the calculations with the results from Energymiser. Moreover, they showed an example of Energymiser in a case study of the high speed TGV trains of SNCF between Lyon and Valance (France) without consideration of regenerative braking. Results indicated that the amount of running time supplement influences the optimal driving strategy. Energy savings of 22.6% can be achieved with 10% running time supplement in relation to time-optimal running.

2.3.3 Exact methods with discrete control

The models considered up to now assumed continuous traction control, which is applicable to most trains nowadays (Liu & Golovitcher, 2003). Nevertheless, there are also trains where traction is controlled using discrete throttle settings. For example, in Australia most freight trains used to have diesel-electric traction with discrete throttle settings (Howlett, 2000). Therefore, the literature also considered energy-efficient train control models where traction control is restricted to a finite number of discrete values. In particular, this changes the cruising regime since not all control settings are possible to maintain an optimal constant cruising speed. Still, for freight trains the distance between two stops is much longer than for suburban trains and therefore some kind of approximate cruising phase would be the dominant phase.

Cheng & Howlett (1992) first described the energy-efficient train control problem with discrete throttle settings as follows. Assume that there are $m+1$ distinct throttle settings f_j, $j = 0, \ldots, m$, with $f_0 = 0$ the zero fuel case corresponding to coasting, and $f_j < f_{j+1}$, $j = 1, \ldots, m$ a sequence of increasing fuel supply rates. Moreover, let t_i, $i = 0, \ldots, n+1$ be a sequence of switching times between throttle

settings with $f_{j_{k+1}}$ the rate of fuel supply maintained in the interval (t_k, t_{k+1}) for a duration of $\tau_{k+1} = t_{k+1} - t_k$. Let $t_0 = 0$ and $t_{n+1} = T$. Furthermore, it is assumed that braking is only applied at the final stage with maximum braking rate b. Then the minimum fuel consumption optimization problem is formulated as

$$\min \sum_{k=0}^{n-1} f_{j_{k+1}} \tau_{k+1} \tag{2.49}$$

subject to

$$\dot{v}(t) = \frac{H f_{j_{k+1}}}{v(t)} - r(v(t)), \qquad t \in [t_k, t_{k+1}) \tag{2.50}$$

for $k = 0, \ldots, n-1$, and

$$\dot{v}(t) = b - r(v(t)), \qquad t \in [t_n, t_{n+1}], \tag{2.51}$$

with the additional constraints (2.4), (2.6) and $v(t) \geq 0$. Here, H is some constant. Note that this first problem formulation assumes flat track. Cheng & Howlett (1992) solved this problem using Lagrange multiplier theory by formulating a Lagrangian function and applying the Karush-Kuhn-Tucker necessary conditions.

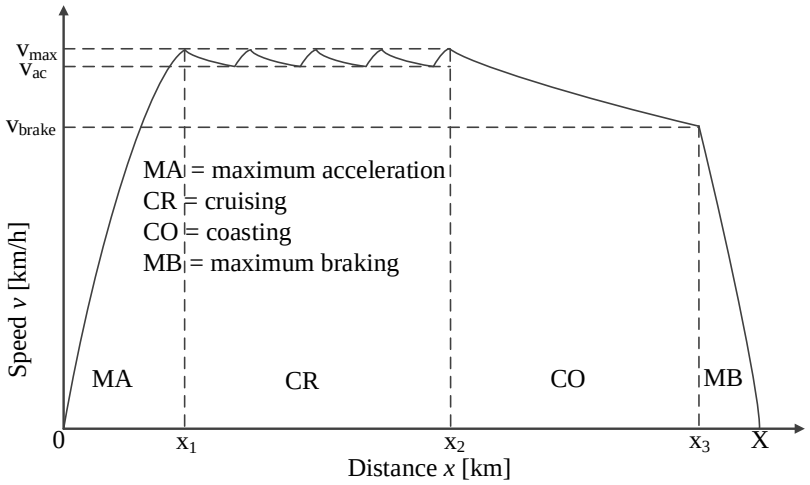

Figure 2.7: Speed profile of an energy-efficient driving strategy with discrete control (throttle settings) with switching points between driving regimes at x_1, x_2 and x_3 (the cruising phase consists of different phases of acceleration and coasting).

Cheng & Howlett (1992) showed that cruising is now approximated by alternating between maximum acceleration and coasting which leads to a sawtooth pattern between two speeds V and W, where a train repetitively accelerates to some critical speed W and then coasts until a certain critical speed $V < W$, where it will accelerate again to the critical speed W, et cetera, see Figure 2.7. This strategy was coined a 'strategy of optimal type'. The critical speeds are obtained from the equation

$$\lambda v - \mu = vr(v), \tag{2.52}$$

where λ and μ are the non-negative Lagrange multipliers corresponding to the fixed distance X and fixed running time T, respectively. Since $vr(v)$ is a convex function, there are exactly two solutions to (2.52), of which V denotes the lower and W the higher. Furthermore, the speed where braking begins was shown to be the solution U to $\lambda v - \mu = 0$. Starting with maximum acceleration, a strategy of optimal type is then characterized by the three speeds $0 < U < V < W$, where λ and μ can be computed in terms of V and W as

$$\lambda = \frac{Wr(W) - Vr(V)}{W - V} \quad \text{and} \quad \mu = \frac{VW\,(r(W) - r(V))}{W - V}.$$

Then the braking speed follows by $U = U(V, W) = \mu/\lambda$. A numerical procedure to solve the optimal control problem for a strategy of optimal type is now obtained by finding speeds V and W such that the resulting errors in the total distance X and time T are zero. With $n = 2p + 3$, for any nonnegative integer p, the solution starts with maximum acceleration to W, oscillates p times with coasting-maximum acceleration between the critical speeds V and W, coasts to the braking speed $U < V$, and then brakes with maximum braking. Cheng & Howlett (1993) showed that the critical speeds V_p and W_p converge to an idealized strategy with speed $V_p = W_p = Z$ as $p \to \infty$ which minimizes the fuel consumption. The oscillation strategy can thus be interpreted as an approximate cruising regime.

Howlett (1996) extended the energy-efficient train control problem with discrete throttle settings to varying gradients using the associated formulation with distance as independent variable. For non-steep gradients again an approximate cruising regime is obtained with oscillations between two critical speeds. The switching points now depend on the gradients and hence the oscillation interval durations τ_k are no longer regular. Recall, that by definition for a non-steep track the speed increases in an acceleration regime and decreases during each coasting or braking regime. The critical speeds and corresponding switching times are computed for a fixed number of acceleration-coasting phases by adjusting the values of the Lagrange multipliers μ and λ. For steep gradients, the approximate cruising regime is interrupted by segments of coasting and traction.

Howlett et al. (1994) extended the problem to varying speed limits. In this case, each segment (x_i, x_{i+1}) of constant speed limit is associated with a separate Lagrange multiplier λ_i that takes a different value on the different segments, and (2.52) is rewritten as

$$\lambda_i = r(v) + \mu / v$$

on (x_i, x_{i+1}). Since the critical speeds for various track segments are defined by different values of the parameter λ_i, the critical speed intervals (V_i, W_i) are nested over the various segments. The models usually consider a train as a point mass. However, Howlett et al. (1994) also showed that a real train with a distributed mass can be treated as a point mass by constructing a modified gradient profile.

Cheng (1997) contained most results for discrete control and also Howlett & Pudney (1995) captured all the results for discrete control with some additional information (next to their results for continuous control up to 1995). The models and algorithms for discrete throttle control setting were used in a DAS named Cruisemiser (Benjamin et al., 1989; Howlett et al., 1994; Cheng, 1997), which extended the ideas of Metromiser (see Section 2.3.1) to long-haul freight trains in Australia.

2.3.4 Direct exact methods

The solution approaches considered so far first derived the optimal driving regimes from the necessary conditions for optimality using Pontryagin's Maximum Principle, and then tried to solve the resulting optimization problem of finding the optimal sequence and switching points of the optimal driving regimes by solving the differential equations of the train movements for the optimal driving regimes. This approach worked well for special cases but the general problem with varying gradients and speed limits is very difficult to solve, while the inclusion of regenerative braking made the problem even harder to solve.

A different approach for solving optimal control problems is obtained by discretizing the dynamic system into a problem with a finite set of variables and then solving the resulting static nonlinear programming problem by nonlinear programming (NLP) methods (Betts, 2010). Only recently this direct approach has been considered for solving EETC problems.

Y. Wang et al. (2011) considered the EETC problem with varying gradients, curves and speed restrictions. They used kinetic energy and time as state variables in the independent variable distance and assumed a linear resistance force as in Franke et al. (2000). As objective function they used a trade-off between energy consumption and driving comfort:

$$\min_u \int_0^X \left(u(x) - \alpha \left| \frac{du(x)}{dx} \right| \right) dx,$$

subject to (2.39)–(2.42), but assuming also a constant maximum traction force, i.e., $u(x) \in [-u_{\min}, u_{\max}]$. Here, α is a weight factor to balance between the two objectives. They then discretized the problem into a discrete-space problem by dividing distance in discrete intervals similar to Franke et al. (2000), where they approximated the nonlinear terms through piecewise affine (PWA) functions, and finally reformulated it into a MILP (mixed integer linear programming) problem. A case study of a 10 km long line was considered with a fixed speed limit, 20 fixed discretization intervals of 500 m, and $\alpha = 500$. Still the computation time was about 10 min and, as a result of the rough discretization, the optimal control and train trajectory were not very accurate.

Y. Wang et al. (2013) reconsidered the EETC problem of Y. Wang et al. (2011) but now considered maximum traction force as a usual nonlinear function of speed, which they approximated by PWA functions. The resistance equation was still assumed linear in the kinetic energy. They now also proposed a Pseudospectral method (Rao et al., 2010b; Ross & Karpenko, 2012) to solve the problem and compared this with the MILP and DDP methods of Franke et al. (2000). For the Pseudospectral method, the optimal control problem was first reformulated into a multiple-phase optimal control problem with each phase corresponding to a constant gradient, curve and speed limit (Betts, 2010). This multiple-phase optimal control problem could then be transformed into a nonlinear programming problem using the Pseudospectral method, where the state and control functions are approximated by orthogonal polynomials based on interpolation of orthogonal collocation points. The PSOPT solver was used to transform and solve the NLP problem. The three approaches were compared in the case study of the 10 km long line where now varying gradients and speed limits were added. The MILP problem used again a 500 m interval while for the DDP method a space interval of 100 m was chosen. The solvers were PSOPT, CPLEX for the MILP problem, and a generic MATLAB Dynamic Programming function for the DDP problem. For a scenario with a constant maximum traction force, PSOPT took 6 min, DDP took 2 min, and CPLEX required 32 seconds, but the DDP and MILP models were highly inaccurate with respect to the PSOPT solution. In a second scenario, the maximum traction was considered as a nonlinear function of speed. Again the DDP and MILP approaches were highly inaccurate compared to the smooth PSOPT solution. The computation time for PSOPT was however very high with 19 min, compared to 2 min and 1 min for the DDP and MILP approaches.

P. Wang et al. (2015) considered the EETC problem (2.20)–(2.24) with the state variables speed and time as function of distance and varying gradients and speed limits, plus additional timetable constraints using the Train Path Envelope (TPE) to model intermediate stops as mandatory target points and through-passing of stations as time windows. The model was reformulated as a multiple-phase

optimal control problem with each phase corresponding to a constant gradient and speed limit, and then solved using the Gauss Pseudospectral Method using the GPOPS solver (Rao et al., 2010b). The model was applied to a case study based on the 50 km corridor Utrecht Central-'s-Hertogenbosch in the Netherlands with eight stations. In a first scenario, a regional train was considered with four scheduled stops from Utrecht Central to Houten Castellum for both the original timetable and an adapted timetable with smaller running times as would be provided by a Traffic Management System (TMS). The solutions are computed within 6 seconds for each train run between two stops, and the speed-distance and force-distance diagrams show a driving behavior as expected from the optimal driving regimes known from applying the PMP. The faster train uses less coasting and needs more energy as a result. In a second scenario, an intercity train is considered from Utrecht Central to 's-Hertogenbosch which overtakes a regional train in a station halfway. Two strategies are computed: one with mandatory target points at all intermediate stations according to the scheduled pass-through times, and another with time windows on the five intermediate stations besides the overtaking and end stations. The optimal trajectories use coasting before all scheduled target points and speed restrictions, while for the time-window case a smoother operation was obtained with a constant cruising speed over all intermediate stations. The case with the time windows saves 4.5% extra energy. The computation time for time-window case was less than 30 seconds for the entire trajectory.

2.3.5 Heuristics

In addition to exact solution methods based on PMP to determine the optimal driving strategy, also artificial intelligence or search algorithms have been applied to directly solve the energy-efficient train control problem.

Chang & Sim (1997) developed a coast control driving strategy for metro systems with varying speed limits and using regenerative braking. They developed an algorithm with the objective to minimize the total traction energy consumption by taking into account punctuality and riding comfort in penalty functions. The riding comfort is described by the jerk, which is the change of acceleration over time. The successive driving regimes are translated into a coast control lookup table, which gives the distance to start each driving regime and could be incorporated in an ATO system. The authors developed a Genetic Algorithm (GA), which was implemented in C++ on an IBM 486 PC. The algorithm was applied to a case study consisting of a track of 923 m between two stops with a speed restriction halfway of 40 km/h. Two scenarios were tested with the model: a normal schedule with 90 s scheduled running time, and a tight timetable in which the scheduled running time between the two stops is assumed 0 s, which forces the algorithm to consider a delay. The model results were compared with a fuzzy ATO controller.

Results indicated that energy savings of 2.5% for the tight timetable to 6.8% for the normal timetable were achieved and that punctuality also increased in both cases. For the normal timetable scenario the jerk was higher than with the fuzzy ATO controller, but it remained within the boundaries of passenger comfort. The results were generated within 30 s.

Lechelle & Mouneimne (2010) developed a GA approach to find energy-efficient speed profiles. A GA generates numerous operating speed profiles according to certain rules specified by the users. In turn, a single-train simulator simulates the movement of a train for each of these speed profiles and computes the corresponding traction energies. Through an iterative process, the GA gradually converges towards an energy-optimised speed profile. This approach was implemented in a tool called OptiDrive and applied on a case study of the tramway network of Rouen in France. Results showed 7% energy saving compared to normal real-time operation.

Domínguez et al. (2011) developed a simulation model for the Madrid metro system driven by ATO. The simulation model includes four independent modules (ATO, engine, train dynamics, and energy consumption). The configuration data for the ATO consists of four parameters: traction, cruising speed, coasting, and braking deceleration rate. The considered ATO system provided only certain discrete values for each parameter, resulting in a solution space of 156 alternative speed profiles per inter-station run, which enabled an exhaustive simulation of all feasible ATO speed profiles. In addition the resulting speed profiles were filtered based on comfort and operational conditions such as a minimum speed throughout the journey (20 km/h), maximum number of reaccelerations, maximum slope for coasting, and minimum speed limits along curves. The resulting running times were plotted against the associated energy consumption, after which a Pareto curve could be used to determine the most energy-efficient speed profile given the available running time, see Figure 2.8. The curves were used to determine a set of four alternative speed profiles per inter-station run associated with the time-optimal running time, the scheduled running time (at most 20 seconds more than the time-optimal running time), and two running times uniformly distributed in between. The approach was applied on the Madrid Metro line 3 in Spain resulting on average in 13% energy savings compared to the previous ATO design without affecting the scheduled running times.

Domínguez et al. (2012) extended the simulation model of Domínguez et al. (2011) by considering the energy in the substations to include regenerative braking. Using the same method as before the model was also tested on the Madrid Metro line 3. Energy savings of 6% to 11% were reported for the optimal speed profiles including optimal use of regenerative braking energy compared to operation without using the optimal speed profiles.

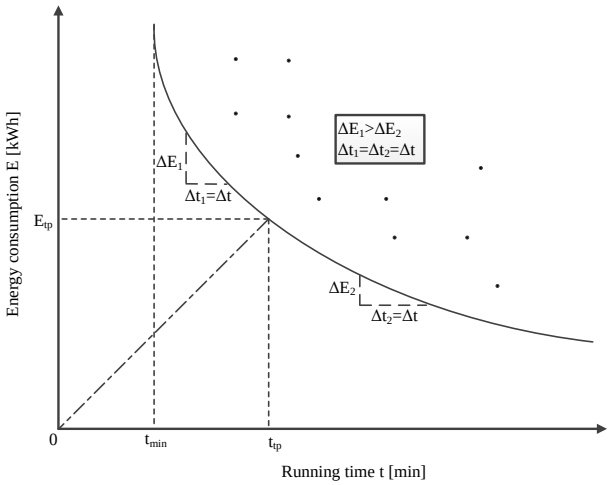

Figure 2.8: Pareto frontier curve of multi-objective function between energy consumption versus running time (t_{min} is the technical minimum running time, solid black line is the Pareto frontier (optimal solutions) and black dots are dominated solutions, t_{tp} and E_{tp} are the turning points, i.e., $\Delta t_1 = \Delta t_2$ and $\Delta E_1 = \Delta E_2$).

Three different optimization algorithms for finding energy-efficient speed profiles were studied by Lu et al. (2013). The authors make use of a graphic model to simplify calculation of the optimal control by avoiding nonlinear complexity. The objective of the optimization is to minimize total traction energy considering punctuality constraints. The optimal speed profile is determined by constructing a complete weighted and directed speed graph. The authors compared the heuristic methods Ant Colony Optimization (ACO) and the Genetic Algorithm, and Dynamic Programming. Varying gradients as well as speed limits were taken into account. The algorithms were applied in different examples in which the total distance was fixed, but the available running time was variable. The results showed that the speed profiles with the lowest total energy consumption were gained with the DP algorithm, but this costs the most computation time. On the other hand, the heuristic algorithms did not guarantee finding an optimal solution.

Sicre et al. (2014) proposed a Genetic Algorithm with Fuzzy parameters based on the accurate simulation of a train motion to determine the optimal driving strategy for delayed high-speed trains. Fuzzy cruising speeds and switching times were used to consider manual train driving. Moreover, regenerative braking was included. The objective of the GA is to find the solution that has the target running time with the minimum energy consumption. A general structure for efficient

manual driving was proposed that was easy to implement for drivers. This structure replaced the cruising regime by a partial traction phase that maintains a speed as long as traction is required. However, if braking is necessary to keep the speed constant on a downhill section braking would not be applied, but the train would coast instead and thus increasing its speed where braking is applied if a speed limit would be reached. The approach requires several runs of the Fuzzy GA with different target running times starting with the scheduled running time where in each iteration the target time is updated by the estimated delay of the former run. To allow a real-time calculation, the algorithm was restricted to two GA runs with a computation time limit of 15 seconds each. The approach was applied in a numerical case of the Spanish High Speed line between Calatayud and Zaragoza in Spain for recovery from a temporary speed restriction at the beginning of the stretch that would lead to a 1:04 min delay if the nominal driving strategy would not be updated. The scheduled running time was 26 min which included 4:08 min (15.9%) running time supplement. Energy savings of 5.5% on pantograph level and 6.7% on substation level were achieved compared to the nominal operations.

Chevrier et al. (2013) proposed a bi-objective optimization approach for computing running times as a trade-off between minimizing running time and energy consumption using a heuristic Evolutionary Algorithm (EA). They consider the time formulation (2.3)–(2.7) with varying gradients and speed limits, but with both the energy consumption J and total time T as objectives to be minimized. They decomposed the problem into $i = 1, \ldots, n$ sections of constant speed limit and in each section i they built the speed profile by splitting the section in two parts with target speeds $v_{a,i}$ and $v_{b,i}$ in the first and second part, respectively, which are the decision variables of the EA. Continuity is guaranteed by incorporating the speed limit in the next section and linking the exit and entry speeds of successive sections. In the first part only maximum acceleration or braking is used to reach the first target speed $v_{a,i}$ from the entry speed. Then in the second part the second target speed $v_{b,i}$ is reached initially by coasting and possibly braking after which cruising is used to complete the rest of the section. The algorithm is followed by a post-processing step for smoothing the speed profile with cruising regimes where a maximum braking regime is followed by either maximum acceleration or acceleration while coasting (on a steep descent). The EA algorithm finds multiple and well-spread non-dominated (Pareto) solutions in a single run that a planner can choose from. The algorithm has been applied in two case studies of a 2.2 km long line with five sections and a 20.2 km long line with also five sections. In both cases the algorithm runs for 60 seconds to produce a wide set of Pareto optimal speed profiles, where a planner can select a solution with given scheduled running time and associated energy consumption. The results show that the energy consumption can be reduced significantly already by slightly increasing the running

times. When more running time is allowed (up to 22% more than the time-optimal running time), energy savings may be even close to 50% in comparison to the technical minimum running time.

2.3.6 Summary on EETC

Table 2.1 gives an overview of the different literature on the EETC. The fourth column 'Method' indicates Approximation (A) if a heuristic method is used or the model contained simplifications. Most research is on the topic of continuous train control using PMP with algorithms for finding exact solutions. All rail modes are considered with an emphasis on metro/urban and regional/IC (intercity) railway systems. To compute realistic speed profiles it is important to take into account nonlinear train traction and resistance, line resistance with in particular varying gradient profiles, and varying speed limits. Curve resistances and tunnels are often ignored.

Some algorithms are applied in a real-time Driver Advisory System. For those algorithms, fast calculation times are achieved by using efficient algorithms, simplifications of the problem, or offline computations of a set of solutions that can be chosen from online. For the analysis of more complex driver behavior or regenerative braking over networks, simulation and/or heuristics like GA have been applied. Also regenerative braking has been considered with still the main focus on a single train (energy consumption at the pantograph).

Finally, there are differences between different modes of rail transport. Table 2.2 shows the main differences. The differences are mostly related to the maximum speed of the trains and the average distance between two stations. The table indicates that cruising becomes more important when the average distance between two stations increases. This can be explained by the fact that at short distances the maximum speed cannot be reached and the running time supplements of the timetable are very small. Therefore any optimal speed to start coasting can be reached, while for longer distances cruising naturally comes in play.

2.4 Energy-efficient train timetabling (EETT)

This section discusses energy-efficient train timetabling, which is the problem of finding a timetable for one or more trains on a railway corridor or network that allows as much as possible energy-efficient driving. The total running time of each train over the corridor may be pre-specified or may still have to be determined. In both cases, the aim is to determine the running time between each pair of consecutive stops for each train such that the total (planned) energy consumption of the involved trains is minimum.

Table 2.1: Summary of energy-efficient train control literature.

Publication	Control	RB	Method	Real-time	Varying features		Mode of transport			
					Speed limits	Gradients	High speed	Regional, IC	Freight	Metro, urban
Ichikawa (1968)	C		E							x
Strobel et al. (1974)	C		E	x						x
Milroy (1980)	C		E	x						x
Asnis et al. (1985)	C	x	E							x
Van Dongen & Schuit (1989a,b, 1991)	C		A		x	x		x		
Howlett (1990)	C		E	x				x		x
Cheng & Howlett (1992)	D		E	x					x	
Cheng & Howlett (1993)	D		E	x					x	
Howlett et al. (1994)	D		E		x	x			x	
Howlett & Pudney (1995)	C, D		E	x	x	x		x	x	x
Howlett (1996)	D		E	x		x			x	
Chang & Sim (1997)	C	x	A		x					x
Cheng (1997)	D		E	x	x	x			x	
Franke et al. (2000)	C	x	A	x	x	x		x		
Howlett (2000)	C, D		E	x		x		x	x	x
Khmelnitsky (2000)	C	x	E	x	x	x		x		x
Oettich & Albrecht (2001)	C		E		x	x		x		x
T. Albrecht & Oettich (2002)	C		E	x						x
Liu & Golovitcher (2003)	C		E	x	x	x		x		x
Vu (2006)	C		E		x	x				
Howlett et al. (2009)	C		E	x	x	x			x	
Lechelle & Mouneimne (2010)	C		A	x	x	x				x
Baranov et al. (2011)	C	x	E		x					x
Domínguez et al. (2011)	C		A		x	x				x
Y. Wang et al. (2011)	C		A		x	x				
Domínguez et al. (2012)	C	x	A		x	x				x
A. Albrecht et al. (2013a)	C		E		x	x				
A. Albrecht et al. (2013b)	C		E	x	x	x		x		
T. Albrecht et al. (2013c)	C		E	x	x	x		x		x
Aradi et al. (2013)	C		E		x	x		x		
Chevrier et al. (2013)	C		E		x	x		x		
Jaekel & Albrecht (2013)	C		E	x	x	x		x		x
Lu et al. (2013)	C		A/E		x	x				x
Rodrigo et al. (2013)	C		E		x			x		
Su et al. (2013)	C		A		x					x
Y. Wang et al. (2013)	C		A, E		x	x				
A. Albrecht et al. (2014)	C		E		x	x		x	x	x
T. Albrecht (2014)	C		E		x	x		x		x
ON-TIME (2014a)	C		E	x	x	x		x	x	
Qu et al. (2014)	C		E		x	x		x		
Sicre et al. (2014)	C	x	A		x	x	x			
Su et al. (2014)	C		A		x	x				x
Scheepmaker & Goverde (2015)	C		E		x	x		x		
P. Wang et al. (2015)	C		E	x	x	x		x		
A. Albrecht et al. (2016a,b)	C		E	x	x	x	x	x	x	

Legend: RB = regenerative braking, C = continuous, D = discrete, E = exact, A = approximation, IC = Intercity .

Table 2.2: Comparison of EETC solutions by mode of transport. Note that the most important driving regime is the regime that has the biggest contribution to the total traction energy savings.

Train type	Driving regimes	Most important driving regime	Maximum speed [km/h]	Average stop spacing [km]	Regenerative braking included	Algorithms
High speed	MA, CR, CO, MB	CR (& CO)	200-300	> 50	Possible	E, A
Regional and IC	MA, CR, CO, MB	CR & CO	120-160	> 25	Possible	E
Freight	MA, CR, CO, MB	CR & CO	80-100	> 30	Possible	E
(Sub)urban	MA, CR, CO, MB	CO	100-120	> 5	Possible	E, A
Metro	MA, CO, MB	CO	80	> 1	Yes	E, A

Legend: MA = maximum acceleration, CR = cruising, CO = coasting, MB = maximum braking, E = exact method, A = approximation, IC = Intercity.

For each trip between two consecutive stations, the planned running time consists of the minimum running time between the stations plus a running time supplement. The minimum energy consumption that is needed on a single trip between two stations is decreasing in the amount of running time supplement. Indeed, if more running time supplement is available, then less energy is needed by running at a lower cruising speed or starting earlier with coasting. This effect is shown in Figure 2.8, which also shows the decreasing added value of more running time supplement. Increasing the amount of running time supplement is often also useful for increasing the robustness of the timetable. However, it also leads to increased (planned) journey times for the passengers.

We used a framework based on EETT with and without regenerative braking. With regenerative braking the models consider synchronization of accelerating and regenerative braking trains. Without regenerative braking the models from literature focus on finding the optimal amount and distribution of the running time supplements. An overview of our framework is given in Figure 2.9.

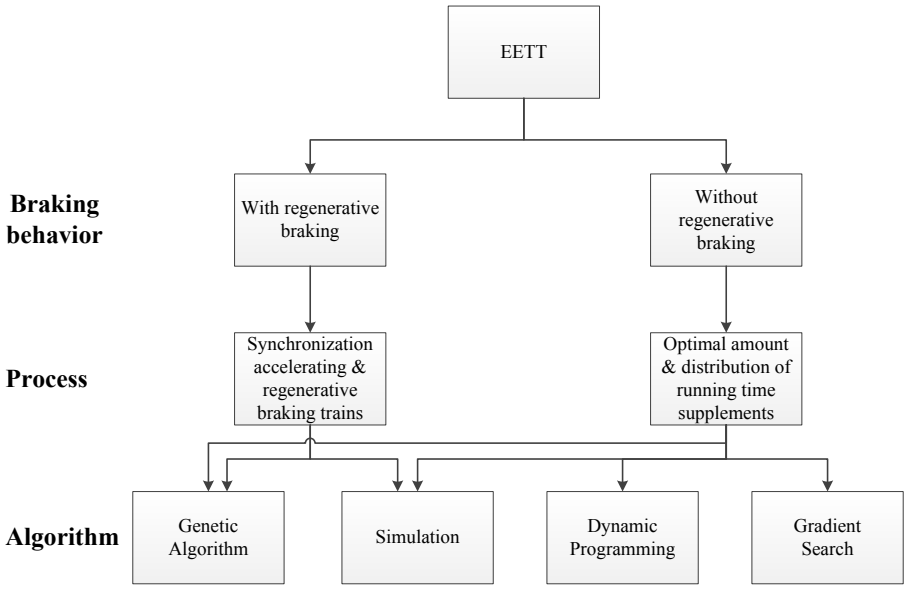

Figure 2.9: Framework of EETT.

Section 2.4.1 first describes a basic version of a model for EETT. Then Section 2.4.2 focuses on EETT without regenerative braking. Finally, Section 2.4.3 reviews the literature including the possibility of regenerative braking.

2.4.1 Basic timetabling model

In this section we give a brief description of a basic timetabling model for a single train. Suppose a single train is to be scheduled along the consecutive trips in the set $Q = \{1, 2, \ldots, n\}$. The minimum running time of trip $q \in Q$ is denoted by r_q, and the dwell time of the stop between trips q and $q+1$ is denoted by d_q.

The basic problem here is to distribute a given amount of time supplement Z in such a way among the trips that the total energy consumption of the train is minimum. To that end, let the decision variables D_q, A_q and S_q denote the departure time, the arrival time and the time supplement of trip $q \in Q$, respectively. Then the timetabling model for scheduling this single train can be described as follows:

$$\min f(D, A, S) \tag{2.53}$$

subject to

$$A_q - D_q = r_q + S_q \qquad \text{for } q = 1, \ldots, n \tag{2.54}$$

$$D_{q+1} - A_q = d_q \qquad \text{for } q = 1, \ldots, n-1 \tag{2.55}$$

$$\sum_{q=1}^{n} S_q \leq Z. \tag{2.56}$$

The objective function (2.53) expresses the total energy consumption of the train in terms of the departure times, the arrival times, and the time supplements of the trips. For evaluating the objective function (2.53), a trade-off curve as shown in Figure 2.8 is used. Constraints (2.54) and (2.55) express the running time and dwell time of trip q in terms of the trip's departure time, arrival time and time supplement. Constraint (2.56) indicates that the total amount of slack time should not exceed the maximum amount of slack time Z.

The above model is a basic model for scheduling just a single train, where minimizing the energy consumption is the only objective. For generating a timetable for more than one train, at least headway constraints and connection constraints must be taken into account as well. Furthermore, regenerative braking requires modeling the interaction between the energy production and the energy consumption of nearby trains. In addition, also other objectives, such as robustness, may be pursued. For different approaches to deal with an objective like robustness, we refer to Cacchiani & Toth (2012).

2.4.2 EETT without regenerative braking

T. Albrecht & Oettich (2002) belonged to the first ones researching EETT and dynamic train operations. They used a simulation model to compute the energy

utilization for each discretized running time between two consecutive stops of a train. Then they calculated the optimal timetable with Dynamic Programming, in which the total running time of each train is optimally distributed along the line. They also aimed at increasing the probability that passenger connections can be maintained in case of delays. Therefore, a multi-objective function was used: minimizing expected waiting time at transfer stations (passengers) and minimizing energy consumption (operator). The final solution was based on the minimum Euclidean distance from the *ideal point*. The results show that the algorithm inserted extra running time supplements to decrease the waiting time at a connection and to reduce energy consumption. The developed method was successfully tested at the suburban railway system of Dresden in Germany: it led to 15-20% reduction in energy consumption compared to using the normal timetable, see T. Albrecht (2005a,b). The EETT algorithm has been implemented in the driver simulator of TU Dresden, see T. Albrecht (2005b).

Ghoseiri et al. (2004) considered an optimization model for scheduling a number of passenger trains on a railway network including single and double track sections and several stations. Their model is a large non-linear mathematical programming model that is solved with the commercial solver LINGO. They consider the multi-objective function of minimizing the total travel time of the passengers and minimizing the fuel consumption costs of the operator. The solution process for the multi-objective problem consists of two steps. In the first step the Pareto curve of the trade-off between running time and energy consumption is determined by the ϵ-constraint method. Then a multi-objective optimization is performed in which different distance-based methods are used to select the final timetable from the Pareto curve. The model was tested on a number of relatively small artificial instances. The results clearly show the trade-off between the two objectives: lower travel times cost more energy. Due to the nature of the model, it is not possible to explicitly describe the resulting optimal driving strategies.

Ding et al. (2011) used a two-level iterative optimization model to determine the energy-efficient driving strategy as well as the optimal timetable for a metro line. They consider the driving regimes acceleration, coasting, and braking. At the first level, an optimization model computes the energy-efficient driving strategy by determining the switching points. At the second level, an optimization model determines the optimal running time supplements. They use a Genetic Algorithm for solving the iterative two-level optimization model. The authors apply their model on a single case study. They report that the energy consumption can be reduced by up to 19.1% compared to the timetable without optimization.

Sicre et al. (2010) considered optimizing the running time distribution for a high speed train. A simulation model computes the relation between the amount of running time supplement and the energy consumption per trip, which results in

trade-off curves between running time and energy consumption per trip between two stops. In this simulation model the energy-efficient driving strategy is based on a 'manual' driving module with heuristic rules to change between the optimal driving regimes known from the EETC literature. An optimization model then distributes the available running time over the trips in order to minimize the total energy consumption. The model only redistributes the available running time supplement, so there is no focus on finding the optimum total amount of running time supplement. The authors report savings of about 33.6% compared to using the commercial timetable with technically minimum running times over a high-speed journey from Madrid to Zaragoza with two intermediate stops.

Cucala et al. (2012) further optimized the model of Sicre et al. (2010) for high speed trains. They included uncertain delays in the model by using fuzzy numbers and punctuality constraints. In addition, they changed the single objective function into a bi-criteria objective function aiming at minimizing total energy consumption and minimizing delays. The preferred timetable is found by distributing the available running time supplement among the trips. For this, first an EETC problem is solved per trip using a Genetic Algorithm and a simulator. As in Sicre et al. (2010), these models determine per trip the trade-off curve between running time and energy consumption. Then a fuzzy mathematical programming model is used to distribute the running time supplement among the trips, where fuzzy models are used to determine uncertainty in delays. Since the problem is solved by a mathematical programming model, no analytical descriptions of the solutions are derived. On a journey from Madrid to Barcelona with four intermediate stops, the authors report a reduction in energy consumption of 5.25% in the optimized timetable without delays, and of 6.67% in the delayed optimized timetable both in comparison with using the commercial timetable. They thus conclude that it is useful to consider delays in the optimization.

L. Yang et al. (2012) considered the EETC problem with variable running times for multiple high-speed trains without regenerative braking and discarding cruising. Their objective was to find a trade-off between total traction energy and total travel time in the railway network, where weight factors are used to determine the balance between the two objectives. Cruising at a fixed speed was not taken into account; the authors mention that cruising is just a special sort of traction operation and could be considered easily. Hence, the optimal driving strategy is a sequence of acceleration and coasting phases until final braking. The EETC was calculated based on a simulation model for determining the driving behavior and a Genetic Algorithm to find the optimal control strategy for multiple trains in a network by taking into account the headway between trains, the speed limits and the riding comfort. Fuzzy variables are included in the simulation part to simulate uncertainty in the performance of the train during operation. Penalty

functions were included to differentiate between the priority of trains. The model was implemented in VC++ 6.0 on a PC with 2.67 GHz processor and was tested on two numerical examples for high speed trains. In the first example, the difference between three objective functions is compared, i.e., technical minimum running times, energy-efficient train operation (single train optimization) and a combination of both (multiple train optimization). Results indicated that a combination of minimizing total travel time and energy consumption is the most realistic. In the second example the weight factor for the objective function was varied. The best total objective function (highest value for the maximization problem) was achieved when the weight factor for total traction energy consumption was set to 0.3 and the weight factor for total travel time was set to 0.7. The computation time of the model varied between 400 s and 2,000 s, depending on the settings of the parameters in the model.

Su et al. (2013) developed an optimization model that determines both an energy-efficient driving strategy and an optimal distribution of the running time supplements in the timetable of a metro line. The aim is to minimize the total energy consumption. To that end, the authors first explicitly calculate the energy-efficient switching points for the different driving regimes. A second algorithm calculates the minimum running time for a train, given the maximum speed limits. Then a third algorithm distributes the running time supplements among consecutive trips in order to minimize the total energy consumption, based on the gradients of the curves between running time and energy consumption. The running time calculations are simplified by assuming constant acceleration, braking, and running resistances. Based on experiments involving the Beijing Yizhuang metro line, the authors conclude that the energy consumption can be reduced on average by 10.3% by applying EETC in the current timetable compared to normal operation. If the timetable is modified based on the results of the model, then the energy consumption can be reduced by 14.5% compared to to normal operation.

In a follow-up paper, Su et al. (2014) aimed at overcoming some of the shortcomings of the model of Su et al. (2013). To that end, they extend the energy-efficient optimization model into an integrated energy-efficient optimization model. In this model they also consider the headway times between consecutive trains in order to incorporate passenger demand and multiple trains. Moreover, the authors now allow variable gradient profiles. In the same way as in Su et al. (2013), the model first calculates the optimal train control per trip. Then the optimal distribution of the running time supplements is determined, again based on the per trip trade-off curves of running time and energy consumption. Finally the headway times between consecutive trains are determined, thereby taking into account passenger demand and fleet size. This is done by iterating over the first two algorithms for different values of the cycle time and the fleet size. In a case

study of the Beijing Yizhuang metro line, the authors determine that the energy consumption could be reduced by 25.4% during peak hours and 15.9% during off-peak hours compared to normal operation. Over a whole day, the energy consumption could be reduced by 24.0% in comparison with normal operation.

Li et al. (2013) described another multi-objective timetable optimization approach. They considered three objectives: minimizing energy consumption, carbon emissions, and passenger travel time. All objectives are equally weighted in the optimization. To solve the problem, a multi-objective optimization model is proposed. This model is a deterministic model, but it is solved by fuzzy multi-objective optimization techniques available in LINGO. The model is applied to the Wuhan-Guangzhou high speed railway line in China, which includes 10 stations. In the resulting timetable, a reduction in energy consumption of about 17.6% is realized in comparison with the timetable that minimizes passenger travel times. However, this comes at a cost of an increase in total passenger travel time of 8.6%. Especially, the journey times increased for the heavier trains with high resistance coefficients and the trains with high carbon emission factors.

Y. Wang et al. (2014) considered the optimal trajectory planning problem for two trains without regenerative braking, and incorporating varying gradients and speed limits. The authors studied the effects of using two different signalling systems, namely a fixed block system (FBS) or a moving block systems (MBS). The objective of their algorithm is to minimize total traction energy consumption for a leading and a following train. The nonlinear terms in the train model and constraints were approximated by piecewise affine functions. In order to separate the two trains, minimum headways were applied. Two different approaches were considered in the paper to solve the problem. A greedy approach where first the leading train is optimized and afterwards the following train, and a simultaneous approach, where the optimization of the two trains is done simultaneously. Two solution approaches were used: a MILP method and a Pseudospectral method, both implemented in MATLAB. The models were applied on a case study of a 1,332 m track between two stops of the Beijing Yizhuang metro line in China. The results indicated that moving block leads to more energy savings, since the headways between two trains can be shorter. Moreover, a simultaneous approach performed better in energy minimization than a greedy approach. The Pseudospectral method performed better in terms of energy consumption and punctual running than the MILP approach, however, the computation times of the MILP approach were much faster. For the instances with parameter values corresponding to the more accurate models the computations times for the MILP approach were above a minute, while the fastest Pseudospectral method took more than several minutes.

P. Wang & Goverde (2016a) considered the train trajectory optimization problem for two successive trains without regenerative braking with consideration of

general infrastructure (varying gradients and speed limits) and operational constraints, as well as signalling constraints. Operational constraints refer to time and speed restrictions from the actual timetable, while signalling constraints refer to the influences of signal aspects and automatic train protection on train operation. They extended the multiple-phase optimal control model of P. Wang et al. (2015) by modelling also signalling constraints in the TPE and applied a Pseudospectral method as solution method. They considered various delays of the first train and computed the resulting optimal trajectory for the second train, with the objective to minimize a trade-off between delays and energy consumption. For this purpose, two optimization policies were developed with either limited or full information of the train ahead. A regional signal response policy only assumed information on the signal ahead such as with a stand-alone DAS that is not connected to a TMS. This policy ensures that the train makes safe responses to different signalling aspects. On the other hand, a global green wave policy assumed that the signal release times by the train ahead are available corresponding to a DAS connected to a centralized Traffic Management System that monitors and predicts the movements of the trains and communicates the corresponding earliest signal approach times to the following trains. The green wave policy then aims at avoiding yellow signals and thus proceeds with all green signals. A case study considered a 50 km corridor with eight stations in the Netherlands operated by regional and nonstop intercity trains in a 15 minute cyclic timetable with the intercity trains overtaking the regional trains halfway. The optimal trajectories were computed for various delays of a regional train. The results showed the benefits on energy consumption and train delay of the following trains if accurate predictive information of the leading train is available. The more delay of the leading train, the better the performance of the green wave policy in both energy consumption and delay.

The combination of timetabling and energy-efficient train operation is also studied by Binder & Albrecht (2013) for the European rail project ON-TIME (ON-TIME, 2014b). They developed a Dynamic Programming algorithm for regional trains that determines the optimal arrival and departure times at intermediate stops in a corridor between two main stations with fixed departure and arrival time, and thus the optimal distribution of the running time supplements and the dwell times along a corridor. The objective includes three criteria: minimization of the expected energy consumption, minimization of the expected arrival delay at the main station at the end of the corridor, and minimization of the expected delay at the intermediate stations. First, Train Path Envelopes are determined which limit the solution space in the optimization. Within a TPE, the optimal train trajectory is computed. The model considers stochastic dwell times, but the running times are assumed to be deterministic and follow the optimal energy-efficient driving strategy for the running time obtained by fixing the arrival and

departure times. Binder & Albrecht (2013) tested the model on a German corridor between two main stations with five intermediate stations. Depending on the weights of the three objectives, the authors report expected energy savings between 4.3% and 12.9% in comparison to the technical minimum running times. In the ON-TIME project the model was applied to fine-tune the arrival and departure times at the intermediate stops of the regional trains on corridors between main intercity stations (Goverde et al., 2016). First, the arrival and departure times of all trains at the intercity stations were optimized using a micro-macro two-level timetabling approach generating a conflict-free timetable with an optimal trade-off between travel times and robustness. Then the energy-efficient speed profiles were computed for the intercity and freight trains with respect to the fixed scheduled running times, after which the TPEs were determined for the regional trains between the intercity stations. Then the Dynamic Programming model was applied to the regional trains. Goverde et al. (2016) applied this method to a Dutch railway network of several interconnected railway lines and report energy savings of 35.5% for all trains over the network with respect to the energy consumption of the minimum running times.

Mills et al. (1991) studied a different version of EETT. They focused on solving the meet-and-pass problem for freight trains in Australia. Since the main part of the Australian railway network is single track, one of the main issues is the meet-and-pass problem for freight trains in different directions. The dynamic rescheduling system they describe aims at rescheduling train movements in such a way that train lateness and energy consumption are minimized. The described model is a non-linear optimization model for determining energy-efficient speed profiles, and a discrete heuristic for solving the meet-and-pass problem. The model was tested on a railway corridor between Port Augusta and Tarcoola (Australia). The reported savings in this experiment are about 6%. The non-linear model used about 21.5 minutes on a HP9000/340 workstation. The discrete heuristic required about 3.3 minutes.

2.4.3 EETT with regenerative braking

Another way to save energy during train operation is by using regenerative braking, i.e., to use the released kinetic energy by regenerative braking of a train as traction energy for other nearby trains. This regenerated energy can be transmitted over the catenary (overhead line) system to the other trains. The effective distance to transfer this regenerated energy over the catenary system depends on the voltage and the current of the power supply. Catenary systems using high voltage alternating current (AC) have less energy loss and thus can transmit the regenerated energy over a larger distance than low voltage direct current (DC) systems. Examples of the former are the German, Swiss and Austrian 15 kV AC electrification systems,

and of the latter are the Belgian, Italian or Spanish 3kV DC or the Dutch 1.5 kV DC catenary systems. For low voltage DC systems it is thus important to have overlapping time intervals of the accelerating and regenerative braking train in the same electrified section to make efficient use of the regenerated energy. Thus the aim is to synchronize the processes between accelerating and regenerative braking of trains, where the gain of the synchronization is higher when the electrical voltage is lower.

One of the first papers studying this topic was T. Albrecht (2004). He considered additional running time for the synchronization of acceleration and regenerative braking instead of additional dwell time at stations for synchronization. The model aims at finding the optimal distribution of the running time supplements in order to minimize total energy consumption and power peaks. The model was solved by a Genetic Algorithm and applied on a case study of the S-Bahn of Berlin. It was shown that, in the case of constant dwell times, regenerative braking may lead to an extra 4% of energy savings in comparison to running time optimization for individual trains. In case of stochastic dwell times, energy consumption is about 6% higher than with constant dwell times.

Regenerative braking is also considered by Peña-Alcaraz et al. (2012). They developed a mathematical programming model to determine a timetable for metro systems that minimizes the total energy consumption by optimally using the regenerative braking energy of the trains. The synchronization of acceleration and braking is modeled by a power flow model, which considers increased running times instead of increased dwell times. Then the timetable model determines the optimally synchronized timetable. However, energy-efficient train control is not considered in the model, because the focus is on maximizing the use of regenerative braking by synchronization of acceleration and regenerative braking. Based on a simulation model of the metro of Madrid, the authors report energy savings of the optimized timetable of about 7% on average compared to using the published timetable without loss of service to the passengers.

X. Yang et al. (2013) studied the topic of synchronization of accelerating and regenerative braking trains for metro systems. They did not explicitly look at regeneration of energy, but at maximizing time overlaps of nearby accelerating and braking trains. The authors first described the problem in terms of a mathematical programming model. Then a Genetic Algorithm was developed to find an efficient synchronized timetable by using headway and dwell time control. On a case study involving the Beijing Yizhuang metro line, the model increased the time overlaps of nearby accelerating and braking trains with 22.1% during peak hours and with 15.2% during off-peak hours. The authors did not consider transmission losses nor converter inefficiency of the regenerated energy.

X. Yang et al. (2014) further developed the model of X. Yang et al. (2013).

In addition to energy savings by using regenerative braking, the authors also take into account passenger waiting time. Again they first described the problem in terms of a mathematical programming model with two objective functions. The model does not take into account uncertainty in the dwell time process at stations: it treats passenger behaviour as deterministic. The model is solved by a Genetic Algorithm. Again in a case study involving the Beijing Yizhuang metro line, the model could reduce the energy utilization by 8.9%, while at the same time the passenger waiting time could be reduced by 3.2% compared to using the published timetable. However, the authors assumed that all regenerative energy is used by another train, while this is not always realistic.

X. Yang et al. (2015) again improved the model of X. Yang et al. (2013). Instead of just focusing on time overlaps of nearby accelerating and braking trains, they consider all trains in the same track interval of electricity supply, and they extend the time horizon to the whole day. The authors assume that trains are operating according to the optimal speed profiles, and aim at synchronizing the arrivals and departures of trains such that as much as possible regenerated energy can be used. They first describe this scheduling problem in terms of a Mixed Integer Programming model. Again they develop a Genetic Algorithm for solving this model. They test their algorithm on the Beijing Yizhuang metro line. Their conclusion is that their algorithm leads to 7.0% reduction in energy consumption in comparison with the currently operated timetable, and to 4.3% reduction in comparison with the algorithm of X. Yang et al. (2013). The improved algorithm leads to an increase of 36.2% in the utilization of regenerated energy.

Next, Li & Lo (2014a) developed an integrated energy-efficient operation model. In their model they both optimize the timetable and the speed profiles by taking into account the headways between trains. They applied a Genetic Algorithm to solve their model. The timetabling part of the model tries to synchronize the accelerating and regenerative braking of trains in order to reuse the regenerated energy. The speed profile part calculates the optimal train control in order to minimize the net energy consumption. The model was again applied to the Beijing Yizhuang metro line. One of the results of the model is that the energy savings are about 25% if the headways between trains are minimal (i.e., 90 seconds). In that case the energy savings of the integrated approach are about 20% higher than those of a two-step approach. The energy savings are smaller when the headways increase, which is also observed by Feng et al. (2013). Also the difference between the integrated approach and the two-step approach gradually decreases for increasing headways. However, Li & Lo (2014a) assumed simplified train dynamics with a constant acceleration rate, deceleration rate, running resistance, and energy transmission loss factor.

Finally, Li & Lo (2014b) developed a model to determine the cycle time, the

headway time, and the speed profiles for a metro line, dynamically depending on the passenger demand and such that the energy consumption is minimized. If the passenger demand is high, then a small cycle time and short headway times are required to be able to handle the passenger demand. If the demand is lower, then the cycle time and the headway times may be longer. The authors make several simplifying assumptions, e.g., they assume that there is no coasting phase, but only a cruising phase. Based on these assumptions, they develop an explicit quadratic expression for the net energy consumption of a train during one cycle, thereby also considering regenerated energy. Then they set up the corresponding KKT conditions, and they solve these in an iterative way. The model was applied to the Beijing Yizhuang metro line. The results obviously depend on the assumptions for the passenger demand. In the experiment with fluctuating passenger demand that was carried out, using a dynamic cycle time and headway time could save up to about 8% energy in comparison with the shortest possible fixed cycle time and headway time that allow satisfying all passenger demand. If the fixed cycle time and headway time are increased, then the corresponding energy consumption may be the same as that of the dynamic ones, but in that case the transport capacity may not be sufficient in the cycles with a high passenger demand.

2.4.4 Summary on EETT

The main results of the literature survey are summarized in Table 2.3. In this table the column "RB" indicates whether regenerative braking is taken into account. Part of the research focuses on optimizing speed profiles of trains in order to minimize the energy consumption, where the total running time is used as a variable to influence the total energy consumption. Another part of the research focuses on optimally distributing running time supplements over the successive train runs according to different multi-criteria objectives including the minimization of total energy consumption. A third research stream focuses on regenerative braking and tries to synchronize the timetable in order to maximize the use of regenerated braking energy.

The models for finding optimal running time supplements over a train line are mainly divided into Gradient Search, Dynamic Programming, Genetic Algorithms, and Simulation. Moreover, when regenerative braking is available, the synchronization of accelerating and braking trains is considered mainly using Genetic Algorithms and Simulation. Different kinds of railway modes have been considered, although most focus is on regional trains and metro trains. Most research considers single-train line optimization, while surrounding trains are mainly considered with regenerative braking.

Table 2.3: Literature on energy-efficient train timetabling.

Publication	Objective(s)	Process	Algorithm	Transport mode	Scope	RB
Mills et al. (1991)	Train lateness, energy consumption	Meet-and-pass problem	Non-linear optimization, discrete heuristic	Freight trains	Several trains on a single track corridor	
T. Albrecht & Oettich (2002)	Expected waiting time, energy consumption	Distribution of running time supplements	Dynamic Programming	Suburban trains with ATO	Single train on a line with 10 stations	
T. Albrecht (2004)	Power peaks, energy consumption	Running time optimization for synchronization	Genetic Algorithm	Suburban trains	One train an a line with 16 stations, taking into account also other trains	x
Ghoseiri et al. (2004)	Travel time, fuel consumption	Timetabling	Non-linear Mathematical Programming, ϵ-constraint method	Passenger trains	Several trains on lines with varying numbers of stations	
Sicre et al. (2010)	Energy consumption	Distribution of running time supplements	Simulation, Optimization	High speed trains	Single train on a line with 4 stations	
Ding et al. (2011)	Energy consumption	Distribution of running time supplements, switching points	Genetic Algorithm	Metro trains	Single train on a line with 6 stations	
Cucala et al. (2012)	Delays, energy consumption	Distribution of running time supplements	Genetic Algorithm, Simulation, Fuzzy Linear Programming,	High speed trains	Single train on a line with 6 stations	
Peña-Alcaraz et al. (2012)	Energy consumption, regenerated energy	Running time optimization for synchronization	Mathematical Programming and DC power flow model	Metro trains	One metro on a line with 36 stations, taking into account also other metros	x
L. Yang et al. (2012)	Travel time, energy consumption	Coasting control	Genetic Algorithm	High speed trains	Three trains in an example network	
Binder & Albrecht (2013)	Expected delays, energy consumption	Distribution of running time supplements	Dynamic Programming	Regional trains	Single train on a line with 7 stations	
Li et al. (2013)	Travel time, carbon emission, energy consumption	Distribution of running time supplements	Fuzzy multi-objective non-linear optimization	Regional trains and high speed trains	Multiple trains on a line with 10 stations	
Su et al. (2013)	Energy consumption	Distribution of running time supplements	Explicit formulas based on simplifying assumptions	Metro trains	Single metro on a line with 14 stations	
X. Yang et al. (2013)	Overlap time	Headway and dwell time optimization for synchronization	Genetic Algorithm	Metro trains	Several metros on a line with 14 stations in two directions	x
Li & Lo (2014a)	Net energy consumption	Timetable optimization for synchronization	Genetic Algorithm	Metro trains	Several metros on a line with 14 stations in two directions	x
Li & Lo (2014b)	Net energy consumption	Dynamic cycle time, headway and speed profiles	Simplifying assumptions, KKT conditions	Metro trains	Several metros on a line with 14 stations in two directions	x
Su et al. (2014)	Energy consumption	Distribution of running time supplements and headway control	Iterative application of the methods from Su et al. (2013)	Metro trains	Multiple metros on a line with 14 stations	
Y. Wang et al. (2014)	Energy consumption	Headway optimization	Mixed integer linear programming and Pseudospectral method	Metro trains	Two following trains between two stops with fixed or moving blocks	
X. Yang et al. (2014)	Passenger waiting time, regenerated energy	Headway and dwell time optimization for synchronization	Genetic Algorithm	Metro trains	Several metros on a line with 14 stations in two directions	x
X. Yang et al. (2015)	Energy consumption	Headway and dwell time optimization for synchronization	Genetic Algorithm	Metro trains	Several metros on a line with 14 stations in two directions	x
P. Wang & Goverde (2016b)	Delays, energy consumption	Headway optimization	Pseudospectral method	Mixed regional and intercity trains	Multiple trains on a line with fixed blocks and 8 stations	

Legend: ATO = automatic train operation, RB = regenerative braking, KKT = Karush-Kuhn-Tucker.

2.5 Conclusions

The general energy-efficient train control problem is characterized by nonlinear dynamics from the traction and train resistance forces as function of speed, distance-dependent state constraints from speed restrictions, bounded controls, and a fixed time horizon. Since the state constraints and the line resistance forces from varying gradients depend on distance, most models in the literature take distance as the independent variable rather than time. The objective is typically minimization of energy consumption, which is the integral of the (scaled) applied forces over distance. The states are mostly speed and time as function of distance, with some authors taking energy as an alternative to speed. To solve the resulting optimal train control problem, distance is typically partitioned into sections of constant gradient and speed limit, and the problem becomes a multiple-phase optimal control problem where each phase (section) is linked with its adjacent phases via continuity constraints in the state variables. In this case, the number and order of driving regimes become less obvious, by which solving the problem becomes numerically challenging.

The optimal train control structure can be derived by applying Pontryagin's Maximum Principle, which gives necessary conditions for the optimal train control. For level track and no or fixed speed limit the optimal train control structure consists of a sequence of the four driving regimes maximum acceleration by full traction, cruising by partial traction, coasting with no traction, and maximum braking, in this order, where cruising and coasting may be absent depending on the time horizon and speed limit. When varying speed limits are considered, additional maximum acceleration regimes may occur in the optimal control structure at each speed limit increase and additional coasting regimes before each speed limit decrease. With varying gradients the cruising regime can be realized by partial traction or partial braking depending on the gradient, while steep gradients may require maximum traction or maximum braking, even in front of a steep uphill or downhill section. When also regenerative braking is possible, the optimal train control structure is extended to seven driving regimes where also (partial or full) regenerative braking can be used for cruising or braking. In addition, recent literature considers further operational constraints such as various target points, flexible time and/or speed windows, or signalling constraints.

Pontryagin's Maximum Principle gives the optimal driving regimes but not the optimal sequence of these regimes nor the optimal switching points between regimes. The literature therefore describes many numerical algorithms to solve the optimal control problem by determining the switching points between driving regimes and associated optimal cruising speeds. Several efficient algorithms have been developed for special cases or assumptions such as level track, absence of steep gradients, assumed linear train resistance, discarding the coasting regime,

or setting the cruising speeds equal to the speed limits. These special cases can be used for suboptimal train control in particular situations. A recent approach based on a direct Pseudospectral method is promising to solve the most general energy-efficient train control problem with varying gradients and speed limits.

The energy consumption is largely determined by the timetable and in particular by the amount of scheduled running time supplements. In the energy-efficient train timetabling problems the running time supplements are the decision variables and the objective is to find the optimal distribution of the running time supplements for a train on one or more legs of its journey, where the objective is mainly a trade-off between minimizing both travel time and energy consumption, and in some cases also delay. The energy-efficient train control problem is mostly used as a subproblem and the overall optimization problem is solved by Gradient Search, Dynamic Programming, Simulation or Genetic Algorithms. When regenerative braking is possible, the focus shifts to synchronizing braking and accelerating trains so that the regenerated braking energy can be used by nearby accelerating trains. Simulation and Genetic Algorithms are here the main solution methods.

The literature on energy-efficient train control is advancing towards developing more accurate advanced models and faster algorithms.he alorithms in the existing DAS and ATO systems rely on some simplifications to be able to compute (sub)optimal driving advice in real-time or are based on offline computed solutions for a large set of scenarios. The main difference between the theoretical models for EETC and a DAS in practice is that the theoretical models try to find the optimal driving strategy, while a DAS often settles for suboptimal solutions using heuristics. The computation time increases for EETC models when more realistic behavior is included, like varying gradients and speed limits. In real-time operation fast algorithms for a DAS are needed. Furthermore, additional constraints may be included in a DAS to provide the train driver with a stable driving advice (i.e., no continuously changing advice) or specific driving regimes may be excluded, such as coasting or cruising at less than the speed limit. This also relates to the drivability of the optimal driving strategy in terms of the number and time intervals between driving regime changes, which applies more to DAS than ATO, as well as how the advice is presented to the driver and the acceptability of a driver to use a DAS. This needs more research from a human factors point of view. Moreover, the option of regenerative braking increases the number of driving regimes even more. In this respect, a comparison of EETC with or without regenerative braking is also required with respect to energy consumption and the complexity of the associated driving strategy. Nevertheless, even suboptimal driving strategies can lead to significant energy savings. In due time, power of computers will increase allowing more advanced algorithms to be used in real-time in a DAS. And of course, there is active research in model and algorithm development where the

increased knowledge about the optimal driving strategies under various conditions and constraints will be a guide to find more evident algorithms.

Recent research also focused on including more operational (schedule and signalling) constraints in the train control problem, which also paves the way to extend the single-train optimal control problem to multi-train optimal control problems where the energy consumption of multiple trains is optimized dynamically including their interaction. This multi-train optimization problem can be included in real-time railway Traffic Management Systems, where the aim is first to avoid real-time conflicts and second to minimize the total traction energy consumption of all trains in a network. An initial study in this area was presented by Mills et al. (1991), but there has not yet been much follow-up research. The additional operational constraints will also be useful for more realistic energy-efficient timetabling problems for multiple trains, which is yet a largely unexplored topic.

Incorporating energy-efficiency in timetable design is another area of future research. There are currently limited papers on this topic, but the attention to this field has been increasing recently. Besides theoretical results, railway undertakings also start showing interest in EETT. For example, recently NS is investigating a change in their timetable design process by redistributing the amount of running time supplements and scheduling more realistic running times, which increases the opportunities for energy-efficient driving. Also the Swiss Federal Railways SBB (*Schweizerische Bundesbahnen*) is investigating EETT for their regional train services by uniformly redistributing the running time supplements over the trajectories and using flexible arrival times. In the future, research will investigate the optimal amount and distribution of the running time supplements as well as the balance between different objectives for timetable design, like minimizing total running time, total delay, energy consumption, and maximizing passenger comfort. Moreover, the efficiency of these models and the interaction with the applied EETC strategies and possible DAS implementations need to be tested in pilots. The awareness of the impact of EETC to exploit time allowances for energy savings will change both operational railway traffic management and timetabling. The review of models and algorithms presented in this chapter may guide future research directions and lead to a further reduction of energy consumption and costs in the railways of the future.

Chapter 3

Energy-efficient train control using nonlinear bounded regenerative braking

---

Apart from minor updates, this chapter has been published as:
Scheepmaker, G. M., Goverde, R. M. P. (2020) Energy-efficient train control using nonlinear bounded regenerative braking, *Transportation Research Part C: Emerging Technologies*, 121, 102852.

3.1 Introduction

The topic of *energy-efficient train control* (*EETC*) or *energy-efficient train trajectory optimization* has been studied a lot in the literature during the last decades. The aim of EETC is to run a train with the least traction energy consumption. Therefore, the train uses the available *running time supplements* in order to arrive exactly on-time (i.e., not too early and not too late) at the next station. The running time supplements are the extra running times above the minimum-time running in order to cope with small delays or to deal with disturbances during operations. The minimum-time running can be computed by solving the the *minimum-time train control* (*MTTC*) problem. Energy-efficient train driving is applied if the train is running punctual (Scheepmaker & Goverde, 2015). A comprehensive overview on the topic of energy-efficient train control can be found in Scheepmaker et al. (2017) and X. Yang et al. (2016).

The EETC problem can be formulated as an optimal control problem. By using *Pontryagin's Maximum Principle* (*PMP*) the optimal control can be shown

to consist of the optimal *driving regimes* maximum acceleration (MA), cruising (CR), coasting (CO) and maximum braking (MB) (Howlett & Pudney, 1995; Khmelnitsky, 2000; Liu & Golovitcher, 2003; Albrecht et al., 2016a,b). The challenge is to derive the optimal order of the driving regimes and the switching points between them. For more details on this topic we refer to Scheepmaker et al. (2017).

Modern trains have the possibility to apply both *mechanical braking* and *regenerative braking*. Braking disks or pads are used in order to convert kinetic energy into heat, while applying mechanical braking. During regenerative braking electricity is generated while using the engine of the train as a generator in order to convert the kinetic energy into electricity. This electricity can be used for the train itself such as heating or lighting, stored within batteries or it can be fed back to the catenary system for other surrounding trains. For urban rail relatively more energy savings can be achieved by energy storage compared to utilizing the regenerated energy by surrounding trains (González-Gil et al., 2014). In this chapter we focus on the utilization of regenerated braking energy by surrounding trains for heavy rail, because a lot of research on regenerative braking is considering the topic of synchronizing accelerating and regenerative braking trains including energy-efficient train control (Scheepmaker et al., 2017). For more details about regenerative braking and different regenerative braking storage techniques for urban rail systems, we refer to the review paper of González-Gil et al. (2013).

The topic of regenerative braking has been studied both for multiple-trains as well as single trains (Scheepmaker et al., 2017). In the multiple train problem, the aim is to synchronize accelerating and regenerative braking trains, in order to maximize the usage of regenerative braking. This leads to the *energy-efficient train timetable* (*EETT*) problem that determines the optimal departure and arrival times within stations, which is mainly focused on urban railway networks. Examples of the EETT problem with regenerative braking can be found in T. Albrecht (2004), Peña-Alcaraz et al. (2012), X. Yang et al. (2013), X. Yang et al. (2014), Li & Lo (2014a), Li & Lo (2014b), Zhou et al. (2018), and Luan et al. (2018a,b). In the single-train problem, the aim is to find the energy-efficient train control with regenerative braking, so the objective function includes regenerated energy during braking, which depends on the efficiency of the regenerative braking system. Asnis et al. (1985) started this research by considering flat tracks. The main difference between the EETC models with mechanical braking is that the driving regimes with mechanical braking are replaced by regenerative braking, such as cruising by partial braking and maximum braking. Later studies include varying gradients and speed limits. Khmelnitsky (2000) and Franke et al. (2000) both used time and energy as state variables to derive analytical expressions for the different driving regimes for the EETC problem including regenerative braking. Moreover,

A. Albrecht et al. (2016a,b) discussed the key principles of optimal train control with regenerative braking using continuous control settings and included speed limits and steep gradients. They generalized the formulations of traction and regenerative braking control by using monotone functions and a generic function for the train resistance. Qu et al. (2014) focused on the optimal cruising speed and regenerative braking for metro trains, where they excluded coasting. In the European project ON-TIME (Optimal Networks for Train Integration Management across Europe) an iterative gradient-based algorithm was developed to determine the energy-efficient driving strategy including regenerative braking that can be used for a Driver Advisory System (DAS) (ON-TIME, 2014a). S. Yang et al. (2018) developed an analytical method to determine the optimal train control for a complete metro line, by subdividing the trajectory in phases with constant speed limits. They included the effect of regenerative braking in order to minimize the total energy consumption, but varying gradients were not considered in their model. Their train control method was part of an optimization method that determined the energy-optimal timetable for a single train for a complete metro line.

The main assumption behind the discussed papers is that they consider regenerative braking only, and assumed it as constant. In practice trains need mechanical braking as well, since the regenerative braking force is limited by the maximum regenerative braking force and the power of the engine (given by the traction/regenerative braking force diagram) (Frilli et al., 2016; Zhou et al., 2018). This is especially the case for high speeds where the power of the traction engine is limited as well as speeds close to zero, where mechanical braking is applied to compensate the total braking force. Up to our knowledge, only Baranov et al. (2011), Lu et al. (2014), Fernández-Rodríguez et al. (2018), and Zhou et al. (2018) investigated the combination of mechanical and regenerative braking. Baranov et al. (2011) considered traction, regenerative braking and mechanical braking. They considered the seven optimal driving regimes including two driving regimes for the combination of regenerative and mechanical braking (i.e., cruising by partial regenerative braking (CR2), maximum regenerative braking (MRB), cruising by maximum regenerative and partial mechanical braking (CR3), and maximum total braking (MB)). However, the derivation of these regimes as well as an algorithm to solve the optimal sequence of the driving regimes were not provided. Lu et al. (2014) only considered the braking part of the trajectory optimization in order to maximize the regenerative braking energy. They made a distinction between mechanical and regenerative braking and they compared the difference between a constant braking rate (or mass-specific train braking force) and the regenerative braking rate depending on the maximum regenerative braking force and the regenerative braking power. Using PMP they derived four regimes consisting of coasting, cruising by braking, maximum regenerative braking, and maximum

total braking, but without considering varying speed limits and varying gradients. Fernández-Rodríguez et al. (2018) considered a dynamic multi-objective optimization model to compute the optimal speed profiles during train driving for high speed trains that minimize total delay and energy consumption. The energy-efficient speed profiles are determined by using a simulation model for the train motion and includes both mechanical and regenerative braking. However, the optimal structure of the speed profiles with the different driving regimes and switching points as well as the comparison between the simulation results and optimal control theory were not discussed in this paper. Moreover, the model results only show where the train is braking, but not if the train applies regenerative and/or mechanical braking. Zhou et al. (2018) developed an integrating model for the train control and timetable optimization in order to minimize the total net energy consumption by synchronizing accelerating and regenerative braking trains. They included the combination of regenerative and mechanical braking and solved train control and the timetabling problem using heuristics. However, they considered the four driving regimes (MA, CR, CO and MB) without the derivation of these regimes, and they did not include varying speed limits. Scheepmaker & Goverde (2016) and Scheepmaker et al. (2020b) compared the difference of EETC between regenerative braking only and mechanical braking only, but they did not consider the combination of regenerative and mechanical braking and they applied the comparison of the different EETC braking strategies only on flat track. Scheepmaker et al. (2020b) included varying speed limits. Most research assumes a constant value for the efficiency of the train due to power losses (i.e., efficiency of the engine). However, Ghaviha et al. (2017) investigated the effect of a dynamic efficiency on the energy-efficient train control problem with regenerative braking that considers the losses due to the inverter, motor and gearbox that sum up to the dynamic total power loss. This leads to a more realistic calculations of the energy consumption of the train and the computed speed profile is more energy-efficient compared to models using a constant efficiency factor. For battery catenary-free electric trains Ghaviha et al. (2019) combine the single mass point mechanical train control model with the electrical train battery model, and indicate that these trains should focus on minimizing the total charge of the battery during catenary-free operation.

The aim of this chapter is to derive the energy-efficient train control with both mechanical and regenerative braking and to apply them within a model on numerical examples including varying speed limits and varying gradients. Therefore, this chapter gives the following contributions to the literature:

1. We consider an optimal train control problem with three control variables (traction, regenerative braking and mechanical braking).

2. We consider the effect of the actual nonlinear bounded regenerative braking

constraints and compare this to the commonly used constant regenerative braking on the energy-efficient train control.

3. We derive the optimal energy-efficient train control with nonlinear bounded regenerative braking and/or mechanical braking.

4. We apply a pseudospectral method considering the EETC problem with a variation of regenerative and/or mechanical braking on different numerical realistic experiments with various scenarios to show their difference.

The chapter outline is as follows. Section 3.2 provides the optimal train control problem for both EETC and MTTC including the necessary optimality conditions. Section 3.3 explains briefly the pseudospectral method applied in this chapter. In order to show the working of the multiple-phase pseudospectral method, a case study is presented in Section 3.4 based on Dutch infrastructure and rolling stock data. Finally, the conclusions are provided in Section 3.5.

3.2 Optimal train control problem

This section gives the optimal train control problem formulation and a derivation of the necessary optimality conditions by applying Pontryagin's Maximum Principle (Lewis et al., 2012; Ross, 2015). These conditions provide a formal derivation of the optimal driving regimes when considering a mixture of mechanical and regenerative braking. We consider both mechanical and regenerative braking like Baranov et al. (2011) and model the train as a point mass (Brünger & Dahlhaus, 2014; Howlett & Pudney, 1995). Moreover, we use time as independent variable. We follow a similar derivation of the necessary optimality conditions for the optimal train control problem as Howlett (2000), Khmelnitsky (2000), Liu & Golovitcher (2003), and A. Albrecht et al. (2016a,b). However, since we include both regenerative and mechanical braking our problem formulation is different. We use the step-wise optimal control analysis and separate the specific control u into specific traction f, specific regenerative braking b_r and specific mechanical braking b_m (i.e., $u = f + b_r + b_m$). Therefore, for the case of both regenerative and mechanical braking, the problem formulation is comparable to Baranov et al. (2011).

First, Section 3.2.1 explains the concept of regenerative braking more in depth. Afterwards, Section 3.2.2 gives the energy-efficient train control problem including both regenerative and mechanical braking. Third, regenerative braking only for EETC is considered in Section 3.2.3. Fourth, mechanical braking only for the EETC problem is discussed in Section 3.2.4. Finally, the minimum-time train control (MTTC) problem is considered in Section 3.2.5 where both mechanical and regenerative braking can be applied.

3.2.1 Regenerative braking

The electric engine of a train can be used both for traction and dynamic braking (González-Gil et al., 2013; Lu et al., 2014). During dynamic braking the electric engine of the train is used to convert dynamic energy into electric energy by using the opposite direction of the torque of the motor compared to the rotating speed. This electric energy can be converted into heat using various resistors, which is called rheostatic braking, or it can be used for the train itself (such as heating or air conditioning), stored in energy storage systems or send to other trains by transmitting the electricity over the catenary system, which is called regenerative braking. In this chapter we focus on regenerative braking where the regenerated energy is transformed into electricity that can be used for other surrounding trains. Since the train uses the electric motor (engine) as a generator during regenerative braking, the regenerative force is bounded by the performance of the engine like the traction force, which can be visualized in the traction/braking force diagram, see Figure 3.1. The traction force has a constant part in which the maximum traction force is limiting the maximum traction force (overheat and adhesion limit) and a hyperbolic part, where the power is limiting the maximum traction force (Steimel, 2008; Brünger & Dahlhaus, 2014). During regenerative braking the same engine is used, therefore, the maximum regenerative force is limited by a constant part (maximum regenerative braking force) and a hyperbolic part (maximum regenerative braking power). In addition, during low speeds regenerative braking cannot be applied, because of the limited kinetic energy that can be converted into energy (low current produced) and it should overcome the power losses in the engine and over the catenary (Pengyu et al., 2009; Yi, 2018). Therefore, trains in practice apply just mechanical braking at speeds below some speed v_1 (close to zero). In this chapter we use the rolling stock data of VIRM-6 of the Netherlands Railways (NS) in the case study which applies zero regenerative braking force below speed $v_1 = 8$ km/h (NS, 2020), see Table 3.1. Finally, we assume that the regenerated energy can be used by another accelerating train and that it is not used by or stored in the train itself, so we consider the regenerative braking energy flow to the engine of the other accelerating train. In addition, we focus on the trajectory optimization of a single train. In practice the utilization of regenerative braking energy by surrounding trains depends on a series of factors such as the operation mode of surrounding trains, the distance between the synchronized accelerating and regenerative braking trains, and the maximum allowable voltage of the power supply system. Including these different aspects requires detailed modelling of the power supply system over the catenary, which requires simulation models such as OpenPowerNet (Stephan, 2008). We focus on the effect of the actual nonlinear bounded regenerative braking instead of the commonly used constant regenerative braking on the energy-efficient train

control. In future work, our train control model can be embedded within a complex electricity simulation model to obtain dynamic condition-dependent estimated parameters of the catenary and the receiving train.

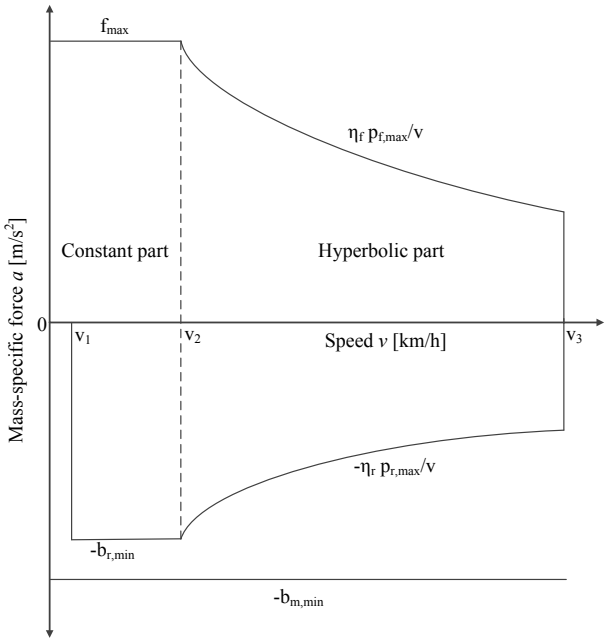

Figure 3.1: Typical mass-specific traction-speed (f) and mass-specific regenerative braking-speed (b_r) diagram with a constant and hyperbolic part, and a constant mass-specific mechanical braking force b_m. The mass-specific regenerative braking force is zero below speed v_1.

3.2.2 Energy-efficient train control with nonlinear bounded regenerative and mechanical braking (RMeB)

In this section we consider the energy-efficient train control problem including regenerative and mechanical braking. The aim for energy-efficient train control is to minimize total mass-specific traction energy E [m^2/s^2] between two consecutive stops given the scheduled running time T [s] (with sufficient running time supplement) according to the timetable:

$$E = \min \int_0^T (f(t) + \eta b_r(t)) v(t) dt, \tag{3.1}$$

subject to the constraints

$$\dot{s}(t) = v(t) \tag{3.2}$$
$$\dot{v}(t) = f(t) + b_r(t) + b_m(t) - r(v) - g(s) \tag{3.3}$$
$$f(t)v(t) \leq \eta_f p_{f,\max} \tag{3.4}$$
$$-b_r(t)v(t) \leq \eta_r p_{r,\max} \tag{3.5}$$
$$0 \leq v(t) \leq v_{\max}(s) \tag{3.6}$$
$$0 \leq f(t) \leq f_{\max} \tag{3.7}$$
$$-b_{r,\min} \leq b_r(t) \leq 0 \tag{3.8}$$
$$b_r(t) = 0 \text{ if } v(t) < v_1 \tag{3.9}$$
$$-b_{m,\min} \leq b_m(t) \leq 0 \tag{3.10}$$
$$b_r + b_m \leq b_{\min} \tag{3.11}$$
$$s(t_0) = 0, s(t_f) = S, v(t_0) = 0, v(t_f) = 0, \tag{3.12}$$

where time t [s] is defined as the independent variable, distance s [m] and speed v [m/s] are the state variables, the derivatives of the state variables to the independent variable are $\dot{s} = ds/dt$ and $\dot{v} = dv/dt$, and the control variables are mass-specific traction force f [m/s^2], mass-specific (negative) regenerative braking force b_r [m/s^2], and mass-specific (negative) mechanical braking force b_m [m/s^2]. Moreover, the total mass-specific braking force is defined by the combination of regenerative and mechanical braking, i.e., $b(t) = b_r(t) + b_m(t)$, which is bounded by the maximum mass-specific braking force $b_{\min}$. The mass-specific traction, regenerative braking and mechanical braking force are defined by the total force (traction force F [N], regenerative braking force B_r [N] and mechanical braking force B_m [N] divided by the total rotating mass (i.e., train mass m [kg] multiplied by rotating mass factor ρ [-]), thus $f = F(t)/(\rho m)$, $b_r = B_r(t)/(\rho m)$ and $b_m = B_m(t)/(\rho m)$. The mass-specific traction force is bounded by $f_{\max}$, the mass-specific regenerative braking force is bounded by $-b_{r,\min}$, and the mass-specific mechanical braking force is bounded by $-b_{m,\min}$. The regenerative braking and mechanical braking are independent of each other and add up to the total braking. The maximum total mass-specific braking force is limited for passenger comfort to b_{min} as stated in (3.11). The traction and regenerative braking forces are functions of speed and consist of a constant part (depending on the maximum traction or regenerative braking force) and a hyperbolic part that depends on traction efficiency η_f [-] or regenerative braking efficiency η_r [-] and the specific power p [m^2/s^3] of the train, see Figure 3.1. Furthermore, regenerative braking cannot be applied below the speed v_1 as explained in Section 3.2.1. The total efficiency for regenerative braking energy η [-] depends on the efficiency of the engine of the train during regenerative braking η_r [-], the efficiency of the catenary η_c [-], and the efficiency of the

engine of the second train during acceleration η_s [-], i.e., $\eta = \eta_r \eta_c \eta_s$. The specific power is limited by the maximum specific power $p_{\max}$. Therefore, the traction control is bounded by $f \leq f_{\max}(v) = \min(f_{\max}, \eta_f p_{f,\max}/v)$ and the regenerative braking control is bounded by $b_r \geq b_{r,\min}(v) = -\min(b_{r,\min}, \eta_r p_{r,\max}/v)$. Note that we explicitly consider both the efficiency of the traction control η_f and regenerative braking control η_r while in literature this is mostly modelled implicitly in the maximum power (e.g., Scheepmaker et al. (2020b)). Moreover, traction and braking control (both regenerative and mechanical) cannot be applied at the same time, i.e., $f \cdot (b_r + b_m) = 0$. The total mass-specific train resistance consists of the mass-specific train resistance $r(v)$ [m/s^2] and the mass-specific line resistance $g(s)$ [m/s^2]. The mass-specific train resistance is defined by Davis equation $r(v) = r_0 + r_1 v + r_2 v^2$, where $r_0, r_1 \geq 0$ and $r_2 > 0$ are non-negative coefficients (Davis, 1926). The mass-specific line resistance is caused by varying gradients, where $g(s) > 0$ denotes uphill slopes and $g(s) < 0$ downhill slopes. We assume a piecewise constant speed limit $v_{\max}$(s) and gradient g(s) over distance. Finally, the difference in the optimal control problem formulation given in (3.1)–(3.12) with current literature is that we include the combination of mechanical and regenerative braking in (3.3) and (3.11) and we consider the nonlinear bounded maximum regenerative braking behavior in (3.5) (i.e., regenerative braking-speed diagram given in Figure 3.1).

With the problem formulation it is now possible to derive the necessary optimality conditions. We start with defining the Hamiltonian H [m^2/s^3] as

$$H(s, v, \lambda_1, \lambda_2, f, b_r, b_m) = (\lambda_2 - v) f + (\lambda_2 - \eta v) b_r + \lambda_2 b_m + \lambda_1 v - \lambda_2 r(v) - \lambda_2 g(s), \quad (3.13)$$

where the costate variables are defined by λ_1(t) [m/s^2] and λ_2(t) [m/s] as functions of the independent variable t. Moreover, the Hamiltonian is independent of time and so $\partial H / \partial t = 0$. Next, the augmented Hamiltonian $\bar{H}(s, v, \lambda_1, \lambda_2, \mu, f, b_r, b_m)$ [m^2/s^3] also takes the additional (mixed) state and control path constraints (3.4)–(3.10) into account which leads to

$$\begin{aligned} \bar{H} =& H + \mu_1 (f_{\max} - f) + \mu_2 (b_r + b_{r,\min}) + \mu_3 (b_m + b_{m,\min}) + \mu_4 (b_{\min} - (b_r + b_m)) \\ &+ \mu_5 (\eta_f p_{f,\max} - f v) + \mu_6 (\eta_r p_{r,\max} + b_r v) + \mu_7 (v_{\max} - v), \end{aligned} \quad (3.14)$$

with the nonnegative Lagrange multipliers μ_1 [m/s], μ_2 [m/s], μ_3 [m/s], μ_4 [m/s], μ_5 [-], μ_6 [-], μ_7 [m/s^2]. The costates satisfy the differential equations $\dot{\lambda}_1(t) = -\partial \bar{H} / \partial s$ and $\dot{\lambda}_2(t) = -\partial \bar{H} / \partial v$ which gives

$$\dot{\lambda}_1(t) = \lambda_2 g'(s) \quad (3.15)$$

$$\dot{\lambda}_2(t) = f + \eta b_r - \lambda_1 + \lambda_2 r'(v) + \mu_5 f - \mu_6 b_r + \mu_7. \quad (3.16)$$

Note that the derivative of the gradients $g'(s)$ is almost everywhere zero, when the

gradient is constant. Therefore, (3.15) indicates that λ_1 is constant when the gradients are constant. We can now apply Pontryagin's Maximum Principle on the optimal control, which states that the Hamiltonian should be maximized (Pontryagin et al., 1962). We define $U = [0, \min(f_{\max}, \eta_f p_f / v)] \times [-\min(b_{r,\min}, \eta_r p_r / v, 0), 0] \times [-b_{m,\min}, 0]$. The optimal controls $\hat{f}(t)$, $\hat{b}_r(t)$ and $\hat{b}_m(t)$ are then defined by:

$$(\hat{f}(t), \hat{b}_r(t), \hat{b}_m(t)) = \arg \max_{(f, b_r, b_m) \in U} H(\hat{s}(t), \hat{v}(t), \hat{\lambda}_1(t), \hat{\lambda}_2(t), f, b_r, b_m), \quad (3.17)$$

where $(\hat{s}, \hat{v})$ and $(\hat{\lambda}_1, \hat{\lambda}_2)$ are the state and costate trajectories associated to the optimal control trajectories $\hat{f}$, $\hat{b}_r$ and $\hat{b}_m$. The Hamiltonian H is linear in the controls f, b_r and b_m with coefficients $\lambda_2 - v$ for f, $\lambda_2 - \eta v$ for b_r, and λ_2 for b_m. Therefore, the value of the speed v relative to the costate λ_2 determines the optimal controls f, b_r and b_m that maximize the Hamiltonian. This results in the following seven cases:

1. If $\lambda_2 > v$ then f must be maximal (i.e., $f = \min(f_{\max}, \eta_f p_{f,\max} / v)$), and $b_r = b_m = 0$.

2. If $\lambda_2 = v$ then $f \in [0, \min(f_{\max}, \eta_f p_{f,\max} / v)]$ is undetermined (first singular solution), and $b_r = b_m = 0$.

3. If $\eta v < \lambda_2 < v$ then $f = b_r = b_m = 0$.

4. If $\lambda_2 = \eta v$ then $b_r \in [-\min(b_{r,\min}, \eta_r p_{r,\max} / v), 0]$ is undetermined (second singular solution), $f = 0$, and $b_m = 0$.

5. If $0 < \lambda_2 < \eta v$ then b_r must be minimal (i.e., $b_{r,\min} = -\min(b_{r,\min}, \eta_r p_{r,\max} / v)$), $f = 0$, and $b_m = 0$.

6. If $\lambda_2 = 0$ then $b_m \in [-b_{m,\min}, 0]$ is undetermined (third singular solution) and b_r must be minimal (i.e., $b_r = -\min(b_{r,\min}, \eta_r p_{r,\max} / v)$), and $f = 0$.

7. If $\lambda_2 < 0$ then b_m must be minimal ($-b_{m,\min}$) and b_r must be minimal (i.e., $-\min(b_{r,\min}, \eta_r p_{r,\max} / v)$), and $f = 0$.

The next step is to apply the Karush-Kuhn-Tucker (KKT) conditions on the augmented Hamiltonian in (3.14) (Bertsekas, 1999). This leads to the following stationary conditions:

$$\frac{\partial \bar{H}}{\partial f}(s, v, \lambda_1, \lambda_2, \mu, f) = \lambda_2 - v - \mu_1 - \mu_5 v = 0 \quad \text{if } f > 0, b_r = b_m = 0 \quad (3.18)$$

$$\frac{\partial \bar{H}}{\partial b_r}(s, v, \lambda_1, \lambda_2, \mu, b_r) = \lambda_2 - \eta v + \mu_2 - \mu_4 + \mu_6 v = 0 \quad \text{if } b_r < 0, f = b_m = 0 \quad (3.19)$$

$$\frac{\partial \bar{H}}{\partial b_m}(s, v, \lambda_1, \lambda_2, \mu, b_m) = \lambda_2 + \mu_3 - \mu_4 = 0 \quad \text{if } b_m < 0, b_r < 0, f = 0, \quad (3.20)$$

and they are undefined for $f = b_r = b_m = 0$. The second part of the KKT conditions consists of the complementary slackness conditions on the path constraints given by $\mu_i \geq 0, i = 1, \ldots, 7$,

$$\begin{aligned}&\mu_1(f_{\max} - f) = 0, \mu_2(b_r + b_{r,\min}) = 0, \mu_3(b_m + b_{m,\min}) = 0, \mu_4(b_{\min} - (b_r + b_m)) = 0,\\ &\mu_5(\eta_f p_{f,\max} - fv) = 0, \mu_6(\eta_r p_{r,\max} + b_r v) = 0, \mu_7(v_{\max} - v) = 0.\end{aligned} \tag{3.21}$$

We can now describe the optimal driving regimes depending on the costate λ_2 by using PMP and the KKT conditions. The driving regimes are as follows:

1. **Maximum acceleration (MA)**. For the first case $\lambda_2 > v$ holds with f maximal ($f_{\max}(v(t))$). With (3.21) leading to the fact that $\mu_1 > 0$ or $\mu_5 > 0$ and, therefore, maximum traction is applied by $f = \min(f_{\max}, \eta_f p_{f,\max}/v)$. Condition (3.21) also indicates $\mu_2 = \mu_3 = \mu_4 = \mu_6 = 0$, since $b_r = b_m = 0$. Moreover, $\mu_7 = 0$, because the maximum speed $v_{\max}$ cannot be maintained during maximum acceleration.

2. **Cruising by partial traction (CR1)**. The singular solution with $\lambda_2 = v$ and $f \in [0, f_{\max}(v(t))]$ holds for the second case. Again since $f > 0$, (3.18) and (3.21) dictates that $\mu_1 = \mu_2 = \mu_3 = \mu_4 = \mu_5 = \mu_6 = 0$. Furthermore, $\lambda_2(t) = v(t)$ holds for a nontrivial interval, and thus $\dot{\lambda}_2(t) = \dot{v}(t)$. Now (3.3) and (3.16) give $f - \lambda_1 + vr'(v) + \mu_7 = f - r(v) - g(s)$, which can be rewritten to

$$h(v) = -\lambda_1 + vr'(v) + \mu_7 + r(v) + g(s) = 0. \tag{3.22}$$

   For a constant gradient, the function $h(v)$ is an increasing convex function with a unique solution $h(v_f) = 0$ for $v_f > 0$. For the case that $v_f < v_{\max}$ resulting in $\mu_7 = 0$, we can rewrite equation (3.22) to

$$v_f r'(v_f) - \lambda_1 + r(v_f) + g(s) = 0, \tag{3.23}$$

   which indicates that the speed v_f depends on λ_1 and $g(s)$, since r_0, r_1 and r_2 are constants. Therefore, the speed has a unique solution v_f, i.e., cruising speed, when the gradient is constant. In the case $v = v_{\max}$, then $\mu_7 = \lambda_1 - v_{\max} r'(v_{\max}) - r(v_{\max}) - g(s)$. We also have $\dot{v}(t) = 0$ and thus the traction force is equal to the total resistance force in order to remain at the cruising speed, i.e., $f(t) = r(v_f) + g(s)$.

3. **Coasting (CO)**. The third case indicates that $\eta v < \lambda_2 < v$ and thus $f = b_r = b_m = 0$. The complementary slackness conditions (3.21) indicate that $\mu_1 = \mu_2 = \mu_3 = \mu_4 = \mu_5 = \mu_6 = 0$. Furthermore, the resistance influences the speed and, therefore, the speed limit can not be maintained, indicating that $\mu_7 = 0$.

4. **Cruising by partial regenerative braking (CR2)**. The fourth case is the second singular solution with $\lambda_2 = \eta v$ and $b_r \in [-\min(b_{r,\min}, \eta_r p_{r,\max}/v), 0]$ and $f = 0$, and $b_m = 0$, since $\lambda_2 > 0$. Since $b_r < 0$ the conditions (3.19) and (3.21) indicates that $\mu_1 = \mu_2 = \mu_3 = \mu_4 = \mu_5 = \mu_6 = 0$. Moreover, $\lambda_2(t) = \eta v(t)$ holds for a nontrivial interval, and thus $\dot{\lambda}_2(t) = \eta \dot{v}(t)$. Now (3.3) and (3.16) give $\eta b_r - \lambda_1 + \eta v r'(v) + \mu_7 = b_r - r(v) - g(s)$, which rewrites to

$$h(v) = -\lambda_1 + \eta v r'(v) + \mu_7 - (1-\eta) b_r + r(v) + g(s) = 0. \tag{3.24}$$

Like the driving regime CR1, we can prove that this equation results in a unique solution v_r for constant gradient. The derivatives of $h(v)$ are $h'(v) = r'(v) + \eta r'(v) + \eta v r''(v) > 0$ and $h''(v) = r''(v) + 2\eta r''(v) + \eta v r'''(v) > 0$, which indicate that $h(v)$ is an increasing convex function with a unique solution v_r. For the condition $v_r < v_{\max}$ and $\mu_7 = 0$, we can derive that the cruising speed must satisfy

$$\eta v_r r'(v_r) - \lambda_1 - (1-\eta) b_r + r(v_r) + g(s) = 0, \tag{3.25}$$

which indicates that v_r depends on λ_1 and $g(s)$, since r_0, r_1 and r_2 are constants. Again, we find a constant cruising speed v_r for constant gradients since we consider piecewise-constant gradients. In the case $v_r = v_{\max}$, μ_7 is defined by $\mu_7 = \lambda_1 + (1-\eta) b_r - r(v_{\max}) - \eta v_{\max} r'(v_{\max}) - g(s)$. During cruising by partial regenerative braking, the regenerative braking force is equal to the total train resistance in order to remain at a constant cruising speed v_b, i.e., $b_r = r(v_r) + g(s)$, which indicates that this regime can only occur on negative slopes.

5. **Maximum regenerative braking (MRB)** The fifth case occurs if $0 < \lambda_2 < \eta v$ with b_r minimal, i.e., $b_r = -\min(b_{r,\min}, \eta_r p_{r,\max}/v)$, and $f = 0$ and $b_m = 0$. From condition (3.19) and (3.21) it follows that $\mu_2 > 0$, $\mu_6 > 0$, and $\mu_1 = \mu_3 = \mu_4 = \mu_5 = 0$. Moreover, the speed is below the speed limit, thus, $\mu_7 = 0$. If $v = v_{\max}$, then the driving regime CR2 with maximum regenerative braking is applied.

6. **Cruising by maximum regenerative and partial mechanical braking (CR3)**. The sixth case is the third singular solution with $\lambda_2 = 0$ and $b_m \in [-b_{m,\min}, 0]$, $b_r = -\min(b_{r,\min}, \eta_r p_{r,\max}/v)$ and $f = 0$. Since $b_m < 0$ and $b_r < 0$, the conditions (3.19), (3.20) and (3.21) indicate that $\mu_1 = \mu_3 = \mu_4 = \mu_5 = 0$, $\mu_2 > 0$ and $\mu_6 > 0$. Moreover, $\lambda_2(t) = 0$ holds for a nontrivial interval, and thus $\dot{\lambda}_2(t) = 0$. Now (3.16) gives

$$\lambda_1 = b_r(\eta - \mu_6) + \mu_7. \tag{3.26}$$

Moreover, we consider the maximized Hamiltonian (3.13) leading to:

$$H = (\lambda_1 - \eta b_r)v. \tag{3.27}$$

The maximized Hamiltonian is constant on sections with constant gradient. Furthermore, λ_1 is constant for $\lambda_2 = 0$ due to (3.15). The Hamiltonian is independent of t and, therefore, the partial derivative to time is zero. Thus, (3.27) gives $\dot{\lambda}_1 v + (\lambda_1 - \eta b_r)\dot{v} = 0 + (\lambda_1 - \eta b_r)(b_r + b_m - r(v) - g(s)) = 0$. Then either the first factor must be zero or the second. In the first case, $\lambda_1 = \eta b_r$ and since λ_1 is a constant, so is b_r and then by (3.27) also speed is constant. In the second case, $b_r + b_m - r(v) - g(s) = 0$ and then by (3.3) speed is constant and then so is b_r by (3.27). In addition, (3.27) indicates that v depends on b_r which leads to a unique cruising speed v_m. If the speed is smaller than the speed limit ($v_m < v_{\max}$), then $\mu_7 = 0$ and $\mu_6 = \eta - \lambda_1/b_r$ by (3.26) and else $\mu_7 > 0$, $\mu_6 \geq 0$ and $v_m = v_{\max}$. During cruising with maximum regenerative and partial mechanical braking, the total braking force is equal to the total train resistance in order to remain at a constant cruising speed v_m, i.e., $b_m = r(v_m) + g(s) - b_r$, which indicates that this regime can only occur on negative slopes.

7. **Maximum braking (MB)** The seventh case is $\lambda_2 < 0$ with b_m and b_r minimal, and $f = 0$. From (3.21) follows $\mu_2 > 0$, $\mu_3 > 0$, $\mu_4 > 0$, and $\mu_6 > 0$. Moreover, since $f = 0$ from (3.21) follows $\mu_1 = \mu_5 = 0$. Furthermore, if the speed is below the speed limit, then $\mu_7 = 0$. If $v = v_{\max}$, then the sixth driving regime (CR3) with maximum total braking is applied bounded by (3.11).

The optimality conditions thus provide the following seven optimal driving regimes comparable to Baranov et al. (2011):

$$(\hat{f}(t), \hat{b}_r(t), \hat{b}_m(t)) =$$

$$\begin{cases} (f_{\max}(v(t)), 0, 0) & \text{if } \lambda_2(t) > v(t) & \text{(MA)} \\ (r(v(t)) + g(s), 0, 0) & \text{if } \lambda_2(t) = v(t) & \text{(CR1)} \\ (0, 0, 0) & \text{if } \eta v(t) < \lambda_2(t) < v(t) & \text{(CO)} \\ (0, r(v(t)) + g(s), 0) & \text{if } \lambda_2(t) = \eta v(t) & \text{(CR2)} \\ (0, -b_{r,\min}(v(t)), 0) & \text{if } 0 < \lambda_2(t) < \eta v(t) & \text{(MRB)} \\ (0, -b_{r,\min}(v(t)), r(v(t)) + g(s) - b_{r,\min}(v(t))) & \text{if } \lambda_2 = 0 & \text{(CR3)} \\ (0, -b_{r,\min}(v(t)), -(b_{\min} - b_{r,\min})) & \text{if } \lambda_2(t) < 0 & \text{(MB),} \end{cases} \tag{3.28}$$

where $b_{r,\min}(v) = -\min(b_{r,\min}, \eta_r p_{r,\max}/v)$. The first driving regime is maximum acceleration (MA) in which the train applies the minimum of the maximum specific traction force $f_{\max}$ and the maximum specific traction power (including

the traction efficiency η_f) divided by speed $\eta_f p_{f,\max}/v$. The train applies coasting (CO) by zero control, i.e., $f = b_r = b_m = 0$. The driving regime maximum regenerative braking (MRB) is applied to brake the train when the speed is below the optimal cruising speed, since then the train only uses the regenerative brakes in order to generate energy during braking. The maximum braking (MB) driving regime is used to brake as fast as possible and is used especially for low speeds, where regenerative braking does not generate (sufficient) energy or regenerative braking is not available (speeds close to zero). The other three driving regimes are cruising and all are singular solutions. If the solution satisfies $\lambda_2(t) = v(t)$ then the train is driving at a constant speed by using partial traction force in order to balance the total resistance (cruising partial traction, CR1). The second singular solution ($\lambda_2(t) = \eta v(t)$) is cruising by partial regenerative braking (CR2) in which the train applies the regenerative braking control in order to balance the total resistance, which might be needed at maximum speed with downhill slopes. The third singular solution ($\lambda_2 = 0$) consist of cruising by partial mechanical braking with maximum regenerative braking (CR3) in order to balance the total resistance. This holds for steep downhill slopes if regenerative braking alone is not sufficient to maintain the cruising speed. Note that the optimal control structure indicates that the mechanical braking control is only applied by the train in case that the regenerative braking control is insufficient to maintain an optimal cruising speed during steep downhill slopes (CR3) or during maximum braking (MB). The driving regimes with the switching points based on the costate λ_2 are the necessary optimality conditions. Algorithms like the pseudospectral method may be used to find the optimal sequence of the different driving regimes. In practice, energy-efficient train driving can be applied if the train is running on-time and the timetable provides sufficient running time supplements (Scheepmaker & Goverde, 2015). The general speed profile of the EETC-RMeB driving strategy for a flat track without varying speed limits and sufficient running time supplements is shown in Figure 3.2. Compared to mechanical braking only (see Section 3.2.3) or regenerative braking only (see Section 3.2.4), there are two different braking regimes consisting of maximum regenerative braking (MRB) and partial mechanical braking with maximum regenerative braking (CR3). In addition, we consider the nonlinear bounded regenerative braking behavior of the engine of the train.

3.2.3 Energy-efficient train control with constant-bounded regenerative braking only (RB)

In this section the EETC problem with just regenerative braking is discussed. Most research on EETC with regenerative braking considers no mechanical braking and just a constant maximal (regenerative) braking rate (Khmelnitsky, 2000; Franke et al., 2000; Albrecht et al., 2016a,b; Scheepmaker et al., 2020b). This is a

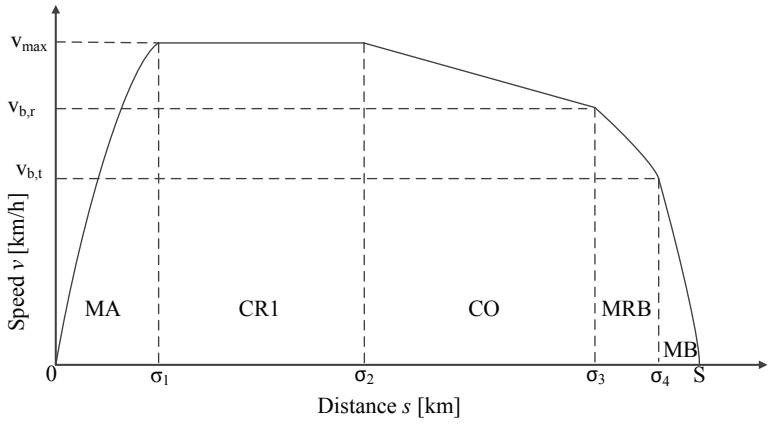

Figure 3.2: Speed profile of a basic energy-efficient driving strategy with regenerative and mechanical braking including switching points between driving regimes at σ_1, σ_2, σ_3, and σ_4 for a flat track without varying speed limits and sufficient running time supplements ($v_{\max}$ = optimal cruising speed, $v_{b,r}$ = speed at the start of the MRB regime, $v_{b,t}$ = speed at the start of the MB regime, MA = maximum acceleration, CR1 = cruising by partial traction, CO = coasting, MRB = maximum regenerative braking, and MB = maximum braking).

special case of the optimal control problem discussed in Section 3.2.2, with $b_m = 0$, without the nonlinear regenerative braking constraint (3.5). Therefore, the objective function is equal to (3.1), subject to the constraints (3.2)–(3.4) and (3.6)–(3.11). It can be shown that this leads to the following optimal control structure:

$$(\hat{f}(t), \hat{b}_r(t)) = \begin{cases} (f_{\max}(v(t)), 0) & \text{if } \lambda_2(t) > v(t) & \text{(MA)} \\ (r(v(t)) + g(s), 0) & \text{if } \lambda_2(t) = v(t) & \text{(CR1)} \\ (0,0) & \text{if } \eta v(t) < \lambda_2(t) < v(t) & \text{(CO)} \\ (0, r(v(t)) + g(s)) & \text{if } \lambda_2(t) = \eta v(t) & \text{(CR2)} \\ (0, -b_{r,\min}(v(t)) & \text{if } \lambda_2(t) < \eta v(t) & \text{(MRB).} \end{cases} \tag{3.29}$$

In this structure maximum braking (MRB) is achieved by applying the maximum regenerative braking force and cruising phase CR2 consists of partial regenerative braking. Therefore, the optimal driving regimes are similar to Section 3.2.2, with the only difference that the train applies only regenerative braking during the different braking regimes. Note that this driving strategy is normally not

possible in practice, since the train needs to apply mechanical braking for speeds around zero in order to brake to standstill. However, we consider this driving strategy, since it is used in literature and so we want to compare the difference between EETC with both regenerative and mechanical braking to EETC with only regenerative braking. For a simple flat track without varying speed limits and sufficient running time supplements, the optimal driving strategy for regenerative braking only is visualized in Figure 3.3 where now MB implies MRB as there is only one type of braking.

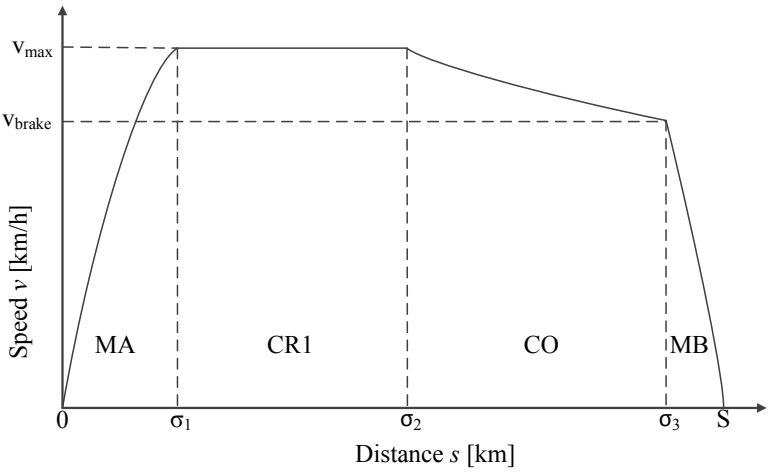

Figure 3.3: Speed profile of a basic energy-efficient driving strategy with regenerative or mechanical braking only including switching points between driving regimes at σ_1, σ_2 and σ_3 for a flat track without varying speed limits and sufficient running time supplements (MA = maximum acceleration, CR1 = cruising by partial traction, CO = coasting, and MB = maximum braking).

3.2.4 Energy-efficient train control with mechanical braking only (MeB)

In this section the EETC problem with only mechanical braking is discussed similar to for instance Howlett (2000) and Scheepmaker et al. (2020b). The optimal control problem is again a special case of the one as discussed in Section 3.2.2, with $b_r = \eta = 0$. This leads to the following objective function:

$$E = \min \int_0^T f(t)v(t)dt, \tag{3.30}$$

subject to the constraints (3.2)–(3.11). This leads to the following optimal control structure:

$$(\hat{f}(t), \hat{b}_m(t)) = \begin{cases} (f_{\max}(v(t)), 0) & \text{if } \lambda_2(t) > v(t) \quad \text{(MA)} \\ (r(v(t)) + g(s), 0) & \text{if } \lambda_2(t) = v(t) \quad \text{(CR1)} \\ (0, 0) & \text{if } 0 < \lambda_2(t) < v(t) \quad \text{(CO)} \\ (0, r(v(t)) + g(s)) & \text{if } \lambda_2(t) = 0 \quad \text{(CR3)} \\ (0, -b_{m,\min}(v(t))) & \text{if } \lambda_2(t) < 0 \quad \text{(MB).} \end{cases} \tag{3.31}$$

The regimes CR3 and MB are achieved by applying the mechanical brakes. Therefore, the optimal driving regimes are similar to Section 3.2.2, with the only difference that the train applies only mechanical during the different braking regimes. For a simple flat track without varying speed limits and sufficient running time supplements, the optimal driving strategy for mechanical braking only is visualized in Figure 3.3. Note that this structure is the same as for regenerative braking only (during MB now mechanical braking is applied instead of regenerative braking).

3.2.5 Minimum-time train control

In this section the minimum-time train control (MTTC) problem is briefly discussed based on the problem formulation defined in Section 3.2.2. The aim of this problem is to minimize total running time of the train t_f [s] which is free. The objective function T [s] is given by

$$\text{Minimize } T = t_f - t_0, \tag{3.32}$$

subject to the constraints (3.2)–(3.11) and the endpoint conditions

$$t_0 = 0, v(t_0) = 0, v(t_f) = 0, s(t_0) = 0, s(t_f) = S. \tag{3.33}$$

Applying an analysis of the necessary optimality conditions similar to Section 3.2.2 leads to the following optimal control structure

$$(\hat{f}(t), \hat{b}(t)) = \begin{cases} (f_{\max}(v(t)), 0) & \text{if } \lambda_2(t) > 0 \quad \text{(MA)} \\ (r(v_{\max}) + g(s), 0) & \text{if } \lambda_2(t) = 0 \text{ and } r(v_{\max}) + g(s) \le 0 \quad \text{(CR1)} \\ (0, r(v_{\max}) + g(s)) & \text{if } \lambda_2(t) = 0 \text{ and } r(v_{\max}) + g(s) > 0 \quad \text{(CR4)} \\ (0, -b_{\min}(v(t))) & \text{if } \lambda_2(t) < 0 \quad \text{(MB).} \end{cases} \tag{3.34}$$

The results indicate a single singular solution (cruising) in which the train applies traction (CR1) or braking force (CR4) in order to remain at the speed limit, depending on the sign of the resistance. The train may apply cruising by partial braking during downhill slopes. The results show that the train accelerates and brakes as fast as possible and remains at the maximum speed in order to minimize

the total running time. The optimal running strategy for a simple flat track without varying gradients is shown in Figure 3.4.

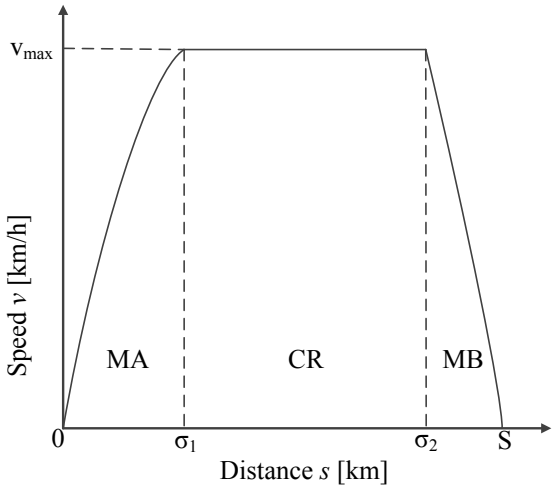

Figure 3.4: Speed profile of a basic minimum time control strategy with switching points between driving regimes at σ_1 and σ_2 for a flat track without varying speed limits (MA = maximum acceleration, CR = cruising, and MB = maximum braking).

In this case, we also have to consider the endpoint equations. The endpoint Lagrangian $\bar{E}$ [s] is

$$\bar{E}(s_f(t_f), v(t_f), t_f) = -t_f + \gamma_1(s(t_f) - S) + \gamma_2 v(t_f), \tag{3.35}$$

where γ_1 [s/m] and γ_2 [s^2/m] are Lagrange multipliers, with the complementary slackness conditions $\gamma_1(s(t_f) - S) = 0$ and $\gamma_2 v(t_f) = 0$. For the endpoint of the Hamiltonian we then have

$$\bar{H}(x_f(t_f), v(t_f), t_f) = -\frac{\partial \bar{E}}{\partial t_f} = 1. \tag{3.36}$$

Thus, the endpoint conditions indicate that the endpoint of the Hamiltonian H is equal to one.

3.3 Pseudospectral method

In this chapter the Radau Pseudospectral Method is applied in which orthogonal collocation at Legendre-Gauss-Radau (LGR) points is applied, which include the initial point. Details are given in of Rao et al. (2010a) and Garg et al. (2009) and the transcription of the optimal train control problem to a discretized nonlinear programming problem is given in P. Wang & Goverde (2016a). We selected the pseudospectral method, because this method can be applied for complex problems, is less sensitive to initial solutions, and no a priori knowledge is needed for the optimal control structure. There are different toolboxes available to solve the optimal control problem, like DIDO (Direct and Indirect Dynamic Optimization) (Ross & Karpenko, 2012; Ross, 2015), PSOPT (Becerra, 2010), and GPOPS (General Pseudospectral OPtimal Control Software) (Rao et al., 2010a). We have chosen for GPOPS (Version 4.1) since this can be applied as a toolbox in MATLAB and evaluation of the costates and Hamiltonian value is possible, to validate whether the results are in line with optimal control theory. The resulting Hamiltonian H and costate variable λ_1 should be constant when the gradient is constant.

We consider the multiple-phase pseudospectral method, where the trajectory consists of different phases. Each phase has its own cost function, dynamic, path and boundary constraints. The different phases are linked using linkage conditions and the total cost function is the sum of the individual cost functions of the different phases. Therefore, the total costs are minimized considering the different constraints within phases and the linkage conditions between phases. Within each phase we consider a constant speed limit and gradient, thus defining the phase boundaries. For the reference scenario without varying speed limits and gradients the model is reduced to the single-phase model. In this scenario we use a single-phase model with 200 collocation points, which was determined by trial-and-error and gave a good balance between the quality of the model results and the computation time. For the other scenarios we used the multiple-phase model where the number of collocation points and their distribution is determined by the algorithm of GPOPS. We refer to P. Wang & Goverde (2016a) for the derivation of the multiple-phase optimal train control problem. For this chapter, we extended the single-phase model developed by Scheepmaker & Goverde (2016) and Scheepmaker et al. (2020b) to a multiple-phase model and we applied it on a laptop with a 2.1 GHz processor and 8 GB RAM.

We use a smoothing function based on a moving average over the control to correct for the numerical oscillations in the pseudospectral approximations during the singular solution of cruising (oscillation of the control). In GPOPS the discretized optimal control is approximated by alternating discrete values around the optimal value with the same objective value as the smooth (feasible) control.

3.4 Results

In this section we apply the multiple-phase pseudospectral model on different cases in order to investigate the effect of different braking strategies (i.e., mechanical and regenerative braking). We have also validated that the model results are in line with the necessary optimality conditions. As illustration, we only show the validation process for the EETC-RMeB driving strategy in the reference scenario. We investigate different driving strategies. First, we have the minimum-time (MT) driving strategy, in which a train runs as fast as possible. Second, we consider the energy-efficient (EE) driving in which total traction energy consumption is minimized given the amount of running time supplements in the timetable. We investigate *combined nonlinear bounded regenerative and mechanical braking* (*RMeB*, see Section 3.2.2), *constant-bounded regenerative braking only* (*RB*, see Section 3.2.3) and *mechanical braking only* (*MeB*, see Section 3.2.4). Our main focus is to compare RMeB with MeB, but we also consider RB since this is used commonly in literature, e.g., Khmelnitsky (2000), Franke et al. (2000), and A. Albrecht et al. (2016a,b). Note that the difference between RMeB and RB is in the maximum braking rate. RMeB considers the regenerative and mechanical braking curve as shown in Figure 3.5 with a nonlinear bounded regenerative braking limited by the maximum braking force. Note that in situations for RMeB where the maximum regenerative braking force is insufficient (i.e., driving regimes CR3 and MB in (3.28)) the train applies additional mechanical braking in order to overcome the gap between the requested braking force and the maximum regenerative braking force. RB uses a constant maximum regenerative braking rate.

We applied the model to a Dutch case study between the stations of Utrecht Central (Ut) and 's-Hertogenbosch (Ht). The total length of the section is 48.531 km. We only consider the double-deck rolling stock type VIRM-6, which is operated by the Netherlands Railways (NS). The static train parameters of the Intercity (IC) train are shown in Table 3.1 and Figure 3.5. The specific parameters of (3.2)–(3.10), i.e., $p_{\max}$, $f_{\max}$, and $r(v)$, are computed by dividing the values of Table 3.1 by the total rotating mass. We assume that the accelerating train is similar to the regenerative braking train, which means that the traction efficiency for the regenerative braking train η_f is the same as for the accelerating train η_s, i.e., $\eta_f = \eta_s = 87.5\%$ (see Table 3.1). Moreover, the traction efficiency of converting electricity into mechanical energy happens to be the same as converting mechanical energy into electricity in the rolling stock data of NS (2020). Therefore, $\eta_f = \eta_r = 87.5\%$ (see Table 3.1). We assume that the Dutch catenary efficiency for the 1.5 kV DC network is equal to $\eta_c = 80\%$ (Scheepmaker & Goverde, 2016). The efficiency of the catenary is used when we consider regenerative braking. In this scenario we consider the energy used by the second (accelerating) train. Therefore, we assume that the total efficiency for regenerative braking energy up to

the traction energy for the accelerating train consists of $\eta = \eta_r \eta_c \eta_s = 0.6125$. After obtaining the relevant traction and braking forces, and speed over the trip by solving the optimal control problems as discussed in Section 3.2, PROMO [1] computes the total energy consumption of the train E [kWh] similar to Scheepmaker et al. (2020b) at the catenary by using

$$E(t) = (P_e + P_c)t, \tag{3.37}$$

with the powers computed by

$$P_e = \left(\frac{F}{\eta_f} + B_r \eta\right) v \text{ and } P_c = \left(\frac{P_e}{V}\right)^2 W, \tag{3.38}$$

where P_e [kW] is the traction power of the train, P_c [kW] is the power over the catenary, V [V] is the voltage, and W [Ω] is the resistance. In addition, we assumed that the average voltage over the catenary is $V = 1500$ V and the average resistance over catenary and tracks is $W = 0.1136$ Ω (Scheepmaker et al., 2020b). We also consider the regenerative braking power of the train P_r [kW] that limits the maximum regenerative braking force for the hyperbolic part in Figure 3.1, which is provided by the rolling stock data (NS, 2020).

We consider different scenarios in order to investigate if the model results of the multiple-phase model are in line with the necessary optimality conditions as discussed in Section 3.2. We begin with the reference case without any varying speed limits and gradients with 15% of running time supplements for the EE driving strategy by using the single-phase model. In this section we also compare the driving strategy RMeB with RB. We consider a long train run (Intercity train run between Ut and Ht) as well as a short train run (Sprinter (SPR) train run between Zaltbommel (Zbm) and Ht). Afterwards, we consider the real-life case for both the IC and SPR train run with the actual speed limit and gradients of the corridor Ut-Ht, also with rolling stock type VIRM-6 for the multiple-phase model. In total we consider four different scenarios, see Table 3.2.

3.4.1 Reference scenario

In this subsection the results of the reference scenario are discussed. We start with a non-stop Intercity train service between Ut and Ht (about 48.5 km). Afterwards, we consider a train run of a Sprinter train between the stops Zbm and Ht (about 14 km). Finally, a summary of the reference scenario is presented.

[1] PROMO (PseudospectRal Optimal train control MOdel) is a MATLAB prototype tool that computes the energy-optimal train trajectory (see Section 1.3.1).

Table 3.1: Basic parameters of a NS Intercity train rolling stock type VIRM-6 (NS, 2020).

Property	Notation	Value
Train mass [t]	m	391
Rotating mass supplement [%]	ρ	6
Max. traction power [kW]	P_e	2157
Max. regenerative power [kW]	P_r	3616
Max. traction force [kN]	F	213.9
Max. RB force [kN]	$-B_{r,\min}$	-142.5
Max. MeB force [kN]	$-B_{m,\min}$	-273.5
Max. braking deceleration [m/s^2]	$-b_{\min}$	-0.66
Min. speed limit for RB [km/h]	v_1	8
Max. speed limit [km/h]	$v_{\max}$	140
Train resistance [kN] (v: [km/h])	R	$5.8584+0.0206v+0.001v^2$
Efficiency of the engine [%]	η_f, η_r, η_s	87.5
Catenary efficiency 1.5 kV DC [%]	η_c	80.0

Legend: Max. = maximum, Min. = minimum, RB = regenerative braking, MeB = mechanical braking, and DC = direct current.

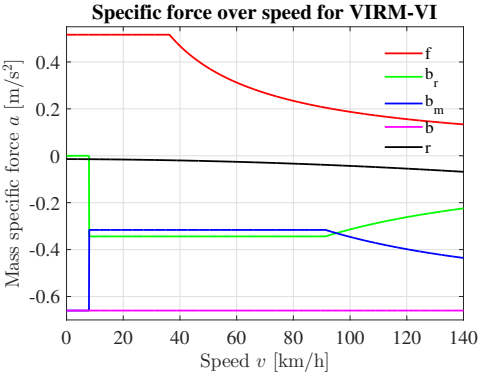

Figure 3.5: Mass-specific force-speed diagram for VIRM-VI (f: mass-specific traction force, r: mass-specific train resistance, b_r: mass-specific regenerative braking force, and b_m: mass-specific mechanical braking force).

Intercity train

The results of the different driving strategies can be found in Figures 3.6–3.9 and Table 3.2. The results of the EETC-RMeB driving strategy are in line with the necessary optimality conditions. First, Table 3.2 shows that the costate λ_1 and Hamiltonian H remain constant, since the gradient is constant as stated in (3.15).

Second, the relation between costate λ_2 and speed v is clearly visible in Figure 3.6 representing the necessary optimality conditions given by (3.28). We see that the train applies maximum acceleration (MA) if $\lambda_2 > v$. Afterwards, cruising (CR1) is applied if $\lambda_2 = v$, followed by coasting (CO) if $0 < \lambda_2 < \eta v$. After CO the train starts to apply maximum regenerative braking (MRB) for $0 < \lambda_2 < \eta v$, followed by maximum braking (MB) with combined mechanical and regenerative braking when $\lambda_2 < 0$. Note that cruising by partial braking does not occur, because there are no downward gradients in this scenario.

The energy consumption of MTTC-MeB is about 549 kWh. The difference between combined regenerative and mechanical braking with mechanical braking only is about 4.4%, and the difference between regenerative braking only versus mechanical braking only is about 9.4% in energy savings. This indicates that the unrealistic MTTC-RB overestimates the energy savings by 5 percent points. The structure of the optimal driving strategy is exactly the same, since the aim is to minimize total travel time. The model results are all generated in about 30 s.

The driving strategy of EETC-RMeB differs from both EETC-RB and EETC-MeB. The main difference betweeen EETC-RMeB and EETC-RB is that RB leads to a an overestimation of the energy savings of 1.0% by the unrealistic assumption of regenerative braking only at a constant braking rate. The RMeB driving strategy includes an extra maximum regenerative braking phase besides the maximum braking (see Figure 3.8 and 3.9) starting below 83 km/h with a deceleration rate of 0.34 m/s^2. Therefore, the train applies a higher cruising speed as well as a shorter coasting phase for RMeB compared to RB and, thus, the results of RMeB show a clear balance between the train applying coasting in order to save energy and regenerative braking in order to regenerate energy. Only at speeds below 27 km/h maximum braking (including mechanical braking) is applied at a deceleration rate of 0.66 m/s^2. Based on the output of the model we computed that the energy saving by regenerative braking in the maximum braking driving regime is 0.3% (1.1 kWh) compared to the total energy consumption. The time the train applies regenerative braking during the maximum braking regime is about 8 s. Therefore, for the EETC-RMeB driving strategy more energy saving can be achieved by coasting than by applying regenerative braking at speeds below 27 km/h. The energy savings of EETC-MeB, EETC-RB, and EETC-RMeB compared to MTTC-MeB are about 28.1%, 31.3%, and 30.6%. Finally, the model results of EETC-MeB, EETC-RB, and EETC-RMeB are generated within 41 s, 92 s, and 43 s.

Sprinter train

Figures 3.10–3.13 and Table 3.2 show the results of the different driving strategies for the Sprinter train. Table 3.2 indicates that costate λ_1 remains constant due

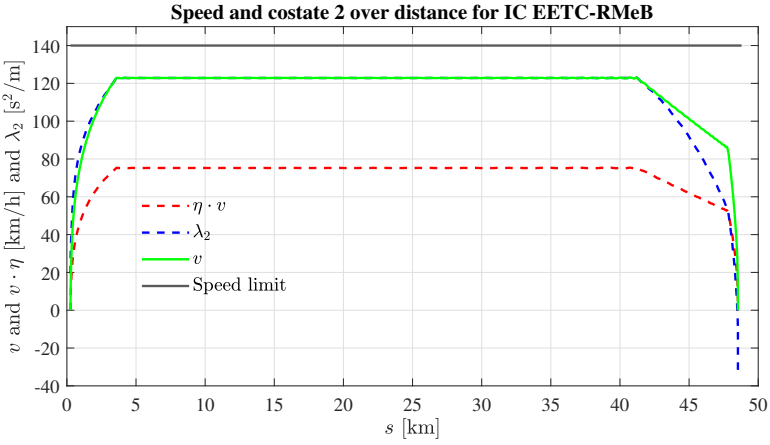

Figure 3.6: Validation of the reference scenario for the IC with the EETC-RMeB driving strategy by using the speed/costate λ_2-distance profile.

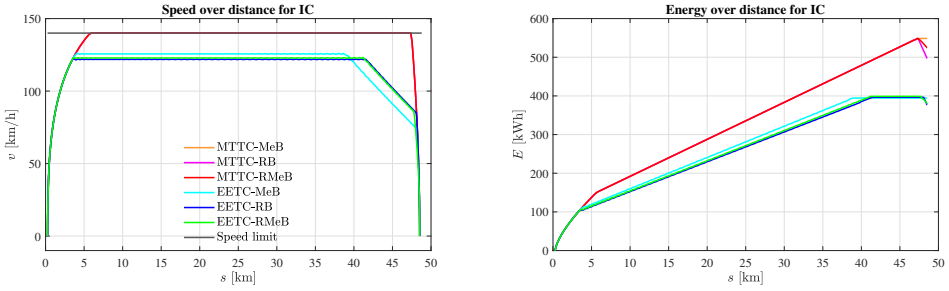

Figure 3.7: Reference scenario for the IC with the speed-distance profile (left) and energy-distance profile of the different driving strategies (right).

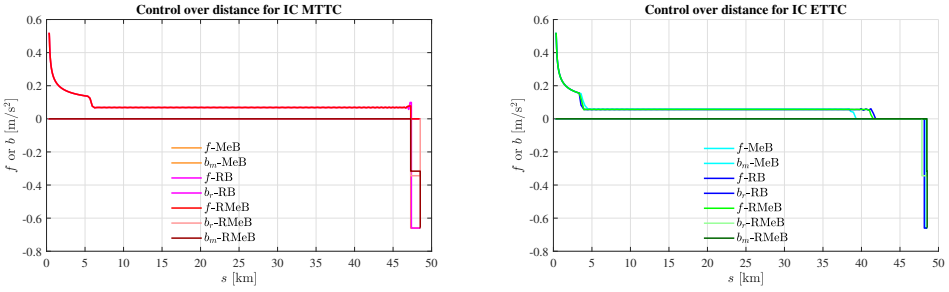

Figure 3.8: Reference scenario for the IC with the control-distance profile for the MTTC (left) and EETC (right) driving strategies.

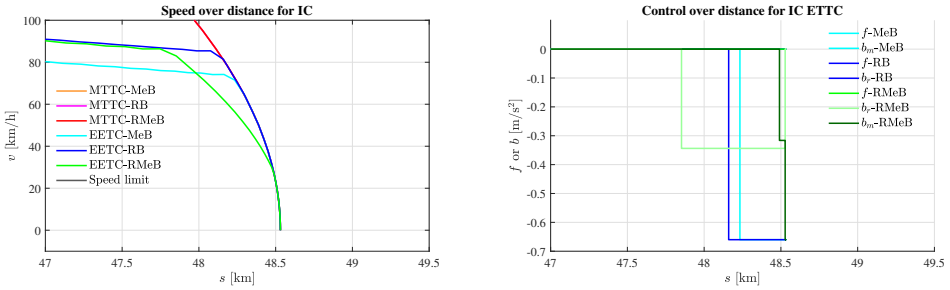

Figure 3.9: Reference scenario for the IC zoomed in for the braking behavior of the energy-efficient driving strategies with the speed-distance profile (left) and control-distance profile (right).

to the constant gradient as stated by (3.15). Costate λ_2 also behaves according to the necessary conditions given in (3.28) as can be seen in Figure 3.10, $\lambda_2 > v$ during the driving regime MA, $\lambda_2 = v$ during cruising (CR1), $\eta v \leq \lambda_2 \leq v$ during CO, $0 \leq \lambda_2 \leq \eta v$ during RMB, and $\lambda_2 < 0$ during MB. The Hamiltonian remains constant. The MTTC-MeB driving strategy uses about 220 kWh. The MTTC-RMeB leads to energy savings of about 11% compared to MTTC-MeB. MTTC-RB leads to the unrealistic highest savings of 23%. The results are generated in 40 s (MTTC-MeB), 39 s (MTTC-RB), and 39 s (MTTC-RMeB).

The results of the shorter train route for the EE driving strategies indicate a clear difference in the optimal speed profile for the different braking strategies. EETC-RMeB and EETC-RB driving strategy have a short cruising phase, which is not included for the EETC-MeB driving strategy. In addition, the coasting phase is shorter for both regenerative braking strategies compared to EETC-MeB, which leads to a higher speed at the beginning of the braking phase. The difference between EETC-RB and EETC-RMeB is that the cruising speed for EETC-RMeB is higher, the coasting phase is shorter and the speed at the beginning of the braking phase is higher. In addition, the EETC-RMeB includes a phase of maximum regenerative braking only at speeds below 89 km/h with a deceleration rate of 0.34 m/s^2, and at speeds below 32 km/h the train applies maximum braking at 0.66 m/s^2 including mechanical braking. Note that below $v_1 = 8$ km/h maximum braking is applied by mechanical braking only, see Table 3.1. Like the Intercity train the results of the Sprinter train indicate that it is more efficient to start coasting earlier instead of applying regenerative braking only at speeds below 32 km/h.

The EETC-MeB leads to a energy saving of 39.6% compared to MTTC-MeB. EETC-RMeB increases the energy savings by 11.2% compared to EETC-MeB (46.3% energy savings compared to MTTC-MeB). EETC-RB would save up to 48.4% energy. The computation time of the EE driving strategies are about 32 s (EETC-MeB), 31 s (EETC-RB), and 34 s (EETC-RMeB).

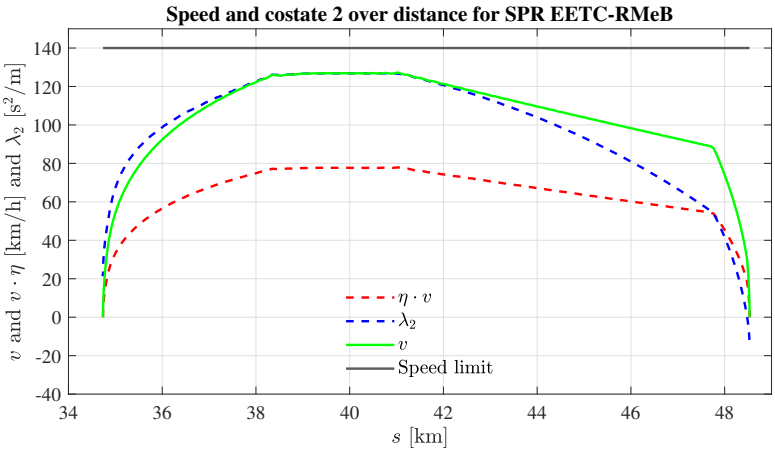

Figure 3.10: Validation of the reference scenario for the SPR with the EETC-RMeB driving strategy by using the speed/costate λ_2-distance profile.

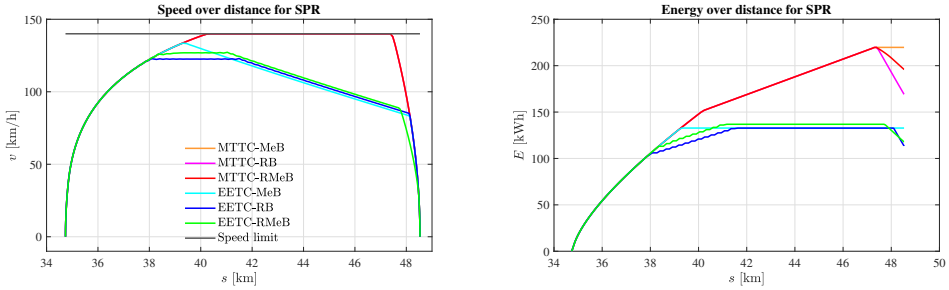

Figure 3.11: Reference scenario for for the SPR with the speed-distance profile (left) and energy-distance profile of the different driving strategies (right).

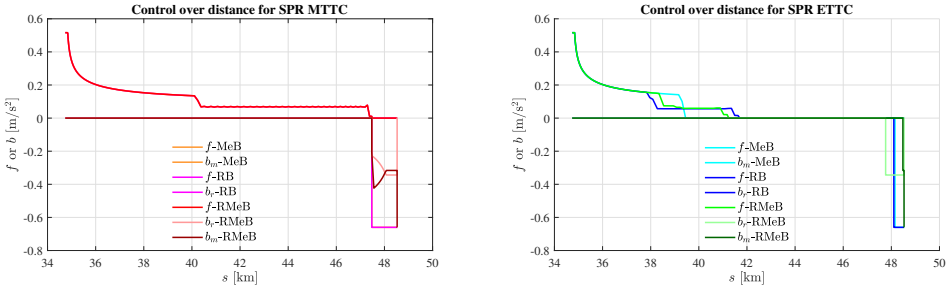

Figure 3.12: Reference scenario for the SPR with the control-distance profile for the MTTC (left) and EETC (right) driving strategies.

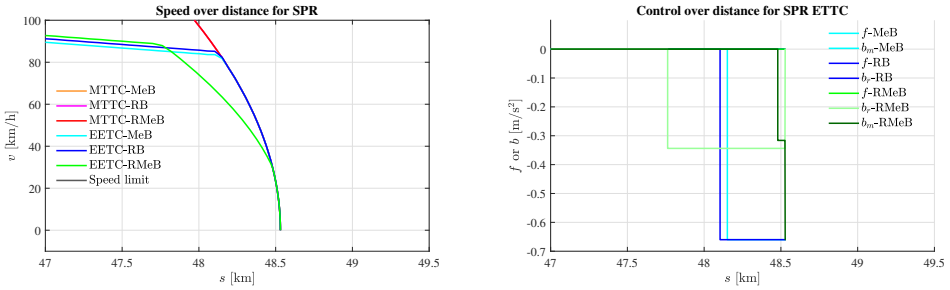

Figure 3.13: Reference scenario for the SPR zoomed in for braking behavior of the energy-efficient driving strategies with the speed-distance profile (left) and control-distance profile (right).

Summary reference scenario

When using regenerative braking (RMeB or RB) for the IC trip the cruising speed is lower, the cruising phase is longer, the coasting phase is shorter and the start of the braking speed is higher compared to pure mechanical braking. For the shorter train route (SPR), regenerative braking leads to a cruising phase, while mechanical braking directly starts to coast after maximum acceleration. The main difference between the driving strategies RMeB and RB for both the long and short trips is that RMeB has a higher cruising speed, a shorter coasting phase and an extra braking phase (maximum regenerative braking) compared to RB, which indicates a balance between coasting and regenerative braking, and mechanical braking is only used for maximum braking. RB overestimates the energy savings compared to RMeB. The results also indicate that the relative energy savings are higher for the shorter trip compared to the longer trip, since the coasting phase is relatively large compared to the other driving regimes.

3.4.2 Real-life case scenario

In this subsection we apply our model on a real-life case study for the train route between Utrecht Central and 's-Hertogenbosch in the Netherlands. We consider 10% running time supplements for the energy-efficient driving strategy. We start with the IC trip of about 48.5 km (Ut-Ht) followed by the SPR trip of about 14 km (Zbm-Ht). Finally, the summary of the case scenario is provided.

Intercity train route

The results of the different driving regimes are shown in Figures 3.14–3.16 and Table 3.2. The energy consumption of MTTC-MeB is about 420 kWh. MTTC-RMeB can lead up to 19.7% extra energy savings. MTTC-RB would lead to extra

energy savings of 14.6% compared to MTTC-RMeB. The computation time of the algorithm is about 164 s for the MTTC-MeB driving strategy, 279 s for the MTTC-RB driving strategy, and 255 s for the MTTC-RMeB driving strategy.

The speed profile of EETC-RMeB differs from EETC-MeB, see Figure 3.14 for the complete trajectory and Figure 3.16 shows specific details for the braking driving regimes by zooming in. The main differences are that the cruising speed is lower, the coasting phase is shorter and the speed at the beginning of the braking phase is higher. The difference between the EETC-RMeB and EETC-RB driving strategy is quite small. The main differences occur during braking as can be seen in the control-distance plots in Figure 3.15. The RMeB driving strategy includes a phase of pure regenerative braking (RMB driving regime) and only at the final braking stage mechanical braking is added to apply maximum braking (MB) for speeds below 20 km/h. The speed and control plots indicate that the train starts to brake earlier with the EETC-RMeB driving strategy compared to the other EE driving strategies. The EETC-MeB driving strategy leads to energy savings of 42.2% compared to MTTC-MeB, and EETC-RMeB can save even 14.5% more energy compared to EETC-MeB (50.6% compared to MTTC-MeB). EETC-RB would lead to the highest energy savings compared to MTTC-MeB of 51.4%. The computation time of EETC-MeB is about 409 s, EETC-RB is about 546 s, and EETC-RMeB takes about 466 s.

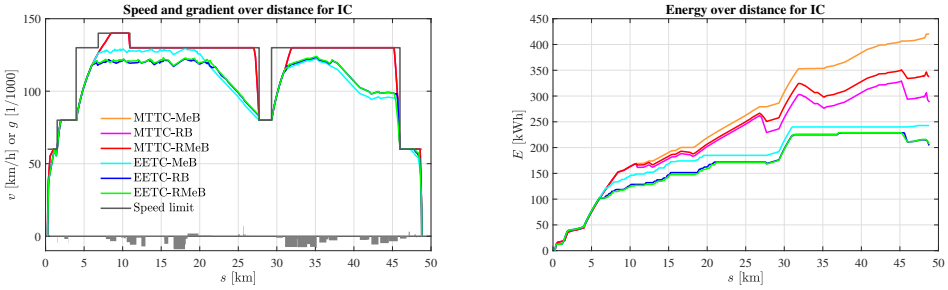

Figure 3.14: Real-life case scenario for the IC (Ut-Ht) with the speed/gradient-distance profile (left) and energy-distance profile of the different driving strategies (right). The grey area in the left figure indicates the gradients [‰].

Sprinter train route

We apply the model also for a Sprinter route between Zaltbommel and 's-Hertogenbosch with the same IC rolling stock. The results of the different driving strategy can be found in Figures 3.17–3.19 and Table 3.2. The energy consumption of MTTC-MeB is about 151 kWh. The MTTC-RMeB driving strategy can save

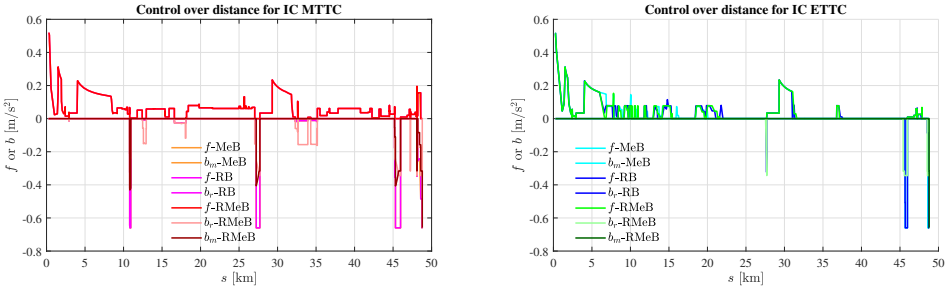

Figure 3.15: Real-life case scenario for the IC (Ut-Ht) with the control-distance profile for the MTTC (left) and EETC (right) driving strategies.

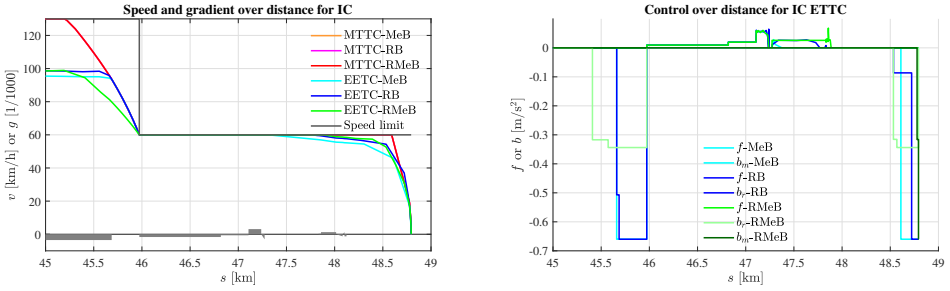

Figure 3.16: Real-life case scenario for the IC (Ut-Ht) zoomed in between 45 km and 49 km for the braking behavior of the energy-efficient driving strategies with the speed/gradient-distance profile (left) and control-distance profile (right). The grey area in the left figure indicates the gradients [‰].

up to 16.1% compared to MTTC-MeB driving strategy, while the MTTC-RB driving strategy can save 31.2% compared to the MTTC-MeB driving strategy. The computation time of the model is 20 s for MTTC-MeB, 28 s for MTTC-RB, and 25 s for MTTC-RMeB.

The energy savings of EETC-MeB are about 40.7% compared to MTTC-MeB. EETC-RMeB can even lead to 55.5% savings compared to MTTC-MeB. EETC-RB would reach energy savings of even 58.6% compared to MTTC-MeB. The biggest difference in the EE driving strategies is between mechanical braking and the other braking strategies. EETC-RMeB accelerates to a higher maximum speed, has a shorter coasting phase and a regenerative braking phase, while mechanical braking is only added at speeds below 25 km/h, see the complete trajectory in Figure 3.17 and Figure 3.18, and for the details of the different braking regimes (by zooming in) see Figure 3.19. The control-distance plots in Figures 3.18 and 3.19 clearly indicate that the EETC-RMeB driving strategy starts the earliest with the braking around 45 km, while the other EE driving strategies starts by applying maximum braking around 45.5 km. The same observations of the difference in braking behavior can be seen around 48.5 km.

Again the resulting speed profiles of EETC-MeB and EETC-RMeB are different, due to the different braking behavior since during braking. EETC-RMeB saves relatively a large amount of energy by regenerative braking compared to the total energy of the trip. During the downhill sections in the coasting phase, the train maintains its speed. In addition, the EETC-MeB and EETC-RB speed profile are almost equal, except at the end of the trip (around 47.5 km) where EETC-MeB is focused on coasting while EETC-RB is focused on both coasting and regenerative braking. The computation time of EETC-MeB is about 53 s, EETC-RB is about 76 s, and EETC-RMeB takes about 57 s.

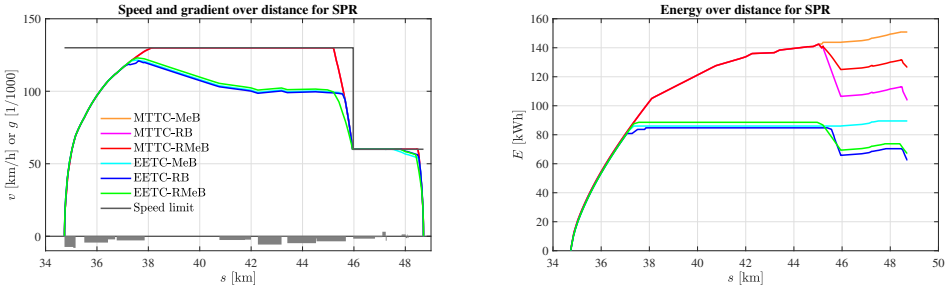

Figure 3.17: Real-life case scenario for the SPR (Zbm-Ht) with the speed/gradient-distance profile (left) and energy-distance profile of the different driving strategies (right). The grey area in the left figure indicates the gradients [‰].

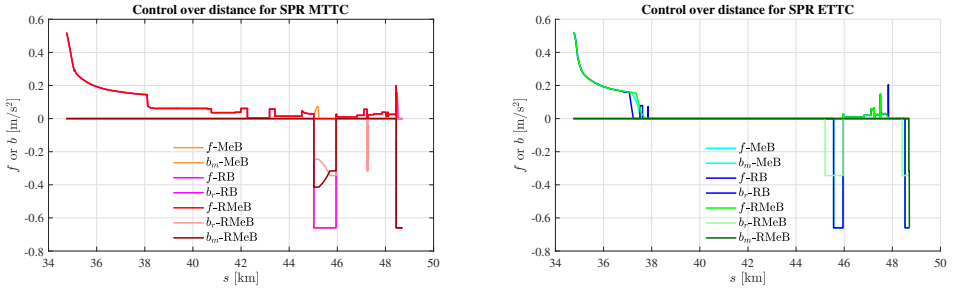

Figure 3.18: Real-life case scenario for the SPR (Zbm-Ht) with the control-distance profile for the MTTC (left) and EETC (right) driving strategies.

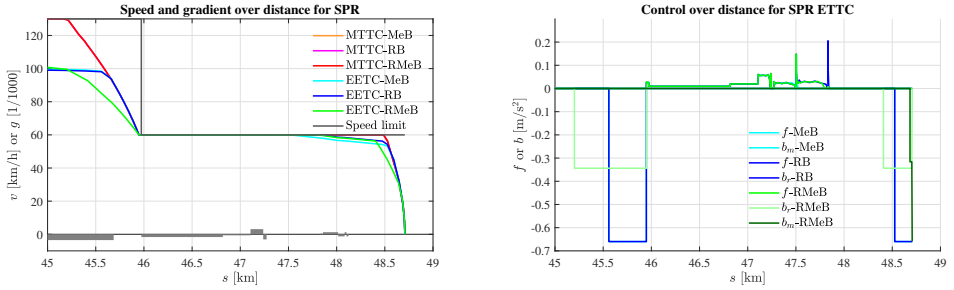

Figure 3.19: Real-life case scenario for the SPR (Zbm-Ht) zoomed in between 45 km and 49 km for the braking behavior of the energy-efficient driving strategies with the speed/gradient-distance profile (left) and control-distance profile (right). The grey area in the left figure indicates the gradients [‰].

Summary real-life case

The application of the different driving strategies in the two real-life cases shows that the braking behavior does influence the structure of the optimal speed profile. In general, the EETC-RB driving strategy leads to the highest energy savings, followed by EETC-RMeB, because during braking energy is regenerated. For the IC case the EETC-RMeB and EETC-RB speed profile are different compared to the EETC-MeB driving strategy. Including (partly) regenerative braking in the EE driving strategy leads to a lower optimal cruising speed, shorter coasting and a higher speed at the beginning of the braking phase. EETC-RMeB applies an earlier braking compared to EETC-RB and only uses maximum braking at the end of the trip (braking for standstill). For the SPR case the driving regime of EETC-RMeB is different compared to EETC-MeB and EETC-RB (EETC-MeB and EETC-RB are quite similar). EETC-RMeB has a higher maximum speed, a shorter coasting phase and a higher speed at the beginning of the braking phase compared to the other EE driving strategies. Finally, the shorter distance scenario (SPR) between stops indicates relatively higher energy savings by the EE driving strategies compared to the longer distance IC scenario, because the coasting phase is a significant part of the total driving strategy. The findings of the real-life case are consistent with the general findings of the reference case.

Table 3.2: Main results of the different scenarios.

Scenario	Figure	Trip time (s)	Running time supplements (%)	Energy consumption (kWh)	Energy saving (%)	Maximum speed (km/h)	Q	N	Costate variable λ_1	Hamiltonian H	Computation time (s)
Reference IC MTTC-MeB	3.7–3.9	1336	0	548.6	0	140.0	1	200	0.026	1.00	30.3
Reference IC MTTC-RB	3.7–3.9	1336	0	496.9	9.4	140.0	1	200	0.026	1.00	30.7
Reference IC MTTC-RMeB	3.7–3.9	1336	0	524.5	4.4	140.0	1	200	0.026	1.00	22.5
Reference IC EETC-MeB	3.7–3.9	1537	15	394.5	28.1	126.1	1	200	0.141	2.88	40.3
Reference IC EETC-RB	3.7–3.9	1537	15	376.9	31.3	122.5	1	200	0.114	2.63	91.2
Reference IC EETC-RMeB	3.6–3.9	1537	15	380.8	30.6	123.2	1	200	0.136	2.69	42.3
Reference SPR MTTC-MeB	3.11–3.13	450	0	219.7	0	140.0	1	200	0.026	1.00	39.3
Reference SPR MTTC-RB	3.11–3.13	450	0	169.2	23.0	140.0	1	200	0.026	1.00	38.7
Reference SPR MTTC-RMeB	3.11–3.13	450	0	196.1	10.8	140.0	1	200	0.026	1.00	38.9
Reference SPR EETC-MeB	3.11–3.13	517	15	132.8	39.6	133.5	1	200	0.169	3.91	32.2
Reference SPR EETC-RB	3.11–3.13	517	15	113.4	48.4	122.9	1	200	0.135	2.67	30.7
Reference SPR EETC-RMeB	3.10–3.13	517	15	117.9	46.3	127.2	1	200	0.143	2.96	33.8
Real-life case IC MTTC-MeB	3.14–3.16	1618	0	420.2	0	140.0	78	4–12	pwc	pwc	164.0
Real-life case IC MTTC-RB	3.14–3.16	1618	0	288.2	31.4	140.0	78	4–12	pwc	pwc	279.0
Real-life case IC MTTC-RMeB	3.14–3.16	1618	0	337.3	19.7	140.0	78	4–12	pwc	pwc	255.2
Real-life case IC EETC-MeB	3.14–3.16	1780	10	242.8	42.2	129.5	78	4–12	pwc	pwc	408.9
Real-life case IC EETC-RB	3.14–3.16	1780	10	204.1	51.4	123.5	78	4–12	pwc	pwc	545.6
Real-life case IC EETC-RMeB	3.14–3.16	1780	10	207.6	50.6	124.1	78	4–12	pwc	pwc	465.6
Real-life case SPR MTTC-MeB	3.17–3.19	545	0	150.9	0	130.0	38	4–12	pwc	pwc	20.0
Real-life case SPR MTTC-RB	3.17–3.19	545	0	103.8	31.2	130.0	38	4–12	pwc	pwc	28.4
Real-life case SPR MTTC-RMeB	3.17–3.19	545	0	126.6	16.1	130.0	38	4–12	pwc	pwc	24.7
Real-life case SPR EETC-MeB	3.17–3.19	599	10	89.5	40.7	121.6	38	4–12	pwc	pwc	53.1
Real-life case SPR EETC-RB	3.17–3.19	599	10	62.5	58.6	121.0	38	4–12	pwc	pwc	75.7
Real-life case SPR EETC-RMeB	3.17–3.19	599	10	67.2	55.5	123.0	38	4–12	pwc	pwc	56.8

Legend: Q = number of phases, N = number of collocation points per phase, pwc = piecewise constant, IC = Intercity, SPR = Sprinter, MTTC = minimum time train control, EETC = energy-efficient train control, MeB = mechanical braking, RB = constant-bounded regenerative braking, RMeB = nonlinear bounded regenerative and mechanical braking.

3.5 Conclusion

This chapter investigated the difference between mechanical and regenerative braking on the energy-efficient driving strategy using a multiple-phase pseudospectral optimal train control method for a single train. We model regenerative braking using the physical nonlinear bounded braking-speed functional relation, which could be supported by mechanical braking when needed, and compare this with pure mechanical braking and pure constant-bounded regenerative braking as is common applied in the literature. We derived the necessary optimality conditions for the energy-efficient driving strategy with mechanical and/or regenerative braking. The optimal control problems were solved using the multiple-phase pseudospectral method. We applied the models on different scenarios where we investigated the effect of the varying speed limit and gradients on the driving strategies.

The main differences between regenerative braking and pure mechanical braking for the EE driving strategies are that regenerative braking EE driving strategies apply a lower optimal cruising speed and have a higher speed at the beginning of the braking phase. For shorter distances EETC-MeB does not have a cruising phase, while EETC-RMeB and EETC-RB do have a cruising phase. The main difference between EETC-RMeB and EETC-RB is that the EETC-RMeB driving strategy considers the nonlinear bounded regenerative braking force diagram with possible additional mechanical braking in order to compensate regenerative braking (for example at low speeds), while EETC-RB considers only a constant regenerative braking. This leads to a higher cruising speed, a shorter coasting phase and a longer braking phase for EETC-RMeB. Therefore, current literature that focused on a constant regenerative braking rate overestimates the energy savings gained by regenerative braking and does not compute to the optimal trajectory in practice for regenerative braking trains. Finally, the relative energy savings for the EE driving strategies are higher for shorter distances, because coasting is relatively the longest driving regime for short train routes and cruising becomes more significant for the longer train routes. Future research on regenerative braking for EETC will focus on the interaction with the neighboring trains including factors such as the driving strategy of the surrounding train, the distance between the synchronizing trains and the maximum allowable voltage of the power supply system.

Chapter 4

Comparing train driving strategies on multiple key performance indicators

---

Apart from minor updates, this chapter has been published as:
Scheepmaker, G. M., Willeboordse, H. Y., Hoogenraad, J. H., Luijt, R. S., Goverde, R. M. P. (2020) Comparing train driving strategies on multiple key performance indicators, *Journal of Rail Transport Planning & Management*, 13, 100163.

4.1 Introduction

Energy consumption is one of the focus points of modern day train operation. In the last decade, almost every train operating company (TOC), and freight operating company (FOC) has taken measures to diminish its carbon footprint, and to save energy. These measures are meant to make rail transport more eco-friendly and cost effective (Luijt et al., 2017). The driving behaviour of the driver has a large impact on energy consumption during train trips. TOCs and FOCs therefore promote energy-efficient driving, and educate their drivers in one or more eco-driving strategies. However, there are more *key performance indicators* (*KPIs*) than energy consumption that determine the performance of train operation. In this study we aimed at determining a set of SMART (i.e., specific, measurable, assignable, realistic and time-related (Doran, 1981)) KPIs relevant to train operation, that are influenced by the driving strategy of the driver. Those KPIs are safety, timeliness, energy consumption, workload of the driver, the environment, cost of maintenance, and the brand image of a TOC. We did a

literature review on KPIs relevant to train operation, but we did not find relevant papers. Therefore, we used the basic KPIs at NS as guidance and extended them by interviewing different experts at NS.

We chose four of the most used train driving strategies to study the effect of the driving strategy on our set of KPIs. The first two are the main eco-driving strategies which are applied by drivers in everyday practice: the *maximal coasting* (*MC*) strategy, which applies maximum speed until coasting, and the *reduced maximum speed* (*RMS*) strategy, which applies an optimal cruising speed and no coasting. Drivers apply any variation of these two strategies, either or not supported by a *driver advisory system* (*DAS*). We also included the *energy-efficient train control* (*EETC*) strategy, which calculates the optimal eco-driving strategy per train trip, and combines coasting and cruising. This strategy is described in multiple studies (Albrecht et al., 2016a,b; Howlett & Pudney, 1995; Howlett, 2000; Khmelnitsky, 2000; Liu & Golovitcher, 2003; Lu et al., 2013). A review of energy-efficient train control can be found in Scheepmaker et al. (2017). The fourth driving strategy is the *minimum time train control* (*MTTC*) strategy. In this strategy the driver minimizes the total running time by driving as fast as possible. While this is not an eco-driving strategy, it is often used to make up for lost time in case of a delay. This driving strategy is mostly used in the literature as a reference scenario (see A. Albrecht et al. (2016a,b) and Scheepmaker & Goverde (2015, 2016)).

The main contributions of this chapter are:

- The definition of a toolbox of KPIs, that can be used to determine the most appropriate driving strategy for a specific TOC or FOC, or even for a specific part of the track.
- A broader view on the effect of train driving strategies, by studying the effect on a set of KPIs relevant to train operation.
- A comparison of eco-driving strategies not only to MTTC, but also to each other.
- Elaborate multiple case studies based on several characteristics (e.g., track length, gradients) and conditions (e.g., speed restrictions, load factor) on three types of rolling stock (i.e., Intercity/long distance, Sprinter/regional and freight).

Although, we are aware that there are many DASs available (see Panou et al. (2013)), based on one or more driving strategies, we refrained from using a DAS in this study. First of all, because the purpose of this study was to establish a toolbox of KPIs to measure the performance of train operation and not to compare the effectiveness of DASs, although it can be used for this. Besides that, in practice it has been shown that significant energy savings can be accomplished by

implementing an eco-driving strategy without the use of a DAS (see Luijt et al. (2017)) and lastly, because we wanted to make an objective comparison between the driving strategies on the KPI workload. Although we admit that it is difficult to apply a driving strategy such as EETC without a DAS.

We applied a mathematical model for different driving strategies based on the optimal control theory. Most of our test scenarios were based on the actual situation at the largest Dutch TOC, the Netherlands Railways (NS or in Dutch: *Nederlandse Spoorwegen*).

In this chapter we first describe the KPIs studied, together with the evaluation criteria used to measure these KPIs (Section 4.2). In Section 4.3 the driving strategies, and the main model used in this chapter are described. This section also includes an explanation on how we solved the optimal train control problem. In Section 4.4 we present our test scenarios, with the key characteristics and conditions on which they are based. We then present our results in Section 4.5. Our interpretation of these results, and the impact of the results will be discussed in Section 4.6. We will conclude this chapter by highlighting the main conclusions based on the findings in this study (see Section 4.7).

4.2 Key performance indicators and evaluation criteria

In this section we describe the set of SMART KPIs, that are relevant to train operation, and that can be influenced by the driving strategy. This set consists of seven KPIs, of which the first three KPIs are the most important for train operation. They are presented in descending order of importance (Clements et al., 2011) in this section: safety (see Section 4.2.1), timeliness (see Section 4.2.2), energy consumption (see Section 4.2.3), workload of the driver (see Section 4.2.4), cost of maintenance (see Section 4.2.5), the environment (see Section 4.2.6), and the brand image of a TOC (see Section 4.2.7). Although the KPIs are selected based on SMART criteria, the T (time-related) of SMART does not apply so much in the process of finding a SMART set of KPIs for train operation. Per KPI we describe the evaluation criteria and the methods used (except for the main method which is described in Section 4.3) to measure these KPIs in this section.

We evaluated the KPI passenger and train conductor comfort during this study as well. However, we found that this KPI does not depend on the driving strategy, because the maximal acceleration and deceleration are the same for all driving strategies in our test scenarios, and the maximum speed hardly differs. Therefore, this KPI is not mentioned further in this chapter. Table 4.1 gives an overview of the different KPIs and evaluation criteria used in this chapter.

Table 4.1: KPIs and evaluation criteria.

KPI	Evaluation Criteria
Safety	Distance remaining (between first and final braking regime) Time remaining (between first and final braking regime)
Timeliness	Deviations from planned time of arrival
Energy consumption	Total amount of energy
Workload	Total interference score
Environment	Average pass-by noise Wear of braking blocks
Cost of maintenance	Wear of braking blocks
Brand image	Risk of unplanned stops

4.2.1 Safety

We defined safety as the absence of the risk of causing a railway accident (Era, 2016). In this chapter we focused on signals passed at danger (SPAD), one of the most common events preceding a railway accident. Note that we only measured this risk for conventional automatic train protection (ATP) systems such as the Dutch NS '54/ATB system. We assumed that under ETCS L2 with continuous braking curve supervision, this risk does not exist. In agreement with NS safety experts we evaluated the KPI safety by choosing the distance and time between the end of the first braking regime (after an unplanned signal passed at warning (SPAW)), and the beginning of the following braking regime (needed to come to a full stop in front of the red signal) as our evaluation criteria. After the SPAW the driver needs to decelerate to a speed of 40 km/h with a minimal ATP enforced braking deceleration of 0.43 m/s^2. For the signal at danger (SAD), a minimum braking deceleration of 0.5 m/s^2 is required. For most of the test scenarios in this chapter, we assumed that the arrival of the test train was not hindered by a previous train at the arrival platform. The KPI safety is not of influence in these scenarios, since there is no unplanned SPAW. In order to study the effect on the KPI safety we introduced a so called platform clearing scenario (see scenario 6.2 in Table 4.4), in which the test train under NS '54/ATB is hindered by a previous train, that has not left the arrival platform. This results in an unplanned SPAW for the test train. The results of this scenario are described in a separate Section 4.5.7.

4.2.2 Timeliness

Timeliness is defined as the ability to depart and arrive exactly to the second of the planned time. Note that we did not use the KPI punctuality, which is defined as arrival or departure within a specified number of minutes of the designated timetable time (see Olsson & Haugland (2004)). At NS for instance, trains are

considered to be punctual if their departure or arrival time is within three minutes (180 seconds) of the planned time. Per train trip we determined the deviation from the designated timetable time in seconds.

4.2.3 Energy consumption

Energy consumption is defined as the use of the least possible amount of energy to complete a train run. We measured this by determining the total amount of energy (in kWh) per train trip i.e., the amount of traction energy used (including electrical losses), minus the amount of regenerative energy gained by braking. The use of, for instance, auxiliary power was excluded from our study, because this is not related to, or influenced by the driving strategy. Since not all the rolling stock of NS is equipped with regenerative brakes we added one test scenario with mechanical braking. We compute the total energy consumption E [kWh] at the catenary by using

$$E = (P_t + P_c)t, \tag{4.1}$$

with the powers computed by

$$P_t = Fv/\eta \tag{4.2}$$

$$P_c = (P_t/V)^2 R, \tag{4.3}$$

where P_t [kW] is the traction power of the train, P_c [kW] is the power over the catenary, t [s] is the time, F [N] is the traction force, v [m/s] is the speed, η [-] is the traction efficiency, V [V] is the voltage, and R [Ω] is the resistance. We consider the Dutch 1.5 kV DC catenary network with an average resistance over catenary and tracks of 0.1136 Ω. For stability of the calculations, we fixed the voltage at the pantograph on 1.5 kV, and added the dissipated power. In this way, the maximal tractive force remains unchanged, and iterations in the calculations were avoided.

4.2.4 Workload

In RSSB (2008, p.125) the workload of the train driver is defined as follows: "Workload refers to the effort demanded from people by the tasks they have to do", and on the same page the following statement is made: "Workload is a problem for safety-critical operations if it's too low - and an even bigger one if it's too high." We evaluated this KPI by measuring the total interference score (TIS) per driving strategy, using the multiple resource model by Wickens (Horrey & Wickens, 2004; Wickens, 2002). We then compared the TISs of different driving strategies to each other. Note that we concentrated on differences in driving strategies, and therefore excluded tasks that are common to all driving strategies such as monitoring signs.

In order to make a valid comparison between driving strategies we assumed that the driver does not use any form of electronic DAS. We are aware that without the use of such a device, a high level of memorization of routes and circumstances is needed to comply with both timeliness and energy consumption. Furthermore, we assumed that the driver in our study is an experienced driver with sufficient route knowledge.

In order to determine the workload we first defined the tasks of the driver, and the order in which these tasks are carried out. For this purpose we used a hierarchical task analysis (based on RSSB (2008)). The initial results of this analysis were based on the expert judgment of the authors, and later verified by two expert drivers.

First we defined the goal per scenario. For the standard (golden) run, i.e., the reference scenario, the goal is: "Driving a train from A to B" (from the moment the driver prepares for driving, until the moment the train comes to a full stop at the next station). Secondly, we defined the starting points of the driving regimes as subgoals, since these are the points at which the driver has to perform one or more tasks. We then made a breakdown of these subgoals into tasks, and determined the order of the tasks, the situation or time the task would be carried out, and the precondition(s) of the task per driving strategy. Note that the workload analysis was only performed on test scenarios besides the reference scenario, which are of influence on workload (e.g., not on scenarios concerning load or mechanical braking see test scenarios in Section 4.5). We used the multiple resource model by Wickens (see Wickens (2002) and Horrey & Wickens (2004)) to determine the total task interference per driving strategy. This model is suitable for the analysis of work environments with a high workload where multiple tasks are performed. It is therefore appropriate for the analysis of train driving, although a train driver can also experience periods of under load. The multiple task model assumes that tasks can claim one or more resources. These resources are limited in capacity. The model is especially suitable to calculate the degree of interference in cases where there are concurrent tasks with a demand on the same resources. The multiple resource model (see Figure 4.1) consists of four dimensions each with two different levels:

- The information processing stage consists of a perception/cognition level and a responding level.
- Perceptual modalities are either visual or auditory.
- Processing codes can be spatial (relating to environment) or verbal (spoken).
- The visual channel (the fourth dimension which is embedded in the visual modality resource) can be focal (e.g., reading a message) or ambient

*Table 4.2: Total task interference for reference scenario (golden run). *Note that tasks 1.2 and 1.3 are concurrent tasks. The TIS for these combined tasks is* $3 \times 3 \times 0.8 = 7.2$*. This value is only presented for task 1.3.*

Nr	Subgoals/tasks	Total interference score					Perceptual				Cognitive		Response		CC
	Reference scenario - Golden run	MTTC	RMS	MC short	MC long	EETC	Vf	Va	As	Av	Cs	Cv	Rs	Rv	
1	**MA - Accelerate to (maximum) speed target**														
1.1	Decide on MTTC (based on assessment of departure time) or on an eco-driving strategy	3.0	3.0	3.0	3.0	3.0	2.0					1.0			
1.2	Determine when to start Coasting	0.0	0.0	0.0	3.0	*						3.0			0.8
1.3	Determine the MA speed target	0.0	3.0	3.0	0.0	7.2						3.0			0.8
1.4	Accelerate to MA speed target	1.0	1.0	1.0	1.0	1.0							1.0		
2	**CR - Starting a cruising regime**														
2.1	Start cruising	2.0	2.0	0.0	2.0	2.0	1.0						1.0		
2.2	Monitor that the cruising speed is not overrun	2.0	2.0	0.0	2.0	2.0		1.0					1.0		
3	**CO - Starting a coasting regime**														
3.1	Start coasting (turn off traction)	0.0	0.0	2.0	2.0	2.0	1.0						1.0		
4	**MB- starting (maximum) braking**														
4.1	Determine when to start braking	1.0	1.0	1.0	1.0	1.0	1.0								
4.2	Turn off traction (before braking)	2.0	2.0	0.0	0.0	0.0	1.0						1.0		
4.3	Start decelerating to a speed limit which enables the driver to come to a full stop at the signal	2.0	2.0	2.0	2.0	2.0	1.0						1.0		
4.4	Start braking and come to a full stop in front of the signal	2.0	2.0	2.0	2.0	2.0	1.0						1.0		
	TIS per driving strategy	15.0	18.0	14.0	18.0	22.2									

Legend: short = short distance variant (SPR), long = long distance variant (IC/FT), SPR = Sprinter, IC = Intercity, FT = freight train, Vf = visual focal, Va = visual ambient, As = auditory spatial, Av = auditory verbal, Cs = cognitive spatial, Cv = cognitive verbal, Rs = response spatial, Rv = response verbal, CC = conflict component, TIS = total interference score, MA = (maximum) acceleration, CR = cruising; CO = coasting; MB = (maximum) braking (see Section 4.3.1).

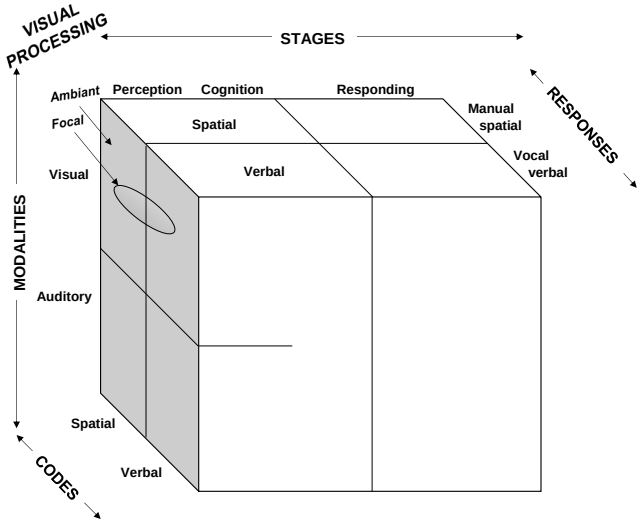

Figure 4.1: The multiple resource model adapted from Wickens (2002, p.163).

(peripheral vision e.g., monitoring signs and signals).

For the test scenarios relevant to the KPI workload we determined the TIS per task and driving strategy in the following three steps (see Table 4.2):

1. Determine demand scalar. Resources demanded by each task are scored according to the demand the task makes on the resource. The resources are scored as follows:

   - 0: the task is not dependent on this particular resource.
   - 1: there is some dependency on this resource.
   - 2: the task demands this resource twice, or this is a more complex task.
   - 3: complex task with a high demand on this particular resource.

   The resource scores of each task form a demand vector. For instance, task 1.1. demands two types of visual perception. Firstly, perception of the departure time on the timetable and secondly perception of the actual time. The score for the visual focal level therefore is 2. On the information processing dimension the driver needs to choose a driving strategy based on his assessment of time. The cognitive verbal level is 1. The demand vector for this task is presented as 2 –1.

2. Determine total demand score. The total demand score is then derived by adding up the scores from the demand vector. In case there is no concurrence of this particular task with another task the total demand score is equal to the TIS for this particular task.

3. Determine the TIS. In cases where two tasks use the same resources simultaneously, a resource-conflict score is derived from a conflict matrix (see Horrey & Wickens (2004)). Then the TIS is calculated as follows: total demand score task 1× total demand score task 2 × conflict component. For instance, tasks 1.2 and 1.3 are concurrent tasks for the driving strategy EETC. The TIS for these combined tasks is $3 \times 3 \times 0.8 = 7.2$ for EETC.

The total workload per driving strategy in a certain scenario is determined by adding up the TISs of the tasks per driving strategy. Table 4.2 gives an elaboration of the TIS for the reference scenario (golden run). The rows in this table represent the tasks in consecutive order. The columns under 'Total interference score' show the interference score per driving strategy and per task. These scores are derived by adding up the demand scalars per task, which are presented under the columns from 'Perceptual' to 'Response'. If a task does not apply for a certain driving strategy the interference score = 0. The interference score for concurrent tasks are determined by multiplying the demand scalars and then multiplying this result with a conflict component (see Wickens (2002) and Horrey & Wickens (2004)). The TIS per driving strategy (see last row of Table 4.2) is then derived by adding up the interference scores per task for a driving strategy.

4.2.5 Cost of maintenance

This KPI is linked to the amount of wear and tear on the braking blocks of the rolling stock. We would have liked to include wear on tracks. However, to our knowledge there was no suitable algorithm available in the literature on the basis of which we could determine this. Since wear on braking blocks is directly proportional to the absorbed energy in the mechanical brakes (this can be concluded from Vernersson & Lundén (2014)), we normalized it by setting wear of the MTTC reference scenario per rolling stock to 100% and compared results of other scenarios to it.

4.2.6 Environment

In this study we focused on two aspects of environmental pollution, namely the average amount of pass-by noise created during driving, and the amount of brake grindings produced during braking (which also depends on the material used in the brakes). In this study the evaluation criterion of the latter is equal to the wear of the braking blocks. We will refer to this as wear throughout the rest of this chapter.

We calculated the average pass-by noise L_p [dB] per train trip by measuring it on every 100 m of the track and then averaging it in dB over the full track length using the following equation (see Ministerie van Infrastructuur en Milieu (2012)):

$$L_p(v) = \frac{1}{n}\sum_{i=1}^{n} b \log_{10}\left(\frac{v(x_i)}{v_{\mathrm{MTTC}}(x_i)}\right), \tag{4.4}$$

with $v(x_i)$ the speed of the given driving style in km/h at location x_i [km] for the n measurements and $v_{\mathrm{MTTC}}(x_i)$ the speed of the MTTC profile in km/h at the same location. The value of b [dB] is prescribed to be 16.1 dB for passenger trains and 19.6 dB for freight trains (Ministerie van Infrastructuur en Milieu, 2012).

We chose this way of averaging over the produced noise energy, because it corresponds best to the way other noise reduction measures are determined (e.g., calculation of surface roughness of rail). In our calculations the average pass-by noise of MTTC in each scenario is set to 0.0 dB, and the results of other driving strategies are compared to it. The influence of train speed on vibrations of the surroundings was excluded from this study, because we learned that this could vary per location, and that in some cases higher speeds result in less vibration (see Van Leeuwen (2017)). In the scope of this chapter, location-independent averaging is used to assess the usefulness of this KPI.

4.2.7 Brand image

Brand image is defined as the view of target customers (i.e., passengers) on the service of a TOC. Note that we limited this KPI to TOCs. We assumed that for passengers the brand image would be influenced negatively by unplanned stops. Therefore, we assessed the likelihood of an unplanned stop for each of the driving strategies at the entry signal.

4.3 Driving strategies

In this section we first describe the four driving strategies used in this study (see Section 4.3.1), and then we give a more elaborate description of the main model in Section 4.3.2, followed by an explanation on how we solved the optimal train control problem in Section 4.3.3.

4.3.1 Four driving strategies

There are several driving strategies that are applied by train drivers. In most of these driving strategies the following *driving regimes* play an important role (see Scheepmaker & Goverde (2015)):

- (Maximum) acceleration;
- Cruising (maintaining a certain speed level);
- Coasting (turning off traction);
- (Maximum) braking.

In this study we compared the following four, in practice and theory most commonly used driving strategies: minimum time train control (MTTC), maximal coasting (MC), reduced maximum speed (RMS), and energy-efficient train control (EETC). We have chosen MTTC as a reference driving strategy to compare the other eco-driving strategies that aim to arrive exactly on-time at the next station (i.e., not too late or not too early). The MC and RMS driving strategy are commonly applied in practice, while the EETC driving strategy is studied a lot in scientific research and gives the theoretical energy optimal solution. We explain the different driving strategies below:

1. The minimum time train control (MTTC), also known as the technical minimum running time strategy. This is not an eco-driving strategy. In this strategy the driver drives as fast as is technically possible, using the maximum permitted speed on every part of the track (see Figure 4.2). This driving strategy is usually in practice applied to make up for lost time (due to delays). In addition, this driving strategy is used as a reference to compare the other driving strategies in this chapter, as this strategy is unambiguously defined.

2. The maximal coasting (MC) strategy, see Figure 4.2. This strategy aims at reducing total traction energy, by coasting as much as possible. In this strategy the driver drives as fast as possible and turns off the traction as soon as possible during the train trip, so that the train can coast to the nearest stop without using energy. This driving strategy uses the *running time supplements* in the timetable to arrive exactly on-time at the next station. The MC driving strategy is applied in practice by train drivers at the Netherlands Railways NS, where they use the UZI method (In Dutch: *Universeel Zuinig rijden Idee*) (Velthuizen & Ruijsendaal, 2011; Scheepmaker & Goverde, 2015; Luijt et al., 2017).

3. The reduced maximum speed (RMS). The driver chooses and maintains a maximum speed in order to arrive exactly on time. This strategy focuses on optimizing a fixed cruising speed (see Figure 4.2). This driving strategy is applied by the Swiss Federal Railways SBB, where the information about the cruising speed is presented in the train driver information system LEA (digital timetable) (Graffagnino et al., 2019).

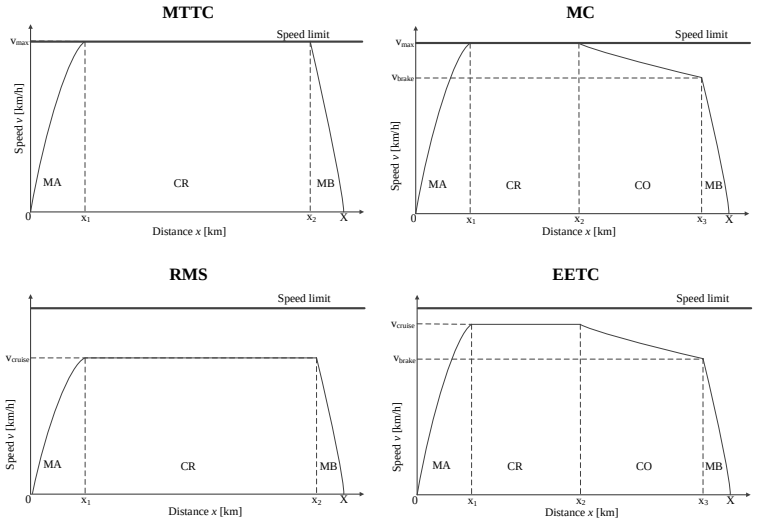

Figure 4.2: The different driving strategies: MTTC (top left), MC (top right), RMS (bottom left), and EETC (bottom right). (MA = maximum acceleration, CR = cruising, CO = coasting and MB = maximum (service) braking, and the switching points x_1, x_2, and x_3 between driving regimes).

4. The energy-efficient train control (EETC) strategy. This strategy focuses on determining and applying the optimal cruising speed and the optimal coasting points for each individual train trip (see Figure 4.2). This strategy combines cruising and coasting and aims to minimize total traction energy consumption given the amount of running time in the timetable. The results of the EETC model are the theoretical optimum. Most scientific research on energy-efficient train driving is focused on the topic of EETC, e.g., Howlett (2000), Khmelnitsky (2000), Liu & Golovitcher (2003), and A. Albrecht et al. (2016a,b). For an overview on the topic of EETC we refer to the review paper of Scheepmaker et al. (2017).

All strategies apply (maximum) acceleration and (maximum) braking. The main difference is the cruising speed, the use of coasting and the speed at the beginning of the braking phase.

4.3.2 Optimal train control

In this section the optimal train control problem is briefly explained and the optimal control structure are derived by using *Pontryagin's Maximum Principle* (*PMP*) (Pontryagin et al., 1962; Lewis et al., 2012; Ross, 2015). Derivations with distance as independent variable can be found in for example A. Albrecht et al.

(2016a,b). In this chapter, we use time as independent variable, because this leads to more stable results for the pseudospectral method compared to distance as independent variable (Goverde et al., 2021). We consider both *mechanical braking* (*MeB*) and *regenerative braking* (*RB*). During mechanical braking the train uses braking disks or pads in order to convert kinetic energy into heat while during regenerative braking the kinetic energy is converted into electricity by using the engine of the train as a generator, which can be used by the train itself, stored in batteries or fed back to the catenary system (González-Gil et al., 2013).

We start with the minimum time train control problem. Afterwards, we consider the energy-efficient train control problem with regenerative braking only and mechanical braking only. Then the maximal coasting problem is explained. Finally, the reduced maximum speed driving strategy is discussed.

Minimum time train control problem

This section briefly discusses the minimum time train control problem (MTTC). For a more detailed derivation of this problem we refer to A. Albrecht et al. (2016a,b). The aim of the MTTC problem is to minimize total running time of the train J [s] with t_f [s] defined as the final time and t_0 [s] as the initial time by

$$\text{Minimize } J = t_f - t_0, \tag{4.5}$$

subject to the constraints and the endpoint conditions

$$\dot{x}(t) = v(t) \tag{4.6}$$
$$\dot{v}(t) = f(t) + b_r(t) + b_m(t) - r(v) - g(x) \tag{4.7}$$
$$f(t)v(t) \leq p_{f,\max} \tag{4.8}$$
$$-b_r(t)v(t) \leq p_{b,\max} \tag{4.9}$$
$$0 \leq v(t) \leq v_{\max}(x) \tag{4.10}$$
$$0 \leq f(t) \leq f_{\max} \tag{4.11}$$
$$-b_{r,\min} \leq b_r(t) \leq 0 \tag{4.12}$$
$$-b_{m,\min} \leq b_m(t) \leq 0 \tag{4.13}$$
$$t_0 = 0, x(t_0) = 0, x(t_f) = X, v(t_0) = 0, v(t_f) = 0, \tag{4.14}$$

where time t [s] is the independent variable, distance x [m] and speed v [m/s] are the state variables with their derivatives to time $\dot{x} = dx/dt$ and $\dot{v} = dv/dt$. Furthermore, the control variables are the mass-specific traction force or acceleration f [m/s^2], mass-specific regenerative braking force b_r [m/s^2], and mass-specific mechanical braking force b_m [m/s^2], which are computed by dividing the total force F [N] over the total rotating mass, e.g., $F(t)/(\rho m)$ with the rotating mass factor ρ [-]

and the train mass m [kg]. The mass-specific traction control is bounded between the minimum of the maximum mass-specific traction force and the maximum mass-specific power divided by the speed, i.e., $f(v) \in [0, \min(f_{\max}, p_{f,\max}/v)]$. The braking forces are bounded between zero and the maximum braking force, i.e., $b_r(v) \in [\min(-b_{r,\min}, -p_{b,\max}/v), 0]$ for regenerative braking and $b_m(v) \in [-b_{m,\min}, 0]$ for mechanical braking. The train cannot apply both traction and braking at the same time, i.e., $f \cdot (b_r + b_m) = 0$. The total resistance W [N] is determined by the train resistance and the line resistance, i.e., $W = R + G$. The train resistance R [N] is given by Davis

$$R(v) = r_0 + r_1 v + r_2 v^2, \tag{4.15}$$

with the non-negative coefficients r_1, r_2, and r_3 (Davis, 1926). The mass-specific train resistance $r(v)$ [m/s^2] is computed by dividing the train resistance force by the total rotating mass, i.e., $r(v) = R(v)/(\rho m)$. The line resistance is mainly determined by the gradient force $G(x)$ [N], which is positive if the gradient is uphill and negative if the gradient force is downhill. The mass-specific line resistance is $g(x) = G(x)/(\rho m)$ [m/s^2]. We do not include curves and tunnel resistance.

The Hamiltonian H [-] is defined by

$$H(x, v, \lambda_1, \lambda_2, f, b_r, b_m, t) = \lambda_2 f + \lambda_2 b_r + \lambda_2 b_m + \lambda_1 v - \lambda_2 r(v) - \lambda_2 g(x), \tag{4.16}$$

with the costate variables $\lambda_1(t)$ [s/m] and $\lambda_2(t)$ [s^2/m]. The augmented Hamiltonian $\bar{H}(x, v, \lambda_1, \lambda_2, \mu, f, b_r, b_m, t)$ [-] is defined by

$$\begin{aligned}\bar{H} =& H + \mu_1(f_{\max} - f) + \mu_2(b_r + b_{r,\min}) + \mu_3(b_m + b_{m,\min}) + \mu_4(p_{f,\max} - fv) \\ &+ \mu_5(p_{b,\max} + b_r v) + \mu_6(v_{\max} - v),\end{aligned} \tag{4.17}$$

with the nonnegative Lagrange multipliers μ_1 [s^2/m], μ_2 [s^2/m], μ_3 [s^2/m], μ_4 [s^3/m^2], μ_5 [s^3/m^2], and μ_6 [s/m]. The costates λ_1 and λ_2 satisfy the following differential equations

$$\dot{\lambda}_1(t) = -\partial \bar{H}/\partial x = \lambda_2 g'(x) \tag{4.18}$$

$$\dot{\lambda}_2(t) = -\partial \bar{H}/\partial v = -\lambda_1 + \lambda_2 r'(v) + \mu_4 f - \mu_5 b_r + \mu_6. \tag{4.19}$$

Note that (4.18) indicates that λ_1 is constant where the gradient is constant.

Pontryagin's Maximum Principle gives the optimal controls by maximizing the Hamiltonian (Pontryagin et al., 1962). Moreover, by applying the *Karush-Kuhn-Tucker* (*KKT*) conditions on the augmented Hamiltonian, we are able to derive the optimal control structure from the necessary optimality conditions:

$$(\hat{f}(t), \hat{b}_r(t), \hat{b}_m(t)) =$$
$$\begin{cases} (f_{\max}(v(t)), 0, 0) & \text{if } \lambda_2(t) > 0 \quad \text{(MA)} \\ (r(v_{\max}) + g(x), 0, 0) \text{ and } r(v_{\max}) + g(s) \leq 0 & \text{if } \lambda_2(t) = 0 \quad \text{(CR1)} \\ (0, r(v_{\max}) + g(x) + b_m, r(v_{\max}) + g(x) + b_r) \text{ and } r(v_{\max}) + g(s) > 0 & \text{if } \lambda_2(t) = 0 \quad \text{(CR2)} \\ (0, -b_{r,\min}(v(t)), -b_{m,\min}(v(t))) & \text{if } \lambda_2(t) < 0 \quad \text{(MB).} \end{cases} \tag{4.20}$$

The results indicate that the MTTC driving strategy consists of three driving regimes, which depends on the value and sign of costate λ_2. The first driving regime is maximum acceleration (MA) in which the train applies the minimum between the maximum specific traction force (4.11) and maximum specific power divided by speed (4.8). Second, during cruising at the speed limit the control is equal to the total train resistance in order to remain at the speed limit (i.e., depending on the sign of the total train resistance using traction (CR1) or braking (CR2)). Note that it is not possible to apply traction and braking at the same time. Finally, the train applies maximum braking force during the maximum braking (MB) regime. Note that there is no preference for regenerative or mechanical braking in this scenario, since the aim is to minimize total travel time and not the energy consumption.

Energy-efficient train control problem with regenerative braking only

The second optimal control problem we consider is the energy-efficient train control (EETC) problem with regenerative braking (RB) only. We included the effect of regenerative braking by the term $(b_r(t) + b_m(t))\eta$, where η [-] considers the total efficiency of both the traction η_t [-] and the catenary η_c [-], so $\eta = \eta_t \eta_c$. EETC with mechanical braking is achieved by replacing b_r by b_m and setting $\eta = 0$, which is discussed in the Section about the MTTC problem. Like A. Albrecht et al. (2016a,b) we assume that the train only applies regenerative braking and no mechanical braking. We briefly provide the EETC problem formulation and we refer to A. Albrecht et al. (2016a,b) for more details about the general EETC problem derivation. The aim of the optimal train control is to minimize total mass-specific energy consumption J [m^2/s^2] between two consecutive stops, while arriving on time given the amount of time within the timetable T [s]:

$$J = \min \int_{t_0}^{t_f} (f(t) + \eta b_r(t)) v(t) dt, \tag{4.21}$$

subject to the constraints (4.6)–(4.12) and the endpoint conditions

$$t_0 = 0, t_f = T, x(t_0) = 0, x(t_f) = X, v(t_0) = 0, v(t_f) = 0. \tag{4.22}$$

We define the Hamiltonian H [m^2/s^3] by

$$H(x,v,\lambda_1,\lambda_2,f,b_r,b_m,t) = (\lambda_2 - v)f + (\lambda_2 - \eta v)b_r + \lambda_1 v - \lambda_2 r(v) - \lambda_2 g(x), \tag{4.23}$$

with the costates $\lambda_1(t)$ [m/s^2] and $\lambda_2(t)$ [m/s]. The augmented Hamiltonian $\bar{H}(x,v,\lambda_1,\lambda_2,\mu,f,b_r,b_m,t)$ [m^2/s^3] is given by

$$\begin{aligned}\bar{H} =& H + \mu_1(f_{\max} - f) + \mu_2(b_r + b_{r,\min}) + \mu_4(p_{f,\max} - fv) \\ &+ \mu_5(p_{b,\max} + b_r v) + \mu_6(v_{\max} - v).\end{aligned} \tag{4.24}$$

where the nonnegative Lagrange multipliers are defined by μ_1 [m/s], μ_2 [m/s], μ_4 [-], μ_5 [-], and μ_6 [m/s^2]. The differential equations of the costates λ_1 and λ_2 state

$$\dot{\lambda}_1(t) = \lambda_2 g'(x) \tag{4.25}$$

$$\dot{\lambda}_2(t) = f + \eta b_r - \lambda_1 + \lambda_2 r'(v) + \mu_4 f - \mu_5 b_r + \mu_6. \tag{4.26}$$

Again, by using the PMP and KKT conditions we can derive the optimal control structure consisting of:

$$(\hat{f}(t), \hat{b}_r(t)) = \begin{cases} (f_{\max}(v(t)), 0) & \text{if } \lambda_2(t) > v(t) & \text{(MA)} \\ (r(v_f) + g(x), 0) & \text{if } \lambda_2(t) = v_f & \text{(CR1)} \\ (0,0) & \text{if } \eta v(t) < \lambda_2(t) < v(t) & \text{(CO)} \\ (0, r(v_r) + g(x)]) & \text{if } \lambda_2(t) = \eta v_r & \text{(CR2)} \\ (0, -b_{r,\min}(v(t))) & \text{if } \lambda_2(t) < \eta v(t) & \text{(MB).} \end{cases} \tag{4.27}$$

The optimal control now depends on the costate λ_2 in relation to speed v. The driving regimes MA and MB are similar to (4.20). The CO driving regime corresponds to coasting, where there is zero control. The driving regime CR1 indicates cruising by partial traction at cruising speed v_f, where a balance exists between the traction force and the total train resistance. The CR2 driving regime is cruising by partial regenerative braking at cruising speed v_r and can only be maintained during downhill gradients. MB indicates maximum braking by applying regenerative braking.

Energy-efficient train control problem with mechanical braking only

In this section we briefly consider mechanical braking (MeB) only for the EETC problem. More details can be found in A. Albrecht et al. (2016a,b). Basically, the optimal control problem is the same as in Section about EETC RB replacing b_r (regenerative braking) by b_m (mechanical braking) and setting $\eta = 0$, thus, mechanical braking does not generate energy. This leads to the following objective

function (J [m^2/s^2]):

$$J = \min \int_{t_0}^{t_f} f(t)v(t)dt, \tag{4.28}$$

subject to constraints (4.6), (4.8), (4.10), (4.11), (4.13), endpoint conditions (4.22), and constraint

$$\dot{v}(t) = f(t) + b_m(t) - r(v) - g(x). \tag{4.29}$$

The Hamiltonian H [m^2/s^3] is defined as

$$H(x, v, \lambda_1, \lambda_2, f, b_m, t) = (\lambda_2 - v)f + \lambda_2 b_m + \lambda_1 v - \lambda_2 r(v) - \lambda_2 g(x). \tag{4.30}$$

The augmented Hamiltonian $\bar{H}(x, v, \lambda_1, \lambda_2, \mu, f, b_m, t)$ [m^2/s^3] is given by

$$\bar{H} = H + \mu_1(f_{\max} - f) + \mu_3(b_m + b_{m,\min}) + \mu_4(p_{f,\max} - fv) + \mu_6(v_{\max} - v), \tag{4.31}$$

where the nonnegative Lagrange multipliers are defined by μ_1 [m/s], μ_3 [m/s], μ_4 [-], and μ_6 [m/s^2]. The costates λ_1 [m/s^2] and λ_2 [m/s] satisfy the following differential equations:

$$\dot{\lambda}_1(t) = \lambda_2 g'(x) \tag{4.32}$$

$$\dot{\lambda}_2(t) = f - \lambda_1 + \lambda_2 r'(v) + \mu_4 f + \mu_6. \tag{4.33}$$

After maximizing the Hamiltonian and applying the KKT conditions we can derive the optimal control structure:

$$(\hat{f}(t), \hat{b}_m(t)) = \begin{cases} (f_{\max}(v(t)), 0) & \text{if } \lambda_2(t) > v(t) \quad \text{(MA)} \\ (r(v_f) + g(x), 0) & \text{if } \lambda_2(t) = v_f \quad \text{(CR1)} \\ (0, 0) & \text{if } 0 < \lambda_2(t) < v(t) \quad \text{(CO)} \\ (0, r(v_m) + g(x)) & \text{if } \lambda_2(t) = 0 \quad \text{(CR3)} \\ (0, -b_{m,\min}(v(t))) & \text{if } \lambda_2(t) < 0 \quad \text{(MB).} \end{cases} \tag{4.34}$$

Compared to (4.27) the only difference is that the cruising by partial regenerative braking CR2 is replaced by cruising by partial mechanical braking CR3 at cruising speed v_m and that the maximum braking (MB) is now applied by mechanical braking instead of regenerative braking.

Maximal coasting

The third driving strategy is maximal coasting (MC). The optimal control problem is equal to (4.21) for RB and to (4.28) for MeB, subject to the constraints (4.6)–

(4.12) for RB, (4.6), (4.8), (4.10), (4.11), (4.13) for MeB, and endpoint conditions (4.22). In addition, we included a constraint that forced the train to apply cruising at the speed limit by:

$$0 \leq v(t) - v_s(t) \leq v_{\max}, \tag{4.35}$$

where $v_s(t)$ is defined as a restricted speed that forces the train to maintain the speed limit during cruising. We also check the MTTC driving strategy to see where the train starts to cruise at the speed limit and we consider this the first distance where the train should apply cruising at the speed limit. For the distance where the model suggests to start cruising below the speed limit (such as suggested by the EETC model) we avoid this by setting $v_s(t) = v_{\max}$ given (4.10), and for all other distance $v_s(t) = 0$. The process to determine the optimal start of the coasting phase by changing $v_s(t)$ is done iteratively. The resulting optimal driving regimes include MA, (CR at speed limit), CO and MB, which are equal to the driving regimes given by (4.27) for RB and (4.34) for MeB. The only difference is the driving regime cruising CR1, CR2, and CR3, where the speed is equal to the speed limit $v_{\max}$ similar to CR1 and CR2 in (4.20).

Reduced maximum speed

The fourth driving strategy considered is the reduced maximum speed (RMS) below the speed limit, which is a cruising driving strategy without coasting. Again the optimal control problem is equal to (4.21) for RB and (4.28) for MeB subject to the constraints (4.6)–(4.11) for RB and (4.6), (4.8), (4.10), (4.11), (4.13) for MeB and endpoint conditions (4.22). In addition, we included an extra path constraint that avoids the train to apply coasting by:

$$f(t) - r(v) - g(x) \geq 0. \tag{4.36}$$

The RMS driving strategy leads to the same driving regimes MA, MB, CR1, CR2, and CR3 as given by (4.27) for RB and (4.34). The only difference is that the driving regime coasting (CO) is not included.

4.3.3 Pseudospectral optimal train control

We use the *Radau Pseudospectral Method* (*RPM*) in order to solve the optimal control problem P. (Wang & Goverde, 2016a). This is a direct solution method, which discretizes the optimal control state and control variables using collocation points (Betts, 2010). Next, the discretized optimal control problem is rewritten to a nonlinear programming (NLP) problem, which is solved using efficient algorithms.

For more details on the translation of the optimal train control problem into a NLP problem, we refer to P. Wang & Goverde (2016a).

The main focus in the literature on pseudospectral optimal train control is on multiple-phase, in which the optimal control problem is divided into subproblems or phases with constant values for speed limit and gradient. The total optimal control problem is then solved for each phase and the phases are connected using linking functions (Wang et al., 2013, 2014; Wang & Goverde, 2016a,c, 2017, 2019). Single-phase pseudospectral methods decrease the computation time and can be applied when the number of discontinuities in the constraints is limited, because the quality of the model results depends strongly on the amount and location of the collocation points (determined by the algorithm) (Scheepmaker et al., 2020a). Therefore, some constraints may be violated between the collocation points such as speed restrictions or gradients, since the descretization points are not exactly at the locations where the speed limit or gradient changes. In this chapter we consider the single-phase model using the software MATLAB with the toolbox of GPOPS version 4.1 (Rao et al., 2011) to develop the model which we call PROMO (PseudospectRal Optimal train control Model) based on Scheepmaker & Goverde (2016) and Scheepmaker et al. (2020a). We use a single core for the computations applied on a 2.1 GHz processor with 8 GB RAM.

4.4 Description case study

In this Section we describe the key characteristics and conditions that formed the basis of our test scenarios. The test scenarios per rolling stock type (see Section 4.4.1) with the different characteristics are summarized in Section 4.5. We first constructed a reference scenario by using what we considered to be standard values for each train type. Then we varied one of the key characteristics or conditions to create a new scenario. Some of these characteristics and conditions are based on the actual situation at NS. One example is the NS timetable, which includes a running time supplement of at least 5%. We measured the KPIs for different driving strategies on a single train without conflicts. We start this section with a description of the fixed characteristics within our study (see Section 4.4.1). We then describe track (see Section 4.4.2), rolling stock (see Section 4.4.3), and timetable related characteristics (see Section 4.4.4). In most scenarios we assume that there are no other trains preceding our test train. However, in Section 4.4.5 we add a train sequencing condition.

4.4.1 Fixed characteristics

The following standard characteristics were used in our study: for all our scenarios we used a single train without conflicts. The ATP in most of our test scenarios uses a braking curve, for instance ETCS L2. There is only one scenario with a conventional ATP (NS '54/ATB). We only considered electrically powered rolling stock (i.e., trains that obtain their power from the catenary system using a pantograph). The catenary voltage amounted to 1.5 kV DC with a maximum of 4 kA per train (Dutch situation). We assume the efficiency of the catenary to be 80% in the case the train applies regenerative braking and its energy is fed back to the catenary system (Scheepmaker & Goverde, 2016). All trains in our model started at the same location at the departure station (at the end of the platform length), and stopped at the end of a platform length of the station of arrival. The timetable was conflict-free in fractions of seconds. The maximum permitted speed (linespeed) on the track was 140 km/h. We used a fixed train length (fixed number of carriages) per rolling stock type. We used three types of rolling stock in our model: an Intercity (IC), a Sprinter (SPR), and a freight train (FT). Details of the the rolling stock characteristics can be found in Table 4.3. A brief overview of the rolling stock is given below:

- For the IC we used the most commonly used type of rolling stock at NS, which is the VIRM (In Dutch: *Verlengd InterRegio Materieel*). We used a VIRM type VI, which has six coaches.
- The SPR was a SLT VI (Sprinter Light Train) consisting of six coaches. This type of rolling stock is used on short distances.
- For the FT we chose the BR186 (In German: *BauReihe* 186). This e-loc is often used for freight transport in the Netherlands. This train consists of a locomotive and 28 freight wagons (type Falns used to transport coal).

The standard track length for both the IC, and the FT was 50 km in most test scenarios. For the SPR we used a track length of 5 km. We used tracks without curves and an amount of cross wind of 10 km/h (this is considered to be the average amount of cross wind in the Netherlands). For the IC and the SPR we chose the set of train resistance coefficients of the tactical Dutch timetable design system, Donna. Our FT train resistance coefficients are based on the data of the strategic timetable design system DONS.

4.4.2 Track related characteristics

Most of our scenarios are based on track lengths between 5 and 50 km, that are common in the Netherlands. For the purpose of a sensitivity analysis we wanted to

Table 4.3: Standard rolling stock characteristics (NS, 2020). Note that the train resistance equation between brackets for FT is only valid for 0% train load scenario.

Rolling Stock Characteristic	IC	SPR	FT
Rolling StockType	VIRM VI	SLT VI	BR186 (Traxx e-loc)
Number of coaches /wagons	6	6	28 (class Fals)
Train length	162 m	101 m	515 m
Total train weight	391,000 kg	198,000 kg	2,400,000 kg
Empty train weight	375,418 kg	189,600 kg	786,000 kg
Train load weight	15,582 kg (35%)	8,400 kg (35%)	1,614,000 kg (100%)
Train resistance equation: $r_0 + r_1\, v + r_2\, v^2$			
r_0	2,711.3 N	1,375.8 N	30,658 (10,949) N
r_1	43.43 Ns/m	37.48 Ns/m	796.97 (284.49) Ns/m
r_2	7.82 Ns^2/m^2	6.75 Ns^2/m^2	141.05 (48.81) Ns^2/m^2
Maximum traction force	213.9 kN	170 kN	236.22 kN
Maximum power	2,157 kW	1,755 kW	5,600 kW
Standard and ATB braking deceleration	0.5 m/s^2	0.5 m/s^2	0.5 m/s^2
Traction efficiency	87.5%	87%	87.7%
Caternary efficiency	80%	80%	80%
Maximum regenerative braking force	142.5 kN	150 kN	–
Maximum speed	160 km/h	160 km/h	95 km/h

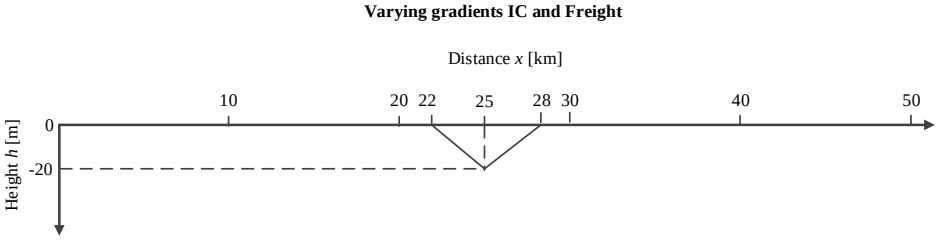

Figure 4.3: Track gradient IC and FT.

study the effects of longer track lengths on the four driving strategies. Therefore, we introduced an additional scenario with a track length of 150 km for both IC and FT.

In order to study the effect of track gradients on the driving strategies, we developed a test scenario in which we introduced one track gradient with a height difference of 20 m over a distance of 3000 m the middle of the track, equal to 20/3000 = 6.67‰ (see Figure 4.3). This was only for IC and FT under the assumption that a track gradient on a short track (SPR) would not add to this study. In this scenario the trains first encounter a downward, and then an upward gradient. We reasoned that this would be more demanding with respect to driver anticipation than a situation with first an upward and then a downward gradient.

4.4.3 Rolling stock related characteristics.

We used a load factor of 0% (zero load), 35% (the default) and of 100%. The latter refers to the weight of the train itself (zero load) including full loading. In passenger trains full loading includes the weight of all the (folding) seats occupied by passengers, the weight of one train driver, and one train train conductor (with an average weight per person of 70 kg (BS-EN-15663, 2017)) plus the rotating mass. For the freight trains the maximum load was the train weight (zero load) plus the maximum cargo weight.

In our model regenerative braking (RB) is standard for SPR and IC. Since not all the NS rolling stock is equipped with regenerative brakes we defined a separate test scenario for mechanical braking (MeB). In this chapter we assume that the SPR train uses 100% regenerative braking and the IC train uses 72.89% regenerative braking (the rest is mechanical braking) with a maximum deceleration rate of 0.5 m/s^2 (NS, 2020). The FTs in the Netherlands only use mechanical brakes. That is why all the FT test scenarios in our model use MeB.

We tested the effectiveness of driving strategies under limited speed restrictions (SR). Besides the standard situation, in which there are no speed restrictions, we introduced an SR in the middle of the route in which the line speed of 140 km/h was lowered to 100 km/h (for IC and SPR), and 80 km/h (for FT) respectively.

4.4.4 Timetable related characteristics

We compared the runs of our four driving strategies with different running time supplements. At NS the advised running time supplement for SPR and IC is at least 5% rounded up to whole minutes (ProRail, 2016). In practice this results in an average running time supplement of 10%. Note that in this study we did not round up the running time supplement. For IC and SPR in this study the standard running time supplement was 10%. We also measured the effects of a running time supplement of 5%, and 15%, and compared the results to a reference value without running time supplement (a situation in which MTTC is applied).

For FT we used a standard running time supplement of 4.3%, based on the difference between the minimum running time with a maximum speed of 90 km/h and of 95 km/h. During timetable design in the Netherlands freight trains are modelled with 0% running time supplements for the heaviest composition (maximum train load) and the slowest train allowed (maximum speed of 90 km/h) (ProRail, 2016). The running time supplements for freight trains are then determined in practice by lighter freight trains as well as freight trains with a higher maximum speed. For freight trains we used alternative running time supplements of 7.5% and 10%.

Figure 4.4: Track characteristics IC/FT entering a station. Total track length = 50 km.

4.4.5 Train sequencing

In a busy, tightly planned network, IC and FT trains cannot run early without encountering the effects of preceding trains. In order to study the effect of driving strategies under this situation we introduced a condition in which a preceding train occupies the entry track of our approaching simulated train. We chose the shortest platform clearing times where the planned timetable was conflict-free for a train entering the station at linespeed. We studied this condition only for IC in both the standard ETCS L2 and the conventional Dutch NS '54/ATB situation.

In these scenarios the speed and time at the signal before the entry signal (km 47) is used as input (see Figure 4.4). We assumed that the driver does not change the driving strategy up to this signal. Braking was taken at 0.5 m/s^2 without reaction times or speed dependence. In this way, braking curve intervention in ETCS L2 was avoided, and at the same time this conformed to minimal braking for NS '54/ATB. Acceleration was likewise taken at 0.5 m/s^2.

4.5 Results

In this section we summarize our findings per group of test scenarios as defined in Table 4.4. Section 4.5.1 contains an elaborate description of our findings in the reference scenarios. In the following sections we will predominantly highlight the differences with the reference scenarios. We start with track related scenarios (see Section 4.5.2), followed by load factor scenarios (in Section 4.5.3), braking characteristics (in Section 4.5.4), speed restrictions in Section 4.5.5, running time supplements in Section 4.5.6, and finally platform clearing scenarios in Section 4.5.7. The values per evaluation criterion based on the KPIs for each of the different test scenarios are presented in Tables 4.5 (for SPR), 4.6 and 4.9 (for IC), and 4.7 (for FT). The columns in Tables 4.5, 4.6, and 4.7 indicate the different KPIs and the evaluation criteria to measure the KPIs. Under 'Timeliness' we find the deviation in seconds from the planned arrival time. For MTTC this is

Table 4.4: Test scenarios per rolling stock type.

Scenario	Track length	Gradient	Load factor	Braking (MeB/RB)	SR	Run. time suppl.	Plat clear	ATP
Train type SPR								
0: Reference	5 km	0 m	35%	RB	No	10%	Yes	L2
2.1: Load factor (zero load)	5 km	0 m	0%	RB	No	10%	Yes	L2
2.2: Load factor (fully loaded)	5 km	0 m	100%	RB	No	10%	Yes	L2
3.1: Braking (MeB)	5 km	0 m	35%	MeB	No	10%	Yes	L2
4.2: SR (100 km/h)	5 km	0 m	35%	RB	100 km/h	10%	Yes	L2
5.1: Run. time suppl. (5%)	5 km	0 m	35%	RB	No	5%	Yes	L2
5.2: Run. time suppl. (15%)	5 km	0 m	35%	RB	No	15%	Yes	L2
Train type IC								
0: Reference	50 km	0 m	35%	RB	No	10%	Yes	L2
1.1: Track length (150 km)	150 km	0 m	35%	RB	No	10%	Yes	L2
1.2: Gradient (20 m)	50 km	20 m	35%	RB	No	10%	Yes	L2
2.1: Load factor (zero load)	50 km	0 m	0%	RB	No	10%	Yes	L2
2.2: Load factor (fully loaded)	50 km	0 m	100%	RB	No	10%	Yes	L2
3.1: Braking (MeB)	50 km	0 m	35%	MeB	No	10%	Yes	L2
4.2: SR (100 km/h)	50 km	0 m	35%	RB	100 km/h	10%	Yes	L2
5.1: Run. time suppl. (5%)	50 km	0 m	35%	RB	No	5%	Yes	L2
5.2: Run. time suppl. (15%)	50 km	0 m	35%	RB	No	15%	Yes	L2
6.1: Platform clear (L2)	50 km	0 m	35%	RB	No	10%	No	L2
6.2: Platform clear (ATB)	50 km	0 m	35%	RB	No	10%	No	ATB
Train type FT								
0: Reference	50 km	0 m	100%	MeB	No	4.3%	Yes	L2
1.1: Track length (150 km)	150 km	0 m	100%	MeB	No	2.5%	Yes	L2
1.2: Gradient (20 m)	50 km	20 m	100%	MeB	No	4.3%	Yes	L2
2.1: Load factor (zero load)	50 km	0 m	0%	MeB	No	4.3%	Yes	L2
4.1: SR (80 km/h)	50 km	0 m	100%	MeB	80 km/h	4.3%	Yes	L2
5.1: Run. time suppl. (7.5%)	50 km	0 m	100%	MeB	No	7.5%	Yes	L2
5.2: Run. time suppl. (10%)	50 km	0 m	100%	MeB	No	10%	Yes	L2

Legend: SPR = Sprinter, IC = Intercity, FT = freight train, SR = speed restriction, MeB = mechanical braking, RB = regenerative braking, NA = not applicable, Run. time suppl. = running time supplement, L2 = ETCS L2, ATB = NS '54/ATB, automatic train protection (ATP), Plat clear = platform is clear on arrival of test train at the signal preceding the entry signal.

usually a negative value, since the train arrives ahead of time. The columns under 'Energy consumption' display the total energy consumption per driving strategy, and in addition the percentage extra energy saved by a particular driving strategy compared to MTTC. The 'Environment' column displays the average noise made during the train trip, and under 'Environment-Maintenance' the percentage of wear (KPI Maintenance) generated by a driving strategy, compared to MTTC in the reference scenario (which is set at 100%) is displayed. This is equal to the amount of brake grindings produced, which is another evaluation criterion for the KPI Environment. The rows contain the driving strategies per scenario as defined in Table 4.4.

The results of the workload analysis are presented separately in Table 4.8 for the scenarios 0 ('Reference'), 1.2 ('Gradient'), 4.1 ('Speed restriction'), 6.1 ('Platform clearing ETCS L2'), and 6.2 ('Platform clearing NS '54/ATB'). Finally, Table 4.9 is focused on the platform clearance scenarios, in which the test train is hindered by a previous train at the arrival platform (scenarios 6.1 and 6.2). This table has basically the same structure as Tables 4.5–4.7, but it also includes the KPI safety for NS '54/ATB, and the KPI brand image (see Section 4.5.7).

Table 4.5: Results SPR for each test scenario per evaluation criterion.

Results SPR	Timeliness	Energy consumption		Environment	Environment-maintenance	Computation time (s)
	Deviation arrival time (s)	(kWh)	P1 (%)	P2 (dB)	PMx = Wear (%)	
Scenario 0. Reference (35% load)						
MTTC-RB	-20.24	40.94	0.0%	0.00	0%	74.40
EETC-RB	0	24.40	40.4%	0.90	0%	10.61
MC-RB	0	24.40	40.4%	0.90	0%	10.61
RMS-RB	0	25.88	36.8%	0.89	0%	13.98
Scenario 2.1. Load factor (zero load)						
MTTC-RB	-21.83	40.18	0.0%	0.00	0%	111.72
EETC-RB	0	23.46	41.6%	0.92	0%	9.74
MC-RB	0	23.46	41.6%	0.92	0%	9.74
RMS-RB	0	24.96	37.9%	0.91	0%	12.42
Scenario 2.2. Load factor (fully loaded)						
MTTC-RB	-17.28	42.64	0.0%	0.00	0%	60.18
EETC-RB	0	26.26	38.4%	0.87	0%	10.44
MC-RB	0	26.26	38.4%	0.87	0%	10.44
RMS-RB	0	27.83	34.7%	0.86	0%	12.19
Scenario 3.1. Braking (MeB)						
MTTC-MeB	-20.24	64.52	0.0%	0.00	100%	74.83
EETC-MeB	0	35.89	44.4%	0.90	49%	10.66
MC-MeB	0	35.89	44.4%	0.90	49%	10.66
RMS-MeB	0	39.36	39.0%	0.89	57%	13.02
Scenario 4.2. SR						
MTTC-RB	-23.35	40.15	0.0%	0.00	0%	104.41
EETC-RB	0	17.17	57.2%	0.83	0%	12.44
MC-RB	0	17.17	57.2%	0.83	0%	12.44
RMS-RB	0	18.19	54.7%	0.82	0%	18.76
Scenario 5.1. Running time supplement (5%)						
MTTC-RB	-10.12	40.94	0.0%	0.00	0%	74.40
EETC-RB	0	29.22	28.6%	0.48	0%	10.88
MC-RB	0	29.22	28.6%	0.48	0%	10.88
RMS-RB	0	30.95	24.4%	0.47	0%	14.86
Scenario 5.2. Running time supplement (15%)						
MTTC-RB	-30.36	40.94	0.0%	0.00	0%	74.40
EETC-RB	0	21.17	48.3%	1.28	0%	11.29
MC-RB	0	21.17	48.3%	1.28	0%	11.29
RMS-RB	0	22.54	44.9%	1.28	0%	14.23

Legend: SPR = Sprinter, PMx = particular matter (brake grindings), SR = speed restriction, MeB = mechanical braking, RB = regenerative braking, P1 = percentage of savings compared to MTTC, P2 = pass-by noise compared to MTTC.

Table 4.6: Results IC for each test scenario per evaluation criterion.

Results IC	Timeliness	Energy consumption		Environment	Environment-maintenance	Computation time (s)
	Deviation arrival time (s)	(kWh)	P1 (%)	P2 (dB)	PMx = Wear (%)	
Scenario 0. Reference (35% load)						
MTTC-RB	-141.35	330.9	0.0%	0.00	100%	140.55
EETC-RB	0.00	248.9	24.8%	0.70	35%	34.90
MC-RB	0.00	249.0	24.8%	0.63	26%	36.21
RMS-RB	0.00	262.5	20.7%	0.72	66%	22.59
Scenario 1.1. Track length (150 km)						
MTTC-RB	-398.54	863.3	0.0%	0.00	101%	18.10
EETC-RB	0.00	702.7	18.6%	0.68	35%	32.10
MC-RB	0.00	743.9	13.8%	0.52	15%	179.66
RMS-RB	0.00	719.0	16.7%	0.68	68%	16.94
Scenario 1.2. Gradient (20 m)						
MTTC-RB	-141.35	339.0	0.0%	0.00	108%	32.45
EETC-RB	0.00	249.2	26.5%	0.69	35%	67.03
MC-RB	0.00	253.1	25.3%	0.63	34%	40.90
RMS-RB	0.00	263.0	22.4%	0.72	68%	67.70
Scenario 2.1. Load factor (zero load)						
MTTC-RB	-142.81	326.3	0.0%	0.00	96%	23.39
EETC-RB	0.00	245.7	24.7%	0.70	33%	38.54
MC-RB	0.00	247.5	24.2%	0.63	24%	51.88
RMS-RB	0.00	258.8	20.7%	0.72	63%	69.26
Scenario 2.2. Load factor (fully loaded)						
MTTC-RB	-138.63	338.7	0.0%	0.00	106%	22.67
EETC-RB	0.00	251.6	25.7%	0.68	38%	30.01
MC-RB	0.00	253.7	25.1%	0.62	30%	54.39
RMS-RB	0.00	269.5	20.4%	0.70	71%	60.29
Scenario 3.1. Braking (MeB)						
MTTC-MeB	-141.35	373.5	0.0%	0.00	181%	149.17
EETC-MeB	0.00	259.9	30.4%	0.65	51%	29.43
MC-MeB	0.00	260.0	30.4%	0.63	47%	82.14
RMS-MeB	0.00	290.7	22.2%	0.72	119%	27.98
Scenario 4.2. SR						
MTTC-RB	-144.76	361.1	0.0%	0.00	100%	26.38
EETC-RB	0.00	247.8	31.4%	0.71	39%	117.11
MC-RB	0.00	248.4	31.2%	0.68	34%	36.02
RMS-RB	0.00	269.3	25.4%	0.73	84%	27.42
Scenario 5.1. Running time supplement (5%)						
MTTC-RB	-70.68	330.9	0.0%	0.00	100%	140.55
EETC-RB	0.00	270.2	18.3%	0.35	40%	28.21
MC-RB	0.00	270.7	18.2%	0.33	40%	49.54
RMS-RB	0.00	286.9	13.3%	0.37	73%	24.95
Scenario 5.2. Running time supplement (15%)						
MTTC-RB	-212.03	330.9	0.0%	0.00	66%	140.55
EETC-RB	0.00	227.9	31.1%	1.03	31%	54.84
MC-RB	0.00	241.2	27.1%	0.87	24%	129.32
RMS-RB	0.00	241.0	27.2%	1.05	58%	25.42

Legend: IC = Intercity, PMx = particular matter (brake grindings), SR = speed restriction, MeB = mechanical braking, RB = regenerative braking, P1 = percentage of savings compared to MTTC, P2 = pass-by noise compared to MTTC.

Table 4.7: Results FT for each test scenario per evaluation criterion.

Results FT	Timeliness	Energy consumption		Environment	Environment-Maintenance	Computation time (s)
	Deviation arrival time (s)	(kWh)	P1 (%)	P2 (dB)	PMx = Wear (%)	
Scenario 0. Reference (running time supplement 4.3% and fully loaded)						
MTTC-MeB	-89.94	3127	0.0%	0.00	100%	29.97
EETC-MeB	0	2730	12.7%	0.36	35%	36.60
MC-MeB	0	2760	11.7%	0.30	25%	33.49
RMS-MeB	0	2837	9.3%	0.39	90%	29.82
Scenario 1.1. Track length (150 km)						
MTTC-MeB	-147.36	8939	0.0%	0.00	100%	14.20
EETC-MeB	0	8428	5.7%	0.33	37%	25.19
MC-MeB	0	8531	4.6%	0.32	18%	28.39
RMS-MeB	0	8491	5.0%	0.36	92%	29.00
Scenario 1.2. Gradient (20 m)						
MTTC-MeB	-84.40	3211	0.0%	0.00	104%	349.23
EETC-MeB	0	2824	12.1%	0.33	33%	122.10
MC-MeB	0	2858	11.0%	0.31	33%	34.35
RMS-MeB	0	2929	8.8%	0.36	99%	418.55
Scenario 2.1. Load factor (zero load)						
MTTC-MeB	-217.25	997.74	0.0%	0.00	35%	24.99
EETC-MeB	0	773.91	22.4%	0.89	10%	36.91
MC-MeB	0	830.44	16.8%	0.64	3%	87.88
RMS-MeB	0	799.25	19.9%	0.92	25%	25.94
Scenario 4.2. SR (80 km/h)						
MTTC-MeB	-81.17	3191	0.0%	0.00	122%	296.52
EETC-MeB	0	2737	14.2%	0.33	35%	114.42
MC-MeB	0	2755	13.7%	0.31	35%	73.42
RMS-MeB	0	2857	10.5%	0.36	99%	35.81
Scenario 5.1. Slack time (7.5%)						
MTTC-MeB	-157.90	3127	0.0%	0.00	100%	29.97
EETC-MeB	0	2560	18.1%	0.64	32%	65.69
MC-MeB	0	2679	14.3%	0.50	15%	39.55
RMS-MeB	0	2636	15.7%	0.67	81%	44.39
Scenario 5.2. Slack time (10%)						
MTTC-MeB	-210.53	3127	0.0%	0.00	100%	29.97
EETC-MeB	0	2439	22.0%	0.85	30%	33.00
MC-MeB	0	2640	15.6%	0.64	10%	93.08
RMS-MeB	0	2516	19.5%	0.89	77%	34.32

Legend: FT = freight train, PMx = particular matter (brake grindings), SR = speed restriction, MeB = mechanical braking, P1 = percentage of savings compared to MTTC, P2 = pass-by noise compared to MTTC.

4.5.1 Reference scenarios

On short distances (SPR) the energy consumption of EETC and MC is identical (see Figure 4.5 and Table 4.5). These driving strategies lead to the highest energy savings i.e., 40.4% compared to the non-eco-driving strategy MTTC. On this distance EETC will not reach the line speed, nor will it apply a cruising regime (CR), but it will switch from maximum acceleration (MA) immediately to coasting (CO). Note that the small oscillations in cruising speeds observed in the speed profiles are due to numerical approximations of the real cruise speed.

In comparison RMS leads to 36.8% more energy savings than MTTC, which is less than EETC and MC. On longer distances (IC) we see that EETC attains an optimal cruising speed of 136 km/h. This amounts to 24.8% more energy savings than MTTC (see Figure 4.5 and Table 4.6). There is a mere 0.01% difference in energy savings between EETC and MC, which makes MC nearly as energy-efficient. RMS has the highest energy consumption of the eco-driving strategies (20.7% less than MTTC). Similar to IC we find that for FT (see Figure 4.5 and Table 4.7) both EETC and MC lead to the highest energy savings with 12.7% (for EETC) and 11.7% (for MC) more than MTTC. RMS has with energy savings of 9.3% more than MTTC again the highest energy consumption of the eco-driving strategies.

The results of the workload analysis of the reference scenario (see Table 4.8) show that on short distances (SPR) MC is the least demanding (TIS = 14.0) and that the workload of MTTC is only slightly higher (TIS = 15.0). On longer distances (50 km) the driver will experience the lowest workload when applying MTTC (TIS = 15.0). EETC causes the highest workload on both short and long distances (TIS = 22.2), while MC (long distance variant) and RMS score equally high (TIS = 18.0). The workload of the latter two is considerably higher than that of MTTC, but at the same time considerably lower than the workload of EETC.

The results of the pass-by noise measurements show that on short runs (SPR) the average pass-by noise produced during a run of MTTC is about 0.9 dB higher than that of the eco-driving strategies (see Table 4.5). On long runs for IC (see Table 4.6) the difference is less (between 0.63 and 0.7 dB higher) and for FT runs (see Table 4.7) it is even smaller (between 0.3 and 0.39 dB). Since the SPR applies full regenerative braking there is no wear on short distances. For the IC we see that (see Table 4.6, under Environment-Maintenance) MC produces the least percentage of wear (26%), EETC results in more wear (35%), and of the three eco-driving strategies RMS has the highest percentage of wear (66%). For FT (see Table 4.7, under Environment-Maintenance) the driving strategies relate to each other in the same way as for IC (MC 25%, EETC 35%), although the scores of RMS on wear are almost as high as MTTC (i.e., 90%).

Note that in general the computation times of our model are quite long as can be

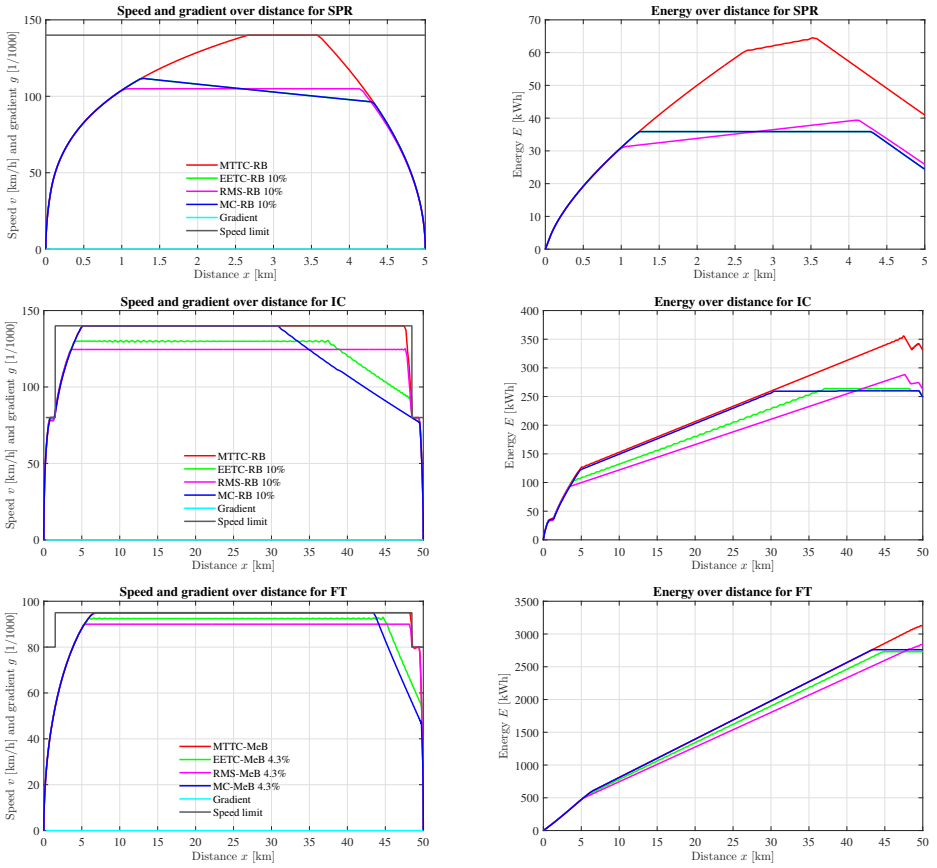

Figure 4.5: Results reference scenario. Note that for SPR the driving strategy EETC is identical to MC and, therefore, is not visible in this figure.

Table 4.8: Results workload (short = short distance variant (SPR), long = long distance variant (IC/FT), SPR = Sprinter, IC = Intercity, FT = Freight Train). Note that the determination of the total interference scores per driving strategy for the reference scenario is described in detail in Table 4.2.

Scenario	Total interference score per driving strategy				
	MTTC	RMS	MC short	MC long	EETC
0. Reference - golden run	15.0	18.0	14.0	18.0	22.2
1.2. Gradient	24.0	26.0	-	27.0	36.4
4.1. Speed restriction	28.0	31.0	24.0	32.0	42.4
6.1. Platform clearing (ETCS L2)	31.0	26.0	-	18.0	22.2
6.2. Platform clearing (NS '54/ATB)	31.0	26.0	-	22.0	26.2

seen in Table 4.5, Table 4.6, and Table 4.7. In the literature, initialization methods exist and allow a strong decrease of the computation time, see, e.g., Lejeune et al. (2016). However, we are not considering a real-time driver advisory system, but we do an offline comparison between different driving strategies. Therefore, we accept longer computation times and we did not include initialization methods to decrease the computation speeds. We just provided the computation times to indicate the performance of our model.

4.5.2 Track related scenarios

On long tracks (150 km) we see that (in contrast to the results of the reference scenario) RMS saves more energy than MC (see Figure 4.6 and Table 4.6). For IC RMS attains 16.7% more energy savings than MTTC, while MC generates extra energy savings of 13.8% compared to MTTC. EETC still saves the most energy with additional savings of 18.6%. For FT (see Figure 4.6 and Table 4.7) we see a comparable result on energy consumption (extra energy savings compared to MTTC amount to 5.7% for EETC, 5.0% for RMS, and 4.6% for MC). We used a running time supplement of 2.5% for FT, because a larger running time supplement could not be accommodated for by MC.

We see that a gradient affects all driving strategies (see Figure 4.7). For IC MTTC applies a braking regime when driving downhill to prevent the train from exceeding the line speed. The energy profile shows that energy is regenerated during this regime. When driving downhill MC applies an extra coasting, and a short braking regime. Similar to MC, EETC applies a coasting regime when driving downhill. In line with Howlett (2016) EETC applies the same cruising speed (130.2 km/h) both before and after the gradient. In Figure 4.7 it seems as if RMS also applies a coasting regime on the downhill slope, however the data

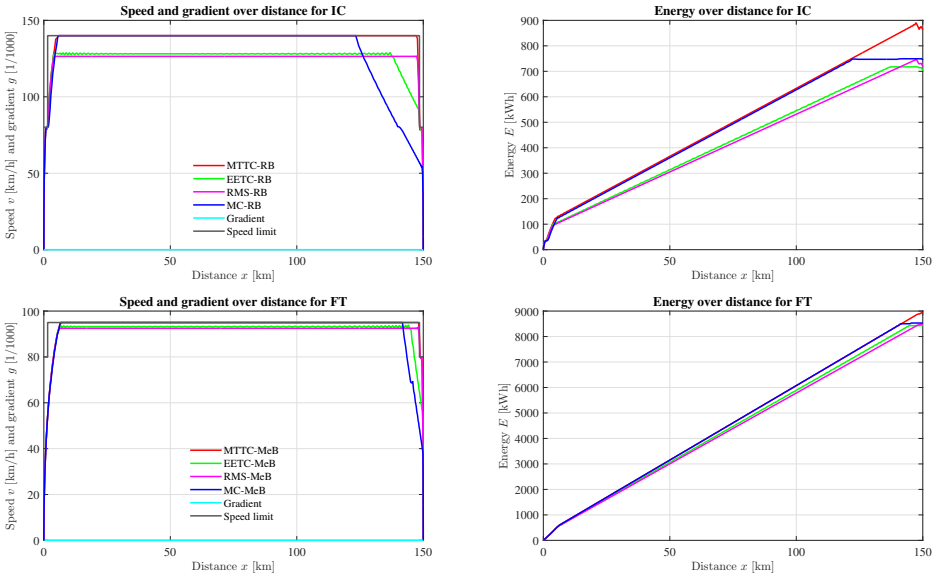

Figure 4.6: Results for scenario with a track length of 150 km for IC and FT.

shows that at this point RMS applies an extremely low amount of traction, since (4.36) restricts RMS from applying a coasting regime. The ranking of the driving strategies, with respect to energy consumption, is the same as in the reference scenario.

For FT we see that the uphill slope is so steep that none of the driving strategies can maintain speed. In this case the optimal cruising speed of EETC before the gradient (95 km/h) differs from the cruising speed after the gradient (90.3 km/h). EETC applies a coasting regime on the uphill slope. This results in a speed profile similar to that of MTTC. The effect of the gradient is the most distinct in the speed curve of MC. As a result of the relatively large percentage of running time supplement (4.3%) MC uses the first coasting phase (on the downhill slope) optimally by coasting maximally to a speed of 50 km/h. This ensures that the (final) coasting curve is almost equal to that of EETC (from 90.3 km/h onwards). RMS maintains the same optimal cruising speed of 90 km/h, both before and after the gradient. On energy savings the driving strategies score similar to the IC runs.

The workload of all the driving strategies increases considerably compared to the reference scenario on a track with a gradient (see Table 4.8). For the driving strategies MTTC (TIS = 24.0), RMS (TIS = 26.0), and MC long distance variant (TIS = 27.0) the TIS is eight or nine points higher than in the reference scenario. EETC, which already had the highest TIS score, scores on this scenario (TIS = 36.4), i.e., 14.2 points higher than in the reference scenario.

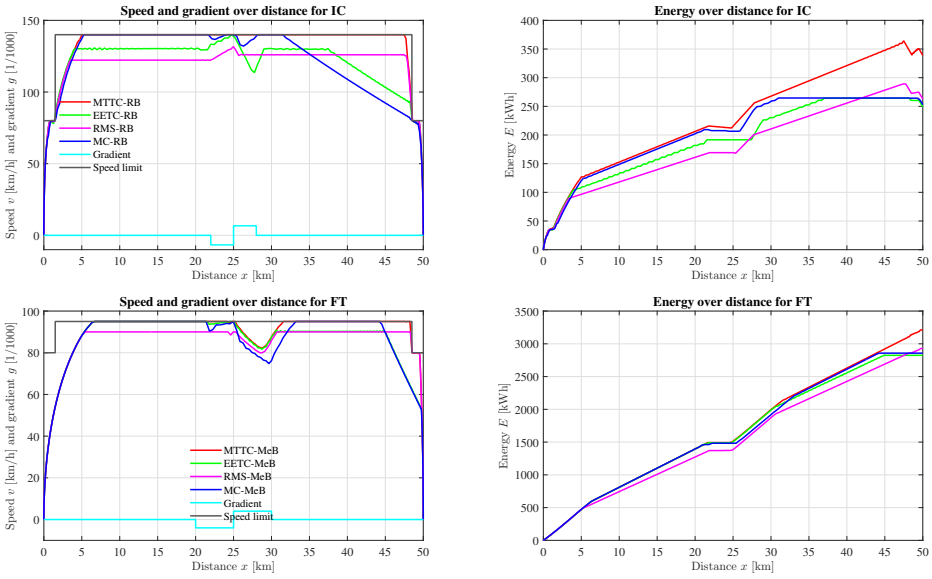

Figure 4.7: Results varying gradient scenario for IC and FT.

In this scenario, wear of MC is considerably higher than in the reference scenario (see Table 4.6 for IC, and Table 4.7 for FT), making it similar to that of EETC. For IC we see that there is a small increase in wear of RMS compared to the reference scenario (from 66% to 68%). However, for FT runs wear of RMS, which was already high in the reference scenario, increases to 99%, making it almost equally high as wear of MTTC.

4.5.3 Load factor

From the load factor scenarios (see Figure 4.8 and 4.9) we learn that the higher the load, the longer the (maximum) acceleration regime. This results in a higher cruising speed for RMS and EETC, and a longer coasting regime for MC and EETC. For MTTC a longer acceleration regime results in higher energy consumption (e.g., see Table 4.6, with a zero load MTTC consumes 326.3 kWh, a 35% load (reference scenario) results in an energy use of 330.9 kWh, and a fully loaded IC consumes 338.7 kWh).

The lighter the train, the more running time is available for eco-driving. For all eco-driving strategies we see that the lighter the train, the more extra savings compared to MTTC can be obtained (e.g., see Table 4.5 driving strategy RMS, train type SPR: a zero load results in 37.9%, a load of 35% in 36.8%, and a fully loaded train in 34.7% extra savings compared to MTTC). Note that for MC (IC),

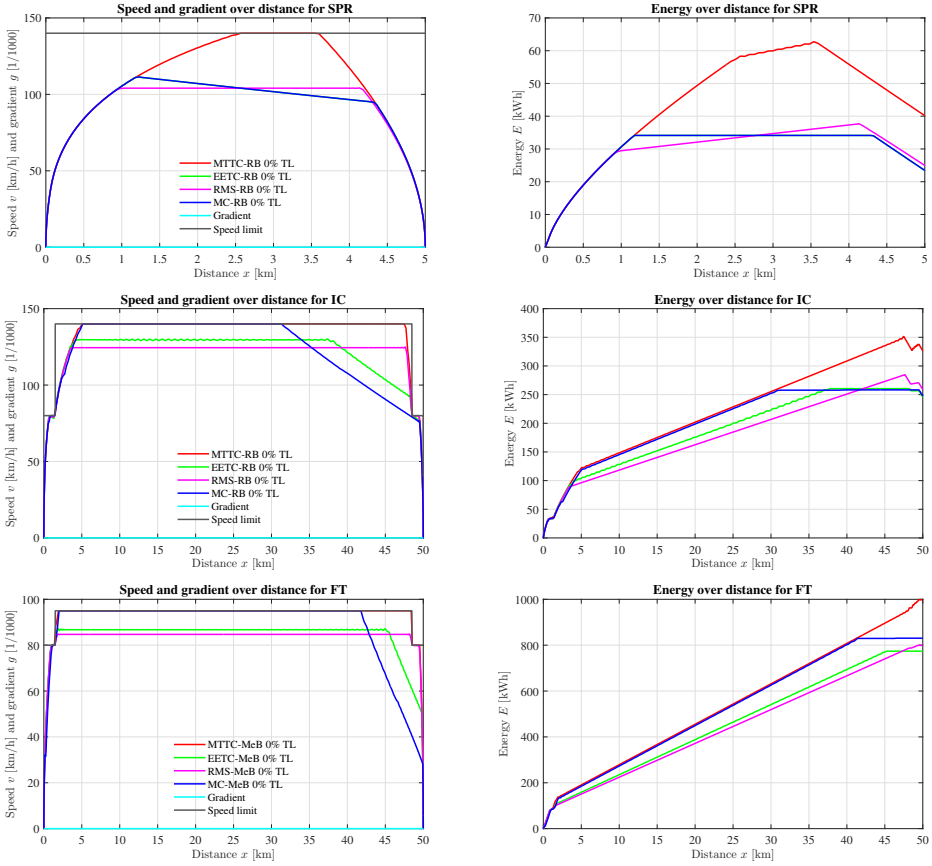

Figure 4.8: Results zero load scenario.

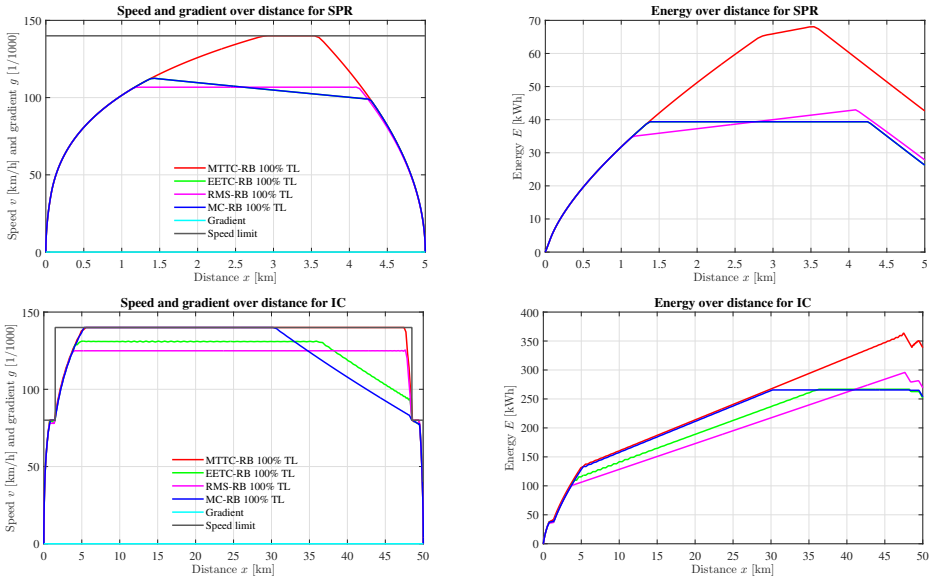

Figure 4.9: Results fully loaded scenario for SPR and IC.

a train with zero load will not be hindered by the speed restriction of 80 km/h at the end of the track, and can maintain the coasting regime longer, see Figure 4.8. The coasting capacity with a zero load is low, so the train will already have reached a speed lower than 80 km/h at that point. As a result, the extra energy savings (compared to MTTC) for MC with a zero load is relatively high compared to scenarios with a higher load (see Table 4.6 under Energy consumption: 24.2% for zero load, 24.8% for a load of 35%, and 25.1% for a fully loaded train).

4.5.4 Braking characteristics

We find that when mechanical braking is applied (see Figure 4.10), the difference in energy savings between MTTC and the eco-driving strategies becomes larger. For SPR, under the driving strategy EETC or MC, the extra savings compared to MTTC amount to 44.4%, as opposed to 40.4% when regenerative braking is applied. For RMS this results in extra savings compared to MTTC of 39% with mechanical braking, and 36.8% with regenerative braking. For IC we see similar results. For IC we see a steep rise (by a factor 2.9 for EETC, and 3.7 for the other driving strategies) in the percentage of wear compared to the reference scenario (see Table 4.6 under PMx=Wear(%)).

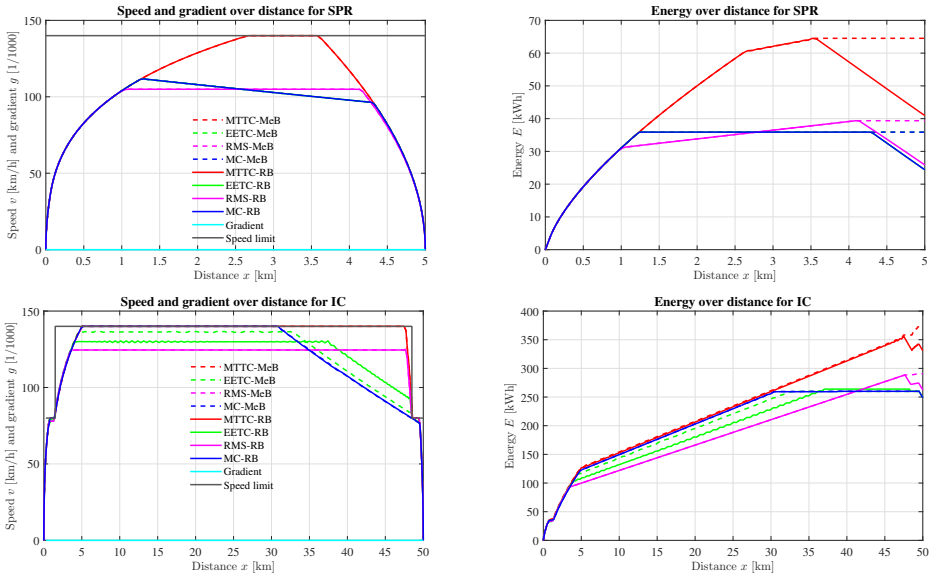

Figure 4.10: Results mechanical versus regenerative braking scenario for SPR and IC.

4.5.5 Speed restrictions

In the results of the speed restriction scenario (see Figure 4.11), we see that the difference in energy savings between MTTC and the eco-driving strategies is larger than in the reference scenario. We see, e.g., that for SPR EETC and MC save 57.2% more energy compared to MTTC (see Table 4.5), while in the reference scenario this amounted to 40.4%. This does not change the ranking of the eco-driving strategies with respect to the total energy consumption, i.e., in this scenario EETC still saves the most energy, followed by MC, and then by RMS.

For both FT and IC we see that in this scenario wear increases for most driving strategies. Only for the driving strategy EETC (for FT) wear remains the same as in the reference scenario, see Table 4.7. For FT the wear of MC becomes 10 percentage points higher than in the reference scenario. Especially for IC we see a substantial increase in the wear of RMS from 66% in the reference scenario to 84% in the speed restriction scenario (see Table 4.6). For FT wear of RMS was already 90% in the reference scenario. In this scenario it becomes similar to MTTC (i.e., 99%), see Table 4.7.

The workload of EETC becomes almost twice as high as in the reference scenario (see Table 4.8) with a TIS of 42.4. On short distances, MC has the lowest TIS of 24.0. This is considerably less than MTTC (TIS = 28.0). On longer

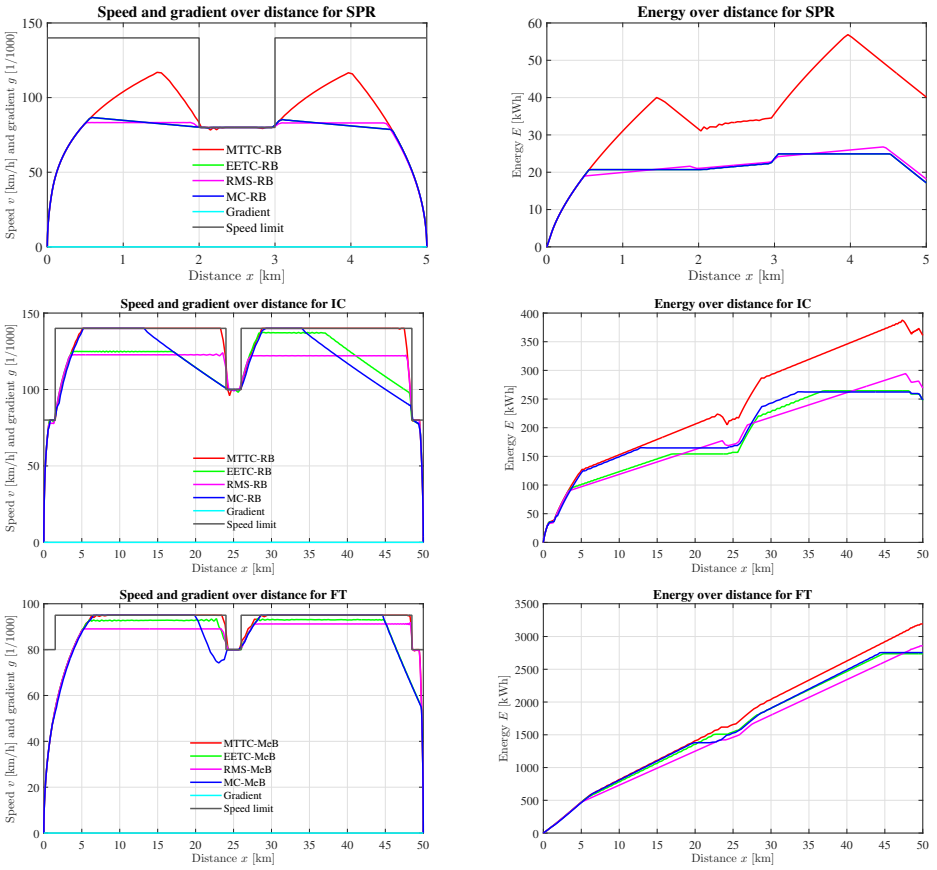

Figure 4.11: Results speed restriction scenario.

distances the score of RMS (TIS = 31.0) and MC (TIS = 32.0) with respect to workload is similar. In this scenario, as in scenario 1.2. Gradient (See Table 4.8), we see that the difference in workload between on the one hand RMS and MC, and on the other hand EETC increases.

4.5.6 Running time supplement

The results of the test scenarios with varying running times show that in general the larger the percentage of running time supplement, the lower the optimal cruising speed, and the longer the coasting regime. In addition, the more running time supplement, the sooner the train starts a coasting regime. On short distances (SPR) EETC and MC refrain from applying a cruising regime. As stated before, extra savings compared to MTTC runs can be attained by applying an eco-driving

strategy. However, these additional energy savings are not directly proportional to the running time supplement. The Pareto curve (see Figure 4.12) shows that the relative energy savings become smaller when the running time is longer i.e., for EETC and MC (SPR) we see that in comparison to MTTC, a 5% running time supplement leads to 28.6% extra energy savings, while a 10% running time supplement leads to additional savings of 40.4%, and a 15% running time supplement leads to 48.3% (see Table 4.5).

On longer distances (IC), EETC starts coasting at more or less the same point for every variation in running time supplement, while MC starts coasting at an earlier point as the percentage of the running time supplement increases. When there is a relatively small percentage of running time supplement (5%) additional energy savings of MC (18.2%) are comparable to those of EETC (18.3%) (see Table 4.6). However, when there is a relatively large percentage of running time supplement (15%) RMS saves slightly more energy than MC (see Table 4.6). In this situation RMS has 27.2% and MC 27.1% additional savings compared to MTTC, while EETC remains the most energy-efficient driving strategy. We see similar results for FT (see Table 4.7). However, energy savings of RMS become significantly higher than those of MC with a running time supplement of either 7.5% or 10%.

We find that wear diminishes as the percentage of running time supplement increases, and that (similar to energy consumption) the rate with which it diminishes is not directly proportional to the percentage of running time supplement (see Tables 4.6, and 4.7 under PMx = Wear(%)), e.g., on long distances (IC) the percentage of wear for RMS with a running time supplement of 5% is 73%, with a running time supplement of 10% it is 66%, and with a running time supplement of 15% it is 58%). Similar to the reference scenario MC produces the least percentage of wear, while of the eco-driving strategies RMS scores the highest.

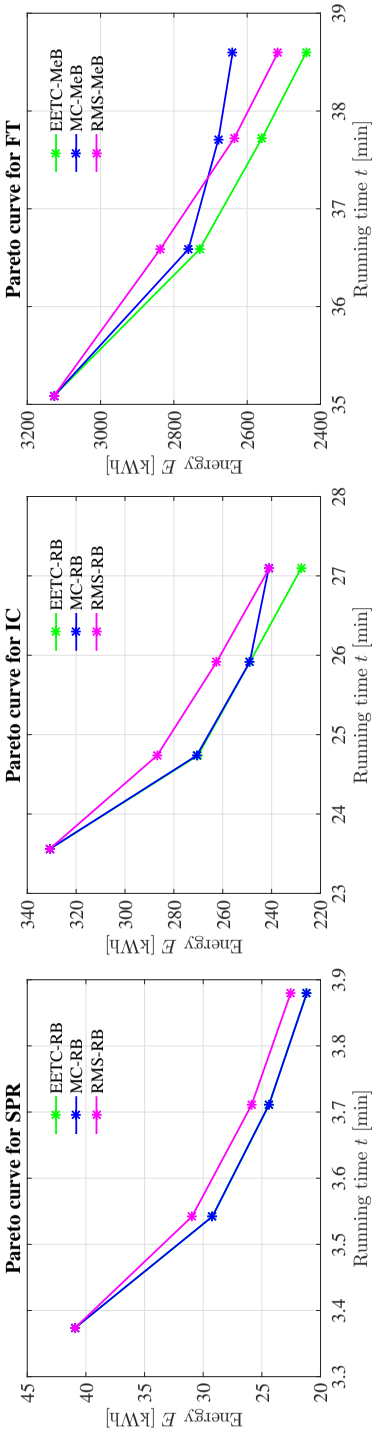

Figure 4.12: Pareto curves varying running time (left SPR, middle IC, and right FT).

4.5.7 Platform clearing scenarios

In this section we will look at the effects of driving strategies in a more dense network in which the platform clearing times of a previous train at the platform can influence the arrival of the test train (see Figure 4.4). The energy consumption of the eco-driving strategies is the same as in the reference scenario. Only MTTC consumes more energy. Therefore, the additional savings of the eco-driving strategies compared to MTTC increase, with approximately 6.5 under ETCS L2 (scenario 6.1), and 1.5 percentage points under NS '54/ATB (scenario 6.2), see Table 4.9.

Under ETCS L2 we see that the workload of an EETC or MC driver is the same as in the reference scenario (see Table 4.8). MTTC has in both platform clearing scenarios the highest workload, which includes making an unplanned stop at the entry signal, and informing passengers (the latter task is mandatory within NS proceedings). The workload of RMS also increases significantly compared to the reference scenario (from a TIS of 18 to a TIS of 26), making RMS the eco-driving strategy with the highest workload in scenario ETCS L2, and a workload similar to EETC under NS '54/ATB. Although, the workload of MC increases in the NS '54/ATB scenario, in relative terms the difference with EETC remains the same, making MC the driving strategy with the lowest workload in this scenario.

Note that only for MTTC an additional braking and acceleration regime is necessary. This can be seen in the results for wear. For the eco-driving strategies this evaluation criterion is the same as in the reference scenario. For MTTC we see an increase in wear of 35 percentage points under the ETCS L2 scenario, and of 9 percentage points under the NS '54/ATB scenario (see Table 4.9).

Safety is measured in scenario 6.2 (see Table 4.9). The results of this scenario show that for MTTC the distance, and time remaining between the first and final braking regime is negative, i.e., -238 m and -21 s, respectively (see Table 4.9). Negative values mean that the driver (in order to avoid a SPAD) will have to brake harder than the minimal required braking deceleration of 0.43 m/s^2, making the risk of a SPAD for this driving strategy high. For RMS, there is a distance of 129 m left to be covered within 12 s. This is a large enough margin for the driver to stop the train in front of the signal at danger. For MC and EETC a distance of more than 600 m remains, to be covered within 60 to 80 s. The margin here is large.

In both these scenarios MTTC experiences hinder from the previous train, that is still at the platform as the MTTC train passes the signal at warning. As a consequence, the train arrives less early than in the reference scenario (-46.88 s under ETCS L2, and -28.37 s under NS '54/ATB, see Table 4.9), but still not timely. Under ETCS L2 all eco-driving strategies manage to arrive timely, but under NS '54/ATB only RMS and EETC are timely. Although, the MC train arrives at the

Table 4.9: Results IC for the platform clearing scenarios.

Results platform clearing scenarios (IC)	Safety			Timeliness	Energy consumption		Environment	Environment-Maintenance	Brand Image
	P1 (km/h)	P2 (km)	P3 (s)	Deviation arrival time (s)	(kWh)	P4 (%)	P5 (dB)	PMx = Wear (%)	Unplanned stop
6.1. Platform Clearing (ETCS L2)									
MTTC-RB	140	-	-	-46.88	361.8	0.0%	0.00	135%	Yes
EETC-RB	98	-	-	0.00	248.9	31.2%	0.69	35%	No
MC-RB	85	-	-	0.00	249.0	31.2%	0.63	26%	No
RMS-RB	125	-	-	0.00	262.5	27.4%	0.72	66%	No
6.2. Platform Clearing (NS '54/ATB)									
MTTC-RB	140	-238	-21	-28.37	338.2	0.0%	0.00	109%	Yes
EETC-RB	98	668	60	0.00	248.9	26.4%	0.54	35%	No
MC-RB	85	879	79	17.20	249.0	26.4%	0.47	26%	No
RMS-RB	125	129	12	0.00	262.5	22.4%	0.56	66%	No

Legend: IC = Intercity, PMx = particular matter (brake grindings), RB = regenerative braking, P1 = speed at 47 km (signal at danger), P2 = distance between the end of the first braking regime and the beginning of the second braking regime, P3 = time left between the end of the first braking regime and the beginning of the second braking regime, P4 = percentage of savings compared to MTTC, P5 = pass-by noise compared to MTTC.

signal at warning a number of seconds earlier than under RMS, it passes this signal with a significantly lower speed (85 km/h). The MC train is then obliged by the ATP to maintain a speed of 40 km/h over a longer period of time than under RMS. This causes the MC train to arrive 17.2 s later than the planned arrival time. Since MTTC causes an unplanned stop in both these scenarios this driving strategy will have a negative impact on the brand image for passengers.

4.6 Discussion

In Section 4.5 we have seen that driving strategies affect the train operator's KPIs in various ways, and that the circumstances of a TOC or FOC determine which driving strategy will be most beneficial for its operation. There is no one size fits all solution, when it comes to selecting an appropriate driving strategy for a TOC or FOC. We see for instance, that it depends on the level of automation, whether or not the minimal energy solution, EETC is an appropriate choice.

In this section we discuss the findings in Section 4.5 in the light of previous studies, conventional wisdom, and the known literature on the subject of train driving strategies. Based on our results in Section 4.5 we first draw some general conclusions as to which driving strategy is, under which circumstance the most beneficial for the KPIs in our toolbox (see Section 4.6.1). We then conclude this section in Section 4.6.2 by discussing the implications of our main results on a number of issues concerning train operation. Some of these issues could be studied further on basis of our results, and could subsequently lead to additional insights into the effects of driving strategies on KPIs relevant to train operation.

Note that, although in this study all seven KPIs in the toolbox are important,

the KPI energy consumption is often mentioned first, and often receives more attention than the other KPIs, because most of our driving strategies are eco-driving strategies, and the focus of research up until now has predominantly been on this KPI.

4.6.1 Choosing an appropriate driving strategy

For fully automated trains the importance of the KPIs energy consumption, environment and cost of maintenance (wear) for a TOC or FOC determine the choice for a driving strategy. The KPI workload is not an issue in this situation and therefore EETC could be an appropriate choice. However for semi-automatic train operation, it is important to consider a fall back scenario (in case there is a manual take-over by the driver) in which either RMS or MC is applied, so that there is a reasonable workload for the driver.

On short (metro-like) distances MC (like EETC), has the lowest energy consumption. This is counter to the findings in previous research (see Li & Lo (2014a)), where for highly regenerating rolling stock, RMS is presented as favorable to MC with respect to energy consumption. For TOCs with many metro-like distances, a high-density network, low running time margins (less than 15%), and manual train control, MC seems to be the most appropriate driving strategy. Under these circumstances, MC has in addition to the lowest energy consumption also the lowest workload. Moreover, it scores best on environmental pollution, and cost of maintenance.

Only when there is a relatively large percentage of running time supplement (15% or more), or a relatively long track, RMS manages to save more energy than MC. A TOC or FOC which only operates on long hauls (more than 50 km) without running the risk of crossing busy tracks, or hinder from other trains, and with predominantly manual operation would be best served with RMS as its preferred driving strategy. However, consideration should be given to the KPI cost of maintenance because RMS causes a relatively large amount of wear, and also to the KPI environment because of the relative large amount of brake grindings generated by this driving strategy.

4.6.2 Train operating issues

It was suggested by Van Dongen & Schuit (1989a) that the reduction in catenary losses by reducing acceleration would change the optimum in the driving strategy. However, our findings show that increased traction at the beginning of a train run does not necessarily lead to higher energy consumption. On the contrary, although MC uses the maximum amount of energy in the acceleration regime (unlike for

instance RMS), we find that the total use of energy during an MC run is usually significantly lower than that of RMS.

In some energy saving programs there was a strong focus on regenerative braking. In this study, we certainly see that regenerative braking makes additional energy savings possible. However, a strict focus on regenerative braking as the only energy saving measurement is a suboptimal approach, because according to our findings, an eco-driving strategy with mechanical braking saves more energy than MTTC, even if MTTC uses regenerative braking. Therefore, energy saving programs should first and foremost focus on choosing, and implementing an appropriate eco-driving strategy (see Luijt et al. (2017)), and only then add regenerative braking as an extra measurement to save more energy.

Although there are eco-driving (training) programs without electronic devices that have brought about substantial energy savings (e.g., see Luijt et al. (2017)), the implementation of a DAS could offer TOCs and FOCs the opportunity to operate more precisely, as calculations can be performed more accurately. A DAS can alleviate tasks of the driver (KPI workload), by calculating the start of the coasting regime and/or the cruising speed. This could require less computation effort of drivers. However, the KPI workload of the driver could be influenced negatively if a DAS gives several updates during a run. This can cause distraction and can increase the workload, depending on the specific implementation. An additional study into the effect of human aspects of each specific DAS implementation should be considered.

Pass-by noise could at certain locations along a track be a critical factor, that limits capacity (i.e., number of trains allowed to pass this location). Our study does not offer a direct solution to this problem (since we compared the average pass-by noise per driving strategy over the full track length), but it can help in a comprehensive weighing of the different KPIs. An analysis on pass-by noise on a specific location might lead to a trade-off between optimal energy savings, and noise reduction, leading possibly to an optimized speed profile with for instance an additional coasting regime at this location.

An interesting addition to our study would be a comparison of driving strategies on a higher line speed (e.g., 160 km/h). In previous field tests in the Netherlands (see Weltevreden (2015)), we saw that a higher line speed with the same timetable led to an increase in energy consumption, because drivers would arrive ahead of time. It would be interesting to study this scenario for our eco-driving strategies, and find out whether the possibility of longer traction in the acceleration regime, and as a consequence a longer coasting regime, could lead to reduced energy consumption under these circumstances.

Under a conventional ATP, all eco-driving strategies are safer compared to MTTC (i.e., have a low risk of a SPAD). This means that under eco-driving a

conventional ATP system offers better protection than under MTTC. The fact that ATP protection under eco-driving is better, does not necessarily reduce the number of SPADs, because drivers who apply eco-driving in the vast majority of their train trips might not be sufficiently aware of this risk, when applying MTTC to make up for lost time. Further study on this subject and in addition on other human factors such as the risk of distraction in this case, could lead to additional insights.

For the four driving strategies studied, the seven KPIs are shown to yield different optimal solutions. None of these four driving strategies scores optimal on all. When applying these results, other driving strategies can be developed that optimize on a (weighted) mix of these KPIs. Such an optimum depends on the specific situation, as the relative importance of (sometimes location-specific impacts) varies. This study establishes the seven KPIs and evaluation methods and establishes a toolbox rather than defining an optimum for a specific situation. In future research TOCs and FOCs can optimize specific preferences with the help of this toolbox.

4.7 Conclusions

In this study we defined a toolbox of SMART KPIs for train operation, that are influenced by the train driving strategy. Those KPIs are safety, timeliness, energy consumption, workload of the driver, environmental pollution, cost of maintenance and brand image (of a TOC). We chose four of the most used train driving strategies to study their effect on the KPIs in the toolbox that enables TOCs and FOCs to evaluate different driving strategies. We considered the driving strategies minimum time train control, energy-efficient train control, maximal coasting and reduced maximum speed. We formulated the optimal control problem for each different driving strategy and implemented them in our algorithm. The general conclusion is that any eco-driving strategy has advantages over MTTC on most of these KPIs. We also conclude that in general the MC driving strategy can best approach the EETC driving strategy, because without the help of a DAS it is very difficult for a train driver to follow the EETC speed profile. In this section we summarize our findings per KPI, and then conclude with suggestions for further research.

All eco-driving strategies score similarly high on safety (under a conventional ATP), and on timeliness. All these strategies make it possible to approach an entry signal at danger without having to brake excessively, so that (in contrast to MTTC) there is a relatively low risk of a SPAD. Furthermore, in most scenarios eco-driving strategies manage to arrive exactly on the second of the planned time, while MTTC usually arrives ahead of time.

There is a significant difference between the eco-driving strategies with respect

to energy consumption. EETC has by definition the lowest energy consumption, and MTTC the highest. Energy savings of MC are equally or nearly as low as of EETC. Only on long tracks (150 km) RMS saves slightly more energy than MC. We can conclude that MC is comparable to EETC in energy consumption, while (counter to our expectations) RMS is not. So coasting is an essential regime for energy savings.

On sparsely used routes MTTC has a low workload compared to the eco-driving strategies. However, on a busy train network where MTTC runs the risk of unplanned stops it has the highest workload, while MC has the lowest workload. When trains do not experience hinder of previous trains clearing the platform, MC has the lowest workload, but only on short distances. On longer distances (50 km) MC and RMS are comparable in workload, while EETC scores significantly higher. In some scenarios the workload of EETC is twice as high as in the reference scenario. In order to ensure both timeliness and energy consumption the support of some sort of electronic device for the driver (DAS) is indispensable. From our findings it is apparent that it will be much harder (near impossible) for a driver to apply EETC than either RMS or MC without the use of a DAS.

Compared to MTTC any eco-driving strategy will diminish the average pass-by noise with more or less the same amount. MC causes the lowest wear on the braking blocks, and therewith produces the least amount of brake grindings per train trip. This makes MC the most environmental friendly strategy with the least maintenance costs. Under EETC wear is usually somewhat higher than under MC. However, RMS causes significantly more wear. In some situations it is almost equal to that of MTTC. MTTC is by definition the least environmental friendly, and has the highest costs in maintenance.

On a busy train network such as in the Netherlands, MTTC runs a higher risk of an unplanned stop near the arrival station, which will have a negative effect on the brand image for passengers. In contrast, none of the eco-driving strategies run the risk of causing an unplanned stop.

Further research on additional characteristics and conditions will increase the insight into the effect of driving strategies on the KPIs presented in this chapter. A few examples are the effects of driving strategies on slippery tracks, the maintenance condition of the bearings, improved catenary capacity for either powering or accepting (regenerated) energy (e.g., 3 kV), a higher line speed (160 km/h), a larger variation in gradients (e.g., for TOCs and FOCs with tracks on mountainous terrain), and different degrees of delays of preceding trains. Furthermore, a more profound research on the KPI cost of maintenance by studying the effect of driving strategies on wear of wheels, rails, and the catenary system could yield additional insights.

Chapter 5

Optimal running time supplement distribution in train schedules for energy-efficient train control

---

Apart from minor updates, this chapter has been published as:
Scheepmaker, G. M., Pudney, P. J., Albrecht, A. R., Goverde, R. M. P., Howlett, P. G. (2020) Optimal running time supplement distribution in train schedules for energy-efficient train control, *Journal of Rail Transport Planning & Management*, 14, 100180.

5.1 Introduction

Energy efficiency is an important topic for railway companies wishing to reduce CO_2 emissions and save money. One of the research areas to improve the energy efficiency of railways is *energy-efficient train control* (*EETC*). EETC is an optimal control problem with the aim of finding the driving strategy or trajectory that meets the timetable with the lowest energy consumption. The potential for EETC is determined by the timetable, because the running time supplements determine how much energy can be saved by energy-efficient driving (Scheepmaker & Goverde, 2015). The *running time supplements* are the extra running time above the minimum running time (computed by the *minimum time train control* (*MTTC*)) in order to recover from small delays or disturbances during operation.

The *Energy-Efficient Train Timetabling* (*EETT*) problem aims to compute a

timetable for trains running between different stops that maximizes the potential of energy-efficient driving. An overview of the topic of EETC and EETT can be found in the literature review papers of X. Yang et al. (2016) and Scheepmaker et al. (2017). One part of the research is focused on maximizing the usage of regenerative braking energy by synchronizing the accelerating and regenerative braking train around the same station within the same catenary section (Scheepmaker et al., 2017). The aim is to minimize the transmission losses and maximize the consumption of the regenerated energy. Other research is focused on the optimal distribution of the running time supplements for energy-efficient train driving. A stream of research on the optimal distribution of the running time supplements aims to find the optimal running time supplement amount for a single journey section between two stops, e.g., Sicre et al. (2010) and Cucala et al. (2012). The objective is to minimize the trade-off between energy consumption and running time loss by creating a cost-curve or Pareto frontier curve. Another stream of research focuses on the multiple-section train control problem that aims to find the optimal distribution of running time supplements for a single train over multiple stops with a fixed overall journey time to minimize energy consumption. This is also the topic considered in this chapter.

Pudney et al. (2009) studied the topic of the optimal running time supplement distribution for energy-efficient train driving. They computed the optimal distribution of the running time supplements over multiple stops with varying speed limits and gradients for freight trains by using the Energymiser model. To determine the speed trajectories, the authors started from the condition that the cruising speed must be the same on each section. The intuitive argument for equal cruising speeds is to consider an optimal trajectory for EETC where the train has to slow down to an arbitrarily low speed for a small distance during the journey. This trajectory will have the same cruising speed throughout the journey. Therefore, results indicate that the optimal distribution of the running time supplements should lead to the same optimal cruising speed between each two consecutive stops of the trajectory. If this unique speed is not achievable on a particular section there should be no cruising on that section. In addition, if this unique speed is higher than the speed limit, then the cruising speed is set at the speed limit. The theoretical framework for this optimal distribution of the running time supplements follows from observations by Isayev (1987) and by Howlett & Pudney (1995). An explicit statement and proof of this result by Howlett (2016) was motivated by the fact that many authors outside of the former Soviet Union were apparently unaware of this result.

Su et al. (2013, 2014) computed the optimal distribution of the running time supplements over multiple stations for energy-efficient driving of metro trains, and focused on finding the energy optimal timetable (i.e., arrival and departure times). Scheepmaker & Goverde (2015) compared a uniform redistribution of the running

time supplements over the complete trajectory with an existing timetable for a regional train. Goverde et al. (2016) proposed a three-level timetabling method, which first constructs a stable robust conflict-free timetable with optimal train orders and then optimizes the time supplements between the stops of regional trains in a corridor between two main stations for energy-efficiency. The time supplements are reallocated to optimize energy-saving train operation, taking into account the stochastic dwell times. The problem is formulated as a multi-stage, multi-criteria decision problem and solved by dynamic programming.

P. Wang & Goverde (2017) considered a multi-train trajectory optimization method to find optimal meeting locations and times, as well as associated train trajectories for single-track lines with the aim to minimize a trade-off between delays and energy. They considered multiple trains simultaneously and added headway constraints and time window constraints to find conflict-free solutions. P. Wang & Goverde (2019) adapted this model to compute the optimal energy-efficient allocation of running time supplements to all trains running over a (single-track and/or double-track) corridor while maintaining a conflict-free timetable and keeping the train orders as determined in a preceding timetabling step. The optimal running time supplement distribution then depends on the interactions between the trains. General principles for optimal driving with fixed arrival times at stops are well known, and several methods for calculating EETC profiles have been described in the literature. These methods include *indirect methods* that indirectly solve the optimal control using the necessary optimality conditions of *Pontryagin's Maximum Principle* (*PMP*) (Pontryagin et al., 1962; Lewis et al., 2012; Ross, 2015), and *direct methods* that transcribe the optimal control problem into a nonlinear optimization problem and directly solve this problem (Betts, 2010). The optimal control and timetabling problem is less well known. For this problem, the aim is to find intermediate arrival times at stops and a driving strategy that minimizes the energy required to complete a multi-stop journey within a given overall journey time. This problem requires the optimal distribution of running time supplements within a journey. Scheepmaker & Goverde (2015) showed that a uniform distribution of running time supplements increases the potential for energy savings, but they did not investigate whether uniform distribution was optimal. Howlett (2016) showed that the optimal cruising speed should be the same on each journey section. This chapter solves example optimal control and timetabling problems using both direct and indirect methods. It shows that these two methods give practically the same solutions, with small differences due to numerical inaccuracies. It also shows that the optimal distribution of running time supplements is not necessarily uniform.

There are different ways to solve the various energy-efficient train control problems: indirect and direct solution methods, and heuristics (Scheepmaker et al.,

2017). Indirect solution methods solve the optimal control problem indirectly by using the optimal control structure derived from Pontryagin's Maximum Principle (Pontryagin et al., 1962; Lewis et al., 2012; Ross, 2015). This leads to the following *driving regimes*: maximum acceleration, cruising at a constant speed by partial traction, coasting without using traction or braking, cruising at a constant speed by partial (regenerative and/or mechanical) braking, and maximum braking. The challenge is to find the optimal sequence and switching points between the regimes, which is computed by constructive algorithms exploiting the knowledge of the optimal control structure. The results of those models are very accurate, but for more complex problems, such as those with varying speed limits and gradients, the problem becomes more difficult to solve. Nevertheless these problems can be solved by the Energymiser package in real-time on board very fast trains. Examples can be found in Howlett & Pudney (1995), Khmelnitsky (2000), Liu & Golovitcher (2003), and A. Albrecht et al. (2016a,b).

A second way to solve the EETC problem is by using direct solution methods, mainly applied in aerospace applications (Ross & Karpenko, 2012). These methods first discretize the optimal control problem and then transcribe it to a nonlinear programming (NLP) problem that is solved using standard NLP solvers (Betts, 2010). The direct solution methods do not assume a priori knowledge of the optimal control structure, but they are in general slower and less accurate than dedicated indirect algorithms. Examples of these methods applied to optimal train control can be found in Y. Wang et al. (2013, 2014), Ye & Liu (2016), P. Wang & Goverde (2016a,c, 2017, 2019), Scheepmaker & Goverde (2016), and Scheepmaker et al. (2020b).

Heuristics approach the optimal control problem by using artificial intelligence or search algorithms, but they do not provide any information about the quality of the solution. Some examples can be found in Chevrier et al. (2013), Sicre et al. (2014), and Haahr et al. (2017). The indirect and direct solution methods give results that numerically approximate the solution of the optimal control problem. However, a comparison of the two methods applied on the same case study is, to our knowledge, not considered in the literature. Therefore, we compare an indirect and a direct solution method in order to determine the advantages and disadvantages of both models and to see if they generate similar results.

The aim of this chapter is to find the optimal distribution of the running time supplements over multiple stops for a single train given a total scheduled running time, and the full availability of the supplements to be used for energy-efficient train driving, and to compare an indirect solution method with a direct solution method in order to compute the optimal control. The purpose of the optimal running time supplement distribution in this chapter is to determine the optimal allocation of supplements over multiple stops in order to minimize total traction

energy consumption of a train run (i.e., to maximize the usage of EETC by the train). These insights can be used for timetable design to determine the energy-optimal timetable. Therefore, the following contributions to the literature are made:

- A model for the optimal running time supplement distribution over multiple stops given a total scheduled running time by including intermediate speed constraints with the objective of minimizing the total traction energy consumption of a single train.
- Implementation and application of the optimal running time supplement distribution model in a generic direct solution method by using the MATLAB toolbox GPOPS.
- Application of an indirect method using the knowledge that the optimal distribution of time supplements must have the same optimal cruising speed between each pair of stops by using the Driver Advisory System (DAS) Energymiser.
- A comparison between the indirect and direct solution methods for both the minimum-time and energy-efficient train control problem on different case studies.

This chapter is structured as follows. In Section 5.2 the optimal control problem is discussed for minimum time and energy-efficient train driving over multiple stops in order to find the optimal running time supplement distribution. Section 5.3 discusses the indirect and direct methods used to compute the driving strategies. Section 5.4 contains a case study that applies both models and compares the results. Finally, the conclusion and discussion are presented in Section 5.5.

5.2 Optimal control and running time supplement distribution

This section considers the optimal control problem for a multiple-section trajectory in order to determine the optimal distribution of the running time supplements given the total scheduled running time. The optimal control problem is formulated and we derive the necessary optimality conditions by applying Pontryagin's Maximum Principle. We consider only mechanical braking (MeB), because we would like to show the general principles of the optimal distribution of the running time supplements and we do not consider interaction with other trains. In addition, Scheepmaker et al. (2020b) showed that regenerative braking has little impact on the structure of an optimal journey.

The derivation of the optimal control problems is based on earlier work of Howlett (2000), Khmelnitsky (2000), Liu & Golovitcher (2003), and A. Albrecht et al. (2016a,b). Although we build on the current literature, we do include new elements and insights. In particular, we consider minimizing the energy consumption over multiple stops (i.e., different objective function see Eq. (5.1)) by including intermediate speed constraints (see Eq. (5.9)). Therefore, we need to derive the optimal control structure to see what the influence is on the necessary optimality conditions. Moreover, these conditions are used to verify if the model results of the direct solution method are in line with the optimality conditions. In our problem formulation we consider distance as the independent variable, because the speed limit and gradient are related to the distance. In addition, we separate the control u [m/s^2] into specific traction force f [m/s^2] and specific mechanical braking force b [m/s^2], that is, $u = f + b$. The specific force is computed by dividing the total traction force F [N] or braking B force [N] over the equivalent mass, which is given by the actual mass m [kg] times the rotating mass factor ρ [-]), that is, $f = F(t)/(\rho m)$ and $b = B(t)/(\rho m)$.

Section 5.2.1 considers the energy-efficient train control problem over multiple stops by including intermediate speed constraints that minimizes the total amount of traction energy of a train run. Section 5.2.2 briefly discusses the minimum time train control problem over multiple stops that minimizes the total running time of a train.

5.2.1 Energy-efficient train control

In this section we discuss energy-efficient train control over multiple sections between successive stops with mechanical braking. The optimal control problem can be defined to minimize total traction energy J [m^2/s^2] over a railway line with n sections over given stop positions $(s_0, \ldots, s_n)$ with a total scheduled running time T [s]:

$$J = \min \int_{s_0}^{s_n} f(s)\, ds, \tag{5.1}$$

subject to the constraints

$$\dot{t}(s) = \frac{1}{v(s)} \tag{5.2}$$

$$\dot{v}(s) = \frac{f(s) + b(s) - r(v) - g(s)}{v(s)} \tag{5.3}$$

$$f(s)v(s) \leq p_{\max} \tag{5.4}$$

$$0 \leq v(s) \leq v_{\max}(s) \tag{5.5}$$

$$0 \leq f(s) \leq f_{\max} \tag{5.6}$$

$$-b_{\min} \leq b(s) \leq 0 \tag{5.7}$$

$$t(s_0) = 0, t(s_n) = T \tag{5.8}$$

$$v(s_i) = 0, \text{ for } i = 1, \ldots, n, \tag{5.9}$$

where distance s [m] is the independent variable, time t [s] and speed v [m/s] are the state variables, $\dot{t} = dt/ds$ and $\dot{v} = dv/ds$, and specific traction f and specific mechanical braking b are control variables. The speed at each stop i at distance s_i is zero, leading to the intermediate event constraints (5.9). The specific traction f is bounded by the maximum specific traction force $f_{\max}$ and the specific braking force b is bounded by the maximum specific braking force $-b_{\min}$. In addition, the specific traction control is also limited by the specific power of the train p [m^2/s^3], which is limited by the maximum specific power $p_{\max}$. The specific traction force is thus bounded by a constant part depending on the maximum specific traction force and a hyperbolic part depending on the specific power of the train, that is, $f \leq f(v) = \min(f_{\max}, p_{\max}/v)$; see Figure 5.1. Note that the train cannot apply both traction and braking at the same time, that is, $fb = 0$. The total specific train resistance consists of the specific train resistance $r(v)$ [m/s^2] and the specific line resistance $g(s)$ [m/s^2]. The Davis equation $r(v) = r_0 + r_1 v + r_2 v^2$ gives the specific train resistance and consists of non-negative coefficients $r_0, r_1 \geq 0$ and $r_2 > 0$ (Davis, 1926). Gradients $g(s)$ determine the specific line resistance with $g(s) > 0$ indicating uphill slopes and $g(s) < 0$ downhill slopes. The speed v is bounded by the speed limit $v_{\max}$. We assume piecewise-constant speed limits and gradients over the complete trajectory.

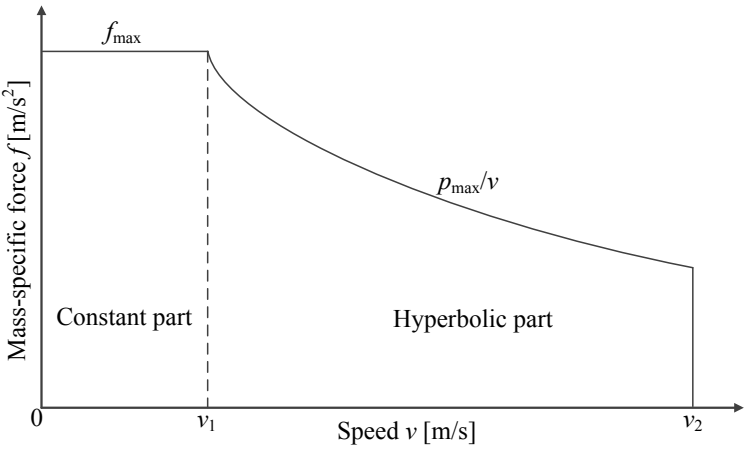

Figure 5.1: Typical specific traction-speed diagram with a constant and hyperbolic part.

We now summarize the necessary optimality conditions. The Hamiltonian H [m/s^2] is defined as

$$H(t,v,\lambda_1,\lambda_2,f,b,s) = -f + \frac{\lambda_1}{v} + \frac{\lambda_2(f+b-r(v)-g(s))}{v}, \tag{5.10}$$

with the costate variables λ_1(s) [m^2/s^3] and λ_2(s) [m/s] as functions of the independent variable s. Note that the Hamiltonian is independent of time since $\partial H/\partial t = 0$. The augmented Hamiltonian $\bar{H}(t,v,\lambda_1,\lambda_2,\mu,f,b,s)$ [m/s^2] is defined by

$$\bar{H} = H + \mu_1(f_{\max}-f) + \mu_2(b+b_{\min}) + \mu_3(p_{\max}-fv) + \mu_4(v_{\max}-v), \tag{5.11}$$

with non-negative Lagrange multipliers μ_1 [-], μ_2 [-], μ_3 [s/m], μ_4 [1/s], with $\mu_i \geq 0$ $(i = 1,\ldots,4)$. The differential equations of the costates $\dot{\lambda}_1(s) = -\partial\bar{H}/\partial t$ and $\dot{\lambda}_2(s) = -\partial\bar{H}/\partial v$ are given by

$$\dot{\lambda}_1(s) = 0 \tag{5.12}$$

$$\dot{\lambda}_2(s) = \frac{\lambda_1 + v\lambda_2 r'(v) + \lambda_2(f+b-r(v)-g(s))}{v^2} + \mu_3 f + \mu_4. \tag{5.13}$$

Differential equation (5.12) shows that costate $\lambda_1(s) \equiv \lambda_1$ is constant.

We are now able to apply Pontryagin's Maximum Principle on the optimal control problem to maximize the Hamiltonian (Pontryagin et al., 1962). In addition, by applying the *Karush-Kuhn-Tucker* (*KKT*) conditions (stationary and complementary slackness) on the augmented Hamiltonian (Bertsekas, 1999), we are able to derive the optimal control structure consisting of the following driving regimes:

$$(\hat{f}(s),\hat{b}(s)) = \begin{cases} (f_{\max}(v(s)),0) & \text{if } \lambda_2(s) > v(s) & \text{(MA)} \\ (r(v(s))+g(s),0) & \text{if } \lambda_2(s) = v(s) & \text{(CR1)} \\ (0,0) & \text{if } 0 < \lambda_2(s) < v(s) & \text{(CO)} \\ (0,r(v(s))+g(s)) & \text{if } \lambda_2(s) = 0 & \text{(CR2)} \\ (0,-b_{\min}(v(s))) & \text{if } \lambda_2(s) < 0 & \text{(MB).} \end{cases} \tag{5.14}$$

The first driving regime is maximum acceleration (MA), in which the train applies the minimum of the maximum specific traction force $f_{\max}$ and the maximum specific traction power divided by speed $p_{\max}/v$. During coasting (CO) the train applies zero control, that is, $f = b = 0$. The driving regime MB uses maximum braking $-b_{\min}$. The other two regimes are singular solutions with cruising, where a balance is found between the traction or braking force and the total resistance force. The driving regime CR1 ($\lambda_2(s) = v(s)$) has cruising with partial traction. The second singular solution CR2 ($\lambda_2(s) = 0$) has cruising with partial braking, which might be needed during steep downhill slopes at the speed limit. The

switching points between the different driving regimes are determined by the value of λ_2.

Although we have established that the optimal speed profile has essentially the same structure on each separate timed section we have not addressed the problem of finding the optimal prescribed times for each such section given that the total journey time must remain fixed. In fact it has been shown elsewhere (Howlett, 2016) that the optimal section running times are those that are obtained by using the same optimal cruising speed on each timed section.

5.2.2 Minimum-time train control

This section considers the minimum-time train control problem over multiple sections. The problem formulation is similar to the energy-efficient problem definition described in Section 5.2.1. The aim of minimum time train control (MTTC) is to minimize the total running time of the train J [s]:

$$\text{Minimize } J = t(s_n), \tag{5.15}$$

subject to the constraints (5.2)–(5.7), (5.9), and the endpoint condition

$$t(s_0) = 0, \tag{5.16}$$

where the final time $t(s_n)$ is free. The derivation of the optimal control structure is similar to the EETC problem in Section 5.2.1. Therefore, we only show the resulting optimal control structure and the resulting value of λ_1 derived from the endpoint Lagrangian.

The optimal control structure consists of the following driving regimes:

$$(\hat{f}(s), \hat{b}(s)) = \begin{cases} (f_{\max}(v(s)), 0) & \text{if } \lambda_2(s) > 0 & \text{(MA)} \\ (r(v_{\max}) + g(s), 0) & \text{if } \lambda_2(s) = 0 \text{ and } r(v_{\max}) + g(s) \leq 0 & \text{(CR1)} \\ (0, r(v_{\max}) + g(s)) & \text{if } \lambda_2(s) = 0 \text{ and } r(v_{\max}) + g(s) > 0 & \text{(CR2)} \\ (0, -b_{\min}(v(s))) & \text{if } \lambda_2(s) < 0 & \text{(MB).} \end{cases} \tag{5.17}$$

Similar to the EETC structure, the MTTC structure includes the driving regimes MA and MB. Moreover, the cruising (CR) phase indicates cruising at the speed limit $v_{\max}$ by traction (CR1) or braking (CR2), depending on the sign of the total resistance. In addition, the transversality conditions of the endpoint Lagrangian indicate that $\lambda_1 \equiv -1$, which can be used to validate the model results.

5.3 Method

Given the optimal control problems (MTTC and EETC) over multiple sections to determine the optimal running time supplement distribution, the next step is to use methods to solve these problems. We consider two different methods to solve the optimal control problems and to find the optimal running time supplement distribution. We first discuss the indirect solution method used by the algorithm of the Energymiser Driver Advisory System. Then we discuss the direct pseudospectral solution method which we call PROMO (PseudospectRal Optimal train control MOdel) that is applied in an algorithm in the toolbox GPOPS in MATLAB to solve the optimal train control problems.

5.3.1 Indirect solution method

The indirect method is used by the algorithm of the Energymiser DAS to calculate driving advice in real time (Albrecht et al., 2016a,b). The Pontryagin Maximum Principle shows that an optimal trajectory for EETC uses only five driving regimes—maximum acceleration, cruising using partial traction, coasting, cruising using partial (regenerative) braking, and maximum braking (see (5.14)). The necessary conditions for an optimal trajectory also determine the optimal sequence of driving regimes and conditions for switching between the different regimes. This structure can be exploited to limit the search space. It is known that a train with distributed mass running on a non-level track can be modelled as a point mass train running along track with a suitably modified gradient (Howlett & Pudney, 1995). The Energymiser algorithm uses distance as the independent variable and uses the known mass distribution of the train to construct a modified gradient profile so that the train can be modelled as a point mass when calculating the optimal speed profile.

The optimal sequence depends on the critical costate value which also determines the constant speed used with partial traction. This critical speed is known as the cruising speed, where the value of λ_2 is equal to the speed as given in (5.14). For some journeys this cruising speed could be higher than the maximum allowable train speed, in which case driving regimes with constant speed using partial traction do not occur except at speed limits. The optimization operates at two different levels. The lowest level finds the optimal trajectory profile for a given cruising speed. However, this journey profile might not meet the timetable constraints. The upper level of the optimization searches for the cruising speeds that generate optimal trajectory profiles that meet the timetable constraints.

Energymiser allows train operators to specify timing windows—earliest desired arrival time and latest desired arrival time—at stops and at intermediate locations given a constant dwell time and a fixed arrival time at the last stop,

and will calculate optimal arrival times and speed profile within these windows. Optimal running time supplements are calculated by setting wide timing windows and running the standard Energymiser optimisation. If we remove arrival time constraints from the problem then Energymiser can find the optimal arrival time. In practice we do this by using wide time windows. Energymiser calculates optimal trajectory profiles with fixed distance steps, typically 20 m, but the differential equation solver will use additional intermediate points to achieve the required accuracy, and switching points between steps are calculated precisely.

The MTTC journey is found by setting the cruising speed to a large value. In practice, a cruising speed that is five times the maximum speed of the train will reduce coasting durations to less than a few seconds. The EETC journey is found by searching for the cruising speed that achieves the required overall journey time. The EETC journey gives the optimal arrival times at each station, and the differences between the EETC section durations and the MTTC section durations give the optimal running time supplements. The calculations were done on a single core of a laptop computer with a 2.9 GHz processor and 8 GB of memory.

5.3.2 Direct solution method

We use the Radau pseudospectral method as a direct method to compute the MTTC and EETC driving strategies. This method uses orthogonal collocation at Legendre–Gauss–Radau (LGR) points to discretize the optimal control problem for the state and control variables and rewrites it as a nonlinear programming problem that can be solved using standard NLP solvers (Betts, 2010). A detailed derivation from the optimal control problem to the nonlinear programming problem is given in P. Wang & Goverde (2016a) and more general background about pseudospectral methods can be found in Garg et al. (2009) and Rao et al. (2010a). We developed the PROMO algorithm by using GPOPS version 4.1 on a laptop with a 2.1 GHz processor and 8 GB RAM. GPOPS (General Purpose OPtimal Control Software) is a MATLAB toolbox based on the Radau pseudospectral method to solve optimal control problems (Rao et al., 2011). The quality of the Radau pseudospectral method is determined by the amount and location of collocation points, because too few collocation points or incorrect locations may lead to violation of the constraints. Especially for cases with changes in the infrastructure data (i.e., changes in the value of the gradient or speed limit), the usage of multiple-phase pseudospectral methods is recommended, because they do not violate the constraints. We use the single-phase model between two stops, because we consider limited changes of the constraints and the single-phase model has lower computation times compared to the multiple-phase model. We used a modified gradient and speed limit profile in order to model the train as a point mass, similar to Energymiser.

The basic single-phase model of Scheepmaker & Goverde (2016) is applied to

compute the optimal trajectory that minimizes total energy consumption between two consecutive stops (i.e., EETC driving strategy) given a total scheduled running time. Although the model in Section 5.2 uses distance as independent variable for ease of formulating the distance-dependent speed and gradient profiles, we use time as the independent variable in the GPOPS model, because this leads to more stable results for the direct solution method compared to distance as the independent variable. Since the varying speed limits and gradients are a function of distance, we used an implicit approach in our algorithm to consider them. During the computation of the differential equations the algorithm searches at each collocation point for the corresponding gradient and speed limit at this specific location. These values are then used in the computation of the differential equations. However, in order to compute the optimal running time supplement distribution over multiple sections for EETC, we extended this model using the multiple-phase model similar to P. Wang & Goverde (2017, 2019). Each phase is defined as the part of the trajectory between two successive stops (i.e., $v = 0$) and is connected using linkage functions. We refer to P. Wang & Goverde (2017, 2019) for more details about the multiple-phase optimal control problem formulation. We included the intermediate stops i by the intermediate event constraint for the speed limit given in (5.9). The algorithm then computes the optimal distribution of the running time supplements in order to minimize total energy consumption over multiple sections. We use a smoothing function based on a moving average over the control to correct for the numerical oscillations in the pseudospectral approximations during the singular solution of cruising (oscillation of the control). Finally, we verified that the model results of the single-phase and multiple-phase models are in line with the necessary optimality conditions (i.e., costates and Hamiltonian).

5.4 Case study

We applied both methods to solve the optimal running time supplement distribution problem for EETC on different scenarios. Our aim is to find the optimal running time supplement distribution and to compare the two different algorithms to compute the optimal control. We start with discussing the input settings for this study in Section 5.4.1. We then apply a reference scenario in Section 5.4.2 in order to see the optimal distribution of the running time supplements and to see how both models behave compared to each other. In Section 5.4.3 we discuss the scenario in which we consider a uniform distribution of the running time supplements on the reference scenario, in order to compare it with the optimal distribution as discussed in Section 5.4.2. The effect of varying gradients and speed limits is discussed in Section 5.4.4. Finally, we consider a real-life case in Section 5.4.5

for the Dutch corridor Utrecht Central–Arnhem Central including varying speed limits and gradients.

5.4.1 Input

This subsection discusses the inputs to the models. We consider the Intercity (IC) rolling stock type VIRM-IV of the Netherlands Railways (NS) in our scenarios running on a 1.5 kV DC Dutch railway network. The parameters used for this rolling stock are shown in Table 5.1. We assume the train applies mechanical braking only and we consider the driving strategies MTTC and EETC.

Table 5.1: Basic parameters of a NS Intercity train rolling stock type VIRM-IV (NS, 2020).

Property	Value
Train mass (excluding rotating mass) [t]	262
Rotating mass supplement [%]	6
Maximum traction power [kW]	1438
Maximum traction force [kN]	142.6
Maximum braking deceleration [m/s^2]	-0.66
Maximum speed limit [km/h]	160
Train resistance [kN] (v in km/h)	$3.9331 + 55.08v + 10.368v^2$
Traction efficiency [%]	87.5
Train length [m]	109

We use a case study based on the Dutch corridor between Utrecht Central (Ut, 0 km) and Arnhem Central (Ah, 60 km) and consider the intermediate stations Driebergen–Zeist (Db, 10 km), Veenendaal–De Klomp (Klp, 33 km), and Ede–Wageningen (Ed, 40 km). We consider a fixed speed limit of 140 km/h and constant gradient for the reference scenario. We analyze the optimal running time supplement distribution and the optimal speed profile for this scenario. In addition, we compare the model results between Energymiser and PROMO to see if both methods generate similar results. For the varying gradient and speed limit scenario in Section 5.4.4 only, we consider a simple track with only three stops (A, B and C) with a distance of 30 km between each two stops. In the real-world case study we analyze the effects of varying speed limits and gradients on the optimal running time supplement distribution.

We include running time supplements above the technical minimum running time for the EETC driving strategy. We schedule 15% total running time supplement for the EETC driving strategy compared to the MTTC driving strategy in all scenarios in order to have an optimal cruising speed below the speed limit.

In addition, the arrival and departure times at intermediate stations are flexible, because the models can change the distribution of the supplements over stops and thus the running time between stops. However, we do not influence the dwell times at the stations.

5.4.2 Reference scenario

In this section we discuss the results of the models for the optimal running time supplement distribution. The model results of Energymiser and PROMO can be found in Figure 5.2, Figure 5.3, Table 5.2, and Table 5.3. The results indicate that the speed profile and energy profile are almost the same. The EETC driving strategy with 15% running time supplement decreases the total energy consumption by about 39% compared to the MTTC driving strategy. The optimal speed profile of the EETC driving strategy indicates that the optimal cruising speed between stations Db and Klp and stations Ed and Ah is similar (about 131 km/h), which is in line with Howlett (2016), however, in our case applied over multiple stops. The results in Figure 5.3 and Table 5.3 for the reference scenario also indicate that the relative amount of running time supplements increases as the distance between two consecutive stops decreases. In other words, the shorter the distance between two stops, the larger the relative running time supplement. For instance, the relative amount of running time supplements over a distance of 7 km (Klp-Ed) is about 18.3%, while the relative amount of running time supplements over a distance of 23 km (Db to Klp) is about 13.1%. This is due to the higher potential for energy saving during coasting between short stops, i.e., there is no cruising so the train only needs energy for maximum acceleration. In addition, the results indicate that the optimal running time supplement distribution leads to the same optimal cruising speed (if achievable by the train) between each two stops over the multiple stop trajectory.

If we take a closer look at Table 5.2 and Table 5.3 we can see that the MTTC driving strategy of Energymiser has a slightly faster total running time of the train compared with PROMO (0.09%). This leads to a slightly higher energy consumption of 0.44%. The difference might be explained by the accuracy of the models (i.e., numerical errors) or by the fact that the computed strategies are slightly different in structure. The Energymiser strategy uses a short coasting phase but PROMO aims for the MTTC driving strategy to minimize total travel time and does not consider a coasting phase. The computation time of Energymiser (0.03 s) is much faster than PROMO (51.62 s).

The comparison of the EETC driving strategy between Energymiser and PROMO indicates minor differences. The energy consumption of PROMO is slightly lower compared to Energymiser (0.71%), due to the accuracy of the models. The optimal speed profile is slightly different, because the optimal cruis-

ing speed of Energymiser is 130.8 km/h for sections Db-Klp and Ed-Ah, while PROMO indicates an optimal cruising speed of 131.6 km/h for section Db-Klp and 131.7 km/h for section Ed-Ah. In general, the results indicate that the optimal cruising speed should be the same between each two stops. The computation time of Energymiser (0.34 s) is much faster compared with PROMO (153.6 s). Energymiser and PROMO runs were done on different laptop computers, but the difference in computation time is much greater than the difference in the computer speeds.

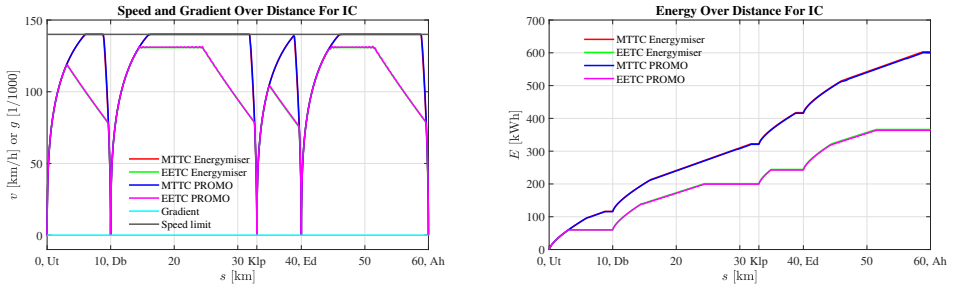

Figure 5.2: Reference scenario IC speed/gradient–distance profile (left) and energy–distance profile (right) of the MTTC and EETC driving strategies of Energymiser and PROMO.

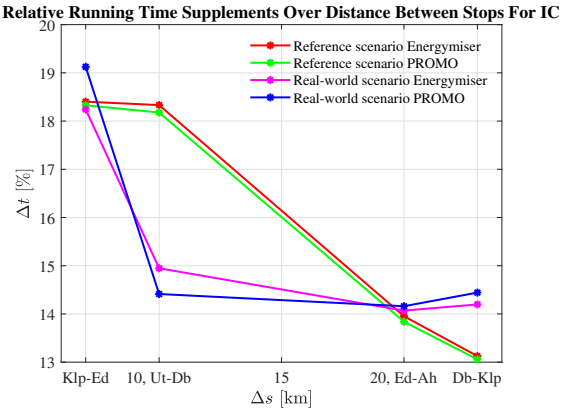

Figure 5.3: Relative running time supplements (Δt) over the distance between two stops (Δs) for the reference scenario and real-world scenario (i.e., including varying gradients and speed limits) by using the models of Energymiser and PROMO.

5.4.3 Uniform distribution

Scheepmaker & Goverde (2015) investigated the effect of a uniform distribution of the running time supplements over multiple stops, i.e., the same percentage of running time supplements on each section. In this scenario we compare the difference between the optimal and the uniform distribution of the running time supplements. We consider a uniform distribution of 15% running time supplements for the EETC driving strategy based on the reference scenario as discussed in Section 5.4.2 (i.e., without varying gradients and/or speed limits). Results for Energymiser and PROMO can be found in Figure 5.4, Table 5.2, and Table 5.3. Since we force the percentage of the supplements to be the same between each two stops, the differences between Energymiser and PROMO are minimal and caused by numerical precision. Energymiser generates the results in 0.35 s, while PROMO takes about 294.50 s. Results indicate energy savings of at most 39.3% compared to the MTTC driving strategy. Therefore, the energy consumption of the uniform distribution is slightly higher (0.24%) compared to the optimal running time supplement distribution as discussed in Section 5.4.2. Thus, the uniform distribution of the running time supplements is not the optimal distribution of the supplements for EETC over multiple stops.

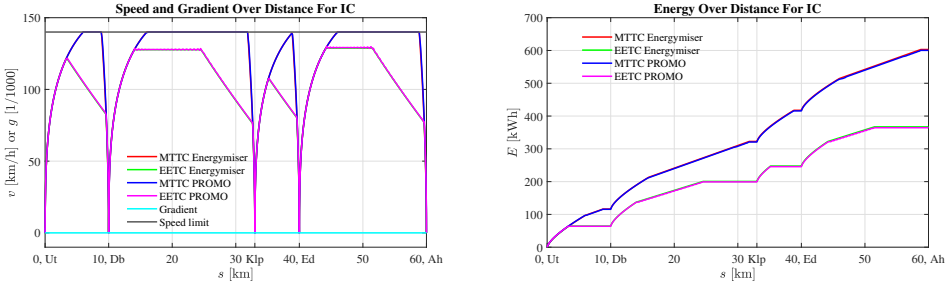

Figure 5.4: Uniform distribution scenario IC speed/gradient–distance profile (left) and energy–distance profile (right) of the MTTC and EETC driving strategies of Energymiser and PROMO.

5.4.4 Varying gradients and speed limits

In this scenario we consider three stations A, B and C with 30 km between each two stations in which we investigate the effect of varying gradients and speed limits on the optimal distribution of the running time supplements for EETC. We included a steep downhill gradient of 6.7‰ followed a bit later by an increase in the speed limit of 20 km/h between stations A and B. For the section between stations B and C we include instead a steep uphill gradient of 6.7‰ followed later by a speed limit

drop of 20 km/h. The total amount of running time supplements between stations A and C is 15% for the EETC driving strategy. Figure 5.5, Table 5.2, and Table 5.3 give the results of both Energymiser and PROMO. The resulting speed profile of the MTTC driving strategy of both Energymiser and PROMO show that the time-optimal solution does not experience any speed effects of the gradient, because during the steep downhill section the train applies the brakes in order to remain at the speed limit, while the total traction force of the train is able to counterbalance the total gradient resistance during the steep uphill sections. The MTTC driving strategy follows the speed limit, because during the increase of the speed restriction the train accelerates to the new increased speed limit and during the decrease of the speed limit, the train brakes to the new decreased speed limit. The results indicate that there is a small difference in the total running time between Energymiser, where PROMO is slightly faster (0.1%) and the resulting energy consumption of PROMO is slightly higher compared to Energymiser (0.74%). The computation time of Energymiser (0.03 s) is again much lower compared to PROMO (398.95 s).

The EETC driving strategy indicates energy savings of about 34% compared to the MTTC driving strategy. Figure 5.5 indicates a difference in the resulting speed profile of Energymiser compared to PROMO. Energymiser uses the theory of Howlett (2016) with a constant optimal cruising speed, while PROMO computes variations in the cruising speed during the steep downhill and uphill gradient. The results of PROMO are not in line with Howlett (2016) and thus are not optimal. The reason for this is that PROMO with time as the independent variable approximates the cruising speeds on different sections separately, which could lead to slightly different cruising speeds depending on the numerical precision. However, the difference in total energy consumption between Energymiser and PROMO is small (0.22%) as can be seen in Figure 5.5 and Table 5.2. Another explanation for the differences is the accuracy of the models. PROMO can also slightly violate some constraints, because the location of the collocation points is fixed and determined by the Radau points. For instance, this can be seen around 10 km, where PROMO starts accelerating earlier compared to Energymiser and, therefore, PROMO violates the end of the reduced speed limit of 120 km/h. Finally, Energymiser is much faster in generating results (0.25 s) compared to PROMO (646.09 s).

5.4.5 Real-world scenario: Utrecht Central–Arnhem Central

This subsection discusses the results of the case study between Utrecht Central and Arnhem Central with real-world data about varying speed limits and gradients. The results of both Energymiser and PROMO are shown in Figure 5.3, Figure 5.6, Table 5.2, and Table 5.3. The EETC driving strategy with about 15% total

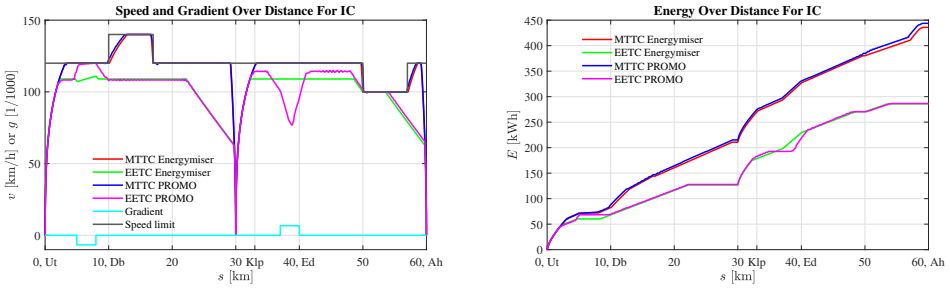

Figure 5.5: Varying gradients and speed limits scenario IC speed/gradient–distance profile (left) and energy–distance profile (right) of the MTTC and EETC driving strategies of Energymiser and PROMO.

running time supplement leads to about 39% energy savings compared to the MTTC driving strategy. The optimal cruising speed on sections Db–Klp and Ed–Ah is below the speed limit. At the sections Ut–Db and Klp–Ed the optimal driving stategy does not include a cruising phase and the train starts to coast after maximum acceleration. Again similar to the results in Section 5.4.2 the results of the optimal running time supplement distribution in seconds or percentage for the real-world scenario (see Figure 5.3 and Table 5.3) show that the shorter the total distance between two consecutive stops, the larger the relative amount of running time supplements becomes. However, in this case the general statement is only valid if there is no cruising in the optimal driving strategy, because between Db and Klp relatively more running time supplements are included compared to Ed and Ah, while the distance is longer. The difference is caused by the gradients (i.e., between Ed and Ah there are uphill gradients, while the line between Ut and Db is more flat).

The detailed results in Table 5.2 and Table 5.3 indicate that the MTTC driving strategy of PROMO is 0.11% faster compared to Energymiser, resulting in a higher energy consumption of about 1.8%. The MTTC driving strategy of PROMO leads to a slightly higher maximum speed between the stations Klp and Ed (135.3 km/h compared to 135.0 km/h). This might be caused by the difference in objective between Energymiser and PROMO as discussed in Section 5.4.2. Furthermore, it can be explained by the use of GPOPS for PROMO where the location of the collocation points is fixed by the amount of points, therefore, PROMO (single-phase part between two stops) might sometimes violate track constraints such as gradients or speed limits. Analysis of the results of PROMO indicate that the location of the collocation points is not exactly the same as the locations of change in speed limit. This causes the model to apply braking a bit too long and apply short acceleration to compensate for the undershoot around the restricted speed limits at 59 km (80 km/h) and 59.5 km (40 km/h), which also explains the difference in

the energy-distance profile for the MTTC driving strategy in Figure 5.6. Finally, numerical errors might occur due to the numerical accuracy of the algorithms. The computation time of Energymiser (0.03 s) is much lower compared to PROMO (573.89 s).

The detailed results of the EETC driving strategy show that PROMO has a slightly lower total energy consumption compared to Energymiser (0.55%). Although the resulting running times are the same, the amount of running time supplements is slightly higher for PROMO (15.0% compared to 14.9%). If we have a closer look at the speed profile, we see a difference between the two models during cruising. Between the stations Db and Klp and between Ed and Ah the optimal cruising speed in Energymiser is the same (128.3 km/h), while for PROMO we see that this is not the case. Between both these two stops PROMO indicates that the cruising speed is lower during uphill gradients and at the change of the gradient increases to a new cruising speed. Therefore, the results of PROMO are not optimal. As explained in Section 5.4.4 the reason for this is the fact that PROMO with time as independent variable approximates the cruising speeds on different sections separately which can lead to slightly different cruising speeds while the objective value already approximates the optimal value within the given numerical precision. Finally, the computation time of Energymiser is much lower compared to PROMO (0.39 s compared to 679.32 s).

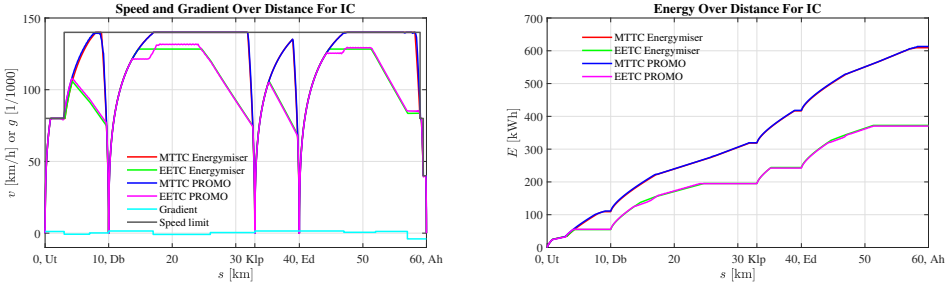

Figure 5.6: Real-world case scenario IC (Ut–Ah) speed/gradient–distance profile (left) and energy–distance profile (right) of the MTTC and EETC driving strategies of Energymiser and PROMO.

Table 5.2: Main results of the different scenarios. Energymiser and PROMO runs were done on different laptop computers, but the difference in computation time is much greater than the difference in the computer speeds.

Scenario	Fig.	Running time (s)	Sup. (%)	Energy (kWh)	Energy savings (%)	N	Comp. time (s)
Ref. MTTC Energymiser	5.2	1928.7	0	603.00	-	3024	0.03
Ref. MTTC PROMO	5.2	1930.5	0	600.35	-	400	51.62
Ref. ETTC Energymiser	5.2	2219.9	15.0	366.14	39.3	3019	0.34
Ref. ETTC PROMO	5.2	2220.1	15.0	363.53	39.4	500	153.56
Uni. ETTC Energymiser	5.4	2220.0	15.1	367.06	39.1	3018	0.35
Uni. ETTC PROMO	5.4	2220.1	15.0	364.40	39.3	500	294.50
Grd. sl. MTTC Energymiser	5.5	1970.9	0	435.82	-	3027	0.03
Grd. sl. MTTC PROMO	5.5	1968.3	0	439.06	-	300	398.95
Grd. sl. ETTC Energymiser	5.5	2263.6	14.9	285.92	34.4	3013	0.25
Grd. sl. ETTC PROMO	5.5	2263.9	15.0	286.56	34.7	400	646.09
Ut–Ah MTTC Energymiser	5.6	2018.7	0	609.35	-	3029	0.03
Ut–Ah MTTC PROMO	5.6	2016.4	0	620.10	-	600	573.89
Ut–Ah ETTC Energymiser	5.6	2318.8	14.9	372.38	38.9	3028	0.39
Ut–Ah ETTC PROMO	5.6	2318.9	15.0	370.32	40.3	600	679.32

Legend: Fig. = Figure, Sup. = running time supplement, N = number of discretization points, Comp. time = computation time, Ref. = reference, Uni. = uniform distribution, Grd. sl. = varying gradient and speed limit, MTTC = mimimum time train control, EETC = energy-efficient train control, Ut = Utrecht Central, and Ah = Arnhem Central.

Table 5.3: Optimal running time supplement distribution and maximum speed for each section of the different scenarios.

Scenario	Fig.	Sup. Ut–Db/A–B (s, %)	Sup. Db–Klp/B–C (s, %)	Sup. Klp–Ed (s, %)	Sup. Ed–Ah (s, %)	Max. speed Ut–Db/A–B (km/h)	Max. speed Db–Klp/B–C (km/h)	Max. speed Klp–Ed (km/h)	Max. speed Ed–Ah (km/h)
Ref. MTTC Energymiser	5.2	0.0, 0.0	0.0, 0.0	0.0, 0.0	0.0, 0.0	140.0	140.0	139.2	140.0
Ref. MTTC PROMO	5.2	0.0, 0.0	0.0, 0.0	0.0, 0.0	0.0, 0.0	140.0	140.0	139.0	140.0
Ref. ETTC Energymiser	5.2	64.8, 18.3	90.3, 13.1	50.9, 18.4	85.2, 14.0	119.0	130.8	104.2	130.8
Ref. ETTC PROMO	5.2	64.4, 18.2	89.9, 13.1	50.7, 18.3	84.6, 13.8	118.8	131.6	104.1	131.7
Uni. ETTC Energymiser	5.4	53.3, 15.1	104.2, 15.1	41.3, 14.9	92.5, 15.1	122.0	127.7	107.8	128.8
Uni. ETTC PROMO	5.4	53.1, 15.0	103.3, 15.0	41.5, 15.0	91.7, 15.0	121.7	128.5	107.7	130.0
Grd. sl. MTTC Energymiser	5.5	0.0, 0.0	0.0, 0.0			140.0	120.0		
Grd. sl.MTTC PROMO	5.5	0.0, 0.0	0.0, 0.0			140.0	120.0		
Grd. sl. ETTC Energymiser	5.5	176.0, 18.5	116.7, 11.4			110.9	109.0		
Grd. sl. ETTC PROMO	5.5	170.6, 18.0	124.6, 12.2			120.0	115.0		
Ut–Ah MTTC Energymiser	5.6	0.0, 0.0	0.0, 0.0	0.0, 0.0	0.0, 0.0	140.0	140.0	135.0	140.0
Ut–Ah MTTC PROMO	5.6	0.0, 0.0	0.0, 0.0	0.0, 0.0	0.0, 0.0	140.0	140.0	135.3	140.0
Ut–Ah ETTC Energymiser	5.6	59.4, 14.9	98.4, 14.2	51.2, 18.2	91.1, 14.1	105.9	128.3	106.2	128.3
Ut–Ah ETTC PROMO	5.6	56.8, 14.4	100.2, 14.4	53.8, 19.1	91.6, 14.2	107.6	131.9	105.1	129.5

Legend: Fig. = Figure, Sup. = running time supplement, Max. = maximum, min = minutes, Ref. = reference, Uni. = uniform distribution, Grd. sl. = varying gradient and speed limit, MTTC = mimimum time train control, EETC = energy-efficient train control, Ut = Utrecht Central, Db = Driebergen–Zeist, A = station A, B = station B, C = station C, Klp = Veenendaal–De Klomp, Ed = Ede–Wageningen, and Ah = Arnhem Central.

5.5 Conclusion and discussion

In this chapter we computed the optimal distribution of running time supplements over multiple stops given a total scheduled running time for energy-efficient train driving where the insights can be used for timetable design. Based on the applications of our models on a realistic Dutch case study between the stations Utrecht Central and Arnhem Central with varying speed limits and gradients, we conclude that the optimal distribution of the running time supplements leads to the same optimal cruising speed between each two stops over the trajectory with multiple sections for flat tracks. For tracks with gradients, PROMO approximates the optimal strategy with different cruising speeds around the gradient segments with a slightly bigger energy consumption within the numerical precision, showing the numerical sensitivity of the solution. We also found that there is a clear relationship between the distance between two stops and the relative amount of running time supplements, which up to our knowledge has not been described in the literature yet. The shorter the distance between two stops, the larger the relative amount of running time supplements. In addition, the effect of gradients influence the relative amount of running time supplements. Relatively more supplements are allocated on sections with downhill gradients compared to uphill gradients, because less traction force and thus energy is used to overcome the gradient resistance. We also conclude that the optimal distribution of the running time supplements leads to higher energy savings compared to a uniform distribution of the running time supplements for EETC over multiple-stops. Future research could focus on finding a general mathematical relationship between the relative amount of the running time supplements and the distance between two stops.

Furthermore, we compared the direct and indirect solution method in order to compute the optimal control. Although both models have different assumptions to compute the optimal running time supplement distribution, they lead, in general, to the same results. The main differences in results are caused by the location of the collocation points for pseudospectral method, and the accuracy of the models (numerical errors). However, for varying gradients the resulting speed profile of PROMO leads to different cruising speeds with approximately the same energy consumption as the resulting speed profiles of Energymiser with the optimal unique cruising speed. The indirect solution method has lower computation time than the direct solution method, because this method exploits information about the optimal control structure (i.e., the same optimal cruising speed between multiple stops). The direct solution method does not use any information about the optimal control structure but nevertheless provides the costates and Hamiltonian required to evaluate the necessary optimality conditions.

While not as fast as the indirect solution method, the direct solution method is able to find the optimal solutions with the same objective value as the indirect

solution method without requiring extensive analysis of the necessary conditions for an optimal strategy, and without requiring highly specialized code to calculate optimal trajectory profiles. The indirect method will be useful for finding optimal solutions to new variants of optimal train control problems. The amount of specialization required to implement practical solutions can then be tailored to the requirements of individual applications.

Chapter 6

Multi-objective railway timetabling including energy-efficient train trajectory optimization

---

Apart from minor updates, this chapter has been published as:
Scheepmaker, G. M., Goverde, R. M. P. (2021) Multi-objective railway timetabling including energy-efficient train trajectory optimization, *European Journal of Transport and Infrastructure Research*, 21(4), pp. 1–42.

6.1 Introduction

Railway undertakings (RUs) try to minimize their energy consumption in order to reduce the CO_2 emissions as well as to save money. One of the methods to reduce the energy consumption is to apply an energy-efficient driving strategy by the train driver. Therefore, most literature is focused on the optimization of driving strategies or determining algorithms for driver advisory systems (DASs) (Panou et al., 2013) or automatic train operation (ATO) (Yin et al., 2017). A stream of research is focused on the *energy-efficient train control* (*EETC*) driving strategy that minimizes the total traction energy consumption of a train, see X. Yang et al. (2016) and Scheepmaker et al. (2017) for overviews on this topic. However, the possibilities for the train to apply the EETC driving strategy depend on the running time supplements in the timetable (Scheepmaker & Goverde, 2015). Therefore, another stream of research is focused on the topic of *energy-efficient train timetabling*

(*EETT*), that aims to incorporate the EETC driving strategy into the timetable design (Scheepmaker et al., 2017). Research on EETT can be classified into two groups: the first group is focused on synchronizing accelerating and regenerative braking trains, while the second group is focused to determine the optimal amount and distribution of the running time supplements. Regenerative braking can be applied by modern electric trains in which the train uses the engine to brake (generator) and to convert kinetic energy into electricity. This electricity can be fed back over the catenary to surrounding accelerating trains. Examples of research on synchronization of accelerating and regenerative braking trains can be found in T. Albrecht (2004), Peña-Alcaraz et al. (2012), Li & Lo (2014a,b), X. Yang et al. (2014), Luan et al. (2018a,b), and Zhou et al. (2018). However, detailed modelling of the power supply system over the catenary should be considered (Scheepmaker & Goverde, 2020), which requires detailed simulation (Stephan, 2008; Arboleya et al., 2020). In this chapter we focus on the second group of research about the optimal amount and distribution of the running time supplements. For more details about EETT we refer to the literature review papers of X. Yang et al. (2016) and Scheepmaker et al. (2017). Scheepmaker et al. (2017) also showed another clustering of papers into two groups based on the type of optimization problem. A first group is focused on the a single objective optimization problem of minimizing the total energy consumption by varying the running time supplements between stops, e.g., Ding et al. (2011), Sicre et al. (2010), Su et al. (2013, 2014), and Scheepmaker & Goverde (2015). Other research considers multiple objective optimization by including the total running time and/or the delays, e.g., Cucala et al. (2012), L. Yang et al. (2012), Binder & Albrecht (2013), and P. Wang & Goverde (2016a). Below we address the most recent studies on the topic of EETT that are published after Scheepmaker et al. (2017). A summary of the literature review for energy-efficient train timetabling can be found in Table 6.1.

Part of the current research aims to find the optimal distribution of the running time supplements for a single train over multiple stops and considers a single objective to minimize total energy consumption. Howlett (2016) proved that the optimal control over multiple stops for the EETC leads to the same cruising speed between each two stops. In addition, Scheepmaker et al. (2020a) found that the shorter the distance between stops, the higher the relative running time supplement.

Another part of the current research is focused on EETT for multiple trains in a railway corridor while considering a single objective. S. Yang et al. (2018) investigated energy-efficient train timetabling for a complete metro line considering the minimization of the total energy consumption including regenerative braking. Although they consider a single-objective optimization problem, they include other objectives related to passenger service and cost of the operator. They did this by taking into account constraints for the cycle time and a time window for the total

Table 6.1: Summary of EETT literature.

Publication	Area	RB	Conflict	Objective(s)				
			detection	TRT	Robust	Cap	Energy	PWT
T. Albrecht (2004)	C	x	H				x	
Sicre et al. (2010)	S		-				x	
Ding et al. (2011)	S		-				x	
Cucala et al. (2012)	S		-		x		x	
Peña-Alcaraz et al. (2012)	C	x	H				x	
Binder & Albrecht (2013)	S		-		x		x	
Su et al. (2013)	S		-				x	
Li & Lo (2014a,b)	C	x	H				x	
Su et al. (2014)	C		H				x	
X. Yang et al. (2014)	C	x	H				x	x
Scheepmaker & Goverde (2015)	S		-				x	
Goverde et al. (2016)	N		B	x	x	x	x	x
Howlett (2016)	S		-				x	
P. Wang & Goverde (2017)	C		H		x		x	
Luan et al. (2018a,b)	C	x	B		x		x	
S. Yang et al. (2018)	C	x	H				x	
Zhou et al. (2018)	C	x	H				x	
P. Wang & Goverde (2019)	C		H				x	
X. Yang et al. (2019)	C		H		x		x	x
A. Albrecht et al. (2020)	T		B				x	
Scheepmaker et al. (2020a)	S		-				x	
Su et al. (2020)	C	x	H				x	
Xu et al. (2020)	C		H	x			x	
This chapter	C		B	x	x	x	x	

Legend: RB = Regenerative Braking, TRT = total running time, Robust = robustness/delays, Cap = capacity utilization, PWT = passenger waiting time, S = single train, T = two trains, C = corridor/line, N = network, H = headway times, B = blocking time.

running time with a buffer time between trains. The speed limits are divided into multiple-phases based on the discrete data of the speed limit and they consider a flat track. Su et al. (2020) also considered the topic of EETT for a complete metro line in both directions and aimed to minimize the total energy consumption. The energy consumption includes the usage of regenerative braking energy by synchronizing the accelerating and regenerative trains near stations in the same power supply area. They developed an iterative integrated approach to compute the energy-optimal timetable. First, the energy-efficient driving strategies are computed with a given total running time using a Dynamic Programming algorithm. Second, a Simulated Annealing heuristic algorithm is used to compute the optimal amount of running time and the headway between trains given the scheduled cycle time and the number of trains in the network, while minimizing the total energy consumption of all trains. The algorithm computes the headway based on the passenger demand at all stations. Constraints are included to guarantee the minimum turn back time at the final stations, the maximum running time between stops, the minimum headway between trains, and the minimum dwell time at stations. A. Albrecht et al. (2020) considered the topic of EETT for two successive trains on a flat track. The authors define a theoretical framework for the optimal driving strategies of two following trains considering safe-separation constraints that aims to minimize the

total energy consumption of both trains given a total running time for both trains, while maintaining a safe separation between the trains. Safe separation means that the leading train must leave each signal point segment before the following train enters that segment. The authors use the Least Action Clearance Time Algorithm (LACTA) to compute the energy-optimal driving strategy for two following trains given a total amount of running time. Basically, LACTA starts by considering a basic separation in time between trains. LACTA then checks for each time overlap in a block section, i.e., whether the leading train left a block section before the following train enters that section. Afterwards, a greedy algorithm includes an additional clearance time constraint for the block section with the biggest time violation and computes the new optimal driving strategies of both trains which is then checked again on the violations. This leads to an iterative process.

Current research on multiple-objective optimization for EETT considers the objectives of total travel time, passenger waiting time, and robustness. X. Yang et al. (2019) focused on the topic of energy-efficient train timetabling by minimizing the energy consumption, passenger waiting time and robustness. Their definition of robustness is different compared to current literature on timetabling, because they are focused on minimizing the effect of perturbations on the energy consumption and passenger waiting time at the stations instead of train delay. They also included the effect of regenerative braking by maximizing the overlap between accelerating and regenerative braking trains. They considered a random dwell time at intermediate stations of the Beijing metro line and used a non-dominated sorting genetic algorithm II to solve the problem and to find the equally optimal solutions (Pareto front). Train separation was considered by headway times and they considered a heuristic method to determine the energy-efficient driving strategy. Xu et al. (2020) considered the topic of EETT by minimizing the total travel time and energy consumption for high-speed trains in a corridor. They included dynamic headway times between trains in order to shorten the travel times compared to fixed headway times. The minimum headway between two trains was determined using an iterative approach by increasing the headway time by one minute if safety space headway was not met. In order to decrease the computation time, they simplified the problem by excluding coasting, varying gradients, and speed limits.

In practice the aim of RUs for timetable design is mainly on other objectives than energy minimization, such as minimizing the total running time, maximizing the capacity utilization and maximizing the robustness of the timetable. The topic of multiple-objective optimization for timetabling (mainly without considering the objective of minimizing the energy consumption) is intensively studied in literature, see the surveys in Caprara et al. (2007), Lusby et al. (2011), and Cacchiani & Toth (2012). Research in timetable optimization can be separated into aperiodic and periodic timetables. In aperiodic timetables the timetable and

number of trains is demand driven providing flexibility, while a periodic timetable provides the same service pattern each period (regularity) (Yan & Goverde, 2019). In this chapter our focus is on periodic timetables. Another difference in timetable optimization is the level of details of the infrastructure data. At a macroscopic level the nodes and link model contains aggregate information of the infrastructure (i.e., nodes are stations and links are the complete railway lines between stations), while at a *microscopic level* the nodes and links contain the highest detail information of the infrastructure (i.e., signals, switches, and track sections) (Radtke, 2014). This also leads to a different methodology for conflict detection: in the macroscopic model headway constraints are considered, while in the microscopic model conflicts are detected based on the block section occupation of trains (i.e., only one train can reserve a section of track between adjacent signals). A standard model for representing macroscopic periodic timetable optimization is based on the Periodic Event Scheduling Problem (PESP) (Serafini & Ukovich, 1989; Kroon et al., 2014). A detailed literature review about macroscopic timetable optimization can be found in Cacchiani & Toth (2012). Research on microscopic timetable optimization is limited (Cacchiani et al., 2014, 2015), because the size of the model increases for the decision variables and constraints when more details are included (Zhang et al., 2019). In addition, multiple-objective timetable optimization research focusing on microscopic timetable optimization including the objective of energy minimization is limited, and is discussed below.

Goverde et al. (2016) considered a three-level iterative framework for timetable design and timetable evaluation which they applied to a Dutch railway network. First, at a macroscopic level they considered a multiple-objective optimization using an Integer Linear programming formulation that minimizes the total running time and dwell time, missed connections, the time of exceeding the nominal transfer time, and cancelled train path requests (i.e., aiming at efficiency). After generating the macroscopic timetable, a delay propagation algorithm is used in order to evaluate the robustness of the macroscopic timetable using a Monte Carlo simulation (Bešinović et al., 2016). Second, at a microscopic level they detect and resolve path of conflicts, and maximize the infrastructure occupation and stability of the timetable (i.e., aiming at feasibility and stability). The model iteratively applies the macro-micro model in order to find a conflict-free, stable and robust timetable that minimizes the objectives on the macroscopic level. Details of this macro-micro interaction can be found in Bešinović et al. (2016). Finally, a mesoscopic fine tuning model is used given the solution from the iterations of the macro-micro model on a corridor level. This mesoscopic model computes the energy-efficient speed profiles considering stochastic dwell time distributions on intermediate stops in order to determine robust energy-efficient speed profiles (i.e., aiming at energy efficiency and robustness). Therefore, energy-efficient train

control was considered sequential in the optimization process (after the other objectives). Details about the mesoscopic fine tuning model can be found in the paper of Binder & Albrecht (2013). P. Wang & Goverde (2017) minimized the total energy consumption and the delays for multiple trains on single-track lines with meeting stations using headway norms. P. Wang & Goverde (2019) extended this approach to re-allocate the running time supplements in a timetable to optimize the joint energy-efficient speed profiles on general railway networks. They used headway norms during the optimization in order to derive a conflict-free timetable, while they checked the feasibility of the optimal timetable afterwards by using the blocking time stairways.

Based on the literature review it can be concluded that research about energy-efficient train timetabling with multiple-objectives is mainly focused on finding the balance between robustness and energy consumption, see Table 6.1. However, in practice the primary objectives for RUs are on minimizing the total running time and maximizing the capacity utilization (i.e., frequencies) and robustness, while energy consumption is at best secondary. In addition, Table 6.1 shows that most research on EETT considers macroscopic timetable feasibility based on normative minimum headway times, while microscopic conflict detection considering the signaling system must be used to guarantee conflict-free timetables in practice (especially closer to the day of operation in order to deliver a realistic and realizable timetable for operation). Only Goverde et al. (2016) considered the multiple objectives of minimizing total running time, robustness, capacity utilization and energy consumption with microscopic conflict detection. However, the objective of energy consumption was considered after a conflict-free, stable and robust timetable structure was determined. Thus, research is missing on simultaneously solving the multiple-objective optimization problem regarding the total running time, capacity utilization using blocking time theory, robustness and energy consumption. In this chapter we include the objective of energy consumption upfront as one of the objectives to minimize (jointly). Therefore, the aim of this chapter is to determine the relationship between the total running time, infrastructure occupation, robustness and energy consumption of trains on a corridor. Specifically, we consider a multiple-objective timetabling problem that aims at a trade-off between minimizing the total running time, extended cycle time, energy consumption and maximizing the buffer time at a microscopic level using the blocking times for conflict detection (blocking time theory). Here, we define the *extended cycle time* as the cycle time including a minimum buffer time between trains. We define the cycle time as the minimum interval that a departure order of successive trains in the same direction repeats itself. Therefore, this chapter gives the following contributions to the literature:

1. We propose the extended cycle time that includes a minimum buffer time.

2. We consider the multiple-objective optimization problem of minimizing total travel time, extended cycle time and energy consumption, and maximizing the buffer time.

3. We find relationships between energy minimization in relation to the other objectives, specifically between energy consumption and capacity consumption, and between energy consumption and robustness.

4. We focus on microscopic timetable optimization using blocking time theory to develop a conflict-free timetable on a railway corridor.

The structure of this chapter is as follows. We first describe the theory regarding the optimal control, blocking time, capacity consumption and robustness in Section 6.2. This leads to the multiple-objective optimization problem formulation regarding the objectives of total running time, extended cycle time, total buffer time and total traction energy consumption. Section 6.3 discusses the method used to compute the optimal solution. Afterwards, we consider a real-world case to investigate the balance between the multiple objectives in Section 6.4. Finally, Section 6.5 discusses the main conclusions of this chapter.

6.2 Theory

This section discusses the theoretical background that is used in the method to tackle the multiple-objective problem. In Section 6.2.1 the optimal control problem is discussed that leads to the optimal driving strategies that are the foundation of our method to compute the optimal timetable. In addition, the optimal control leads to the objectives of minimizing total energy consumption and total running time. Section 6.2.2 discusses the blocking time theory that is used in order to derive a conflict-free timetable on a railway corridor for multiple following trains. Afterwards, Section 6.2.3 discusses the UIC 406 method of timetable compression in order to derive the capacity consumption and extended cycle time of a timetable, which is one of the objectives to optimize. Finally, the fourth objective in this chapter is to maximize the robustness of the timetable by maximizing the total buffer time. Therefore, the topic of timetable robustness is discussed in Section 6.2.4.

6.2.1 Optimal train control

In this section we discuss the optimal train control problems in order to derive the two driving strategies considered in this chapter: the energy-efficient train control (EETC) and the minimum time train control (MTTC). We consider mechanical braking only and we model the train as a point mass (Brünger & Dahlhaus, 2014;

Howlett & Pudney, 1995). The derivation of the EETC and MTTC optimal control structure between two consecutive stops by using distance as independent variable is discussed in Scheepmaker et al. (2020a). Therefore, in this chapter we only provide the optimal control problem formulation and briefly discuss the different driving regimes for the optimal driving strategies. First we discuss the EETC problem formulation and afterwards the MTTC problem formulation is discussed.

Energy-efficient train control

The EETC driving strategy aims to minimize total traction energy consumption Z_E [m^2/s^2] over a railway line with total distance S [m] and $l-1$ sections over stop positions $(s_0, \ldots, s_l)$ with a total scheduled running time T [s]:

$$Z_E = \min \int_{s_0}^{s_l} f(s) ds, \tag{6.1}$$

subject to the constraints

$$\dot{t}(s) = \frac{1}{v(s)} \tag{6.2}$$

$$\dot{v}(s) = \frac{f(s) + b(s) - r(v) - g(s)}{v(s)} \tag{6.3}$$

$$0 \leq v(s) \leq v_{\max}(s) \tag{6.4}$$

$$f(s)v(s) \leq p_{\max} \tag{6.5}$$

$$0 \leq f(s) \leq f_{\max} \tag{6.6}$$

$$-b_{\min} \leq b(s) \leq 0 \tag{6.7}$$

$$t(s_0) = 0,\ t(s_l) = T \tag{6.8}$$

$$v(s_i) = 0, \text{ for } i = 1, \ldots, l, \tag{6.9}$$

where distance s [m] is the independent variable, time t [s] and speed v [m/s] are the state variables. Eqs. (6.2) and (6.3) are the dynamic equations describing the derivatives of the state variables to the independent variable s, i.e., $\dot{t} = dt/ds$ and $\dot{v} = dv/ds$. Eq. (6.4)–(6.7) describe the path constraints. The control variables are the mass-specific traction f [m/s^2] and mass-specific mechanical braking b [m/s^2]. The mass-specific forces are computed by dividing the total force force F [N] over the total rotating mass ρm (rotating mass factor ρ [-] multiplied by the train mass m [kg]), i.e., $F(t)/(\rho m)$. The mass-specific traction force f (see Eq. (6.6)) is bounded between zero and the minimum of the maximum mass-specific traction force and the maximum mass-specific power p [m^2/s^3] divided by the speed (see Eq. (6.5)), i.e., $f(v) \in [0, \min(f_{\max}, p_{\max}/v)]$. The mass-specific mechanical braking force is bounded between zero and the maximum braking force, i.e.,

$b(v) \in [-b_{\min}, 0]$, see Eq. (6.7). Traction and braking control cannot be applied at the same time, i.e., $fb = 0$. Combining the mass-specific train resistance $r(v)$ [m/s^2] and the mass-specific line resistance $g(s)$ [m/s^2] leads to the total mass-specific train resistance. We use the general mass-specific train resistance based on Davis equation $r(v) = r_0 + r_1 v + r_2 v^2$ that consists of non-negative coefficients $r_0, r_1 \geq 0$ and $r_2 > 0$ (Davis, 1926). The mass-specific line resistance is determined by gradients $g(s)$ with $g(s) > 0$ indicating uphill slopes and $g(s) < 0$ downhill slopes. The speed is limited between 0 and the speed limit $v_{\max}$ that depends on distance, see Eq. (6.4). In this chapter a piecewise-constant speed limit and gradient is considered over the complete trajectory. The boundary conditions are described by Eqs. (6.8) for the time and (6.9) for the speed. Note that we do not provide time constraints on the intermediate stops, so the optimal arrival and departure times will be determined by the optimization problem. Intermediate event constraints (6.9) force the speed at stop i at distance s_i to be zero.

Similar to Scheepmaker et al. (2020a) we can define the Hamiltonian, augmented Hamiltonian and costates using the EETC optimal control structure. Pontryagin's Maximum Principle (PMP) gives the optimal controls by maximizing the Hamiltonian, and the necessary optimally conditions are determined by applying the Karush-Kuhn-Tucker (KKT) conditions on the augmented Hamiltonian. Scheepmaker et al. (2020a) showed that the general optimal control structure over multiple stops is similar to the optimal control structure between two successive stops.

In general, the optimal control structure consists of the *driving regimes* maximum acceleration by maximum traction force, cruising at a constant speed by partial traction/braking (i.e., balance between the traction or braking force and the total train resistance), coasting (zero control), and maximum braking. Note that the optimal cruising speed can be lower than the speed limit. In addition, for short distances between two stops the optimal control structure does not include cruising (Scheepmaker et al., 2017, 2020b).

Minimum time train control

The aim of minimum time train control (MTTC) is to minimize the total running time of the train Z_R [s]:

$$Z_R = \min t(s_l), \tag{6.10}$$

subject to the constraints (6.2)–(6.9), and where here the final time $t(s_l)$ is free and will be minimized. Similar to the EETC problem formulation the Hamiltonian, augmented Hamiltonian and costates can be derived. The PMP and the KKT conditions can be applied on them in order to derive the optimal control structure. The structure consists of the driving regimes maximum acceleration, cruising at

the speed limit and maximum braking. The general optimal control structure for the MTTC driving strategy is similar to the optimal control structure between two successive stops (Scheepmaker et al., 2020a).

6.2.2 Blocking time theory

The railway infrastructure is partitioned in different block sections for safe train operation. Each block section is covered by a signal that indicates if the next block section is available for the train approaching the signal. A three-aspect two-block signalling system is assumed, which means that an approach signal in advance indicates if the train needs to brake for the next (stop) signal. The time duration in which a specific block section is allocated to a specific train and thus blocked for other trains is called blocking time. The following components are considered for the blocking times, see Figure 6.1 (a):

1. Setup time: time to set and lock the route in the block.
2. Sight and reaction time: the time for the train driver to see and anticipate on the approach signal.
3. Approach time: the time for the train to run from the approach signal to the signal at the end of the approaching block section.
4. Running time: the time to run the train through the block section and possible overlap.
5. Clearing time: the time needed for the train to clear the block section over the train length.
6. Release time: the time to release the route in the block. Part of a block section might be released earlier after the full train length passed the clearing point of a switch within a block section according to the sectional release route locking principle.

We refer to Pachl (2009) and Pachl (2014) for more information about the blocking time theory. One of the results of blocking time theory is the timetable compression method that provides the minimum headway between trains of two conflict-free train paths (Bešinović & Goverde, 2018).

In addition, a timetable must include scheduled buffer time between two trains. Buffer time is an empty time slot between two successive trains on top of their minimum headway time (Pachl, 2014). The minimum (line) headway time on a corridor is defined as the minimal conflict-free inter-departure time between two train paths given the speed profiles of the two trains (Pachl, 2014). Buffer times are used to avoid or reduce the propagation of delays to other trains, the so called

secondary or knock-on delays (Goverde & Hansen, 2013). In practice, infrastructure managers and RUs consider a minimum buffer time between two trains as a measure to deal with scheduled deviations (also called critical buffer time by Jensen et al. (2017)). Therefore, we define the concept of extended blocking time, which includes a minimum buffer time (see Figure 6.1 (a)). Plotting successive extended blocking times in a time-distance diagram leads to the extended blocking time stairway, as shown in Figure 6.1 (b). The extended blocking time stairway gives the extended minimum line headway between two successive trains as can be seen in Figure 6.1 (b).

Conflicts occur when blocking times of two trains overlap. In addition, buffer time conflicts occur when the required minimum buffer time is overlapping with the blocking time of another train. In this chapter we aim at a conflict-free timetable. Detailed information about blocking time theory can be found in Pachl (2009) and Pachl (2014).

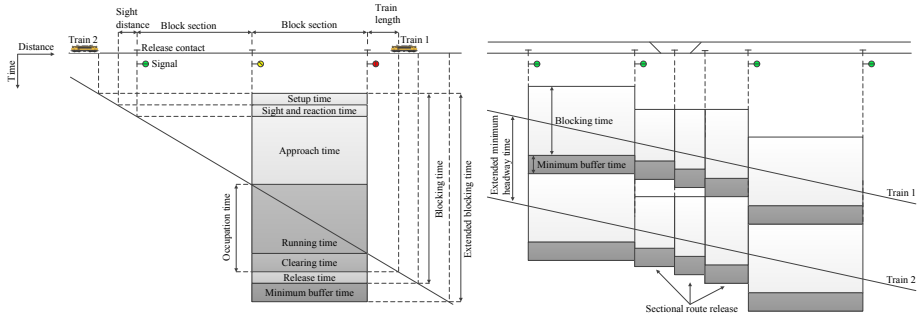

(a) Components of the extended blocking time (b) Extended blocking time stairway

Figure 6.1: The left plot (a) shows the attributes for the extended blocking time stairway including the minimum buffer time for a three-aspect signalling system. The right plot (b) indicates a partial blocking time stairway for two successive trains including the (minimum) buffer time.

6.2.3 Capacity consumption

There are different timetable performance indicators to assess a timetable. One of them is the *infrastructure occupation*, which is defined as the amount of time that the infrastructure is blocked by train paths from a given timetable structure in a given time window (UIC, 2013). This performance indicator provides insight in the potential bottlenecks in a network and is related to the capacity consumption of a corridor. The *capacity consumption* includes the required buffer time between trains on top of the infrastructure occupation (UIC, 2013; Jensen et al., 2017).

The infrastructure occupation depends on the infrastructure (route, speed limits, block lengths, and signalling system), the rolling stock characteristics (such as the train composition, acceleration and braking, maximum speed, and length), and timetable (frequencies, heterogeneity, and dwell times) (Goverde & Hansen, 2013; Bešinović & Goverde, 2018). The UIC 406 timetable compression method can be used to compute the infrastructure occupation on a line (UIC, 2013). The location where the blocking stairways of two trains touch each other are the critical block sections. The infrastructure occupation can be extended to extended infrastructure occupation where the extended blocking time stairways, as described in Section 6.2.2, are compressed, see Figure 6.2. Note that then the capacity consumption consists of the extended infrastructure occupation plus possible additional buffer time on top of the minimum buffer times. The capacity consumption is analyzed over a certain defined time period, for instance 30 min. The extended infrastructure occupation time t_o [s] is then defined from the start of the first train to the start of the compressed first train of the next time period t_p [s], see Figure 6.2. The extended infrastructure occupation time t_o is thus computed as the sum of the minimum line headway times t_{ij}^h [s] for the successive trains (Bešinović et al., 2017)

$$t_o = \sum_{(i,j)\in W_p} t_{ij}^h, \tag{6.11}$$

where W_p is the pattern of successive train pairs (i, j) over the scheduled time period, and t_{ij}^h is the minimum headway time from train i to train j calculated over the corridor with n_b blocks as (Bešinović et al., 2017)

$$t_{ij}^h = \max_{k\in 1,\ldots,n_b} (t_{ik}^e - t_{jk}^b), \tag{6.12}$$

where t_{ik}^e is the end of the blocking time of train i in block section k including the minimum buffer time, and t_{jk}^b is the begin of the blocking time of train j in block section k. The capacity consumption C_s [%] includes additional scheduled buffer time t_a [s] on top of the minimum buffer time due to, e.g., rounding of the timetable to whole minutes or for robustness. This capacity consumption can be computed by

$$C_s = \frac{t_o + t_a}{t_p} \cdot 100\%. \tag{6.13}$$

We consider a cyclic timetable consisting of one or more train cycles, thus the extended infrastructure occupation time is equal to a multiple of the extended cycle time. Therefore, in order to minimize the infrastructure occupation we can also minimize the extended cycle time instead. The extended cycle time t_c [s] considers the minimum periodic pattern of all trains. In case that all trains have

the same frequency f_l, the extended cycle time the cyclic pattern of all train lines can be computed by:

$$t_c = \frac{t_o}{f_l}. \tag{6.14}$$

Finally, we aim to to minimize the extended cycle time Z_c [s] by

$$Z_c = \min t_c. \tag{6.15}$$

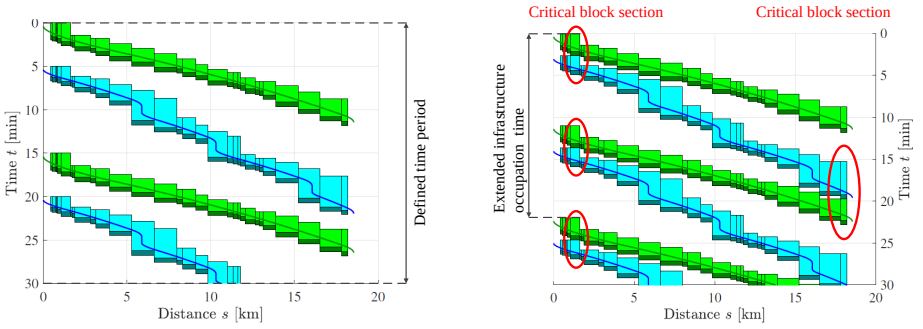

Figure 6.2: The left plot shows the timetable compression method with timetable before compression. The right plot indicates the timetable compression method with timetable after compression including the minimum buffer time and the critical blocks. Note that the darker area below the blocks indicates the minimum buffer time between trains that are included in the extended blocking times.

6.2.4 Robustness

The topic of robustness in railway planning is considered in the literature review paper of Lusby et al. (2018). They noticed that there is no common definition of robustness for all stakeholders, but that it in general is focused on the capacity for the railway system to function during disturbances (i.e., how the timetable functions during uncertainty by small deviations from train paths). Cacchiani & Toth (2012) also discussed the topic of robustness for timetabling problems. They indicate that robust timetables try to avoid delay propagation in the railway network during disruptions. Goverde & Hansen (2013) define different performance indicators for railway timetables of which one of them is timetable robustness, which are applied in the three-level timetable design framework of Goverde et al. (2016). They consider robustness as the ability of the timetable to cope with design errors, parameter variations, and changing operational conditions, which depend on stochastic processes such as running, dwelling and turning. The aim is

to minimize the primary delays (caused by variations in a process that takes longer than the scheduled process time) and secondary or knock-on delays (caused by delays exceeding the scheduled buffer time between two trains at a critical block section) (Vromans et al., 2006; Goverde et al., 2016). Therefore, running time supplements and buffer times between trains are included in order to improve the robustness of the timetable. *Running time supplements* are the extra running time above the minimum running time in order to minimize primary delays caused by variations of the process times (Goverde et al., 2013; Scheepmaker & Goverde, 2015).

In this chapter we consider *the total buffer time* t_b as a measure of the *robustness* of the timetable, which we aim to maximize. The buffer time is also considered in practice for timetable design and evaluation in the Netherlands, where a minimum buffer time (a wake) behind each passenger train is considered for timetable robustness, which is analyzed using a deterministic simulation run. We use a similar approach as considered by NS for timetable robustness. The total buffer time consists of the total minimum buffer time and the additional buffer time. For a cyclic timetable the total buffer time t_b can be computed as:

$$t_b = \frac{T}{f_l} - t_c. \tag{6.16}$$

Finally, we aim to maximize the robustness of the timetable by maximizing the total buffer time Z_b [s]:

$$Z_b = \max t_b. \tag{6.17}$$

6.3 Method

This section discusses the method used for the multiple-objective optimization problem. In this chapter we apply a brute force algorithm to generate the optimal solutions by considering the running time supplements as a variable for the train and then compute the optimal driving strategy for a single train including the blocking times. We consider a corridor of different train types in a specified time window, and compute the associated total running time as well as the total energy consumption of all trains. Next, we apply the UIC 406 timetable compression method on the corridor in order to determine the extended cycle time and buffer time.

Section 6.3.1 explains the model PROMO (PseudospectRal Optimal train control MOdel) that is used to compute the different driving strategies and blocking times, that are necessary for the blocking time theory. The brute force search is explained in Section 6.3.2. In this search we use two methods to compute the optimal solutions.

6.3.1 PROMO

We used the Radau pseudospectral method to compute the MTTC and EETC driving strategies. In this method orthogonal collocation is applied at the Legendre-Gaus-Radau (LGR) points in order to discretize the optimal control problem. The optimal control problem is then rewritten to a nonlinear programming (NLP) problem that is solved using standard NLP solvers (Betts, 2010). We refer to P. Wang & Goverde (2016a) and Goverde et al. (2021) for more details about the discretization of the optimal control problem and to Garg et al. (2009) and Rao et al. (2010a) for general background about the pseudospectral method.

We used the model called PROMO as described in Scheepmaker et al. (2020a) to compute the MTTC and EETC driving strategies. PROMO uses the GPOPS (General Purpose OPtimal Control Software) toolbox of MATLAB, which implements a Radau pseudospectral method to solve the optimal control problem (Rao et al., 2011). We applied PROMO in GPOPS version 4.1 using a laptop with a 2.1 GHz processor and 8 GB RAM. We consider two different train types, an Intercity (IC) or long distance train that stops only at main stations and a Sprinter (SPR) or regional train that stops at all stations. We applied the multiple-phase model of Scheepmaker et al. (2020a) to compute the optimal trajectory for the trains, in which we define a phase between each two stops (i.e., no separate phases for the speed limits and gradients). We also considered time as independent variable for our algorithm, because this leads to more stable results compared to distance as independent variable. We refer to Section 5.3.2 for a description of how we considered the varying gradients and speed limits that dependent on distance. Each stop needs to be a new phase, because then a collocation point at that stop is guaranteed in GPOPS. The objective is to determine the optimal distribution of the running time supplements over the trajectory in order to minimize the total traction energy consumption over the multiple runs. The model results are verified to see if they are in line with the necessary optimality conditions.

In addition, PROMO computes the extended blocking time for each block section over the trajectory for a single train using the blocking time theory as described in Section 6.2.2. The computation is done for multiple trains over a corridor. Afterwards, the extended cycle time (and maximum frequency) over the corridor is computed by applying the UIC 406 compression method as described in Section 6.2.3. The total buffer time is computed by using Eq. (6.16). Finally, a balance between different objectives can be determined by comparing the running time, extended cycle time, buffer time and energy consumption for each different combination of running time supplements for the IC and SPR. These combinations are determined by varying the running time supplements of the trains over the corridor.

6.3.2 Brute force search

In this section we explain the approach of the brute force search algorithm in order to determine the optimal solutions for the single and multiple-objective optimizations. We selected the brute force algorithm, because it is a simple approach to solve the multiple-objective problem. In addition, with this method it is possible to analyze multiple solutions close to the optimal solution to see the difference in each single objective value, and the effect on the running time supplements for the IC and SPR. We consider the running time supplements as the main variables in this chapter, because they influence all objectives. In general, increasing the running time supplements increases the total running time and decreases the energy consumption. The effect of the running time supplements on the cycle time and buffer time depends on the infrastructure, timetable and rolling stock. Therefore, by adjusting the running time supplements the interaction between the different objectives can be investigated.

The brute force search consist of the following four main steps (see Algorithm 1):

1. Compute the energy-efficient driving strategy for both the IC and SPR for running time supplements ranging from 0% until 15% with a step-size of 0.5% using PROMO. We define x as the total running time of the IC and y as the total running time of the SPR, where the MTTC driving strategy is the reference. PROMO generates the speed profile, energy consumption, as well as the blocking time per train for each given running time. For readability we only show the results of the step-size of 1% in the tables and figures. We define combination xy for each running time supplement combination for an IC-SPR cycle, where m is the total number of running time supplements for the IC and n is the total number of running time supplements for the SPR. Thus in total we have mn combinations of xy IC-SPR cycles.

2. Apply the UIC 406 compression method to compute the minimum extended cycle time for an IC-SPR cycle and the buffer time for all combinations of xy between 0% and 15% running time supplements (step-size of 0.5%) for the IC and SPR.

3. Develop four matrices with the values of the objectives of the total running time Z_R, extended cycle time Z_c, total buffer time Z_b and energy consumption Z_E for each combination of running time supplements (xy) of the IC-SPR cycle. Each entry in the table consists of a combination of the given running time supplement of the IC (columns) and SPR (rows).

4. Compute the optimal solution using two different methods. The first method is the *weighted sum method* in which we minimize the weighted sum given

a weight factor for each of the objective functions (Yan & Goverde, 2019). The second method is based on the optimal standardized Euclidean distance (*standard Euclidean distance method*) (Yan et al., 2019). We use these methods because they are most common and relative simple methods, and the weighted sum method considers the importance of the railway undertakings for each single objective by the weight factors.

We start by explaining the weighted sum method. Basically the weighted sum method is a scalarization method which combines all objectives into a single objective (Marler & Arora, 2004). However, when all weights are positive the Pareto optimal solution is achieved by minimizing the weighted sum. Before we can apply the weighted sum method, we need to scale the different objectives with different weight factors in order to compare them (Yan & Goverde, 2019). Since the objectives of total running time, extended cycle time and total buffer time are defined in seconds, we consider this basic scaling to compare the different objectives. We consider the total running time as reference with value 1. We compute the scaling by comparing for each running time supplement combination xy the two objectives with each other with the total average ratio as a scaling factor. This leads to the following scaled formulation of the different single objectives:

$$V_R^{xy} = Z_R^{xy},\ V_c^{xy} = \left(\frac{1}{mn}\sum_{x=1}^{m}\sum_{y=1}^{n}\frac{Z_c^{xy}}{Z_R^{xy}}\right)^{-1} Z_c^{xy},\ V_b^{xy} = \left(\frac{1}{mn}\sum_{x=1}^{m}\sum_{y=1}^{n}\frac{Z_b^{xy}}{Z_R^{xy}}\right)^{-1} Z_b^{xy}. \tag{6.18}$$

Since buffer times should be maximized, we rewrite this to minimize the negative value of the buffer time in order to minimize all objectives (i.e., $\max Z_b = -\min Z_b$). In addition, we apply a sensitivity analysis where we see the effect of the optimal solution by varying between the minimum and maximum ratio given the data. Since energy consumption is measured in a complete different unit (kWh), it is difficult to scale this objective with the other objectives that have units in s. Therefore, a scaling factor ω is used and varied using a sensitivity analysis to find a balance between energy consumption and the other objectives:

$$V_E^{xy} = \omega Z_E^{xy}. \tag{6.19}$$

The weighted sum (affine combination) with weight factors w_i for $i = 1,\ldots,4$ (for each of the four objectives) and $\sum_{i=1}^{4} w_i = 1$ for the xyth solution can be computed by:

$$\alpha_{xy} = w_1 V_R^{xy} + w_2 V_c^{xy} - w_3 V_b^{xy} + w_4 V_E^{xy}. \tag{6.20}$$

A sensitive analysis is applied in order to determine the weight factors, which will

be discussed in Section 6.4.4.

Second, we explain the steps to derive the standard Euclidean distance. We first need to standardize the results on the interval $[0,1]$ for each element in the different tables by using the min-max normalization (Yan et al., 2019), i.e., for the objective of running time the normalized objective value is

$$\tilde{Z}_R^{xy} = \frac{Z_R^{xy} - Z_R^{\min}}{Z_R^{\max} - Z_R^{\min}}, \tag{6.21}$$

where $Z_R^{\min}$ and $Z_R^{\max}$ are respectively the minimum and maximum over the entire matrix of Z_R. The normalized objective values of the other objectives Z_c and Z_E are computed in the same way. Since the buffer times are to be maximized, we compute first Z_b the same way as Z_R and afterwards we compute the normalized objective value for the buffer time by $\tilde{Z}_b^{xy} = 1 - \tilde{Z}_b^{xy}$, in order to minimize all the objectives. Finally, we determine the optimal standardized Euclidean distance for each combination xy as:

$$\beta_{xy} = \sqrt{(\tilde{Z}_R^{xy})^2 + (\tilde{Z}_c^{xy})^2 + (\tilde{Z}_b^{xy})^2 + (\tilde{Z}_E^{xy})^2}. \tag{6.22}$$

Algorithm 1: Brute-force search algorithm.

Data: Infrastructure, rolling stock, interlocking, and timetable.
Result: The optimal solutions for the single and multiple-objective optimizations;
Compute MTTC driving strategy for the IC ($x = 1$) and SPR ($y = 1$) ;
for $x = 1.005, 1.010, 1.015, ..., 1.15$ **do**
  Compute EETC driving strategy for the IC with x running time supplement;
end
for $y = 1.005, 1.010, 1.015, ..., 1.15$ **do**
  Compute EETC driving strategy for the SPR with y running time supplement;
end
for $x = 1, 1.005, 1.010, ..., 1.15$ **do**
  for $y = 1, 1.005, 1.010, ..., 1.15$ **do**
    Apply UIC 406 compression method for each xy IC-SPR cycle combination;
    Compute Z_R, Z_c, Z_b, and Z_E for each xy IC-SPR cycle combination;
  end
end
Compute weighted sum method α;
Compute standard Euclidean distance method β;

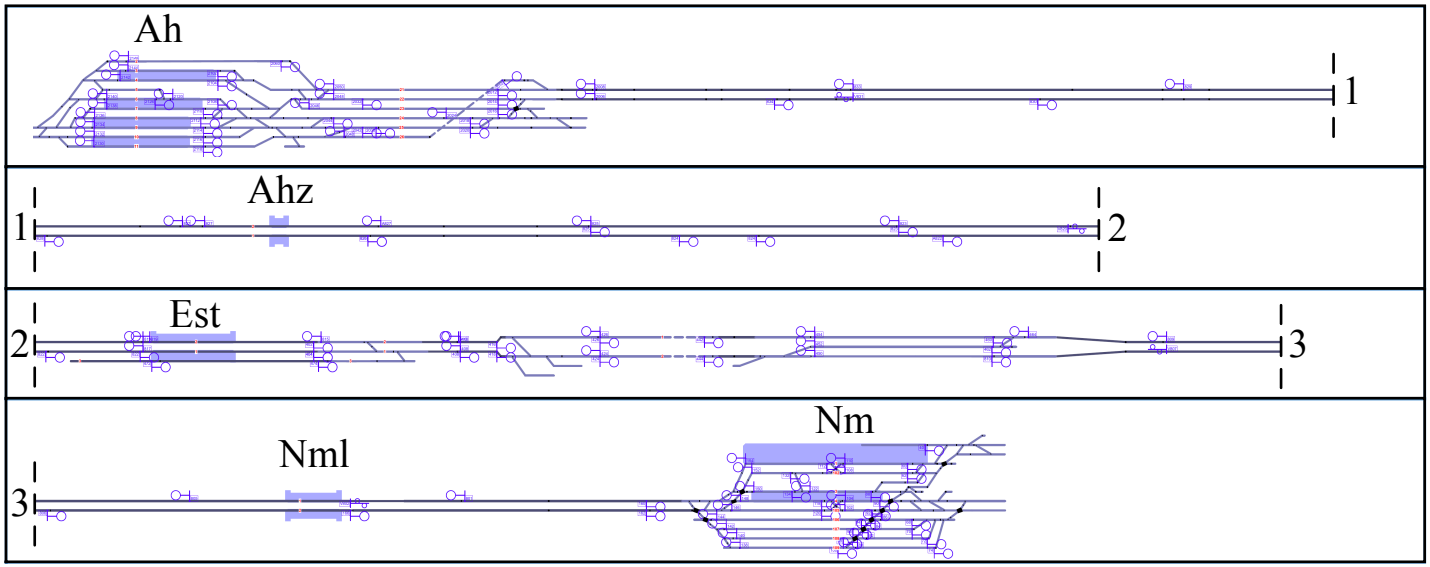

Figure 6.3: Detailed track layout of railway line Arnhem Central (Ah)–Nijmegen (Nm).

6.4 Case Study

In this section we apply our models to different scenarios in a case study in order to find a balance between the objectives of minimizing total travel time for the passengers, extended cycle, and energy consumption as well as maximizing the buffer time for robustness. We start by providing the input of the case study, see Section 6.4.1. In Section 6.4.2 we discuss the results for the different single objectives. We make a comparison between the different objectives in Section 6.4.3. Afterwards, we consider the optimization of the multiple objectives in Section 6.4.4. We analyze the effect of varying the minimum buffer time on the multiple objectives in Section 6.4.5. Finally, a discussion of the main results is presented in Section 6.4.6.

6.4.1 Case study description

The case study considers the railway line between the main stations Arnhem Central (Ah) and Nijmegen (Nm) in the Netherlands with the intermediate stations Arnhem South (Ahz), Elst (Est) and Nijmegen Lent (Nml). The detailed track layout of this railway line can be seen in Figure 6.3 and the details in one direction about the location of the gradients, speed limits and signals can be found in Table A.1 in Appendix A, which is based on the infrastructure data from ProRail (ProRail, 2020). The trains are running over the right-hand tracks for the double track sections. We consider two different electrified train types operating on this network: an Intercity (IC) or long distance train only stopping at the main stations Ah and Nm, and a Sprinter (SPR) or regional train stopping at all stations. The IC and SPR share the same route over the infrastructure, except at the first and last block section due to different track and platform use at Ah and Nm (i.e., we do not consider overtaking on the open track between these stations). We set the maximum passenger comfort braking to 0.5 m/s^2, according to practice in the timetable design at the Netherlands Railways (NS). The trains receive their electricity from the 1.5 kV DC catenary system. We develop microscopic conflict-free timetables using the blocking time theory as described in Section 6.2.2, therefore, we assume that there is only a red signal approach at the final platform signal at Nm. The general characteristics and parameter setting times can be found in Appendix A Table A.2 and A.3 that are partially adopted from Goverde et al. (2013) and Scheepmaker et al. (2020b).

The Dutch timetable is cyclic and in general repeats itself every half hour. In the current Dutch timetable trains operate with frequencies of at least two trains per hour. Therefore, we use a half hour time interval. We consider the running time supplements and the minimum buffer time between trains as basic measures for timetable robustness. In the Netherlands the current minimum buffer time is

60 s. However, the aim is to reduce this buffer time to 30 s by for instance using ATO in order to increase the number of trains in the network without expensive infrastructure cost. In this chapter we set the minimum buffer time to 30 s, but we also investigate the effect of increasing the minimum buffer time to 60 s. The minimum extended cycle time is computed using the UIC 406 compression method as described in Section 6.2.3. Finally, we consider an increase in the frequency of the IC-SPR train when this is enabled by the extended cycle time, because this leads to a higher service to the passengers. For instance an extended cycle time of 720 s leads to 4 IC-SPR cycles per hour, while an extended cycle time of 719 s gives 5 IC-SPR cycles per hour. However, the increase in the frequency of the IC-SPR cycles reduces the total buffer time.

6.4.2 Results of the indicators

In this section we discuss the results of different indicators where we differentiate between the separate IC and SPR, and the IC-SPR cycle. First, we analyze the separate results of the IC (Figure 6.4) and SPR (Figure 6.5) in terms of speed profile and energy consumption. The results of the driving strategies of the IC and SPR with varying running time supplements are shown in Table B.1 (Appendix B), while the optimal distribution of the running time supplements over multiple-stops for the SPR is shown in Table B.2 (Appendix B).

We start by analyzing the results of the speed-distance and energy-distance profiles of the IC (Figure 6.4) and SPR (Figure 6.5), where we varied the amount of running time supplements. Figure 6.4 indicates for the IC that the higher the amount of running time supplement, the earlier the train starts to coast. With limited running time supplement up to 4% the speed-distance plot indicates two coasting phases: one before and one after the reduced speed limit of 130 km/h after Est with possibly a short distance of maximum acceleration after the reduced speed limit of 130 km/h before coasting. In case that the running time supplements are at least 10% we see that the optimal driving strategy does not include cruising at the speed limit, but the train starts to coast directly after maximum acceleration. Table B.1 indicates that the energy savings of the EETC driving strategy for the IC vary between 24% and 57% compared to the MTTC driving strategy. The resulting speed-distance profile of the SPR is shown in Figure 6.5. In general, the figure indicates that when there are sufficient running time supplements, the optimal driving regime between each of the stops consists of maximum acceleration, coasting and maximum braking, with a possible cruising regime at the speed limit where the speed limit is reached. The results in Figure 6.5 and Table B.2 also indicate that relatively more running time supplement is included for shorter distance sections where the train can start coasting at relatively lower speeds, which is in line with the results of Scheepmaker et al. (2020a). The exception is at the

short section Nml-Nm (2.4 km) that includes a speed limit restriction of 40 km/h. The results indicate that coasting below 70 km/h takes relatively much running time supplement while the energy savings are limited. The energy savings of the SPR by the EETC driving strategy vary between 18% and 56% compared to the MTTC driving strategy (see Table B.1).

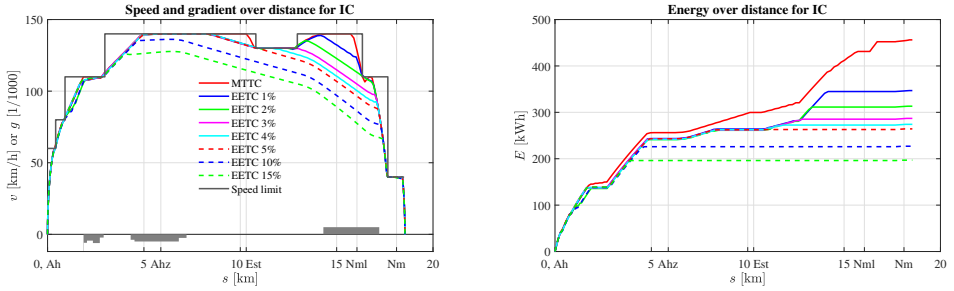

Figure 6.4: The left plot shows for the case Ah-Nm IC with varying running time supplements the speed/gradient–distance profile of the MTTC and EETC driving strategies. The right plot indicates the energy–distance profile of the MTTC and EETC driving strategies for the case Ah-Nm IC.

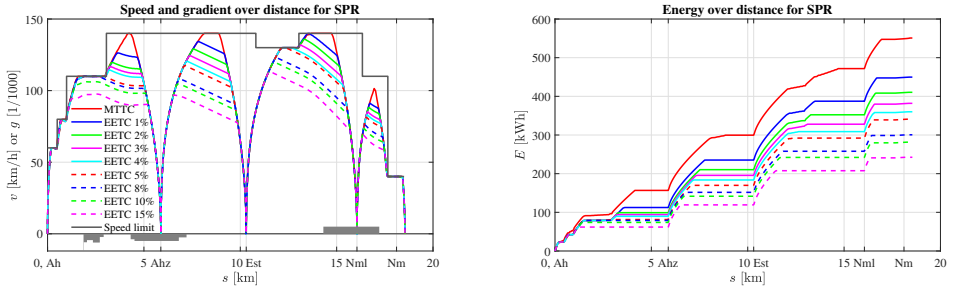

Figure 6.5: The left plot shows for the case Ah-Nm SPR with varying running time supplements the speed/gradient–distance profile of the MTTC and EETC driving strategies. The right plot indicates the energy–distance profile of the MTTC and EETC driving strategies for the case Ah-Nm SPR.

Afterwards, we continue on the interaction of the trains by analyzing the IC-SPR cycles. We analyze the results of the IC-SPR cycle for the total running time, followed by the extended cycle time and buffer time. Then, we discuss the results of the energy consumption of the IC-SPR cycle. Table B.3 (Appendix B) gives the total running time per IC-SPR cycle and the extended cycle time per IC-SPR cycle is shown in Table B.4 (Appendix B). Table B.5 (Appendix B) gives

the buffer time per IC-SPR cycle and the total energy consumption per IC-SPR cycle is provided by Table B.6 (Appendix B). The results of the different driving strategies and IC-SPR cycles are also visualized in Figures 6.6–6.10.

Table B.3 and the contour plot in the left plot of Figure 6.6 obviously indicate that more running time supplements for the IC and/or SPR leads to a higher total running time. The MTTC driving strategy provides the solution that minimizes total travel time. For the MTTC driving strategy the resulting compressed timetable is shown in the left part of Figure 6.7, indicating that the critical blocks are block 3 after Ah (IC-SPR) and block 17 at Nm (SPR-IC).

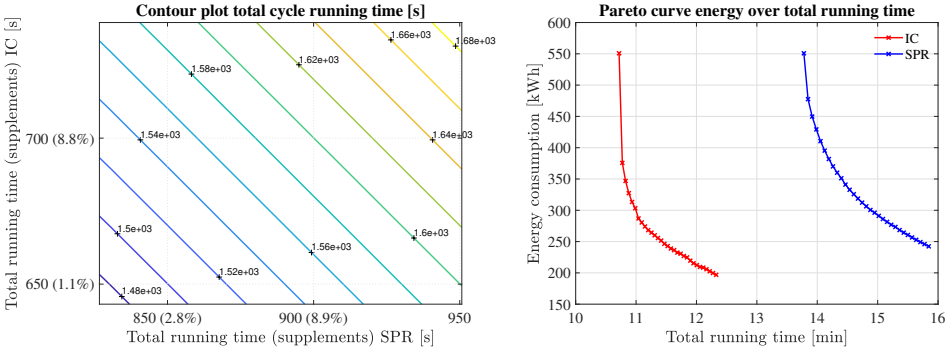

Figure 6.6: The left plot shows the contour plot for the case Ah-Nm for the total cycle running time over the total running time (supplements) for the SPR and IC. The right plot indicates the Pareto frontier curve of the energy consumption over the total running time for the IC and SPR for the case Ah-Nm.

Table B.4 shows that more running time supplement for the IC leads to a lower extended cycle time, while including more running time supplement for the SPR increases the extended cycle time. This effect can also be seen in the contour plot of the total extended cycle time in the left plot in Figure 6.8. The contour plot shows that the curves with low values of the extended cycle times (i.e., 640 s and 660 s) intersect the vertical axis of the varying running time (supplements) of the IC, indicating that with 0% running time supplements for the SPR and high amount of running time supplements of the IC, the smallest extended cycle time can be achieved. The resulting compressed timetable of the driving scenario with 15% running time supplements for the IC and 0% for the SPR is shown in the left part of Figure 6.9, indicating that block 7 at Ahz (IC-SPR) and block 17 at Nm (SPR-IC) are the critical blocks. Lower extended cycle times enable higher frequencies of the IC-SPR train cycles. The results are in line with common knowledge in practice that homogenization leads to a lower cycle time and thus may enable a possible increase in frequency. Homogenization is defined as decreasing the differences

between running times on the same track section of successive trains, which can be achieved by slowing down the IC (i.e., increasing the running time supplements) or speeding up the SPR (i.e., decreasing the running time supplements). In general, homogenization has a positive effect on the infrastructure occupation.

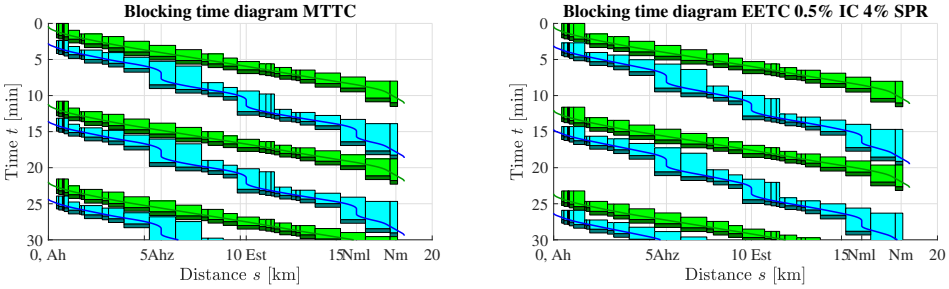

Figure 6.7: The left plot shows for the case Ah-Nm for the IC (green) and SPR (blue) compressed blocking time diagram of the MTTC driving strategies. The right plot indicates for the IC (green) and SPR (blue) compressed blocking time diagram EETC driving strategies for the case Ah-Nm. The EETC driving strategy has 0.5% running time supplements for the IC and 4% running time supplements for the SPR. The dark green and dark blue blocks are the minimum buffer time of 30 s.

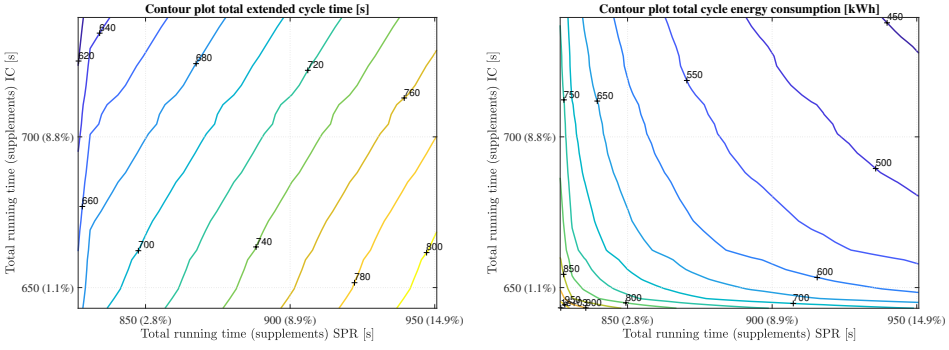

Figure 6.8: The left plot shows the contour plot for the case Ah-Nm for the extended cycle time over the total running time (supplements) for the SPR and IC. The right plot indicates the contour plot for the total total cycle energy consumption over the the total running time (supplements) for the SPR and IC for the case Ah-Nm.

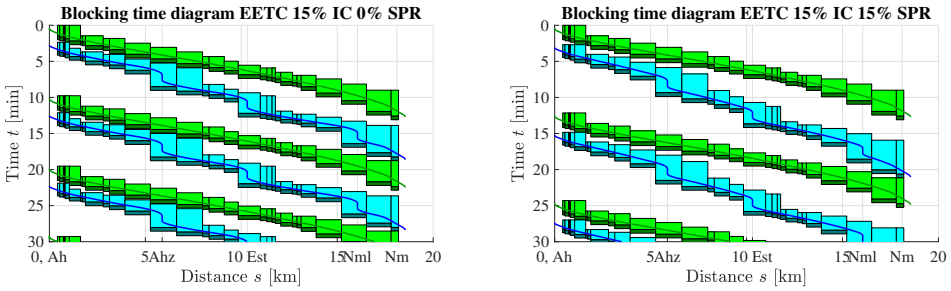

Figure 6.9: The left plot shows for the case Ah-Nm for the IC (green) and SPR (blue) compressed blocking time diagram for the EETC driving strategies with 15% running time supplements for the IC and 0% running time supplements for the SPR. The right plot indicates the IC (green) and SPR (blue) compressed blocking time diagram for the case Ah-Nm for the EETC driving strategies with 15% running time supplements for both the IC and SPR.

The results of the buffer time in Table B.5 show that the buffer time increases until the frequency of the number of IC-SPR train cycles can be increased for a higher service to the passengers. This effect is shown in Figure 6.10. For instance there is a switching point at 720 s (from 60 s to 240 s). The mesh plot of the buffer time on the left side of this figure shows the effect of the different running time supplements of the SPR (x-axis) and IC (y-axis) over the buffer time (z-axis). The vertical drop in buffer time indicates the increase in frequency of both trains by one train per hour. The right plot in Figure 6.10 shows the effect of the extended cycle time (x-axis) over the buffer time (y-axis), which indicates a piecewise linear relationship between the two conform Eq. (6.16) with a jump where sufficient buffer allows an increase of the frequency. Basically, the higher the extended cycle time, the lower the buffer time. If we consider a fixed frequency of 4 IC-SPR train cycles per hour, the highest buffer time can be achieved by considering 15% running time supplements for the IC and 0% running times for the SPR, which will lead to a buffer time of 350.2 s that is determined based on extrapolation of the results in Table B.5. The results of the compressed timetable are shown in the left part of Figure 6.9.

The results of the energy consumption in Table B.6 show that the total energy consumption decreases if the running time supplements of the IC and/or SPR increase. The highest energy savings are achieved by 15% running time supplements for both IC and SPR. The associated compressed timetable is shown in the right plot of Figure 6.9, indicating that the critical blocks are block 3 (after Ah for the IC-SPR order) and block 17 (at Nm for the SPR-IC order). The results are also shown in the right contour plot of Figure 6.8. This contour plot indicates the

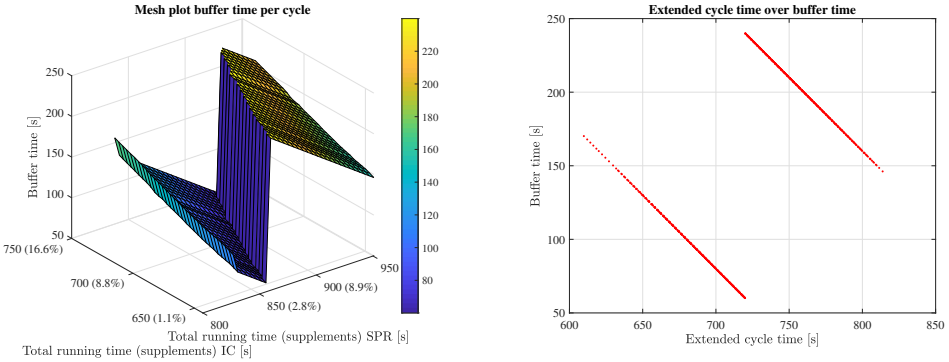

Figure 6.10: The left plot shows the mesh plot for the case Ah-Nm for the buffer time per cycle over the running time (supplements) of the SPR and IC. The right plot indicates the buffer time over extended cycle time for the case Ah-Nm.

effect of varying the running time (supplements) of the SPR (x-axis) and varying the running time (supplements) of the IC (y-axis) on the total energy consumption. The closer the lines, the steeper the relative decrease in energy consumption compared to the extra running time. The highest relative savings are achieved with the smallest time supplement (i.e., diminishing returns) (Scheepmaker et al., 2017, 2020b). The right contour plot in Figure 6.8 shows that relatively higher energy savings can be achieved by including extra running time supplements for the SPR compared to the IC. For instance, the line of 700 kWh intersects the x-axis, while not intersecting the y-axis. The Pareto curve of the varying running time supplements of the IC and SPR is shown in the right plot of Figure 6.6. The figure clearly indicates that the steepest gradient occurs between 0% and 0.5% running time supplement, leading to the relatively largest energy savings.

6.4.3 Balance between objectives

In this section the balance between the different objectives of minimizing the total running time, extended cycle time and energy consumption as well as maximizing the buffer time for robustness is discussed. Optimizing each of the different objectives leads to different solutions as shown in Section 6.4.2. We focus both on the effect of the IC-SPR cycle as well as the effects on the IC and SPR separately. The relationship between the different single objectives is shown in the causal loop for the Intercity and Sprinter in Figure 6.11.

First, the causal loop in Figure 6.11 indicates that for the IC there is a positive relationship (reinforcing) between the objective of total running time and buffer time, i.e., an increase in the total running time for the IC leads to an increase in

the total buffer time for the IC-SPR cycles. For the SPR there is only a positive relationship between the total running time and extended cycle time, i.e., an increase in the total running time for the SPR leads to an increase in the extended cycle time. The relationship with all the other objectives for the IC and SPR is negative (balancing), i.e., an increase in total running time for the IC and/or SPR leads to a decrease in the other objectives. If we focus on the IC-SPR train cycle, we notice that the objective of minimizing total running time leads to the MTTC driving strategy for all trains (0% running time supplements), while considering the objectives of maximizing robustness, minimizing capacity or energy consumption leads to a certain optimal amount of running time supplements. The most clear trade-off is between minimizing the total running time and minimizing the energy consumption, because for energy minimization the trains should have the maximum possible amount of running time supplements. However, as explained in Section 6.4.2 the relative energy savings achieved by extra running time supplements decreases for higher supplements (diminishing returns).

Second, we see that there is a clear relationship between infrastructure occupation and robustness. As stated in Section 6.2.4 by Eq. (6.16) and also shown in the right plot in Figure 6.10 there is a negative linear relationship between the extended cycle time and buffer time. This can also be observed from the causal loop in Figure 6.11 (balancing between the extended cycle time and buffer time for both the IC and SPR). If we consider a fixed frequency of IC-SPR train cycles per hour, we see that higher extended cycle times lead to lower buffer time.

Third, there is a reinforcing relationship between the extended cycle time and energy consumption for the IC and a balancing relationship between the extended cycle time and energy consumption for the SPR, see Figure 6.11. This can also be seen in Figure 6.12. Each of the lines in the left plot in the figure represents the fixed percentage of running time supplements of the IC, while the running time supplements of the SPR are varied. The right plot in the figure indicates the opposite by fixing the running time supplements of the SPR and varying the running time supplements of the IC. The figures clearly indicate that higher amount of supplements for the SPR leads to a higher extended cycle time, while higher amounts of supplements for the IC leads to a lower extended cycle time (homogenization). Moreover, Figure 6.12 shows the effect of diminish returns of the extra running time compared to the extra extended cycle time by the gradient of the curve.

Fourth, the relationship between buffer time and energy consumption is balancing for the IC and reinforcing for the SPR, see Figure 6.11. Robustness can be improved by increasing the buffer time, which is achieved by adding large amount of running time supplements to the IC and none to the SPR (MTTC). This means that the fastest train gains the highest running time supplements. However,

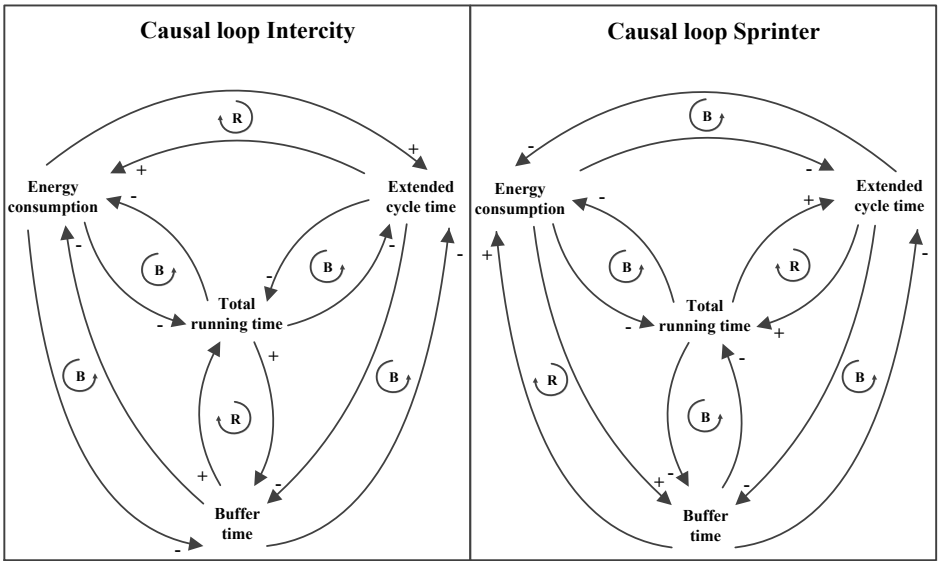

Figure 6.11: The left plot shows for the case Ah-Nm the causal loop diagram between the objectives for the IC. The right plot indicates for the case Ah-Nm the causal loop diagram between the objectives for the SPR (legend: R = Reinforcing, B = Balancing, + = objective at the end of the arrow is moving in the same direction as the objective at the beginning of the arrow, and − = objective at the end of the arrow is moving in the opposite direction as the objective at the beginning of the arrow).

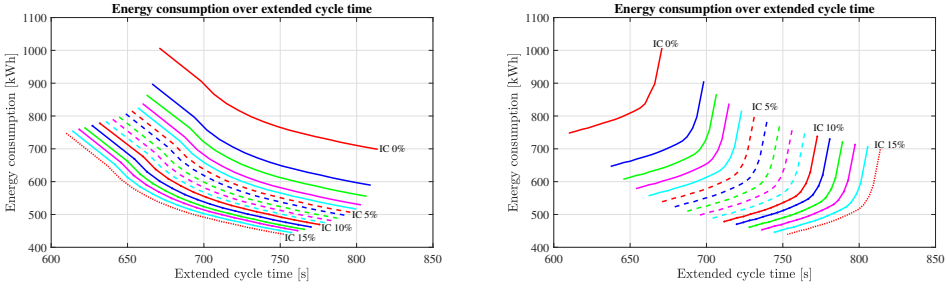

Figure 6.12: The left plot shows the energy consumption over the extended cycle time for the case Ah-Nm for fixed running time supplements of the IC and varying running time supplements for the SPR. The right plot indicates the energy consumption over the extended cycle time for fixed running time supplements of the SPR and varying running time supplements for the IC for the case Ah-Nm.

for the objective of minimizing the energy consumption relatively more energy savings can be achieved by adding extra running time supplement to the slowest train (SPR), while overall the most energy can be saved by giving all trains the maximum amount of running time supplements.

6.4.4 Multiple objectives

In this section we consider the optimal solution of the multiple objectives as described in Section 6.4.2. We use two different methods to compute the optimal solutions. The first method is based on the weighted sum and the second method is based on the standard Euclidean distance. We start with a sensitivity analysis for determining the scaling and weight factors that are needed for the weighted sum method. Afterwards, we discuss the results of the optimization with the three objectives of minimizing total travel time, extended cycle time and maximizing the buffer time. Finally, the effects of including energy minimization to the other three objectives is discussed.

Sensitivity analysis scaling and weight factors

In this section we discuss the sensitivity analysis to determine the scaling and weight factors for the weighted sum method. We first give the outline of the approach in five steps. Afterwards, we present the main results of the sensitivity analysis. The results are used to compute the different multiple objective values using the two methods.

We started by doing a sensitivity analysis to determine the scaling factors of the three-objective optimization function, i.e., the total running time, extended cycle time, and total buffer time. We considered the minimum, medium and maximum relationship instead of the average relationship as given by Eq. (6.18). Second, we did a sensitivity analysis for the weight factors of the three objectives, where we assumed $w_4 = 0$. We started by finding the correlation between the total running time and extended cycle time by varying the weight factor w_1 (and w_2) on the interval $[0, 0.66]$, with a constant weight factor for the buffer time (i.e., $w_3 = 0.33$). Afterwards, we looked for the correlation between the extended cycle time and total buffer time by varying the weight factor w_2 (and w_3) on the interval $[0, 0.66]$ given a constant value of the weight factor for the total running time (i.e., $w_1 = 0.33$). Third, we determined the scaling factor for energy consumption ω by including the energy consumption objective with the three other objectives and varying the scaling factor. We varied the scaling factor ω on the interval $[0, 20]$ while using equal weight factors for all objectives in order to scale the energy consumption objective (i.e., $w_1 = w_2 = w_3 = w_4 = 0.25$). Fourth, given the relationship between the three objectives and the scaling factor for the

energy consumption we applied the sensitivity analysis of the weight factor w_4 on the interval $[0,1]$ for the energy consumption considering the four-objective optimization problem. We varied the value of w_4 and we assumed the other weight factors to be equal to each other (i.e., $w_1 = w_2 = w_3$). Fifth, we investigated the relationship between the extended cycle time that is related to the infrastructure occupation, and the total energy consumption by doing two sensitivity analyses. During the first sensitivity analysis we varied the weight factors w_2 and w_4 between 0 and 0.5 and we set the other weight factors equal to 0.25 (i.e., $w_1 = w_3 = 0.25$). We added a second sensitivity scenario in which we considered only the objectives of extended cycle time and energy consumption by setting $w_1 = w_3 = 0$, and we varied the values of w_2 and w_4 between 0 and 1.

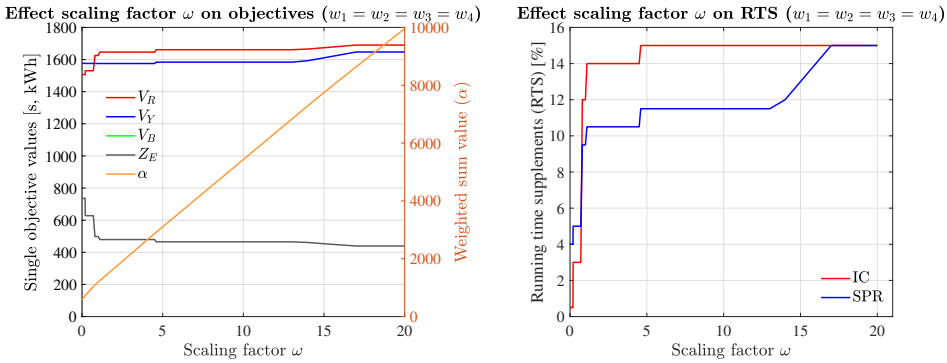

Figure 6.13: The left plot shows the sensitivity analysis by varying the scaling factor of the energy consumption ω related to the single objectives (left y-axis) and weighted sum value (right y-axis). The right plot indicates the running time supplements (RTS) for the IC and SPR given the varying weight factor of the energy consumption ω.

The results of the scaling factors given in Eq. (6.18) show that the scaling factors are robust. The sensitivity analysis of the weight factors of the three different objectives indicate that three objectives are stable for varying the different single weight factors. Since the three objectives are already scaled by Eq. (6.18), we choose equal weights for them, i.e., $w_1 = w_2 = w_3 = 0.33$. The results of the sensitivity analysis of the scaling factor ω for the energy consumption are shown in Figure 6.13. The left plot in this figure indicates the effect of varying the scaling factor of the energy consumption ω for the single objectives (left y-axis) and for the multiple objectives (right y-axis), due to the different magnitude. The right plot shows the optimal solution for the relative amount of running time supplements for the IC and SPR that leads to the optimal value given the scaling factor value ω. The results indicate that Z_E is not sensitive on different intervals of ω. Stability for the objectives is reached when $\omega \in [4.6, 13]$, however, this leads to relatively large

amount of running time supplements (15% IC and 11.5% SPR). From a practical perspective the running time supplements at NS should be at least 8% and not too big, therefore, we choose the 12% for the IC and 9.5% for the SPR which leads to a scaling factor $\omega = 1$. We choose equal weight factors for all objectives in the remainder of the chapter based on the sensitivity analysis of weight factor w_4, i.e., $w_1 = w_2 = w_3 = w_4 = 0.25$, because V_R, V_c, V_B and V_E are not sensitive on different intervals of w_4. The results of the first sensitivity analysis between the extended cycle time and energy consumption indicate that both V_c and V_B are relatively stable for the varying weight factor for the energy consumption, and the capacity consumption is about 80%. The results of the second sensitivity analysis indicate that the lower the value of w_4, the higher the total energy consumption and the lower the extended cycle time, and thus the lower the infrastructure occupation when the frequency remains the same (i.e., 4 IC-SPR cycles per hour). In addition, low values of w_4 lead to a low amount of running time supplements for the SPR (i.e., homogenization), while high values of w_4 lead to a high amount of running time supplement for the SPR. The relative amount of running time supplements for the IC remains constant for varying values of w_4 (15% running time supplements).

Results for multiple objectives without energy consumption

We start by analyzing the results considering the multiple-objective function with the three objectives: total running time, extended cycle time and total buffer time (thus without energy consumption). The top 10 Pareto-optimal solutions can be found in Table 6.2. The top 10 of optimal values are sorted according to the order of the weighted sum (from low to high), because in this method the different objectives are scaled and weighted. The optimal solution ($\alpha = 193.7$) is achieved by 0.5% running time supplements for the IC and 4% running time supplements for the SPR. This leads to relatively low amount of total running time (1506 s) for the IC-SPR cycle as well as high amount of buffer time (239 s, close to the maximum buffer time in Table B.5). The total energy consumption is about 736 kWh and the capacity consumption is about 80%. The drawback for this solution is that the extended cycle time is relatively high, which leads to a maximum frequency of 4 IC-SPR cycles per hour. In addition, the optimal solution considering the weighted sum method is the same as considering the Euclidian distance, although their value is different ($\alpha = 193.7$ and $\beta = 0.5674$). This is caused by the fact that the total running time is close to its minimum value and the buffer time is almost its maximum value. The right plot in Figure 6.7 shows the resulting compressed timetable for the optimal solution with the critical block sections 3 (IC-SPR) and 17 (SPR-IC). The top 10 of α-optimal solutions shows that optimal solutions consider very low amount of running time supplements for the IC and slightly higher amount of running time supplements for the SPR. In addition, the

top-10 order of the α-optimal solutions are different compared to the β-optimal solutions, due to the scaling of the objectives in the weighted sum method.

In the Netherlands the norm for running time supplements for each train is at least 8% for timetable stability. If we include this NS constraint to determine the optimal solution according to the weighted sum method, the running time supplements should be 10.5% for the IC and 8.5% for the SPR ($\alpha = 225.6$) as can be seen in Table 6.2. The result is far away from the optimal solution without the constraint of at least 8% running time supplements for the IC and SPR, which leads to relatively a high amount of running time. The compressed timetable of this scenario is shown in the left plot in Figure 6.14, indicating the critical block sections 3 (IC-SPR) and 17 (SPR-IC). The main difference compared to the top 10 α-optimal solutions is the increase in total running time. Therefore, this optimal solution could only be achieved by adding the constraints of at least 8% running time supplements given the three-objective optimization.

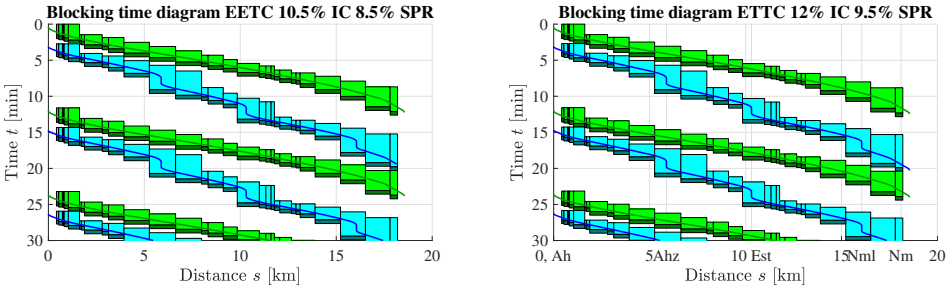

Figure 6.14: The left plot shows for the case Ah-Nm for the IC (green) and SPR (blue) compressed blocking time diagram for the EETC driving strategies with 10.5% running time supplements for the IC and 8.5% running time supplements for the SPR. The right plot indicates the IC (green) and SPR (blue) compressed blocking time diagram for the case Ah-Nm for the EETC driving strategies with 12% running time supplements for the IC and 9.5% running time supplements for the SPR.

Results for all objectives including energy consumption

Here we consider the four objectives in the multiple-objective optimization: total running time, extended cycle time, buffer time, and energy consumption. The results can be found in Table 6.3. The optimal solution according to the weighted sum method ($\alpha = 298.3$) is achieved by 12% running time supplements for the IC and 9.5% running time supplements for the SPR. This solution complies to the NS constraint optimal solution of at least 8% running time supplements for

Table 6.2: First 10 Pareto-optimal solutions and NS constrained optimal solution (No. α 21) with 30 s minimum buffer time considering the objectives total running time Z_R, extended cycle time Z_c and buffer time Z_b for the real-world case Ah-Nm using the weighted sum method (sorted from low to high according to α).

No. α	No. β	RTS IC (%)	RTS SPR (%)	Z_R (s)	Z_c (s)	Z_b (s)	Z_E (kWh)	f (-)	C (%)	α	β
1	1	0.5	4.0	1506.0	720.6	239.4	735.8	4	80.1	193.7	0.5674
2	11	1.5	4.5	1516.6	721.2	238.8	678.6	4	80.1	199.7	0.5858
3	20	3.0	5.0	1530.4	720.3	239.7	628.0	4	80.0	200.5	0.6073
4	2	0.0	4.5	1502.8	723.0	237.0	816.3	4	80.3	202.6	0.5748
5	13	1.0	4.5	1513.3	722.6	237.4	698.1	4	80.3	204.2	0.5869
6	32	4.0	5.5	1540.9	721.4	238.6	606.9	4	80.2	208.6	0.6350
7	22	2.5	5.0	1527.2	722.8	237.2	644.4	4	80.3	209.7	0.6118
8	14	0.5	4.0	1510.1	724.8	235.2	727.0	4	80.5	212.5	0.5929
9	42	5.0	6.0	1551.5	721.6	238.4	590.0	4	80.2	213.0	0.6616
10	21	2.0	5.0	1523.9	724.0	236.0	654.3	4	80.4	213.7	0.6114
21	204	10.5	8.5	1607.5	720.2	239.8	520.8	4	80.0	225.6	0.8265

Legend: α = weighted sum, β = standardized Euclidean distance, IC = Intercity, SPR = Sprinter, RTS = running time supplements, Z_R = minimum running time objective, Z_c = minimum extended cycle time objective, Z_b = maximum buffer time objective, Z_E = minimum energy consumption objective, f = frequency of IC-SPR cycles per hour, C = capacity consumption.

the IC and the SPR. The compressed timetable of this scenario can be seen in the right plot in Figure 6.14, indicating that the critical block sections are block section 3 (IC-SPR) and 17 (SPR-IC). The optimal solution leads to a total running time of 1625 s, an extended cycle time of 720 s (frequency of 4 IC-SPR cycles per hour), 240 s buffer time, a capacity consumption of 80%, and an energy consumption of 498 kWh. We can see that including the energy consumption into the multiple-objective optimization leads to higher running times, but the resulting extended cycle time and buffer time are almost the same. Therefore, including energy consumption in the multiple-objective optimization only influences the total running time (i.e., balance total running time and energy consumption). Analyzing the top 10 optimal solutions according to the weighted sum method shows that the running time supplements of the IC vary between 7% and 14.5% while the running time supplements of the SPR vary between 7.5% and 11% and are in general relatively smaller than the IC. The optimal values of the extended cycle time and buffer time remain about the same (small fluctuations), while there are bigger fluctuations in the total running time and energy consumption. Moreover, the results of the top 10 α-optimal solutions are completely different compared to the β-optimal solutions, because in the weighted sum method all different objectives are scaled to each other, and in the standardized Euclidean distance the variables are only normalized on the interval [0, 1].

Table 6.3: First 10 Pareto-optimal solutions with 30 s minimum buffer time considering the objectives total running time Z_R, extended cycle time Z_c, buffer time Z_b and energy consumption Z_E for the real-world case Ah-Nm using the weighted sum method (sorted from low to high according to α).

No. α	No. β	RTS IC (%)	RTS SPR (%)	Z_R (s)	Z_c (s)	Z_b (s)	Z_E (kWh)	f (-)	C (%)	α	β
1	205	12.0	9.5	1625.4	720.2	239.8	498.4	4	80.0	298.3	0.8955
2	271	13.0	10.0	1636.0	720.1	239.9	489.9	4	80.0	298.4	0.9319
3	344	14.0	10.5	1646.5	720.1	239.9	479.4	4	80.0	298.5	0.9694
4	116	10.5	8.5	1607.5	720.2	239.8	520.8	4	80.5	299.4	0.8389
5	152	13.0	9.0	1614.9	720.6	239.4	510.6	4	80.1	299.9	0.8624
6	44	8.0	7.5	1583.2	721.5	238.5	545.2	4	80.2	303.7	0.7741
7	68	9.0	8.0	1593.7	721.8	238.2	532.9	4	80.2	303.9	0.8028
8	25	7.0	7.0	1572.6	721.4	238.6	558.6	4	80.2	303.9	0.7489
9	197	11.5	9.5	1622.2	722.1	237.9	501.4	4	80.2	304.3	0.8905
10	414	14.5	11.0	1653.9	722.0	238.0	473.1	4	80.2	304.9	1.0020

Legend: α = weighted sum, β = standardized Euclidean distance, IC = Intercity, SPR = Sprinter, RTS = running time supplements, Z_R = minimum running time objective, Z_c = minimum extended cycle time objective, Z_b = maximum buffer time objective, Z_E = minimum energy consumption objective, f = frequency of IC-SPR cycles per hour, C = capacity consumption.

6.4.5 Effect of varying minimum buffer time

We investigated the effect of varying the minimum buffer time on the optimal solution. Therefore, we included two scenarios: one with 0 s (Table 6.4) and one with 60 s (Table 6.5) minimum buffer time for each train instead of 30 s (Table 6.3). Since the minimum buffer time is constant for all trains over the complete trajectory, the results indicate that the optimal solutions considering the weighted sum and the Euclidean distance remain the same, except the value of the weighted sum. The change in buffer time only leads to a different total buffer time, extended cycle time, frequency and capacity consumption. In general larger minimum buffer time leads to lower frequencies of IC-SPR cycles per hour. If we consider a fixed frequency of IC-SPR cycles per hour, then the larger the minimum buffer time, the larger the capacity consumption. We can thus conclude that the change in minimum buffer time does not influence the results for the weighted sum and the standard Euclidean distance.

6.4.6 Discussion of the main results

In this section we discuss the main results achieved by the case study. We make a distinction between results of the single objectives, the interaction between objectives, the sensitivity analysis for the scaling and weight factors, and the multiple objectives. The main results of the case study are the causal loop diagram in Figure 6.11 that indicates the relationship between the objectives, and the application of two methods to compute the optimal solutions, which show that

Table 6.4: First 10 Pareto-optimal solutions with 0 s minimum buffer time considering the objectives total running time Z_R, extended cycle time Z_c, buffer time Z_b and energy consumption Z_E for the real-world case Ah-Nm using the weighted sum method (sorted from low to high according to α).

No. α	No. β	RTS IC (%)	RTS SPR (%)	Z_R (s)	Z_c (s)	Z_b (s)	Z_E (kWh)	f (-)	C (%)	α	β
1	205	12.0	9.5	1625.4	720.2	179.8	498.4	5	91.7	455.0	0.8955
2	271	13.0	10.0	1636.0	720.1	179.9	489.9	5	91.7	455.2	0.9319
3	344	14.0	10.5	1646.5	720.1	179.9	479.4	5	91.7	455.3	0.9694
4	116	10.5	8.5	1607.5	720.2	179.8	520.8	5	91.7	456.2	0.8389
5	152	13.0	9.0	1614.9	720.6	179.4	510.6	5	91.7	456.7	0.8624
6	44	8.0	7.5	1583.2	721.5	178.5	545.2	5	91.9	460.4	0.7741
7	68	9.0	8.0	1593.7	721.8	178.2	532.9	5	91.9	460.7	0.8028
8	25	7.0	7.0	1572.6	721.4	178.6	558.6	5	91.9	460.7	0.7489
9	197	11.5	9.5	1622.2	722.1	177.9	501.4	5	92.0	461.0	0.8905
10	414	14.5	11.0	1653.9	722.0	178.0	473.1	5	92.0	461.7	1.0020

Legend: α = weighted sum, β = standardized Euclidean distance, IC = Intercity, SPR = Sprinter, RTS = running time supplements, Z_R = minimum running time objective, Z_c = minimum extended cycle time objective, Z_b = maximum buffer time objective, Z_E = minimum energy consumption objective, f = frequency of IC-SPR cycles per hour, C = capacity consumption.

Table 6.5: First 10 Pareto-optimal solutions with 60 s minimum buffer time considering the objectives total running time Z_R, extended cycle time Z_c, buffer time Z_b and energy consumption Z_E for the real-world case Ah-Nm using the weighted sum method (sorted from low to high according to α).

No. α	No. β	RTS IC (%)	RTS SPR (%)	Z_R (s)	Z_c (s)	Z_b (s)	Z_E (kWh)	f (-)	C (%)	α	β
1	205	12.0	9.5	1625.4	720.2	299.8	498.4	4	86.7	141.5	0.8955
2	271	13.0	10.0	1636.0	720.1	299.9	489.9	4	86.7	141.6	0.9319
3	344	14.0	10.5	1646.5	720.1	299.9	479.4	4	86.7	141.7	0.9694
4	116	10.5	8.5	1607.5	720.2	299.8	520.8	4	86.7	142.6	0.8389
5	152	13.0	9.0	1614.9	720.6	299.4	510.6	4	86.7	143.1	0.8624
6	44	8.0	7.5	1583.2	721.5	298.5	545.2	4	86.8	146.9	0.7741
7	68	9.0	8.0	1593.7	721.8	298.2	532.9	4	86.9	147.2	0.8028
8	25	7.0	7.0	1572.6	721.4	298.6	558.6	4	86.8	147.2	0.7489
9	197	11.5	9.5	1622.2	722.1	297.9	501.4	4	86.9	147.5	0.8905
10	414	14.5	11.0	1653.9	722.0	298.0	473.1	4	86.9	148.2	1.0020

Legend: α = weighted sum, β = standardized Euclidean distance, IC = Intercity, SPR = Sprinter, RTS = running time supplements, Z_R = minimum running time objective, Z_c = minimum extended cycle time objective, Z_b = maximum buffer time objective, Z_E = minimum energy consumption objective, f = frequency of IC-SPR cycles per hour, C = capacity consumption.

only the total running time is influenced by including the energy consumption in the multiple-objective optimization.

First, we focus on the main results for the single objectives. Basically, optimizing for the different single objectives leads to different results. The MTTC driving strategy gives the optimal timetable considering the total running times. Homogenization by increasing the running times of the SPR and decreasing the running times of the IC leads to the optimal solution for minimizing the extended cycle time, which also results into the highest buffer times (if the frequency remains the same). Minimizing the total traction energy consumption leads to maximum amount of running time supplements for the EETC driving strategy of both IC and SPR.

Second, the main results regarding the interaction between the different single objectives indicates the clear linear balancing relationship between the extended cycle time and the buffer time. There is also a balancing relationship between the objectives of total running time and energy consumption. The interaction with the other objectives depends for the IC or SPR whether it is balancing or reinforcing.

Third, in order to apply the weighted sum method, we defined the scaling and weight factors. The result indicate that the average ratio between the extended cycle time and total running time, and between the total buffer time and total running time can be used as scaling factor, where the the total running time is the reference (scaling factor 1). In addition, the sensitivity analysis indicates that the scaling factor 1 for the total energy consumption leads to the best balanced optimal results given the practical constraint of at least 8% running time supplements for each train. We also applied a sensitivity analysis for the weight factors and found that equal weight factors for all objectives leads to the best balanced results, because the objective values were already scaled. Finally, we did a sensitivity analysis for the weight factors of extended cycle time and energy consumption, which indicates that the extended cycle time varies limited. Only by excluding the objectives of total running time and total buffer time, we found that the extended cycle time (and thus the infrastructure occupation) varies for different weight factors and that there is a balancing relationship between the extended cycle time and total energy consumption.

Fourth, the main results regarding the multiple objectives show that only the objective of total running time is influenced by including the objective of total energy consumption in the multiple-objective optimization (i.e., the extended cycle time and buffer time remain the same). The results also indicates that (considering the three objectives of total running time, extended cycle time and buffer time) there is only a trade-off between the extended cycle time (and thus frequency) and the buffer time (i.e., the total running time remain the same). In addition, the results show that changing the minimum buffer time does not influence the optimal

results (only changes the extended cycle time and total buffer time). Finally, the results of the weighted sum and standard Euclidean distance method are different when all four objectives are considered. This is caused by the the fact that the weighted sum method includes scaling of the different single objectives, which is not considered for the standard Euclidean distance method.

6.5 Conclusions

We considered the topic of energy-efficient train timetabling by investigating the multiple-objective optimization problem for a cyclic pattern of trains on a railway line. The aim was to minimize the total running time, the infrastructure occupation (by the extended cycle time) and energy consumption and to maximize the robustness (by the total buffer time) of the timetable, while guaranteeing a conflict-free timetable using the blocking time theory. We introduced the term extended cycle time that expanded the cycle time with a fixed minimum buffer time that is commonly applied by railway undertakings and infrastructure managers to cope with robustness. We investigated the effect of including energy consumption to the multiple-objective timetable optimization problem of total running time, infrastructure occupation and robustness.

We used a constructive brute force search algorithm in order to determine the optimal objective values. We first computed the different driving strategies including the blocking times by varying the running time supplements for all trains. Then we applied the timetable compression method to compute the minimum extended cycle time and the buffer time between each train cycle. Thus, we computed the single objective values for the total running time, extended cycle time, buffer time and energy consumption, using the given amount of running times of the trains. Finally, we used two different methods to compute the multiple-objective solution: the weighted sum and the standard Euclidean distance method. The methods used in this chapter basically transform the multiple-objective optimization functions into a single objective function. Future research will focus on different methods to solve the multiple-objective optimization problem directly by determining the Pareto frontier instead of a single Pareto optimal solution, such as the ε-constraint method (Yan et al., 2019).

We applied the methods to a real-world case study on the Dutch railway corridor with alternating Intercity and Sprinter train services without intermediate overtaking. There is a clear linear balancing relationship between the extended cycle time and buffer time, which indicates that an increase in the extended cycle time leads to a decrease in the buffer time. In addition, we found a balancing relationship between the total running time and energy consumption without influencing the infrastructure occupation and robustness. We also observed a balancing

relationship between the extended cycle time and total energy consumption. Finally, we found that changing the minimum buffer time does not influence the optimal solution.

We conclude that taking energy consumption into account is a good method for RUs to balance total running time without affecting capacity and robustness. Including energy consumption into the multiple objective optimization problem leads to timetables with at least the minimum requested amount of supplements for each train. In addition, realistic speed profiles are generated during timetable design when the minimization of the energy consumption is considered, which is necessary for the implementation of the speed profile in a DAS or ATO. RUs should note that minimizing the infrastructure occupation results into homogenization, which leads to limited running time supplements for the slowest train, while high amount of running time supplements are allocated to the fastest train. Minimizing the cycle times enables RUs to increase the frequency of trains, but this reduces the total buffer time. Moreover, RUs should consider timetable optimization instead of manual timetable design to improve the quality of the timetable or to evaluate different scenarios.

In this chapter we focused on changing the extended cycle time by influencing the running times. The extended cycle time can also be improved by including overtaking possibilities for the IC, skipping stops for the SPR or changing the rolling stock formation. Future research will focus on the effect of these measures on the results of the multiple-objective optimization.

Regenerative braking can lead to extra energy savings and can reduce the power peak supply around stations, but can also influence the trade-off with the other three objectives. Therefore, future research will focus on synchronizing accelerating and regenerative braking trains by including the transmission of regenerated energy over the power supply system in the multiple-objective optimization problem.

Finally, we applied an integrated approach for the multiple-objective timetable optimization problem. However, this approach increases the complexity of the model. In addition, the results also indicated relationships between mainly two objectives (with limited effect on the other objectives). Therefore, similar to Goverde et al. (2016), future research could focus on a sequential approach to solve the problem, while still approaching the optimal solution. However, instead of considering the energy consumption after the other objectives, the sequential approach could start by first optimizing both the objectives of total running time and energy consumption. Afterwards, the infrastructure occupation and robustness can be optimized, given constraints regarding the total running time and energy consumption.

Chapter 7

Conclusions

This thesis developed models for computing energy-efficient train trajectories and incorporating energy-efficient train driving into timetabling. It answers the research question of the Netherlands Railways (NS) to investigate the possibilities to incorporate energy-efficient train driving into the timetable design process (*energy-efficient train timetabling* (*EETT*)). Energy-efficient train trajectory optimization optimizes the use of the actual *running time supplements* to improve on-time and energy-efficient train driving and thus contributes to increasing timetable robustness, and decreasing energy costs and CO_2 emissions. Several models and algorithms have been developed and applied on various cases in this thesis in order to compute the energy-optimal driving strategy, the distribution of the running time supplements between successive train stops, and a balanced multiple-objective conflict-free timetable. This chapter gives the conclusions and recommendations.

The main findings are discussed in Section 7.1. This research also led to recommendations for practice that are presented in Section 7.2. Finally, recommendations for future research are considered in Section 7.3.

7.1 Main findings

This subsection answers the research questions as given in Chapter 1, which supports the final aim of this thesis.

Energy-efficient train control

To arrive at the effect of including energy-efficient train driving in timetabling, it is first needed to determine the energy-optimal driving strategy which is discussed by answering the first research question (Chapter 2). *How can the optimal driving strategy be determined that minimizes total traction energy consumption?*

The energy-optimal driving strategy depends on the timetable and the infrastructure, such as the available running time, track length, varying speed limits and varying gradients. Chapters 2 and 3 gave the theoretical background about the energy-optimal driving strategy and Chapter 2 also provided a thorough literature review on this topic. This driving strategy can be derived using optimal control theory, which leads to the *energy-efficient train control* (*EETC*) problem. The EETC problem consists of an objective function that minimizes total traction energy consumption subject to a number of constraints. These constraints consist of dynamic equations, describing the differential equations of time and speed over distance, and inequality (path) and terminal constraints for the state and control variables. The optimal control structure (i.e., the driving regimes) is derived using *Pontryagin's Maximum Principle* (*PMP*). According to this principle the Hamiltonian associated to the optimal control problem should be maximized. By applying the Karush-Kuhn-Tucker conditions on the augmented Hamiltonian, the necessary optimality conditions are derived. The main *driving regimes* with mechanical braking only or constant-bounded regenerative braking only are: maximum acceleration, cruising at an optimal speed, coasting by rolling without traction, and maximum braking. Next, efficient algorithms are used in order to solve this optimal control problem, which can be classified into indirect solutions methods, direct solution methods and heuristics. The result is an optimal sequence of driving regimes and their switching points. In this thesis a pseudospectral (direct) method was used to solve the optimal control problem. The advantage of this method compared to the indirect method that solves the derived PMP necessary optimality conditions, is that no prior knowledge about the optimal control structure is necessary. Next to the states and controls, pseudospectral methods provide approximations of the costates and Hamiltonian. This enables verification of the pseudospectral results with the necessary optimality conditions derived from PMP.

Including nonlinear regenerative braking in the energy-optimal strategy

One of the driving regimes for the energy-optimal driving strategy is braking. Trains can nowadays apply mechanical and regenerative braking. The type of braking influences the structure of the energy-optimal driving strategy. Research question 2 discusses the differences between them. *How can nonlinear regenerative braking be included in the energy-optimal driving strategy?* Regenerative braking is commonly modelled in literature with a constant braking rate without mechanical braking. However, in practice regenerative braking depends on the maximum regenerative braking force and the regenerative braking power of the train, which results in a nonlinear regenerative braking-speed diagram. In addition, mechanical braking is also applied to compensate the limits of regenerative

braking. In Chapter 3 nonlinear regenerative braking and mechanical braking are included in the EETC problem formulation by extra constraints for both nonlinear regenerative braking (maximum regenerative braking force and maximum regenerative power) and mechanical braking. Afterwards, the optimal control structure and the necessary optimality conditions are derived. The solution to the EETC with nonlinear regenerative and mechanical braking extends the two driving regimes of cruising by partial braking and maximum braking into cruising by partial regenerative braking, cruising by maximum regenerative braking plus partial mechanical braking, maximum regenerative braking, and maximum braking with both maximum regenerative and mechanical braking. To determine the effects of regenerative braking on EETC different algorithms were developed in MATLAB which were implemented in the prototype PROMO. The algorithms are based on a multiple-phase Radau pseudospectral method by using the GPOPS toolbox in MATLAB. PROMO computes different driving strategies such as the EETC with different braking behavior.

The main effects of regenerative braking on EETC are that regenerative braking leads to higher energy savings compared to mechanical braking and that the optimal driving strategy is different. Chapter 3 indicated that higher energy savings can be achieved, because the train generates energy during braking. This regenerated energy can be used by the train itself or fed back to the catenary system for surrounding trains. The effects of regenerative braking mainly depend on the efficiency of the catenary system, of the traction and regenerative braking efficiency of the trains, and the total distance towards the surrounding train. EETC with regenerative braking has a lower cruising speed, a shorter coasting regime, and a higher speed at the beginning of the braking regime compared to EETC with mechanical braking. Other than assuming a constant regenerative braking rate, nonlinear bounded regenerative braking considers a nonlinear function of speed similar to a reversed nonlinear traction-speed diagram. This results in lower energy savings for nonlinear regenerative braking compared to constant regenerative braking and an optimal driving strategy with a higher cruising speed, shorter coasting, and a longer braking regime for nonlinear bounded regenerative braking. A constant regenerative braking rate as commonly used in literature is an unrealistic assumption, and, therefore, existing models based on that assumption overestimate the effect of regenerative braking.

Improving existing train driving strategies to minimize energy consumption

Different driving strategies are applied in practice. However, the relationship between the energy-optimal driving strategy and other strategies has not been investigated. Therefore, the differences are considered by answering the third research question. *How can existing train driving strategies be improved to minimize*

energy consumption? In this thesis the energy-efficient train control driving strategy was compared with a coasting strategy (*maximal coasting*, *MC*) and a cruising strategy (*reduced maximum speed*, *RMS*) that are often applied in practice. We derived the optimal control problems for the MC and RMS driving strategy, and, we compared these driving strategies with the energy-optimal (EETC) driving strategy on different evaluation criteria. We showed how the existing driving strategies MC and RMS can be improved regarding minimizing total energy consumption. The different driving strategies were implemented in the prototype PROMO. The EETC driving strategy optimizes both the cruising speed and the coasting regime in order to minimize total traction energy consumption, which leads to the lowest total traction energy consumption. The other driving strategies are based on only finding an optimal cruising speed (without coasting) or the optimal coasting point with the fixed maximum speed as cruising speed, which are easier to apply by the train driver (lower workload). Chapter 4 showed that the MC strategy leads in general to higher energy savings compared to the RMS strategy. Furthermore, for short stop spacing (e.g., 5 km) the MC driving strategy is equal to the EETC driving strategy when the optimal cruising speed cannot be reached within the given time. For long stop spacing (e.g., 50 km) the other driving strategies can be improved by including both an optimal cruising speed (below the speed limit) and coasting. Note that a driver advisory system is necessary to follow the energy-optimal speed profile by a train driver. Without a DAS the MC driving strategy can approach the energy-optimal solution and is easier to apply in practice by a train driver.

Optimal running time supplement distribution for energy-efficient train driving of a single train over multiple stops

Energy-efficient train driving can be incorporated into timetabling by finding the optimal distribution of running time supplements for a complete train trajectory over a train line. The fourth research question gives answers about this distribution which leads to energy-efficient timetable design principles. *How can the optimal distribution of running time supplements be determined to optimize energy-efficient driving of a train over multiple stops along the line?* The EETC problem for a single train over multiple stops was formulated and the optimal control structure and the necessary optimality conditions were derived. The algorithms of PROMO solved the EETC problem and determined the optimal distribution of the running time supplements between all stops. The results in Chapter 5 showed (similar to Howlett (2016)) that if multiple stops are considered for a single train, the optimal cruising speed between the stops should be equal. In addition, the shorter the distance between stops, the larger the relative running time supplement which is added insight compared to current literature. Gradients influence the distribution

of the running time supplements. Relatively more running time supplements are allocated at downhill sections than uphill sections, because less traction is used at these gradients.

Including energy-efficient train driving in timetable optimization

Past research on timetable optimization focused on the objectives of total travel time, infrastructure occupation and robustness, while energy-efficient train driving is generally not considered during the timetable design. Research question 5 gives answers for EETT by considering the running time supplements and buffer times between trains. *How can energy-efficient train driving be included in timetable optimization considering multiple objectives?* This research question also contributes to the final aim of this thesis (Chapter 1): *the aim of this thesis is to incorporate energy-efficient train driving into timetable design.* A multiple-objective optimization timetabling problem is formulated in Chapter 6 considering the total running time, infrastructure occupation, robustness and energy consumption based on train trajectories computed by the the EETC. Our contribution to literature is that we consider microscopic timetable optimization and we include the objective of energy consumption upfront as one of the objectives to optimize. A brute force search algorithm was applied in order to determine the various objective values for a conflict-free timetable based on blocking times. The driving strategies and the resulting blocking times are computed by the algorithms of PROMO. Afterwards, the weighted sum method and the standard Euclidean distance method were used to compute an optimal solution. Experiments indicated that there is a balancing (negative) relationship between the total running time and energy consumption without influencing the infrastructure occupation and robustness. This means that an increase in the total running time leads to a decrease in the total energy consumption and vice versa. Therefore, a balanced trade-off between the total running time and infrastructure occupation can be achieved by including energy consumption into the multiple-objective optimization problem.

7.2 Recommendations for practice

This thesis has led to five practical recommendations that can be applied during real-time train operation and/or timetable design. The practical recommendations are as follows:

1. The actual optimal driving strategy depends on the weight factors used by railway undertakings for each different *KPI* (*key performance indicator*). Therefore, RUs can use the developed KPI toolbox to determine their preferred driving strategy.

2. Railway undertakings should first focus on determining the optimal cruising speed and coasting regimes, and second on optimizing the regenerative braking energy, because the energy savings by focusing only on optimizing the cruising speed and coasting regime are larger compared to only focusing on regenerative braking. In addition, a surrounding train should be present that needs the regenerated energy, or otherwise this energy is lost due to conversion into heat (i.e., energy loss) by the train resistors.

3. The speed profile of the scheduled running times should be considered during timetable design. The speed profile enables timetable planners to determine a realistic timetable for train drivers. In addition, this enables train drivers to better follow the scheduled timetable and thus reduce the fluctuations of the running times.

4. For incorporating energy-efficient train driving in timetable design, relatively more running time supplements should be allocated to shorter distances, because this leads to the highest energy savings. In addition, the optimal cruising speed between stops should be the same for trains that apply the EETC driving strategy. The established practice of a running time supplement based on a percentage of the minimum running time does not lead to energy-optimal timetables. Advanced optimization algorithms could be applied by RUs in order to derive the optimal distribution of the running time supplement for energy-efficient train driving.

5. Infrastructure managers (IMs) and RUs can incorporate multiple-objective optimization including energy-efficient train driving in order to balance the optimal timetable between running times and robustness. In addition, optimization might help IMs and RUs to generate and evaluate different timetable variants using different weight factors for different objectives.

7.3 Future research

This thesis has made a first start on the topic of energy-efficient train timetabling. However, the developed models are subject to limitations which need future research in order to improve the quality of the model results. Therefore, this section discusses the recommendations for future research.

A first suggestion for future research is to apply EETT to more complex problems. The problem can gradually be extended by including overtaking and crossing trains on a corridor or even a bigger network. In addition, regenerative braking can be incorporated by including detailed models for the power supply system in order to determine the energy-optimal timetable over a network of

interacting trains. Moreover, these complex problems become more realistic for railway undertakings that might enable them to balance different timetable variants depending on the weight factors used for the multiple-optimization problem.

Second, future research could be focused on the interaction between the timetable (including computed train trajectories) and traffic management, in particular the train path envelopes (TPEs) for *driver advisory systems* (*DASs*) and/or *automatic train operation* (*ATO*). TPEs are input for the DASs and ATO and they are defined as sequences of time windows, that define the earliest and latest time to arrive, departure or pass-by at timetable points. The constraints used in the timetable to determine the TPEs should be consistent with the constraints used in operation, because else the speed advice for the DAS and ATO is unrealistic and might lead to hindrance between trains (i.e., causing yellow and red signal approaches). These constraints consider the signalling and train protection system as well as (real-time) conflict detection.

Third, the actual automatic train protection (ATP) system characteristics should be considered, in addition to the block signalling system, to compute the EETC and the resulting blocking times with more realistic operational braking constraints. This leads to a more realistic train trajectory and timetable which is especially necessary when the output is used for DAS and/or ATO.

Another suggestion for future research is on the topic of validation and calibration of the input data to compute the energy-efficient train control driving strategy. Research and practice are more and more focused on DAS and ATO that can use the EETC driving strategy. However, the quality and stability of the advice depends on its input. In practice most infrastructure and rolling stock characteristics are not validated and calibrated using realization data, but are based on infrastructure drawings or input from a manufacturer of rolling stock. Therefore, research could focus on methods to validate and calibrate the infrastructure and rolling stock characteristic parameters in order to provide accurate input to compute the optimal driving strategy for a DAS or ATO.

Finally, future research could focus on the combination of energy-efficient train timetabling and rolling stock planning. The energy-efficiency at RUs is not only determined by energy-efficient train driving, but also by the rolling stock composition. The rolling stock influences the performance of trains in terms of the traction and braking control, maximum speed, and train resistance. Moreover, the rolling stock also influences the occupation rate of trains, which is the balance between the number of (expected) passengers in the train and the train capacity. For instance, at NS the traction energy efficiency is computed as kWh per passenger km. This indicator can be influenced by the rolling stock type that affects the energy consumption (such as single/double deck or locomotive hauled/multiple unit train) and by the demand-supply balance of the number of

seats in trains that affects the passenger km. The demand is influenced by the number of passengers per train and supply by the available seating capacity per train. Passenger demand can be influenced by for instance special tickets at reduced cost during off-peak hours (filling empty seats in trains), while the supply can be influenced by for instance decreasing the size of the train composition during off-peak hours (reducing the number of available seats in trains). Therefore, research on a combined optimization of timetable design and rolling stock planning can improve the energy efficiency for railway undertakings.

Appendix A

Infrastructure details

This appendix presents the input used for the case study in Chapter 6. Table A.1 shows the infrastructure data used for the case study in this chapter with information about the gradients, speed limits and signal locations. The details about the rolling stock characteristics are shown in Table A.2 and the timetable characteristics are visualized in Table A.3.

Table A.1: Infrastructure elements and related distance towards station Ah divided into block sections (ProRail, 2020). Legend: speed marker board indicates speed limit by multiplying the value by 10 (km/h), i.e., speed marker board 11 means speed limit of 110 km/h.

Infrastructure element	Distance from Ah (km)	Infrastructure element	Distance from Ah (km)
Station Ah & speed marker board 6 & gradient 0‰	0	Block signal 824	7.981
Entry/exit signal 2104 & speed marker board 8	0.420	Entry/exit signal A822	9.111
Speed marker board 11	0.906	Block signal 822	9.841
Entry/exit signal 2032	1.041	Station Est	10.309
Entry/exit signal 2014	1.621	Speed marker board 13	10.808
Gradient -11.6‰	1.866	Entry/exit signal 404	10.933
Gradient -5.9‰	1.882	Entry/exit signal 408	11.775
Gradient -4.4‰	2.045	Entry/exit signal 444	12.665
Gradient -6.1‰	2.353	Speed marker board 14	12.960
Gradient -2.25‰	2.711	Block signal 810	13.898
Block signal 834	2.807	Gradient 5.0‰	14.311
Gradient 0‰	2.911	Block signal 806	15.221
Speed marker board 14	2.973	Station Nml	16.054
Block signal 830	3.936	Speed marker board 11	16.336
Gradient -3.8‰	4.311	Entry/exit signal 166	16.521
Gradient -5.0‰	4.511	Speed marker board 4	17.656
Block signal 828	5.261	Gradient 0‰	17.211
Station Ahz	5.877	Entry/exit signal 162	17.791
Block signal 826	6.628	Station Nm	18.500
Gradient -2.5‰	6.811	Entry/exit signal 118	18.542
Gradient 0‰	7.211		

Table A.2: Standard rolling stock characteristics (NS, 2020).

Rolling stock characteristic	IC	SPR
Rolling stock type	VIRM-1 XII	FLIRT-HRN IX
Number of coaches/wagons	12 (6+6)	9 (3+3+3)
Train length	324 m	189.6 m
Total train weight	782,000 kg	400,245 kg
Rotating mass factor	1.06	1.08
Maximum traction force	427.8 kN	387.0 kN
Maximum power	4,314.0 kW	4,407.0 kW
Maximum service braking deceleration	0.5 m/s^2	0.5 m/s^2
Traction efficiency	87.5%	90.6%
Maximum allowed speed	140 km/h	140 km/h
Train resistance equation: $r_0 + r_1\ v + r_2\ v^2$		
r_0	5,440.90 N	3,253.82 N
r_1	100.08 Ns/m	525.00 Ns/m
r_2	18.144 Ns^2/m^2	4.239 Ns^2/m^2

Table A.3: Timetable characteristics and blocking time parameters.

Characteristic	Value
Gravitational acceleration g	9.81 m/s^2
Setup time interlocking area	12 s
Setup time open track	0 s
Driver sight and reaction time	9 s
Release time	2 s
Minimum dwell time SPR at intermediate stations	42 s
Minimum buffer time between two trains	30 s

Appendix B

Main results

This appendix presents the tables of the main results of Chapter 6. Table B.1 and Table B.2 focus on the individual results of the IC and SPR train regarding the speed profile and running time supplement distribution. Table B.1 shows the results of the different driving strategies of the IC and SPR by varying the running time supplements. The optimal running time supplement distribution for the SPR over the complete trajectory is shown in Table B.2. Afterwards, the Tables B.3–B.6 are focused on the results of the IC-SPR cycle. Table B.3 shows the total running time per IC-SPR cycle for different running times for the IC and SPR. The extended cycle time for the IC-SPR cycles can be found in Table B.4. The total buffer time for the different IC-SPR cycles is shown in Table B.5. Finally, Table B.6 shows the energy consumption of the different IC-SPR cycles.

Table B.1: Results of the different driving strategies with varying running time supplements of the IC and SPR for the real-world case Ah-Nm.

Scenario	Figure	Trip time (s)	Running time supplements (%)	Energy consumption (kWh)	Energy saving (%)	N	Computation time (s)
Case Ah-Nm IC MTTC	6.4	643.1	0	456.2	0	200	36.8
Case Ah-Nm IC EETC 1%	6.4	649.6	1.0	346.9	24.0	200	53.0
Case Ah-Nm IC EETC 2%	6.4	656.0	2.0	313.2	31.3	200	34.4
Case Ah-Nm IC EETC 3%	6.4	662.4	3.0	286.9	37.1	200	28.0
Case Ah-Nm IC EETC 4%	6.4	668.9	4.0	274.1	39.9	200	29.6
Case Ah-Nm IC EETC 5%	6.4	675.3	5.0	264.3	42.1	200	50.9
Case Ah-Nm IC EETC 6%	6.4	681.7	6.0	255.7	44.0	200	56.2
Case Ah-Nm IC EETC 7%	6.4	688.2	7.0	246.4	46.0	200	48.2
Case Ah-Nm IC EETC 8%	6.4	694.6	8.0	238.9	47.6	200	47.7
Case Ah-Nm IC EETC 9%	6.4	701.0	9.0	232.4	49.1	200	36.0
Case Ah-Nm IC EETC 10%	6.4	707.4	10.0	227.0	50.2	200	61.0
Case Ah-Nm IC EETC 11%	6.4	713.9	11.0	219.5	51.9	200	30.0
Case Ah-Nm IC EETC 12%	6.4	720.3	12.0	212.4	53.4	200	81.5
Case Ah-Nm IC EETC 13%	6.4	726.7	13.0	208.4	54.3	200	43.8
Case Ah-Nm IC EETC 14%	6.4	733.1	14.0	202.6	55.6	200	83.5
Case Ah-Nm IC EETC 15%	6.4	739.6	15.0	196.9	56.8	200	27.7
Case Ah-Nm SPR MTTC	6.5	826.7	0	550.8	0	500	94.5
Case Ah-Nm SPR EETC 1%	6.5	834.9	1.0	449.7	18.4	600	238.4
Case Ah-Nm SPR EETC 2%	6.5	843.1	2.0	410.4	25.5	600	263.6
Case Ah-Nm SPR EETC 3%	6.5	851.4	3.0	381.9	30.7	600	262.0
Case Ah-Nm SPR EETC 4%	6.5	859.6	4.0	360.1	34.6	600	185.5
Case Ah-Nm SPR EETC 5%	6.5	867.9	5.0	341.1	38.1	600	323.3
Case Ah-Nm SPR EETC 6%	6.5	876.2	6.0	325.7	40.9	600	223.2
Case Ah-Nm SPR EETC 7%	6.5	884.5	7.0	312.2	43.3	600	171.9
Case Ah-Nm SPR EETC 8%	6.5	892.7	8.0	300.6	45.4	600	389.6
Case Ah-Nm SPR EETC 9%	6.5	901.0	9.0	291.0	47.2	650	311.4
Case Ah-Nm SPR EETC 10%	6.5	909.2	10.0	281.5	48.9	650	276.3
Case Ah-Nm SPR EETC 11%	6.5	917.5	11.0	273.4	50.4	670	325.2
Case Ah-Nm SPR EETC 12%	6.5	925.8	12.0	264.3	52.0	670	497.4
Case Ah-Nm SPR EETC 13%	6.5	934.1	13.0	256.6	53.4	670	348.7
Case Ah-Nm SPR EETC 14%	6.5	942.3	14.0	249.2	54.8	700	685.9
Case Ah-Nm SPR EETC 15%	6.5	950.6	15.0	242.4	56.0	700	471.3

Legend: N = number of collocation points, IC = Intercity, SPR = Sprinter, MTTC = minimum time train control, EETC = energy-efficient train control.

Table B.2: Optimal running time supplement distribution for SPR for each section of the different real-world case Ah-Nm scenarios.

Scenario	RTS Ah–Ahz (s)	RTS Ahz–Est (s)	RTS Est–Nml (s)	RTS Nml–Nm (s)	RTS speed Ah–Nm (s)	Max. speed Ah–Ahz (km/h)	Max. speed Ahz–Est (km/h)	Max. speed Est–Nml (km/h)	Max. Nml–Nm (km/h)
Case Ah–Nm SPR MTTC	0.0 (0.0%)	0.0 (0.0%)	0.0 (0.0%)	0.0 (0.0%)	0.0 (0.0%)	140.0	140.0	140.0	101.5
Case Ah–Nm SPR EETC 1%	3.0 (1.2%)	2.2 (1.2%)	1.7 (0.8%)	1.3 (0.7%)	8.2 (1.0%)	126.3	134.4	140.0	91.2
Case Ah–Nm SPR EETC 2%	5.8 (2.3%)	4.6 (2.5%)	3.9 (1.8%)	2.2 (1.2%)	16.4 (2.0%)	119.6	129.2	135.9	88.1
Case Ah–Nm SPR EETC 3%	7.5 (3.0%)	7.3 (4.0%)	6.5 (3.0%)	3.4 (1.9%)	24.7 (3.0%)	116.9	124.3	131.8	85.2
Case Ah–Nm SPR EETC 4%	8.9 (3.6%)	10.2 (5.6%)	9.4 (4.3%)	4.5 (2.5%)	32.9 (4.0%)	114.4	120.5	130.0	83.3
Case Ah–Nm SPR EETC 5%	12.1 (4.9%)	12.7 (7.0%)	10.9 (5.0%)	5.4 (3.0%)	41.2 (5.0%)	110.0	117.5	130.0	81.4
Case Ah–Nm SPR EETC 6%	12.9 (5.2%)	15.9 (8.7%)	13.3 (6.2%)	7.4 (4.1%)	49.5 (6.0%)	110.0	114.4	128.7	78.8
Case Ah–Nm SPR EETC 7%	13.2 (5.3%)	18.9 (10.4%)	17.3 (8.0%)	8.4 (4.7%)	57.8 (7.0%)	110.0	111.2	125.6	77.4
Case Ah–Nm SPR EETC 8%	13.3 (5.3%)	22.4 (12.3%)	21.1 (9.7%)	9.3 (5.2%)	66.0 (8.0%)	110.0	108.0	122.9	76.3
Case Ah–Nm SPR EETC 9%	15.3 (6.1%)	24.5 (13.5%)	23.7 (11.0%)	10.8 (6.0%)	74.3 (9.0%)	108.5	106.5	121.4	74.6
Case Ah–Nm SPR EETC 10%	18.1 (7.3%)	26.6 (14.6%)	25.9 (12.0%)	11.9 (6.6%)	82.5 (10.0%)	106.3	104.6	120.0	73.5
Case Ah–Nm SPR EETC 11%	18.3 (7.4%)	27.6 (15.2%)	27.3 (12.6%)	17.6 (9.8%)	90.8 (11.0%)	106.0	103.9	119.2	69.0
Case Ah–Nm SPR EETC 12%	22.5 (9.0%)	30.7 (16.9%)	31.7 (14.7%)	14.2 (7.9%)	99.1 (12.0%)	102.6	101.8	116.9	71.7
Case Ah–Nm SPR EETC 13%	25.7 (10.3%)	33.3 (18.3%)	34.1 (15.8%)	14.3 (8.0%)	107.4 (13.0%)	100.6	100.0	115.6	71.7
Case Ah–Nm SPR EETC 14%	27.8 (11.2%)	35.6 (19.6%)	35.8 (16.6%)	16.3 (9.1%)	115.6 (14.0%)	99.1	98.4	114.7	70.1
Case Ah–Nm SPR EETC 15%	30.5 (12.2%)	37.9 (20.9%)	38.6 (17.9%)	16.9 (9.4%)	123.9 (15.0%)	97.6	97.1	113.4	69.5

Legend: RTS = running time supplement, Max. = maximum, IC = Intercity, SPR = Sprinter, MTTC = minimum time train control, EETC = energy-efficient train control, Ah = Arnhem Central, Ahz = Arnhem South, Est = Elst, Nml = Nijmegen Lent, Nm = Nijmegen.

Table B.3: Total running time (s) per IC-SPR cycle for different running time supplements for the real-world case study Ah-Nm.

Running time supplements	IC 0%	IC 1%	IC 2%	IC 3%	IC 4%	IC 5%	IC 6%	IC 7%	IC 8%	IC 9%	IC 10%	IC 11%	IC 12%	IC 13%	IC 14%	IC 15%
SPR 0%	1469.8	1476.3	1482.7	1489.1	1495.6	1502.0	1508.4	1514.9	1521.3	1527.7	1534.1	1540.6	1547.0	1553.4	1559.8	1566.3
SPR 1%	1478.0	1484.4	1490.9	1497.3	1503.7	1510.1	1516.6	1523.0	1529.4	1535.9	1542.3	1548.7	1555.2	1561.6	1568.0	1574.5
SPR 2%	1486.3	1492.7	1499.1	1505.6	1512.0	1518.4	1524.8	1531.3	1537.7	1544.1	1550.6	1557.0	1563.4	1569.9	1576.2	1582.7
SPR 3%	1494.5	1500.9	1507.4	1513.8	1520.2	1526.7	1533.1	1539.5	1545.9	1552.4	1558.8	1565.2	1571.7	1578.1	1584.5	1591.0
SPR 4%	1502.8	1509.2	1515.6	1522.1	1528.5	1534.9	1541.4	1547.8	1554.2	1560.6	1567.1	1573.5	1579.9	1586.4	1592.7	1599.2
SPR 5%	1511.1	1517.5	1523.9	1530.4	1536.8	1543.2	1549.7	1556.1	1562.5	1569.0	1575.4	1581.8	1588.2	1594.7	1601.0	1607.5
SPR 6%	1519.3	1525.8	1532.2	1538.6	1545.1	1551.5	1557.9	1564.4	1570.8	1577.2	1583.7	1590.1	1596.5	1602.9	1609.3	1615.8
SPR 7%	1527.6	1534.0	1540.5	1546.9	1553.3	1559.7	1566.2	1572.6	1579.0	1585.5	1591.9	1598.3	1604.8	1611.2	1617.6	1624.1
SPR 8%	1535.9	1542.3	1548.7	1555.1	1561.6	1568.0	1574.4	1580.9	1587.3	1593.7	1600.2	1606.6	1613.0	1619.5	1625.8	1632.3
SPR 9%	1544.1	1550.6	1557.0	1563.4	1569.9	1576.3	1582.7	1589.2	1595.6	1602.0	1608.4	1614.9	1621.3	1627.7	1634.1	1640.6
SPR 10%	1552.4	1558.8	1565.2	1571.7	1578.1	1584.5	1591.0	1597.4	1603.8	1610.3	1616.7	1623.1	1629.6	1636.0	1642.3	1648.8
SPR 11%	1560.7	1567.1	1573.5	1579.9	1586.4	1592.8	1599.2	1605.7	1612.1	1618.5	1625.0	1631.4	1637.8	1644.3	1650.6	1657.1
SPR 12%	1568.9	1575.4	1581.8	1588.2	1594.7	1601.1	1607.5	1614.0	1620.4	1626.8	1633.2	1639.7	1646.1	1652.5	1658.9	1665.4
SPR 13%	1577.2	1583.6	1590.1	1596.5	1602.9	1609.4	1615.8	1622.2	1628.7	1635.1	1641.5	1647.9	1654.4	1660.8	1667.2	1673.7
SPR 14%	1585.4	1591.9	1598.3	1604.7	1611.2	1617.6	1624.0	1630.5	1636.9	1643.3	1649.8	1656.2	1662.6	1669.1	1675.4	1681.9
SPR 15%	1593.7	1600.2	1606.6	1613.0	1619.5	1625.9	1632.3	1638.7	1645.2	1651.6	1658.0	1664.5	1670.9	1677.3	1683.7	1690.2

Legend: IC = Intercity, SPR = Sprinter.

Table B.4: Extended cycle time (s) per IC-SPR cycle for different running time supplements for the real-world case study Ah-Nm.

Running time supplements	IC 0%	IC 1%	IC 2%	IC 3%	IC 4%	IC 5%	IC 6%	IC 7%	IC 8%	IC 9%	IC 10%	IC 11%	IC 12%	IC 13%	IC 14%	IC 15%
SPR 0%	670.8	666.1	662.5	659.8	656.8	652.8	648.9	644.5	640.3	635.8	631.9	627.0	622.2	618.4	614.3	609.8
SPR 1%	698.3	693.7	690.9	687.3	684.3	680.4	676.4	671.9	667.9	664.0	660.2	654.5	650.0	645.8	641.7	637.3
SPR 2%	706.5	701.9	699.2	695.6	692.5	688.6	684.7	680.1	676.1	672.2	668.4	662.8	658.3	654.0	649.9	645.6
SPR 3%	714.8	710.2	707.5	703.8	700.8	696.9	692.9	688.4	684.4	680.5	676.7	671.0	666.5	662.3	658.2	653.8
SPR 4%	723.0	718.4	715.7	712.1	709.0	705.1	701.2	696.6	692.6	688.7	684.9	679.3	674.8	670.5	666.4	662.1
SPR 5%	731.3	726.7	724.0	720.3	717.3	713.4	709.4	704.9	700.9	697.0	693.2	687.5	683.0	678.8	674.7	670.3
SPR 6%	739.5	734.9	732.2	728.6	725.5	721.6	717.7	713.2	709.2	705.2	701.5	695.8	691.3	687.0	682.9	678.6
SPR 7%	747.8	743.2	740.5	736.8	733.8	729.9	725.9	721.4	717.4	713.5	709.7	704.0	699.5	695.3	691.2	686.8
SPR 8%	756.0	751.5	748.7	745.1	742.0	738.2	734.2	729.7	725.7	721.8	718.0	712.3	707.8	703.5	699.5	695.1
SPR 9%	764.3	759.7	757.0	753.4	750.3	746.4	742.5	737.9	733.9	730.0	726.2	720.6	716.1	711.8	707.7	703.3
SPR 10%	772.6	768.0	765.3	761.6	758.6	754.7	750.7	746.2	742.2	738.3	734.5	728.8	724.3	720.1	716.0	711.6
SPR 11%	780.7	776.1	773.4	769.8	766.7	762.8	758.9	754.4	750.4	746.4	742.7	737.0	732.5	728.2	724.2	719.8
SPR 12%	789.1	784.5	781.8	778.1	775.1	771.2	767.2	762.7	758.7	754.8	751.0	745.3	740.8	736.6	732.5	728.1
SPR 13%	797.3	792.7	790.0	786.4	783.3	779.4	775.5	770.9	766.9	763.0	759.2	753.6	749.1	744.8	740.7	736.4
SPR 14%	805.6	801.0	798.3	794.6	791.6	787.7	783.7	779.2	775.2	771.3	767.5	761.8	757.3	753.1	749.0	744.6
SPR 15%	813.8	809.2	806.5	802.9	799.8	795.9	792.0	787.5	783.5	779.5	775.8	770.1	765.6	761.3	757.3	752.9

Legend: IC = Intercity, SPR = Sprinter.

Table B.5: Total buffer time (s) including the minimum buffer time (60 s) per IC-SPR cycle for different running time supplements for the real-world case study Ah-Nm. Note that the drop in the buffer time is caused by the frequency increase of the IC-SPR cycle (from 4 to 5 trains per hour).

Running time supplements	IC 0%	IC 1%	IC 2%	IC 3%	IC 4%	IC 5%	IC 6%	IC 7%	IC 8%	IC 9%	IC 10%	IC 11%	IC 12%	IC 13%	IC 14%	IC 15%
SPR 0%	109.2	113.9	117.5	120.2	123.2	127.2	131.1	135.5	139.7	144.2	148.1	153.0	157.8	161.6	165.7	170.2
SPR 1%	81.7	86.3	89.1	92.7	95.7	99.6	103.6	108.1	112.1	116.0	119.8	125.5	130.0	134.2	138.3	142.7
SPR 2%	73.5	78.1	80.8	84.4	87.5	91.4	95.3	99.9	103.9	107.8	111.6	117.2	121.7	126.0	130.1	134.4
SPR 3%	65.2	69.8	72.5	76.2	79.2	83.1	87.1	91.6	95.6	99.5	103.3	109.0	113.5	117.7	121.8	126.2
SPR 4%	237.0	61.6	64.3	67.9	71.0	74.9	78.8	83.4	87.4	91.3	95.1	100.7	105.2	109.5	113.6	117.9
SPR 5%	228.7	233.3	236.0	239.7	62.7	66.6	70.6	75.1	79.1	83.0	86.8	92.5	97.0	101.2	105.3	109.7
SPR 6%	220.5	225.1	227.8	231.4	234.5	238.4	62.3	66.8	70.8	74.8	78.5	84.2	88.7	93.0	97.1	101.4
SPR 7%	212.2	216.8	219.5	223.2	226.2	230.1	234.1	238.6	62.6	66.5	70.3	76.0	80.5	84.7	88.8	93.2
SPR 8%	204.0	208.5	211.3	214.9	218.0	221.8	225.8	230.3	224.3	238.2	62.0	67.7	72.2	76.5	80.5	84.9
SPR 9%	195.7	200.3	203.0	206.6	209.7	213.6	217.5	222.1	226.1	230.0	233.8	239.4	63.9	68.2	72.3	76.7
SPR 10%	187.4	192.0	194.7	198.4	201.4	205.3	209.3	213.8	217.8	221.7	225.5	231.2	235.7	239.9	64.0	68.4
SPR 11%	179.3	183.9	186.6	190.2	193.3	197.2	201.1	205.6	209.6	213.6	217.3	223.0	227.5	231.8	235.8	60.2
SPR 12%	170.9	175.5	178.2	181.9	184.9	188.8	192.8	197.3	201.3	205.2	209.0	214.7	219.2	223.4	227.5	231.9
SPR 13%	162.7	167.3	170.0	173.6	176.7	180.6	184.5	189.1	193.1	197.0	200.8	206.4	210.9	215.2	219.3	223.6
SPR 14%	154.4	159.0	161.7	165.4	168.4	172.3	176.3	180.8	184.8	188.7	192.5	198.2	202.7	206.9	211.0	215.4
SPR 15%	146.2	150.8	153.5	157.1	160.2	164.1	168.0	172.5	176.5	180.5	184.2	189.9	194.4	198.7	202.7	207.1

Legend: IC = Intercity, SPR = Sprinter.

Table B.6: Total traction energy consumption (kWh) per IC-SPR cycle for different running time supplements for the real-world case study Ah-Nm.

Running time supplements	IC 0%	IC 1%	IC 2%	IC 3%	IC 4%	IC 5%	IC 6%	IC 7%	IC 8%	IC 9%	IC 10%	IC 11%	IC 12%	IC 13%	IC 14%	IC 15%
SPR 0%	1007.0	897.7	864.1	837.8	825.0	815.2	806.5	797.2	789.8	783.2	777.8	770.4	763.2	759.3	753.4	747.7
SPR 1%	905.9	796.6	763.0	736.7	723.9	714.1	705.4	696.1	688.6	682.1	676.7	669.3	662.1	658.1	652.3	646.6
SPR 2%	866.6	757.3	723.7	697.4	684.6	674.8	666.1	656.8	649.4	642.8	637.4	630.0	622.8	618.9	613.0	607.3
SPR 3%	838.1	728.8	695.1	668.8	656.0	646.2	637.6	628.3	620.8	614.3	608.9	601.4	594.3	590.3	584.4	578.8
SPR 4%	816.3	706.9	673.3	647.0	634.2	624.4	615.7	604.4	599.0	592.4	587.0	579.6	572.4	568.5	562.6	556.9
SPR 5%	797.3	687.9	654.3	628.0	615.2	605.4	596.7	587.4	580.0	573.4	568.0	560.6	553.4	549.5	543.6	536.9
SPR 6%	781.9	672.6	638.9	612.6	599.8	590.0	581.3	572.1	564.6	558.1	552.6	545.2	538.1	534.1	528.2	522.5
SPR 7%	768.4	659.1	625.5	599.2	586.4	576.6	567.9	558.6	551.2	544.6	539.2	531.8	524.6	520.7	514.8	509.1
SPR 8%	756.8	647.4	613.8	587.5	574.7	564.9	556.2	547.0	539.5	532.9	527.5	520.1	513.0	509.0	503.1	497.4
SPR 9%	747.2	637.9	604.3	578.0	565.2	555.4	546.7	537.4	529.9	523.4	518.0	510.6	503.4	499.4	493.6	487.9
SPR 10%	737.7	628.4	594.7	568.4	555.6	545.8	537.1	527.9	520.4	513.9	508.4	501.0	493.9	489.9	484.0	478.4
SPR 11%	729.6	620.3	586.7	560.4	547.5	537.8	529.1	519.8	512.3	505.8	500.4	493.0	485.8	481.8	476.0	470.3
SPR 12%	720.5	611.2	577.5	551.2	538.4	528.6	520.0	510.7	503.2	496.7	491.3	483.8	476.7	472.7	466.9	461.2
SPR 13%	712.8	603.4	569.8	543.5	530.7	520.9	512.2	502.9	495.5	488.9	483.5	483.5	470.4	466.5	460.6	460.6
SPR 14%	705.4	596.1	562.4	536.1	523.3	513.5	504.9	495.6	488.1	481.6	476.2	468.7	461.6	457.6	451.8	446.1
SPR 15%	698.6	589.3	555.6	529.3	516.5	506.7	498.1	488.8	481.3	474.8	469.3	461.9	454.8	450.8	444.9	439.3

Legend: IC = Intercity, SPR = Sprinter.

Bibliography

Albrecht, A. R., P. G. Howlett, P. J. Pudney (2020) Optimal driving strategies for two successive trains on level track with safe separation, *IEEE Transactions on Intelligent Transportation Systems*, pp. 1–16.

Albrecht, A. R., P. G. Howlett, P. J. Pudney, X. Vu (2013a) Energy-efficient train control: From local convexity to global optimization and uniqueness, *Automatica*, 49(10), pp. 3072–3078.

Albrecht, A. R., P. G. Howlett, P. J. Pudney, X. Vu, P. Zhou (2013b) Using timing windows to allow energy-efficient driving, in: *10th World Congress on Rail Research*.

Albrecht, A. R., P. G. Howlett, P. J. Pudney, X. Vu, P. Zhou (2015) Energy-efficient train control: The two-train separation problem on level track, *Journal of Rail Transport Planning & Management*, 5(3), pp. 163–182.

Albrecht, A. R., P. G. Howlett, P. J. Pudney, X. Vu, P. Zhou (2016a) The key principles of optimal train control−Part 1: Formulation of the model, strategies of optimal type, evolutionary lines, location of optimal switching points, *Transportation Research Part B: Methodological*, 94, pp. 482–508.

Albrecht, A. R., P. G. Howlett, P. J. Pudney, X. Vu, P. Zhou (2016b) The key principles of optimal train control−Part 2: Existence of an optimal strategy, the local energy minimization principle, uniqueness, computational techniques, *Transportation Research Part B: Methodological*, 94, pp. 509–538.

Albrecht, A. R., P. G. Howlett, P. J. Pudney, X. Vu, P. Zhou, D. Chen (2014) Using maximum power to save energy, in: *IEEE 17th International Conference on Intelligent Transportation Systems (ITSC)*, pp. 1205–1208.

Albrecht, T. (2004) Reducing power peaks and energy consumption in rail transit systems by simultaneous train running time control, in: Allen, J., A. Brebbia, R. J. Hill, G. Sciutto, S. Sone, eds., *Computers in Railways IX*, WIT Press, Southampton, UK, pp. 885–894.

Albrecht, T. (2005a) *A contribution to the utilization of Genetic Algorithms for optimal control and planning of a flexible urban rail transport (in German: "Ein Beitrag zur Nutzbarmachung genetischer Algorithmen für die optimale Steuerung und Planung eines flexiblen Stadtschnellbahnbetriebes")*, PhD Thesis, Dresden University of Technology, Germany.

Albrecht, T. (2005b) Energy-efficient train control in suburban railways: experiences gained from onboard tests of a driver assistance system, in: *1st International Seminar on Railway Operations Modelling and Analysis (RailDelft2005)*.

Albrecht, T. (2014) Energy-Efficient Train Operation, in: Hansen, I. A., J. Pachl, eds., *Railway Timetabling & Operations*, chap. 5, Eurailpress, Hamburg, Germany, pp. 91–116.

Albrecht, T., A. Binder, C. Gassel (2013c) Applications of real-time speed control in rail-bound public transportation systems, *IET Intelligent Transport Systems*, 7(3), pp. 305–314.

Albrecht, T., S. Oettich (2002) A new integrated approach to dynamic schedule synchronization and energy-saving train control, in: Allen, J., R. J. Hill, C. A. Brebbia, G. Sciutto, S. Sone, eds., *Computers in Railways VIII*, WIT Press, Southampton, UK, pp. 847–856.

Aradi, S., T. Becsi, P. Gaspar (2013) A predictive optimization method for energy-optimal speed profile generation for trains, in: *2013 IEEE 14th International Symposium on Computational Intelligence and Informatics (CINTI)*, pp. 135–139.

Arboleya, P., C. Mayet, B. Mohamed, J. A. Aguado, S. De la Torre (2020) A review of railway feeding infrastructures: Mathematical models for planning and operation, *eTransportation*, 5, p. 100063.

Asnis, I. A., A. V. Dmitruk, N. P. Osmolovskii (1985) Solution of the problem of the energetically optimal control of the motion of a train by the maximum principle, *USSR Computational Mathematics and Mathematical Physics*, 25(6), pp. 37–44.

Baranov, L. A., I. S. Meleshin, L. M. Chin' (2011) Optimal control of a subway train with regard to the criteria of minimum energy consumption, *Russian Electrical Engineering*, 82(8), pp. 405–410.

Becerra, V. M. (2010) Solving complex optimal control problems at no cost with psopt, in: *2010 IEEE International Symposium on Computer-Aided Control System Design*, pp. 1391–1396.

Benjamin, B. R., A. M. Long, I. P. Milroy, R. L. Payne, P. J. Pudney (1987) Control of railway vehicles for energy conservation and improved timekeeping, in: *Conference on Railway Engineering 4th edition 1987*, pp. 41–47.

Benjamin, B. R., I. P. Milroy, P. J. Pudney (1989) Energy-efficient operation of long-haul trains, in: *Fourth International Heavy Haul Railway Conference*, Institution of Engineers, Australia, pp. 369–372.

Bertsekas, D. P. (1999) *Nonlinear Programming*, Athena Scientific, Belmont, MA, USA.

Betts, J. T. (2010) *Practical Methods for Optimal Control and Estimation Using Nonlinear Programming*, Advances in Design and Control, SIAM, Philadelphia, PA, USA.

Bešinović, N., R. M. P. Goverde (2018) Capacity assessment in railway networks, in: Borndörfer, R., T. Klug, L. Lamorgese, C. Mannino, M. Reuther, T. Schlechte, eds., *Handbook of Optimization in the Railway Industry*, Springer International Publishing, Cham, Switzerland, pp. 25–45.

Bešinović, N., R. M. P. Goverde, E. Quaglietta (2017) Microscopic models and network transformations for automated railway traffic planning, *Computer-Aided Civil and Infrastructure Engineering*, 32(2), pp. 89–106.

Bešinović, N., R. M. P. Goverde, E. Quaglietta, R. Roberti (2016) An integrated micro–macro approach to robust railway timetabling, *Transportation Research Part B: Methodological*, 87, pp. 14–32.

Binder, A., T. Albrecht (2013) Timetable evaluation and optimization under consideration of the stochastical influence of the dwell times, in: *Proceedings of the 3rd International Conference on Models and Technologies for Intelligent Transportation Systems 2013*, pp. 471–481.

Brünger, O., E. Dahlhaus (2014) Running time estimation, in: Hansen, I. A., J. Pachl, eds., *Railway Timetabling & Operations*, Eurailpress, Hamburg, Germany, pp. 65–89.

BS-EN-15663 (2017) Railway applications - vehicle reference masses, Tech. rep., BSI Group.

Cacchiani, V., L. Galli, P. Toth (2015) A tutorial on non-periodic train timetabling and platforming problems, *EURO Journal on Transportation and Logistics*, 4(3), pp. 285–320.

Cacchiani, V., D. Huisman, M. Kidd, L. G. Kroon, P. Toth, L. P. Veelenturf, J. C. Wagenaar (2014) An overview of recovery models and algorithms for real-time railway rescheduling, *Transportation Research Part B: Methodological*, 63, pp. 15–37.

Cacchiani, V., P. Toth (2012) Nominal and robust train timetabling problems, *European Journal of Operational Research*, 219(3), pp. 727–737.

Caprara, A., L. G. Kroon, M. Monaci, M. Peeters, P. Toth (2007) *Chapter 3 Passenger Railway Optimization*, vol. 14, Elsevier, pp. 129–187.

Chang, C. S., S. S. Sim (1997) Optimising train movements through coast control using genetic algorithms, *Electric Power Applications, IEE Proceedings*, 144(1), pp. 65–73.

Cheng, J. (1997) *Analysis of Optimal Driving Strategies for Train Control Problems*, PhD Thesis, University of South Australia, Adelaide, Australia.

Cheng, J., P. G. Howlett (1992) Application of critical velocities to the minimisation of fuel consumption in the control of trains, *Automatica*, 28(1), pp. 165–169.

Cheng, J., P. G. Howlett (1993) A note on the calculation of optimal strategies for the minimization of fuel consumption in the control of trains, *IEEE Transactions on Automatic Control*, 38(11), pp. 1730–1734.

Chevrier, R., P. Pellegrini, J. Rodriguez (2013) Energy saving in railway timetabling: A bi-objective evolutionary approach for computing alternative running times, *Transportation Research Part C: Emerging Technologies*, 37, pp. 20–41.

Clements, M., R. Minson, L. Moisio, J. Moll, J. Moore, A. Scott (2011) Eco-driving: understanding the approaches, benefits and risks, Tech. Rep. T839, Rail Safety and Standards Board.

Coleman, D., P. G. Howlett, P. J. Pudney, X. Vu, R. Yee (2010) The Freightmiser driver advice system, in: *Proceedings of the First International Congress on Rail Transport Technology*.

Cucala, A. P., A. Fernández, C. Sicre, M. Domínguez (2012) Fuzzy optimal schedule of high speed train operation to minimize energy consumption with uncertain delays and driver's behavioral response, *Engineering Applications of Artificial Intelligence*, 25(8), pp. 1548–1557.

Davis, W. (1926) The tractive resistance of electric locomotives and cars, *General Electric Review*, 29.

De Jong, M. P. (2019) *RTA manual (in Dutch: "Gebruiksaanwijzing RTA")*, NS, Utrecht, The Netherlands.

Ding, Y., H. Liu, Y. Bai, F. Zhou (2011) A Two-level Optimization Model and Algorithm for Energy-Efficient Urban Train Operation, *Journal of Transportation Systems Engineering and Information Technology*, 11(1), pp. 96–101.

Domínguez, M., A. Fernández, A. P. Cucala, P. Lukaszewicz (2011) Optimal design of metro automatic train operation speed profiles for reducing energy consumption, *Proceedings of the Institution of Mechanical Engineers, Part F: Journal of Rail and Rapid Transit*, 225(5), pp. 463–474.

Domínguez, M., A. Fernández-Cardador, A. P. Cucala, R. R. Pecharromán (2012) Energy savings in metropolitan railway substations through regenerative energy recovery and optimal design of ATO speed profiles, *IEEE Transactions on Automation Science and Engineering*, 9(3), pp. 496–504.

Doran, G. T. (1981) There's a S.M.A.R.T. way to write managements's goals and objectives, *Management Review*, 70(11), pp. 35–36.

EEA (2021) Rail and waterborne — best for low-carbon motorised transport, URL https://www.eea.europa.eu/publications/rail-and-waterborne-transport/rail-and-waterborne-best.

Era (2016) Railway Safety in the European Union 2016. Biennial Report, URL http://www.era.europa.eu/Document-Register/Documents/RailwaySafetyPerformance2016finalE.pdf.

Feng, X., H. Zhang, Y. Ding, Z. Liu, H. Peng, B. Xu (2013) A review study on traction energy saving of rail transport, *Discrete Dynamics in Nature and Society*, 2013, pp. 1–9.

Fernández-Rodríguez, A., A. Fernández-Cardador, A. P. Cucala (2018) Real time eco-driving of high speed trains by simulation-based dynamic multi-objective optimization, *Simulation Modelling Practice and Theory*, 84, pp. 50–68.

Franke, R., P. Terwiesch, M. Meyer (2000) An algorithm for the optimal control of the driving of trains, in: *Proceedings of the 39th IEEE Conference on Decision and Control*, vol. 3, pp. 2123–2128.

Frilli, A., E. Meli, D. Nocciolini, L. Pugi, A. Rindi (2016) Energetic optimization of regenerative braking for high speed railway systems, *Energy Conversion and Management*, 129, pp. 200–215.

Garg, D., M. A. Patterson, W. W. Hager, A. V. Rao, D. A. Benson, G. T. Huntington (2009) An overview of three pseudospectral methods for the numerical solution of optimal control problems, *Advances in the Astronautical Sciences*, 135(1), pp. 475–487.

Ghaviha, N., M. Bohlin, C. Holmberg, E. Dahlquist (2019) Speed profile optimization of catenary-free electric trains with lithium-ion batteries, *Journal of Modern Transportation*, 27(3), pp. 153–168.

Ghaviha, N., M. Bohlin, C. Holmberg, E. Dahlquist, R. Skoglund, D. Jonasson (2017) A driver advisory system with dynamic losses for passenger electric multiple units, *Transportation Research Part C: Emerging Technologies*, 85, pp. 111–130.

Ghoseiri, K., F. Szidarovszky, M. J. Asgharpour (2004) A multi-objective train scheduling model and solution, *Transportation Research Part B: Methodological*, 38(10), pp. 927–952.

Golovitcher, I. M. (2001) Energy efficient control of rail vehicles, in: *IEEE International Conference on Systems, Man, and Cybernetics*, vol. 1, pp. 658–663.

González-Gil, A., R. Palacin, P. Batty (2013) Sustainable urban rail systems: Strategies and technologies for optimal management of regenerative braking energy, *Energy Conversion and Management*, 75, pp. 374–388.

González-Gil, A., R. Palacin, P. Batty, J. P. Powell (2014) A systems approach to reduce urban rail energy consumption, *Energy Conversion and Management*, 80, pp. 509–524.

Goverde, R. M. P., N. Bešinović, A. Binder, V. Cacchiani, E. Quaglietta, R. Roberti, P. Toth (2016) A three-level framework for performance-based railway timetabling, *Transportation Research Part C: Emerging Technologies*, 67, pp. 62–83.

Goverde, R. M. P., F. Corman, A. D'Ariano (2013) Railway line capacity consumption of different railway signalling systems under scheduled and disturbed conditions, *Journal of Rail Transport Planning & Management*, 3(3), pp. 78–94.

Goverde, R. M. P., I. A. Hansen (2013) Performance indicators for railway timetables, in: *2013 IEEE International Conference on Intelligent Rail Transportation Proceedings*, pp. 301–306.

Goverde, R. M. P., G. M. Scheepmaker, P. Wang (2021) Pseudospectral optimal train control, *European Journal of Operational Research*, 292(1), pp. 353–375.

Graffagnino, T., R. Schäfer, M. Tuchschmid, M. Weibel (2019) Energy savings with enhanced static timetable information for train drivers, in: *Rail Norrköping Conference*.

Graffagnino, T., M. Tuchschmid (2019) eco2.0: further development of ADL eco (in German: *"eco2.0: Weiterentwicklung ADL eco"*), Report.

Haahr, J. T., D. Pisinger, M. Sabbaghian (2017) A dynamic programming approach for optimizing train speed profiles with speed restrictions and passage points, *Transportation Research Part B: Methodological*, 99, pp. 167–182.

Horrey, W. J., C. D. Wickens (2004) Driving and Side Task Performance: The Effects of Display Clutter, Separation, and Modality, *Human Factors: The Journal of the Human Factors and Ergonomics Society*, 46(4), pp. 611–624.

Howlett, P. G. (1990) An optimal strategy for the control of a train, *The ANZIAM Journal*, 31(04), pp. 454–471.

Howlett, P. G. (1996) Optimal strategies for the control of a train, *Automatica*, 32(4), pp. 519–532.

Howlett, P. G. (2000) The optimal control of a train, *Annals of Operations Research*, 98(1), pp. 65–87.

Howlett, P. G. (2016) A new look at the rate of change of energy consumption with respect to journey time on an optimal train journey, *Transportation Research Part B: Methodological*, 94, pp. 387–408.

Howlett, P. G., I. P. Milroy, P. J. Pudney (1994) Energy-efficient train control, *Control Engineering Practice*, 2(2), pp. 193–200.

Howlett, P. G., P. J. Pudney (1995) *Energy-Efficient Train Control*, Springer, London, UK.

Howlett, P. G., P. J. Pudney, X. Vu (2008) Freightmiser: an energy-efficient application of the train control problem, in: *30th conference of Australian Institutes of Transport Research (CAITR)*.

Howlett, P. G., P. J. Pudney, X. Vu (2009) Local energy minimization in optimal train control, *Automatica*, 45(11), pp. 2692–2698.

IAE, UIC (2014) *Railway Handbook 2014*, Paris, France.

Ichikawa, K. (1968) Application of optimization theory for bounded state variable problems to the operation of train, *Bulletin of JSME*, 11(47), pp. 857–865.

Isayev, I. P. (1987) *Electric Traction Theory (in Russian: "Teoriya Electricheskoy Tyagi")*, vol. 3rd edition, Moscow, Soviet Union.

Jaekel, B., T. Albrecht (2013) Interfacing conflict resolution and driver advisory systems in railway operations, in: *Proceedings of the 3rd International Conference on Models and Technologies for Intelligent Transportation Systems 2013*, TUDpress, pp. 333–343.

Jensen, L. W., A. Landex, O. A. Nielsen, L. G. Kroon, M. Schmidt (2017) Strategic assessment of capacity consumption in railway networks: Framework and model, *Transportation Research Part C: Emerging Technologies*, 74, pp. 126–149.

Kent, S. (2009) Driver advisory information for energy management and regulation Stage 1 Report - Appendices, Report, DeltaRail.

Khmelnitsky, E. (2000) On an optimal control problem of train operation, *IEEE Transactions on Automatic Control*, 45(7), pp. 1257–1266.

Kroon, L. G., D. Huisman, G. Maróti (2014) Optimisation models for railway timetabling, in: Hansen, I. A., J. Pachl, eds., *Railway Timetabling & Operations*, book section 8, Eurailpress, Hamburg, Germany, pp. 155–173.

Lechelle, S. A., Z. S. Mouneimne (2010) OptiDrive: A practical approach for the calculation of energy-optimised operating speed profiles, in: *IET Conference on Railway Traction Systems (RTS 2010)*, pp. 1–8.

Lejeune, A., R. Chevrier, P. Vandanjon, J. Rodriguez (2016) Towards eco-aware timetabling: evolutionary approach and cascading initialisation strategy for the bi-objective optimisation of train running times, *IET Intelligent Transport Systems*, 10(7), pp. 483–494.

Lewis, F. L., D. L. Vrabie, V. L. Syrmos (2012) *Optimal Control*, John Wiley & Sons, Hoboken, NJ, USA.

Li, X., H. K. Lo (2014a) An energy-efficient scheduling and speed control approach for metro rail operations, *Transportation Research Part B: Methodological*, 64, pp. 73–89.

Li, X., H. K. Lo (2014b) Energy minimization in dynamic train scheduling and control for metro rail operations, *Transportation Research Part B: Methodological*, 70, pp. 269–284.

Li, X., D. Wang, K. Li, Z. Gao (2013) A green train scheduling model and fuzzy multi-objective optimization algorithm, *Applied Mathematical Modelling*, 37(4), pp. 2063–2073.

Liu, R. R., I. M. Golovitcher (2003) Energy-efficient operation of rail vehicles, *Transportation Research Part A: Policy and Practice*, 37(10), pp. 917–932.

Lu, S., S. Hillmansen, T. K. Ho, C. Roberts (2013) Single-train trajectory optimization, *IEEE Transactions on Intelligent Transportation Systems*, 14(2), pp. 743–750.

Lu, S., P. Weston, S. Hillmansen, H. B. Gooi, C. Roberts (2014) Increasing the regenerative braking energy for railway vehicles, *IEEE Transactions on Intelligent Transportation Systems*, 15(6), pp. 2506–2515.

Luan, X., Y. Wang, B. De Schutter, L. Meng, G. Lodewijks, F. Corman (2018a) Integration of real-time traffic management and train control for rail networks - part 1: Optimization problems and solution approaches, *Transportation Research Part B: Methodological*, 115, pp. 41–71.

Luan, X., Y. Wang, B. De Schutter, L. Meng, G. Lodewijks, F. Corman (2018b) Integration of real-time traffic management and train control for rail networks - part 2: Extensions towards energy-efficient train operations, *Transportation Research Part B: Methodological*, 115, pp. 72–94.

Luijt, R. S., M. P. F. van den Berge, H. Y. Willeboordse, J. H. Hoogenraad (2017) 5 years of dutch eco-driving: Managing behavioural change, *Transportation Research Part A: Policy and Practice*, 98, pp. 46–63.

Lusby, R. M., J. Larsen, S. Bull (2018) A survey on robustness in railway planning, *European Journal of Operational Research*, 266(1), pp. 1–15.

Lusby, R. M., J. Larsen, M. Ehrgott, D. Ryan (2011) Railway track allocation: models and methods, *OR Spectrum*, 33(4), pp. 843–883.

Marler, R. T., J. S. Arora (2004) Survey of multi-objective optimization methods for engineering, *Structural and Multidisciplinary Optimization*, 26(6), pp. 369–395.

Mills, R. G. J., S. E. Perkins, P. J. Pudney (1991) Dynamic rescheduling of long-haul trains for improved timekeeping and energy conservation, *Asia Pacific Journal of Operational Research*, 8(2), pp. 146–165.

Milroy, I. P. (1980) *Aspects of Automatic Train Control*, Phd thesis, Loughborough University, Loughborough, UK.

Ministerie van Infrastructuur en Milieu (2012) Reken- en meetvoorschrift geluid (in Dutch), report.

National Geographic (2017) Effects of Global Warming, URL http://www.nationalgeographic.com/environment/global-warming/global-warming-effects/.

NS (2020) *TreinPlein*, https://treinplein.net.

Oettich, S., T. Albrecht (2001) A contribution of resource-saving and connection-optimizing flexibility of the S-Bahn operation (in German: *"Ein Beitrag zur ressourcenschonenden und anschlussoptimierenden Flexibilisierung des S-Bahn-Betriebes"*), in: *18. Verkehrswissenschaftliche Tage (TU) Dresden*.

Olsson, N. O. E., H. Haugland (2004) Influencing factors on train punctuality - results from some Norwegian studies, *Transport Policy*, 11(4), pp. 387–397.

ON-TIME (2013) Assessment of State-of-Art of Driver Advice Systems, Report Task 6.1, ON-TIME project.

ON-TIME (2014a) DAS on-board algorithms, Report D6.3, ON-TIME project.

ON-TIME (2014b) Methods and algorithms for the development of robust and resilient timetables, Report D3.1, ON-TIME project.

Pachl, J. (2009) *Railway Operation and Control*, VTD Rail Publishing, Mountlake Terrace, WA, USA.

Pachl, J. (2014) Timetable design principles, in: Hansen, I. A., J. Pachl, eds., *Railway Timetabling & Operations*, Eurailpress, Hamburg, Germany, pp. 13–46.

Panou, K., P. Tzieropoulos, D. Emery (2013) Railway driver advice systems: Evaluation of methods, tools and systems, *Journal of Rail Transport Planning and Management*, 3(4), pp. 150–162.

Peña-Alcaraz, M., A. Fernandéz, A. Cucala, A. Ramos, R. R. Pecharromán (2012) Optimal underground timetable design based on power flow for maximizing the use of regenerative-braking energy, *Proceedings of the Institution of Mechanical Engineers, Part F: Journal of Rail and Rapid Transit*, 226(4), pp. 397–408.

Pengyu, W., W. Qingnian, Wangwei, Z. Naiwei (2009) The affect of motor efficiency on regenerative braking at low-speed stage, in: *2009 International Conference on Energy and Environment Technology*, vol. 1, pp. 388–391.

Pontryagin, L. S., V. G. Boltyanskii, R. V. Gamkrelidze, E. F. Mishchenko (1962) *The Mathematical Theory of Optimal Processes*, Wiley, Hoboken, NY, USA.

ProRail (2016) Network statement 2018.

ProRail (2020) *RailDocs*, https://www.raildocs.nl/raildocs/tekeningen.

Pudney, P. J., P. G. Howlett (1994) Optimal driving strategies for a train journey with speed limits, *Journal of the Australian Mathematical Society, Series B*, 36, pp. 38–49.

Pudney, P. J., C. Stolz, P. Campbell (2009) Using energy-efficient journeys and ARTC to calculate section running times, in: *AusRAIL PLUS 2009*.

Qu, J., X. Feng, Q. Wang (2014) Real-time trajectory planning for rail transit train considering regenerative energy, in: *IEEE 17th International Conference on Intelligent Transportation Systems (ITSC 2014)*, pp. 2738–2742.

Radtke, A. (2014) Infrastructure modelling, in: Hansen, I. A., J. Pachl, eds., *Railway Timetabling & Operations*, Eurailpress, Hamburg, Germany, pp. 47–63.

Rao, A. V. (2014) Trajectory optimization: A survey, in: Waschl, H., I. Kolmanovsky, M. Steinbuch, L. del Re, eds., *Optimization and Optimal Control in Automotive Systems*, Springer, Cham, Germany, pp. 3–21.

Rao, A. V., D. Benson, C. Darby, B. Mahon, C. Francolin, M. A. Patterson, I. Sanders, G. T. Huntington (2011) User's Manual for GPOPS Version 4.x: A MATLAB Software for Solving Multiple-Phase Optimal Control Problems Using hp-Adaptive Pseudospectral Methods, Report.

Rao, A. V., D. A. Benson, C. Darby, M. A. Patterson, C. Francolin, I. Sanders, G. T. Huntington (2010a) Algorithm 902: GPOPS, a MATLAB software for solving multiple-phase optimal control problems using the Gauss pseudospectral method, *ACM Transactions on Mathematical Software (TOMS)*, 37(2), pp. 22:1–22:39.

Rao, A. V., D. A. Benson, C. L. Darby, G. T. Huntington (2010b) User's manual for GPOPS version 3.3: A MATLAB software for solving optimal control problems using pseudospectral methods, Report.

Rodrigo, E., S. Tapia, J. Mera, M. Soler (2013) Optimizing electric rail energy consumption using the Lagrange multiplier technique, *Journal of Transportation Engineering*, 139(3), pp. 321–329.

Ross, I. M. (2005) A historical introduction to the covector mapping principle, in: *Advances in the astronautical sciences*, vol. 123, Univelt Inc., San Diego, CA, USA, pp. 1257–1278.

Ross, I. M. (2015) *A Primer on Pontryagin's Principle in Optimal Control*, Collegiate Publishers, San Fransisco, CA, USA.

Ross, I. M., M. Karpenko (2012) A review of pseudospectral optimal control: from theory to flight, *Annual Reviews in Control*, 36(2), pp. 182–197.

RSSB (2008) Understanding Human Factors a guide for the railway industry, Tech. rep., RSSB.

Scheepmaker, G. M. (2013) *Running time supplements in railway timetables: Energy-efficient operation versus robustness (in Dutch: "Rijtijdspeling in treindienstregelingen: energiezuinig rijden versus robuustheid")*, MSc thesis, Delft University of Technology, Delft, The Netherlands.

Scheepmaker, G. M., R. M. P. Goverde (2015) The interplay between energy-efficient train control and scheduled running time supplements, *Journal of Rail Transport Planning & Management*, 5(4), pp. 225–239.

Scheepmaker, G. M., R. M. P. Goverde (2016) Energy-efficient train control including regenerative braking with catenary efficiency, IEEE International Conference on Intelligent Rail Transportation (ICIRT), pp. 116–122.

Scheepmaker, G. M., R. M. P. Goverde (2020) Energy-efficient train control using nonlinear bounded regenerative braking, *Transportation Research Part C: Emerging Technologies*, 121, 102852.

Scheepmaker, G. M., R. M. P. Goverde, L. G. Kroon (2017) Review of energy-efficient train control and timetabling, *European Journal of Operational Research*, 257(2), pp. 355–376.

Scheepmaker, G. M., P. J. Pudney, A. R. Albrecht, R. M. P. Goverde, P. G. Howlett (2020a) Optimal running time supplement distribution in train schedules for energy-efficient train control, *Journal of Rail Transport Planning & Management*, 14, 100180.

Scheepmaker, G. M., H. Y. Willeboordse, J. H. Hoogenraad, R. S. Luijt, R. M. P. Goverde (2020b) Comparing train driving strategies on multiple key performance indicators, *Journal of Rail Transport Planning & Management*, 13, 100163.

Serafini, P., W. Ukovich (1989) A mathematical model for periodic scheduling problems, *SIAM Journal on Discrete Mathematics*, 2(4), pp. 550–581.

Sicre, C., A. P. Cucala, A. Fernández-Cardador (2014) Real time regulation of efficient driving of high speed trains based on a genetic algorithm and a fuzzy

model of manual driving, *Engineering Applications of Artificial Intelligence*, 29, pp. 79–92.

Sicre, C., A. P. Cucala, A. Fernández-Cardador, J. A. Jiménez, I. Ribera, A. Serrano (2010) A method to optimise train energy consumption combining manual energy efficient driving and scheduling, *WIT Transactions on The Built Environment*, 114, pp. 549–560.

Steimel, A. (2008) *Electric Traction Motive Power and Energy Supply*, Oldenbourg Industrieverlag, München, Germany.

Stephan, A. (2008) OpenPowerNet – Simulation of railway power supply systems, *WIT Transactions on The Built Environment*, 103, pp. 449–459.

Stoer, J., R. Bulirsch (2002) *Introduction to Numerical Analysis*, 3rd ed., Springer, New York, NY, USA.

Strobel, H., P. Horn, M. Kosemund (1974) A contribution to optimum computer-aided control of train operation, in: *2nd IFAC/IFIP/IFORS Symposium on Traffic Control and Transportation Systems*, pp. 377–387.

Su, S., L. Li, T. Tang, Z. Gao (2013) A subway train timetable optimization approach based on energy-efficient operation strategy, *IEEE Transactions on Intelligent Transportation Systems*, 14(2), pp. 883–893.

Su, S., T. Tang, X. Li, Z. Gao (2014) Optimization of multitrain operations in a subway system, *IEEE Transactions on Intelligent Transportation Systems*, 15(2), pp. 673–684.

Su, S., X. Wang, Y. Cao, J. Yin (2020) An energy-efficient train operation approach by integrating the metro timetabling and eco-driving, *IEEE Transactions on Intelligent Transportation Systems*, 21(10), pp. 4252–4268.

UIC (2012) Moving towards sustainable mobility, Paris, France.

UIC (2013) UIC code 406: Capacity, Report, UIC.

Van Dongen, L. A. M., J. H. Schuit (1989a) Energy-efficient driving patterns in electric railway traction, in: *International Conference on Main Line Railway Electrification*, pp. 154–158.

Van Dongen, L. A. M., J. H. Schuit (1989b) Energy-efficient train operation (in Dutch: *"Energie zuinig rijden"*), *KwaliteitsSeinen, Special Edition, December 1989*.

Van Dongen, L. A. M., J. H. Schuit (1991) Energy-efficient driving patterns (in Dutch: *"Energiezuinige rijpatronen"*), Report, Netherlands Railways (NS).

Van Leeuwen, J. J. A. (2017) Trillingshinder - Gedifferentieerd rijden. Samenvatting onderzoek naar het effect van rijsnelheid van goederentreinen op trillingsopwekking in de bodem uitgevoerd op zes locaties in Nederland plus een analyse van andere oorzaken van trillingen (in Dutch), Report, DGMR.

Velthuizen, F., S. Ruijsendaal (2011) UZI BASIC method (In Dutch: *"De UZI BASIS methode"*), Utrecht, The Netherlands.

Vernersson, T., R. Lundén (2014) Wear of brake blocks for in-service conditions-Influence of the level of modelling, *Wear*, (1-2), pp. 125–131.

Vromans, M. J. C. M., R. Dekker, L. G. Kroon (2006) Reliability and heterogeneity of railway services, *European Journal of Operational Research*, 172(2), pp. 647–665.

Vu, X. (2006) *Analysis of necessary conditions for the optimal control of a train*, PhD Thesis, University of South Australia, Adelaide, Australia.

Wang, P., R. M. P. Goverde (2016a) Multiple-phase train trajectory optimization with signalling and operational constraints, *Transportation Research Part C: Emerging Technologies*, 69, pp. 255–275.

Wang, P., R. M. P. Goverde (2016b) Train trajectory optimization of opposite trains on single-track railway lines, in: *2016 IEEE International Conference on Intelligent Rail Transportation (ICIRT)*, pp. 23–31.

Wang, P., R. M. P. Goverde (2016c) Two-train trajectory optimization with a green-wave policy, *Transportation Research Record: Journal of the Transportation Research Board*, 2546, pp. 112–120.

Wang, P., R. M. P. Goverde (2017) Multi-train trajectory optimization for energy efficiency and delay recovery on single-track railway lines, *Transportation Research Part B: Methodological*, 105, pp. 340–361.

Wang, P., R. M. P. Goverde (2019) Multi-train trajectory optimization for energy-efficient timetabling, *European Journal of Operational Research*, 272(2), pp. 621–635.

Wang, P., R. M. P. Goverde, L. Ma (2015) A multiple-phase train trajectory optimization method under real-time rail traffic management, in: *18th IEEE International Conference on Intelligent Transportation Systems (ITSC)*, pp. 771–776.

Wang, Y., B. De Schutter, B. Ning, N. Groot, T. Van den Boom (2011) Optimal trajectory planning for trains using Mixed Integer Linear Programming, in: *14th IEEE International Conference on Intelligent Transportation Systems (ITSC)*, pp. 1598–1603.

Wang, Y., B. De Schutter, T. Van den Boom, B. Ning (2013) Optimal trajectory planning for trains – A pseudospectral method and a mixed integer programming approach, *Transportation Research Part C*, 29, pp. 97–114.

Wang, Y., B. De Schutter, T. Van den Boom, B. Ning (2014) Optimal trajectory planning for trains under fixed and moving signaling systems using mixed integer linear programming, *Control Engineering Practice*, 22, pp. 44–56.

Weltevreden, M. (2015) Wat is het verschil in energieverbruik ERTMS versus ATB ritten? (in Dutch), *Kennisbank ERTMS*.

Wickens, C. D. (2002) Multiple resources and performance prediction, *Theoretical Issues in Ergonomics Science*, 3(2), pp. 159–177.

Xu, Y., B. Jia, X. Li, M. Li, A. Ghiasi (2020) An integrated micro-macro approach for high-speed railway energy-efficient timetabling problem, *Transportation Research Part C: Emerging Technologies*, 112, pp. 88–115.

Yan, F., N. Bešinović, R. M. P. Goverde (2019) Multi-objective periodic railway timetabling on dense heterogeneous railway corridors, *Transportation Research Part B: Methodological*, 125, pp. 52–75.

Yan, F., R. M. P. Goverde (2019) Combined line planning and train timetabling for strongly heterogeneous railway lines with direct connections, *Transportation Research Part B: Methodological*, 127, pp. 20–46.

Yang, L., K. Li, Z. Gao, X. Li (2012) Optimizing trains movement on a railway network, *Omega*, 40(5), pp. 619–633.

Yang, S., J. Wu, X. Yang, H. Sun, Z. Gao (2018) Energy-efficient timetable and speed profile optimization with multi-phase speed limits: Theoretical analysis and application, *Applied Mathematical Modelling*, 56, pp. 32–50.

Yang, X., A. Chen, X. Li, B. Ning, T. Tang (2015) An energy-efficient scheduling approach to improve the utilization of regenerative energy for metro systems, *Transportation Research Part C*, 57(1), pp. 13–29.

Yang, X., X. Li, Z. Gao, H. Wang, T. Tang (2013) A cooperative scheduling model for timetable optimization in subway systems, *IEEE Transactions on Intelligent Transportation Systems*, 14(1), pp. 438–447.

Yang, X., X. Li, B. Ning, T. Tang (2016) A survey on energy-efficient train operation for urban rail transit, *IEEE Transactions on Intelligent Transportation Systems*, 17(1), pp. 2–13.

Yang, X., B. Ning, X. Li, T. Tang (2014) A two-objective timetable optimization model in subway systems, *IEEE Transactions on Intelligent Transportation Systems*, 15(5), pp. 1913–1921.

Yang, X., J. Wu, H. Sun, Z. Gao, H. Yin, Y. Qu (2019) Performance improvement of energy consumption, passenger time and robustness in metro systems: A multi-objective timetable optimization approach, *Computers & Industrial Engineering*, 137, 106076.

Ye, H., R. Liu (2016) A multiphase optimal control method for multi-train control and scheduling on railway lines, *Transportation Research Part B: Methodological*, 93, pp. 377–393.

Yi, S. (2018) *Principles of Railway Location and Design*, Academic Press, London, UK.

Yin, J., T. Tang, L. Yang, J. Xun, Y. Huang, Z. Gao (2017) Research and development of automatic train operation for railway transportation systems: A survey, *Transportation Research Part C: Emerging Technologies*, 85, pp. 548–572.

Zhang, Y., A. D'Ariano, B. He, Q. Peng (2019) Microscopic optimization model and algorithm for integrating train timetabling and track maintenance task scheduling, *Transportation Research Part B: Methodological*, 127, pp. 237–278.

Zhou, Y., Y. Bai, J. Li, B. Mao, T. Li (2018) Integrated optimization on train control and timetable to minimize net energy consumption of metro lines, *Journal of Advanced Transportation*, 2018, p. 19.

Summary

Railways in Europe need to reduce CO_2 emissions and energy usage to contribute to sustainability. One of the measures that railway undertakings can apply with low investment cost and both high reductions in CO_2 emission and energy consumption, is energy-efficient train driving using energy-efficient train trajectory optimization that computes the optimal speed profile and corresponding time-distance path of a train. Another efficient measure is incorporating energy-efficient train driving in the timetable design. The aim of this thesis is to incorporate energy-efficient train driving in the timetable design in order to improve the potential for energy-efficiency of railways. The thesis formulates and develops algorithms for the *energy-efficient train control* (*EETC*) problem for a single train over (multiple) stops with both mechanical and regenerative braking behavior. In addition, energy-efficient train driving is incorporated in timetabling by formulating and developing algorithms for a multiple-objective optimization problem applied on a corridor with multiple interacting trains.

First, the EETC problem was formulated, and the optimal control structure and the necessary optimality conditions were derived. The optimal control structure was derived using *Pontryagin's Maximum Principle* and the Karush-Kuhn-Tucker conditions were used to derive necessary optimality conditions. This leads to the general optimal control structure consisting of the *driving regimes*: maximum acceleration, cruising, coasting, and maximum braking. We extended the original EETC problem by including nonlinear regenerative braking, and derived the resulting optimal control structure and the necessary optimality conditions. The thesis showed that the EETC problem with nonlinear regenerative braking leads to a slightly different optimal driving strategy compared to mechanical or constant regenerative braking only. The driving regime cruising by partial braking is divided into cruising by partial regenerative braking, and cruising by maximum regenerative braking and partial mechanical braking. The maximum braking regime is separated into maximum regenerative braking, and maximum regenerative and mechanical braking.

The EETC problems in this thesis were solved using a multiple-phase Radau pseudospectral method implemented in the prototype called PROMO. This method

uses collocation to discretize the optimal control problem and rewrites it to a nonlinear programming (NLP) problem, which is then solved with efficient NLP solvers. The algorithms of PROMO are capable to compute different driving strategies: *minimum time train control* (*MTTC*), energy-efficient train control, *maximal coasting* (*MC*) and *reduced maximum speed* (*RMS*). In addition, both mechanical braking and constant/nonlinear regenerative braking are implemented in PROMO. The algorithms of PROMO also compute the blocking times based on the blocking time theory for the case of a three-aspect two-block signalling system.

Second, we investigated how existing train driving strategies can be improved to minimize energy consumption. The EETC driving strategy is compared with the RMS and MC driving strategies that are common driving strategies applied in practice. For short stop spacing say 5 km) the MC driving strategy is the same as the EETC driving strategy. For longer stop spacing (say 50 km) the current driving strategies can be improved by optimizing both the optimal cruising speed and the coasting regimes.

Third, this thesis considered the optimal distribution of the *running time supplements* over multiple stops for a single train while minimizing total traction energy consumption. Experiments indicated that the optimal cruising speed between stops should be equal. Moreover, the shorter the distance between the stops, the relatively larger the running time supplement. Gradients also influence the distribution, because relatively more running time supplements are allocated at downhill sections.

Fourth, energy-efficient train driving was considered in timetable optimization. A multiple-objective optimization problem was formulated that considers the total running time, infrastructure occupation, robustness and energy consumption. A conflict-free timetable based on blocking times is generated by a brute force search algorithm. Optimal solutions are determined by the weighted sum method and the standard Euclidean distance method. The methods used the algorithms of PROMO on a railway corridor. A balancing (negative) relationship was derived between the total running time and energy consumption without influencing the infrastructure occupation and robustness.

In summary, this thesis demonstrates that energy-efficient train trajectory optimization in timetable optimization balances the other objectives, and contributes to energy efficiency and sustainability.

Samenvatting

Het spoorvervoer in Europa dient te verduurzamen door de hoeveelheid CO_2-emissies te reduceren. Een van de maatregelen die een vervoerder kan toepassen tegen lage investeringskosten en met zowel een grote reductie van de CO_2-emissies als de verlaging van het energieverbruik, is *energiezuinig rijden* (*EZR*) of energie-efficiënte treintrajectorie (snelheidsprofiel en tijd-wegpad van een trein) optimalisatie. Een ander effiënte maatregel is het meenemen van EZR in het dienstregelingsontwerp. Het doel van dit promotieproefschrift is om EZR in het dienstregelingsontwerp mee te gaan nemen, waarmee de energie-efficiëntie voor het spoorvervoer toeneemt. In het proefschrift zijn algoritmes geformuleerd en ontwikkeld voor de *energie optimale* (*EO*) rijstrategie voor één trein tussen (meerdere) stops, waarbij zowel mechanisch als regeneratief remgedrag onderzocht is. Bovendien is EZR meegenomen in het dienstregelingsontwerp door het formuleren en ontwikkelen van algoritmes voor een multi-doelen optimalisatie probleem op een corridor met meerdere interactieve treinen.

Ten eerste is het besturingsprobleem geformuleerd voor de EO rijstrategie en zijn de structuur van de optimale besturing en de noodzakelijke optimalisatie voorwaarden afgeleid. De structuur van de energie optimale besturing is bepaald met behulp van het *maximum principe van Pontryagin* en de Karush-Kuhn-Tucker condities zijn toegepast om de noodzakelijke optimalisatie voorwaarden te bepalen. Dit leidt tot de algemene optimale besturingsstructuur bestaande uit de *rijregimes*: maximale acceleratie, kruisen (kruissnelheid), uitrollen en maximaal remmen. Het originele energie optimalisatie probleem is uitgebreid door niet-lineair regeneratief remmen mee te nemen, wat tot een kleine aanpassing in de optimale besturingsstructuur leidt ten opzichte van mechanisch of enkel constant regeneratief remmen. Het rijregime 'kruisen met gedeeltelijk remmen' is onderverdeeld in 'kruisen met gedeeltelijk regeneratief remmen', 'kruisen met maximaal regeneratief remmen', en 'kruisen met maximaal regeneratief remmen en gedeeltelijk mechanisch remmen'. Het rijregime 'maximaal remmen' is onderverdeeld in 'maximaal regeneratief remmen', en 'maximaal regeneratief en mechanisch rem-

men'. Het energie optimale besturingsprobleem is opgelost door het toepassen van een multi-fase Radau pseudospectrale methodiek die is geïmplementeerd in het prototype genaamd PROMO. Deze methodiek gebruikt collocatie om het optimale besturingsprobleem te discretiseren en herschrijft dit probleem naar een niet-lineair programmeringsprobleem (NLP-probleem). Het NLP-probleem is opgelost met behulp van een NLP-oplossingsmethode. De algoritmes van PROMO zijn in staat om verschillende rijstrategieën te berekenen, te weten: *minimale rijtijd* (*MR*), energie optimaal, *maximaal uitrollen* (*MU*) en *gereduceerde maximum kruissnelheid* (*GMK*). Bovendien zijn zowel mechanisch remmen als constant/niet-lineair remmen meegenomen in PROMO. De algoritmes van PROMO zijn ook in staat om de blokbezettingstijden op basis van de bloktraptheorie te berekenen, waarbij is uitgegaan van het drie-aspecten twee-blok seinstelsel.

Ten tweede is onderzocht hoe bestaande rijstrategieën verbeterd kunnen worden voor het minimaliseren van het energieverbruik. De energie optimale rijstrategie is vergeleken met de GMK en MU rijstrategie die beide veelal in de praktijk door vervoerders worden toegepast. Voor korte halteafstanden (bijv. 5 km) is de MU rijstrategie gelijk aan de EO rijstrategie. Voor langere halteafstanden (bijv. 50 km) kunnen de bestaande rijstrategieën verbeterd worden door het optimaliseren van zowel de optimale kruissnelheid als de uitrolfase.

Ten derde is in dit proefschrift de optimale verdeling van de *rijtijdspeling* voor één trein over meerdere stops onderzocht, met als doel het totale tractie-energieverbruik te minimaliseren. Experimenten laten zien dat de optimale kruissnelheid tussen stops gelijk dient te zijn. Bovendien geldt dat hoe korter de halteafstand is, hoe relatief meer rijtijdspeling toebedeeld dient te worden. Daarnaast zijn ook hellingen van invloed op de verdeling van de rijtijdspeling, omdat relatief meer speling is toebedeeld aan neergaande hellingen.

Ten vierde is EZR meegenomen in de dienstregelingsoptimalisatie. Een multi-doelen optimalisatieprobleem is geformuleerd die rekening houdt met de totale rijtijd, de bezetting van de infrastructuur, de robuustheid en het energieverbruik. Een conflictvrije dienstregeling gebaseerd op de blokbezettingstijden is gegeneerd door een brute kracht algoritme. De optimale resultaten zijn bepaald door een gewogen som methode en een standaard Euclidische afstand methode. De methodes zijn toegepast in de algoritmes van PROMO voor een spoorcorridor. Een (negatieve) gebalanceerde relatie is afgeleid tussen de totale rijtijd en het energieverbruik, zonder de bezetting van de infrastructuur en de robuustheid te beïnvloeden.

Samenvattend, dit proefschrift heeft laten zien dat energie-efficiënte trajectorie optimalisatie in de dienstregeling leidt tot een balans tussen de andere doelen en bijdraagt aan energie-efficiëntie en duurzaamheid.

About the author

Gerben Scheepmaker (1988) was born in Alkmaar, the Netherlands. In 2010 he obtained his BSc degree with distinction in Civil Engineering at the University of Twente. Afterwards, he continued his master's degree in Civil Engineering at Delft University of Technology (TU Delft). He did his master thesis in collaboration with the Netherlands Railways (NS) on the possibilities to better incorporate energy-efficient train driving into the railway timetable by redistributing the running time supplements. In 2013 he graduated with distinction for his MSc degree.

In 2013 Gerben started to work for NS, beginning at the short term rolling stock department, followed in 2014 at the strategic timetable design department, and since 2017 he works at the innovation department. His main work as a Business Consultant at NS focuses on researching, developing and implementing new methods and tools for timetable design, simulation and evaluation. In addition, he advises NS on energy-efficient train driving. His research interests include timetable design, simulation and evaluation, and energy-efficient train driving.

Furthermore, commissioned and funded by NS, Gerben started his part time PhD research at the Department of Transport and Planning (TU Delft) in 2014. His PhD research focused on incorporating energy-efficient train driving into timetable design under the supervision of Prof. Dr. Rob M.P. Goverde. During his PhD research Gerben was a visiting researcher at the University of South Australia in Adelaide in 2017. In 2020 the Swiss Federal Railways (SBB) purchased the prototype PROMO developed in his PhD research, in order to do further research on energy-efficient train driving.

Publications

Journal papers

1. **Gerben M. Scheepmaker**, Rob M. P. Goverde (2021) Multi-objective railway timetabling including energy-efficient train trajectory optimization, *European Journal of Transport and Infrastructure Research*, 21(4), 1–42.

2. Rob M. P. Goverde, **Gerben M. Scheepmaker**, Pengling Wang (2021) Pseudospectral optimal train control, *European Journal of Operational Research*, 292(1), 353–375.

3. **Gerben M. Scheepmaker**, Rob M. P. Goverde (2020) Energy-efficient train control using nonlinear bounded regenerative braking, *Transportation Research Part C: Emerging Technologies*, 121, 102852.

4. **Gerben M. Scheepmaker**, Peter J. Pudney, Amie R. Albrecht, Rob M. P. Goverde, Phil G. Howlett (2020) Optimal running time supplement distribution in train schedules for energy-efficient train control, *Journal of Rail Transport Planning & Management*, 14, 100180.

5. **Gerben M. Scheepmaker**, Helen Y. Willeboordse, Jan H. Hoogenraad, Ralph S. Luijt, Rob M. P. Goverde (2020) Comparing train driving strategies on multiple key performance indicators, *Journal of Rail Transport Planning & Management*, 13, 100163.

6. **Gerben M. Scheepmaker**, Rob M. P. Goverde, Leo G. Kroon (2017) Review of energy-efficient train control and timetabling, *European Journal of Operational Research*, 257(2), 355–376.

7. **Gerben M. Scheepmaker**, Rob M. P. Goverde (2015) The interplay between energy-efficient train control and scheduled running time supplements, *Journal of Rail Transport Planning & Management*, 5(4), 225–239.

Conference articles

1. **Gerben M. Scheepmaker**, Peter J. Pudney, Amie R. Albrecht, Rob M. P. Goverde, Phil G. Howlett (2019) Optimal running time supplement distribution for energy-efficient train control, RailNorrköping 2019 conference. Norrköping, Sweden.

2. Roel G. van Huet, **Gerben M. Scheepmaker**, Ralph S. Luijt (2017) Energy-efficient train driving in order to drive on time (*Energiezuinig rijden van treinen om op tijd te rijden*) (in Dutch), in: Colloqium Vervoersplanologisch Speurwerk (CVS). Gent, Belgium.

3. **Gerben M. Scheepmaker**, Rob M. P. Goverde (2016) Energy-efficient train control including regenerative braking with catenary efficiency, IEEE International Conference on Intelligent Rail Transportation. Birmingham, UK, 116–122.

4. **Gerben M. Scheepmaker**, Rob M. P. Goverde (2015) Effect of regenerative braking on energy-efficient train control, CASPT 2015. Rotterdam, the Netherlands.

5. **Gerben M. Scheepmaker**, Rob M. P. Goverde (2015) Running time supplements: energy-efficient train control versus robust timetables, RailTokyo 2015 conference. Tokyo, Japan.

TRAIL Thesis Series

The following list contains the most recent dissertations in the TRAIL Thesis Series. For a complete overview of more than 275 titles see the TRAIL website: www.rsTRAIL.nl.

The TRAIL Thesis Series is a series of the Netherlands TRAIL Research School on transport, infrastructure and logistics.

Scheepmaker, G.M., *Energy-efficient Train Timetabling*, T2022/1, January 2022, TRAIL Thesis Series, the Netherlands

Chen, N., *Coordination Strategies of Connected and Automated Vehicles near On-ramp Bottlenecks on Motorways*, T2021/29, December 2021, TRAIL Thesis Series, the Netherlands

Onstein, A.T.C., *Factors influencing Physical Distribution Structure Design*, T2021/28, December 2021, TRAIL Thesis Series, the Netherlands

Olde Kalter, M.-J. T., *Dynamics in Mode Choice Behaviour*, T2021/27, November 2021, TRAIL Thesis Series, the Netherlands

Los, J., *Solving Large-Scale Dynamic Collaborative Vehicle Routing Problems: an Auction-Based Multi-Agent Approach*, T2021/26, November 2021, TRAIL Thesis Series, the Netherlands

Khakdaman, M., *On the Demand for Flexible and Responsive Freight Transportation Services*, T2021/25, September 2021, TRAIL Thesis Series, the Netherlands

Wierbos, M.J., *Macroscopic Characteristics of Bicycle Traffic Flow: a bird's-eye view of cycling*, T2021/24, September 2021, TRAIL Thesis Series, the Netherlands

Qu, W., *Synchronization Control of Perturbed Passenger and Freight Operations*, T2021/23, July 2021, TRAIL Thesis Series, the Netherlands

Nguyen, T.T., *Highway Traffic Congestion Patterns: Feature Extraction and Pattern Retrieval*, T2021/22, July 2021, TRAIL Thesis Series, the Netherlands

Pudāne, B., *Time Use and Travel Behaviour with Automated Vehicles*, T2021/21,

July 2021, TRAIL Thesis Series, the Netherlands

Gent, P. van, *Your Car Knows Best*, T2021/20, July 2021, TRAIL Thesis Series, the Netherlands

Wang, Y., *Modeling Human Spatial Behavior through Big Mobility Data*, T2021/19, June 2021, TRAIL Thesis Series, the Netherlands

Coevering, P. van de, *The Interplay between Land Use, Travel Behaviour and Attitudes: a quest for causality*, T2021/18, June 2021, TRAIL Thesis Series, the Netherlands

Landman, R., *Operational Control Solutions for Traffic Management on a Network Level*, T2021/17, June 2021, TRAIL Thesis Series, the Netherlands

Zomer, L.-B., *Unravelling Urban Wayfinding: Studies on the development of spatial knowledge, activity patterns, and route dynamics of cyclists*, T2021/16, May 2021, TRAIL Thesis Series, the Netherlands

Núñez Velasco, J.P., *Should I Stop or Should I Cross? Interactions between vulnerable road users and automated vehicles*, T2021/15, May 2021, TRAIL Thesis Series, the Netherlands

Duivenvoorden, K., *Speed Up to Safe Interactions: The effects of intersection design and road users' behaviour on the interaction between cyclists and car drivers*, T2021/14, April 2021, TRAIL Thesis Series, the Netherlands

Nagalur Subraveti, H.H.S., *Lane-Specific Traffic Flow Control*, T2021/13, March 2021, TRAIL Thesis Series, the Netherlands

Beirigo, B.A., *Dynamic Fleet Management for Autonomous Vehicles: Learning- and optimization-based strategies*, T2021/12, March 2021, TRAIL Thesis Series, the Netherlands

Zhang, B., *Taking Back the Wheel: Transition of control from automated cars and trucks to manual driving*, T2021/11, February 2021, TRAIL Thesis Series, the Netherlands

Boelhouwer, A., *Exploring, Developing and Evaluating In-Car HMI to Support Appropriate use of Automated Cars*, T2021/10, January 2021, TRAIL Thesis Series, the Netherlands

Li, X., *Development of an Integrity Analytical Model to Predict the Wet Collapse Pressure of Flexible Risers*, T2021/9, February 2021, TRAIL Thesis Series, the Netherlands